



Norwegian University of
Science and Technology

Expansion of the port in Ustka. Simulation of wave conditions.

Hubert Konkol

Wiktor Mateusz Wickland

Coastal and Marine Civil Engineering

Submission date: July 2016

Supervisor: Raed Khalil Lubbad, BAT

Norwegian University of Science and Technology
Department of Civil and Transport Engineering



**NTNU - Trondheim
Norwegian University of
Science and Technology**

ABSTRACT

Along with the development of port cities and conducting new market research and analysis it often turns out that the current port infrastructure is insufficient to exploit the full potential of the location. Then a modernization and expansion of the current port is needed. This is also the case of Port in Ustka, Poland, which is a small harbour handling mainly small fishing boats and yachts. With the ensuing need for a port being able to handle larger vessels, such as military units or vessels used during the construction and service of offshore wind farms, a decision for the port expansion has been made.

Designing a new harbour or a harbour expansion is always a very complex task, where a vast variety of complex phenomena and aspects have to be taken into account. One has to consider such aspect as technical requirements, environmental impact and financial feasibility and cost effectiveness of such an investment.

The research carried out in this thesis aims to choose the best harbour layout of new Harbour of Ustka out of four concepts provided by Maritime Office in Słupsk. As the decisive criterion wave climate inside the designed harbour was chosen. The best breakwater layout should ensure waves as small as possible in order not to disturb berthing of vessels and cargo handling operations inside the port. Wave propagation towards and inside harbour was modelled using MIKE 21 - numerical software developed by DHI. It is comprehensive tool containing numerous models and toolboxes that help to prepare all input data needed for the simulation. It includes also a module called MIKE C-MAP that contains global bathymetry and tidal data. As scarce data on waves and tides is available in the nearest proximity of the site of interest, the nesting approach has been used. Firstly, using all available information Spectral Wave model was prepared. It is a phase averaging model, that calculates wave statistics and allows for wave calculations in large scale. It was used to obtain reliable information about wave climate near the harbour of Ustka. Period of two months, January and February, was simulated, as major and most severe storms occur in this time. Output from Spectral Wave simulation was used to determine the input condition for a models prepared in much greater resolution. The four proposed breakwater layouts were tested using Boussinesq Wave models. Boussinesq Wave model is a phase resolving model, commonly used to investigate wave propagation and transformation in coastal area and wave interaction with the structures, as it is capable of resolving such wave phenomena as diffraction, refraction and reflection. Every layout was tested against waves coming from main direction, which is north-west, and most unfavourable direction of incoming waves, that is north-east.

After successful completion of numerical calculation, the results were summarized, compared and discussed. Conducted analysis allowed for choosing the best proposed breakwater layout in terms of provided wave conditions inside harbour basins and at the entrance to the harbour. In conclusion, limitations of the prepared models are listed, and ways of improvement are suggested. What is more a scope of future research is outlined.

MASTER THESIS
(TBA4920 Marine Civil Engineering, master thesis)

Spring 2016

for

Wiktor Wickland, Hubert Konkol

Expansion of the port in Ustka: simulation of wave conditions.

BACKGROUND

This master thesis concerns a new port in Ustka, which is located in the northern part of Poland. There is a need for a new port to handle specialized vessels servicing the wind farms. In order to ensure that the new harbour fulfils all of its functions properly, tentative concepts have to be evaluated and the especially the waves conditions inside the harbour basin must be examined to guarantee minimal undesirable wave effects. To achieve this, numerical models will be prepared and run using diverse software.

TASK DESCRIPTION

Description of task

The master thesis has the following scope:

- 1) Describe demands and functions of the new port.
- 2) Identify the current technical condition - problems and damages.
- 3) Collect available input data from the physical environment, e.g. bathymetry, wind, waves, current.
- 4) Discuss different layouts of breakwater.
- 5) Describe the theoretical background for the numerical models used in this thesis.
- 6) Simulation of wave conditions in the close proximity and inside the harbor using numerical models.
- 7) Conclusion, summary and recommendations for future work.

Aims and purpose

The purpose is to choose the best breakwater layout that will provide the best wave conditions inside harbour basin. In the same time, it has to be sufficient for the proper operation of the port and meet the standards.

General about content, work and presentation

The text for the master thesis is meant as a framework for the work of the candidate. Adjustments might be done as the work progresses. Tentative changes must be done in cooperation and agreement with the professor in charge at the Department.

In the evaluation thoroughness in the work will be emphasized, as will be documentation of independence in assessments and conclusions. Furthermore the presentation (report) should be well organized and edited; providing clear, precise and orderly descriptions without being unnecessary voluminous.

The report shall include:

- Standard report front page (from DAIM, <http://daim.idi.ntnu.no/>)
 - Title page with abstract and keywords.(template on: <http://www.ntnu.no/bat/skjemabank>)
CoMEM students must include CoMEM as one of the keywords.
 - CoMEM page (Only CoMEM students)
 - Preface
- Summary and acknowledgement. The summary shall include the objectives of the work, explain how the work has been conducted, present the main results achieved and give the main conclusions of the work.
- Table of content including list of figures, tables, enclosures and appendices.
- A list explaining important terms and abbreviations should be included.
- List of symbols should be included
- The main text.
 - Clear and complete references to material used, both in text and figures/tables. This also applies for personal and/or oral communication and information.
 - Thesis task description (these pages) signed by professor in charge as Attachment 1.
- The report must have a complete page numbering.

The thesis can as an alternative be made as a scientific article for international publication, when this is agreed upon by the Professor in charge. Such a report will include the main points as given above, but where the main text includes both the scientific article and a process report.

Submission procedure

Procedures relating to the submission of the thesis are described in IVT faculty webpage <http://www.ntnu.edu/ivt/master-s-thesis-regulations>

On submission of the thesis the candidate shall submit to the professor in charge a CD/DVD('s) or a link to a net-cloud including the report in digital form as pdf and Word (or other editable form) versions and the underlying material (such as data collection, time series etc.).

Documentation collected during the work, with support from the Department, shall be handed in to the Department together with the report.

According to the current laws and regulations at NTNU, the report is the property of NTNU. The report and associated results can only be used following approval from NTNU (and external cooperation partner if applicable). The Department has the right to make use of the results from the work as if conducted by a Department employee, as long as other arrangements are not agreed upon beforehand.

Start and submission deadlines

The work on the Master Thesis starts on 15th January 2016

The thesis report as described above shall be submitted digitally in DAIM at the latest 10th July at 3pm.

Delayed deadline: 04.07.2016

Professor in charge: Raed Lubbad

Trondheim, 18.01.2015 (revised: May 2016)

Professor in charge (sign)

ACKNOWLEDGEMENTS

It is a great pleasure to express our sincere gratitude to everyone who helped, guided and motivated us during our MSc study. At the beginning, we would like to express our deepest gratitude to our thesis supervisor, Raed Lubbad. His guidance, patience, understanding and encouragement were invaluable. We would like to thank all the members and employees of the department of Civil and Transport Engineering. We are especially grateful to Øivind Asgeir Arntsen and Mohammad Saud Afzal, for their openness, advice and constant willingness to help. We wish to express our sincere appreciation to all professors and employees of Gdańsk University of Technology, which is our home institution, for all the great years we have spent studying there, especially to Professor Adam Bolt, who is our supervisor there.

We are very grateful to all institutions that provided data for our simulations. We would like to thank all the people at German Federal Waterways and Shipping Administration, German Federal Institute of Hydrology and Swedish Meteorological and Hydrological Institute for providing all the wave and water level data. We would like to thank the employees of the Maritime Office in Słupsk, for providing all the background information about the Port of Ustka. A special thanks to Adam Borodziuk, former Technical Director, who prepared the concepts of the breakwater layouts. We would like to mention the support from people at DHI, in providing software used for this thesis and for their quick and helpful answers to every question related to the software.

Finally, we would like to express our deepest thanks to all my family and friends, for their endless love, support and encouragement through our study.

CONTENTS

Abstract	ii
Acknowledgements	vi
CONTENTS	vii
List of figures	ix
List of tables	xiii
1. Introduction	1
2. Port of Ustka.....	3
2.1. Area description and history	3
2.2. Current situation and technical problems	4
2.3. Demands and planned functions of the new harbour	7
2.4. Proposed breakwater layouts for Ustka new harbour	8
3. Port design.....	14
3.1. Technical requirements.....	14
3.2. Environmental aspects	19
3.3. Economy aspects	21
3.4. Aspects covered in the master thesis	21
4. Numerical modelling of Waves.....	23
4.1. Wave modelling State-of-the-art	23
4.2. Theoretical background of the numerical models used in this master thesis	24
4.2.1. Spectral Wave model	24
4.2.2. Boussinesq Wave model	26
5. Numerical model for waves in the new Ustka harbour	29
5.1. Approach	29
5.2. SW model	29
5.2.1. Domain Description	29
5.2.2. Boundary Conditions.....	31
5.2.3. Wind forcing	37
5.2.4. Water level	40
5.2.5. Summary of all input data and parameters used	43
5.3. BW model.....	45
5.3.1. Domain Description	45
5.3.2. Boundary Conditions.....	55
5.3.3. Summary of all input data and parameters	60
6. Results and discussion.....	67
6.1. Spectral Wave Model	67
6.2. Spectral Wave Model + HD	71

6.3. Boussinesq Wave Model	81
6.3.1. Regular waves	81
6.3.2. Random waves	83
6.4. Comparison and discussion of the results.....	111
7. Conclusions and recommendations for further reaserch	118
References	120
APPENDICES.....	122
1. Mike Zero License Agreement.....	122
2. Sample log files from Linear Spectra Analysis.....	125
2.1. Layout 1 point 3, waves from north-east	125
2.2. Layout 1 point 4, waves from north-east	127

LIST OF FIGURES

Figure 1 Location – Harbour in Ustka (Source: Google Earth)	3
Figure 2 Location - Port in Ustka with coordinates (Source: Google Maps).....	4
Figure 3 Plan of the current port in Ustka. Pilot Quay marked with red ellipse.	6
Figure 4 Southern Baltic Sea areas proposed for installation of maritime wind farms (Source: Renewable Energy)	8
Figure 5 The cross section of the chosen breakwater type. (Source: Maritime Office in Słupsk; Designer: Borodziuk A.)	9
Figure 6 Proposed layout no. 1. (Source: Maritime Office in Słupsk; Designer: Borodziuk A.)	10
Figure 7 Proposed layout no. 2. (Source: Maritime Office in Słupsk; Designer: Borodziuk A.)	11
Figure 8 Proposed layout no. 3. (Source: Maritime Office in Słupsk; Designer: Borodziuk A.)	12
Figure 9 Proposed layout no. 4. (Source: Maritime Office in Słupsk; Designer: Borodziuk A.)	13
Figure 10 Basic wave parameters.....	17
Figure 11 Sediment transport processes on the coastline. [Sawaragi (1995)].....	20
Figure 12 Bathymetry of Baltic Sea generated by Mike Zero software.....	30
Figure 13 The view on the generated mesh. Zoomed into local area of interest. Prepared using Mike Zero Software	30
Figure 14 Position of the measuring buoys (Source: Google Maps)	31
Figure 15 Northern, Eastern and Western boundaries of the defined domain	32
Figure 16 Plot of the input data from FinO2 WR Buoy –Western boundary	34
Figure 17 Plot of the input data from Sodra Ostersjon Buoy – Eastern boundary.....	35
Figure 18 Plot of the input data from Knolls Grund Buoy – Northern boundary	36
Figure 19 Wind velocity contour plan over the area (Source: ECMWF)	37
Figure 20 Relationship between x and y velocity component.	37
Figure 21 The comparison of the mean wind speed from Ustka measurements (blue) and ECMWF data (red). (Generated by: Mike Zero by DHI)	38
Figure 22 The comparison of the mean wind direction from Ustka measurements (blue) and ECMWF data (red). (Generated by: Mike Zero by DHI)	38
Figure 23 The rose plots of the mean wind speed for Ustka from ECMWF (on the bottom) model and NOAA (top). (Generated by: Mike Zero by DHI)	39
Figure 24 Pressure snapshot over the area (Source: ECMWF).....	40
Figure 25 Water level at western, northern and eastern boundary respectively. Generated by Mike Zero Plot Composer.	41
Figure 26 Dialog window from Setup Planner, part 1. Source: Mike 21 by DHI.....	46
Figure 27 Dialog window from Setup Planner, part 2. Source: Mike 21 by DHI.....	47
Figure 28 General view of the created bathymetry. Generated by Mike Zero software.....	49
Figure 29 View of the breakwater joint with coast. Different edge values. Generated by Mike Zero software.....	50
Figure 30 Dialog window from Bathymetry Grid Editor, view on a place where breakwater connects with the coast. Generated by Mike Zero Bathymetry Editor.	51
Figure 31 Visualization of the first concept. View from the north-east. Generated by Mike Animator Plus.....	52
Figure 32 Visualization of the first concept. View from the north-west. Generated by Mike Animator Plus.....	53

Figure 33 Recommended values for sponge layer coefficients. Source: Mike Toolbox user guide.	54
Figure 34 Visualization of the sponge layer. Generated by Mike Zero software.	54
Figure 35 Visualization of the porosity layer. Generated by Mike Zero software.	55
Figure 36 Mike Zero - Random Wave Generator.	56
Figure 37 Position of the generating lines. Created by Mike Zero software.	57
Figure 38 Angle convention. Source: Mike 21 BW User Guide.	58
Figure 39 Bathymetry of concept no 2 with marked results points. Generated by Mike Zero software.	61
Figure 40 Bathymetry of concept no 3 with marked results points. Generated by Mike Zero software.	62
Figure 41 Bathymetry of concept no 4 with marked results points. Generated by Mike Zero software.	62
Figure 42 Model domain showing significant wave height and wave vectors.	67
Figure 43 Model domain showing isolines with significant wave height.	68
Figure 44 Model domain showing wave period T_{01}	68
Figure 45 Plot of the area of interest showing significant wave height and wave vectors. Wave refraction can be easily seen.	69
Figure 46 Plot of the area of interest showing significant wave height (isolines).	69
Figure 47 Plot of the area of interest showing wave period T_{01}	70
Figure 48 Time series showing significant wave height at the location of the head of the eastern breakwater.	70
Figure 49 Time series showing wave period T_{01} at the location of the head of the eastern breakwater.	71
Figure 50 Model domain showing significant wave height and wave vectors.	72
Figure 51 Model domain showing isolines with significant wave height.	73
Figure 52 Model domain showing wave period T_{01}	74
Figure 53 Plot of the area of interest showing significant wave height and wave vectors. Wave refraction can be easily seen.	75
Figure 54 Plot of the area of interest showing significant wave height (isolines).	75
Figure 55 Plot of the area of interest showing wave period T_{01}	76
Figure 56 Time series showing significant wave height at the location of the head of the eastern breakwater.	76
Figure 57 Time series showing wave period T_{01} at the location of the head of the eastern breakwater.	77
Figure 58 Time series of the surface elevation caused by tides and currents. Generated by Mike Zero.	78
Figure 59 Plot of the speed and direction of the current in proximity of Ustka. Generated by Mike Zero.	78
Figure 60 Time series showing comparison of significant wave height at the location of the head of the eastern breakwater. Red line shows SW+HD output and blue one shows output from SW without HD.	79
Figure 61 The comparison of total wave height (blue) and wave height for wind sea (red). (Generated by: Mike Zero by DHI)	79
Figure 62 The comparison of total wave height (blue) and wave height for swell (red). (Generated by: Mike Zero by DHI)	80
Figure 63 The rose plot of the significant wave height at the proximity of Ustka (Generated by: Mike Zero by DHI)	81
Figure 64 First layout, regular waves: Snapshot of the waves at the beginning of the simulation.	82

Figure 65 First layout, regular waves: Snapshot of propagating waves at the time of the occurrence of the highest waves at the harbour entrance.	82
Figure 66 Time series of surface elevation for regular wave conditions at the detached breakwater (top) and centre of new harbour basin (bottom).	83
Figure 67 First concept with marked points of interest. Generated by Mike Zero.	84
Figure 68 First layout, random waves from north-west: Plot of the time series for point 1-6 from Figure 67, from the top to the bottom respectively	85
Figure 69 First layout, random waves from north-west: Snapshot of the waves at the beginning of the simulation.	86
Figure 70 First layout, random waves from north-west: Snapshot of propagating waves at the time of the occurrence of the highest waves at the harbour entrance.	86
Figure 71 Visualisation of the first layout. Snapshot taken at 47th time step when the highest wave occurs at the harbour entrance. Black line symbolize generation line.	87
Figure 72 First layout, random waves from north-east: Plot of the time series for point 1-6 from Figure 67, from the top to the bottom respectively	89
Figure 73 First layout, random waves from north-east: Snapshot of the waves at the beginning of the simulation.	89
Figure 74 First layout, random waves from north-east: Snapshot of propagating waves at the time of the occurrence of the highest waves inside new harbour basin.	89
Figure 75 Visualization corresponds to Fig. 74. Snapshot taken at 43th time step. Waves are propagating from north-east.	90
Figure 76 Second concept with marked points of interest. Generated by Mike Zero.	91
Figure 77 Second layout, random waves from north-west: Plot of the time series for point 1-6 from Figure 76, from the top to the bottom respectively	92
Figure 78 Snapshot of the second layout, random waves from north-west: Plot of the waves at the beginning of the simulation.	93
Figure 79 Snapshot of the second layout, random waves from north-west: Propagating waves at the time of the occurrence of the highest waves at the harbour entrance.	93
Figure 80 Visualization corresponds to Fig. 77. Snapshot taken at 15th time step. Waves are propagating from north-west.	94
Figure 81 Second layout, random waves from north-east: Plot of the time series for points 1-6 from Figure 76, from the top to the bottom respectively	95
Figure 82 Snapshot of the second layout, random waves from north-east: Plot of the waves at the beginning of the simulation.	96
Figure 83 Snapshot of the second layout, random waves from north-east: snapshot of propagating waves at the time of the occurrence of the highest waves at the harbour entrance.	96
Figure 84 Close-up on the breakwaters showing raising wave heights along the structure.	97
Figure 85 Visualization of the second layout. Snapshot of the 77 th time step.	97
Figure 86 Third concept with marked points of interest. Generated by Mike Zero.	98
Figure 87 Third layout, random waves from north-west: Plot of the time series for points 1-6 from Figure 86, from the top to the bottom respectively.	99
Figure 88 Snapshot of the third layout, random waves from north-west: Snapshot of the waves at the beginning of the simulation.	100
Figure 89 Snapshot of the third layout, random waves from north-west: Plot of propagating waves at the time of the occurrence of the highest waves at the harbour entrance.	100
Figure 90 Visualization of the third layout. Snapshot of the 16 th time step when the highest wave occurs at the entrance to the harbour.	101
Figure 91 Third layout, random waves from north-east: Plot of the time series for points 1-6 from Figure 86, from the top to the bottom respectively	102

Figure 92 Snapshot of the third layout, random waves from north-east: snapshot of the waves at the beginning of the simulation.	103
Figure 93 Snapshot of the third layout, random waves from north-east: snapshot of propagating waves at the time of the occurrence of the highest waves at the harbour entrance.	103
Figure 94 Visualisation of the third layout. Snapshot of the 9 th time step. Waves propagating from north-east. First waves entered into the new basin.	104
Figure 95 Visualisation of the third layout. Snapshot of the 39 th time step. Reflected waves creates standing wave at the corner of the new basin.	104
Figure 96 Fourth concept with marked points of interest. Generated by Mike Zero.	105
Figure 97 Fourth layout, random waves from north-west: Plot of the time series for points 1-6 from Figure 96, from the top to the bottom respectively	106
Figure 98 Snapshot of the fourth layout, random waves from north-west: snapshot of the waves at the beginning of the simulation.	107
Figure 99 Snapshot of the fourth layout, random waves from north-west: snapshot of propagating waves at the time of the occurrence of the highest waves at the harbour entrance.	107
Figure 100 Visualisation of the fourth layout, waves from north-west.. Snapshot of the 14 th time step shows standing wave.	108
Figure 101 Fourth layout, random waves from north-east: Plot of the time series for points 1-6 from Figure 96, from the top to the bottom respectively	109
Figure 102 Snapshot of the fourth layout, random waves from north-east: snapshot of the waves at the beginning of the simulation.	110
Figure 103 Snapshot of the fourth layout, random waves from north-east: snapshot of propagating waves at the time of the occurrence of the highest waves at the harbour entrance.	110
Figure 104 Visualisation of the fourth layout., random waves from north-east: snapshot of propagating waves at the time of the occurrence of the highest waves at the harbour entrance.	111
Figure 105 Compared wave height time series for waves coming from north-west (Points 1-3)	113
Figure 106 Compared wave height time series for waves coming from north-west (Points 4-6)	114
Figure 107 Compared wave height time series for waves coming from north-east (Points 1-3)	115
Figure 108 Compared wave height time series for waves coming from north-east (Points 4-6)	116

LIST OF TABLES

Table 1 The geometrical properties of the proposed layouts.	13
Table 2 The Beaufort wind scale [Huler (2004)]	15
Table 3 Reference Values of Threshold Wave Height for Cargo Handling Works [OCDI-2002].....	18
Table 4 Maximum wave heights [Thoresen (2010)]......	18
Table 5 Specification of the Hydrodynamic model (HD)	42
Table 6 Specification of the SW model + HD	43
Table 7 Summary of prepared generation lines	58
Table 8 Final setup of simulation of regular wave.....	63
Table 9 Final setup of simulation of random waves from northwest.....	64
Table 10 Final setup of simulation of random waves from northeast.....	65
Table 11 Summary of the results obtained in SW simulation.in at the location of the head of the eastern breakwater	77
Table 12 Summary of max. wave height obtained from simulation with random waves from north-west. Colour green symbolize the lowest value while red the highest values.....	117
Table 13 Summary of max. wave height obtained from simulation with random waves from north-east. Colour green symbolize the lowest value while red the highest values.....	117
Table 14 Summary of mean wave period obtained from LSA of random waves from north-west.....	117
Table 15 Summary of mean wave period obtained from LSA of random waves from north-east.....	117

1. INTRODUCTION

1.1. Background and motivation

From the dawn of time coastline protection and its proper management had been providing great benefits to cities and countries which were developing in its vicinity. Nowadays also harbours play strategic role, and have great meaning for both regional and national economies.

Port is a place which is sheltered from severe sea conditions, equipped with devices used for the transshipment and storage of cargo, and vessels and passengers service. To fulfil this task, the port must have an appropriately shaped water areas (basins and channels) to ensure an adequate manoeuvrability and protection against: waves, currents and ice actions. It must also have the appropriate port facilities - places and warehouse spaces equipped with roads, railways, cranes and other cargo handling equipment.

Coastal Structures such as breakwaters or quays are very important for coastline protection and for port construction. In order to design all these structures accurate knowledge of sea state and meteorological conditions and their changes is required. This can be very troublesome, because it often happens, that we do not have the enough amount of data or the conditions are too much complicated to proceed with analytical calculations or use previous experience. To deal with this problem numerical simulations are often used. Motivation of this master thesis is to gain profound knowledge of the process of numerical modelling of waves.

In addition to presenting the theoretical aspects of wave modelling and factors determining harbour design, in this master thesis a real life case is shown. Our area of interest is Ustka port, which is located in north coast of Poland in Pomerania region. Ustka is a summer resort and as a most of polish coast is characterized with a lot of gently sloped sandy beaches. Here is also located an estuary of Śłupia river where an old port is placed.

Maritime office in Słupsk did an analysis of market forecasts and revealed that, taking into account the high potential of this region, there is high demand for a port expansion. It should be noted, however, that Ustka is a summer resort and investments in facilities of this type do not increase the attractiveness of tourist resorts. To reconcile the recreational character of Ustka with the possibility of industrial development, the authorities decided to build a new port and divide its functions between new and existing object. Four different breakwater layouts were prepared, from which the final one must be chosen. The purpose of this thesis is to choose the layout which provides the best wave climate inside the harbour, such that it will not affect safety of moored vessels and provide acceptable conditions for cargo handling operations.

The aim of the current research is to prepare a numerical model representing wave transformation from the offshore conditions to the coastal zone, their propagation into the harbour basin and action on structures using MIKE 21. MIKE by DHI is a powerful tool able to utilize flexible mesh and contains several modules designed for preparation of bathymetry data and calculating wave conditions at required time steps using both spectral (SW) and Boussinesq wave (BW) models. After discussion and comparison of the results for few breakwater layouts tested, the best option will be chosen.

1.2. Structure of the Thesis

Chapter 2 describes current situation at Ustka site, giving the readers necessary background knowledge about existing port structures and challenges with regards to wave conditions, predicted new functions and demands and proposed breakwater layouts. Chapter 3 discusses factors affecting design of new ports. Chapter 4 describes the state-of-the-art in the field of wave modelling and explains the basic equations of both the Spectral Wave (SW) model and Boussinesq Wave (BW) model. Chapter 5 shows the model setup for the simulation conducted and outlines all the available input data. This chapter consists of the short introduction discussing the approach and two subsections describing both models prepared in the research. Afterwards, in Chapter 6 the results are shown, compared and discussed. Chapter 7 summarizes and concludes the work done and gives some recommendation for future research.

2. PORT OF USTKA

2.1. Area description and history

Port of Ustka is located in Ustka as shown in Figure 1. Ustka is a town in the Middle Pomerania region of north-western Poland. Ustka is located on the Coast Słowińskie, at the mouth of the river Słupia to the Baltic Sea. It is a port city and a health resort. According to data from 31 December 2014, the city had 16 056 inhabitants.

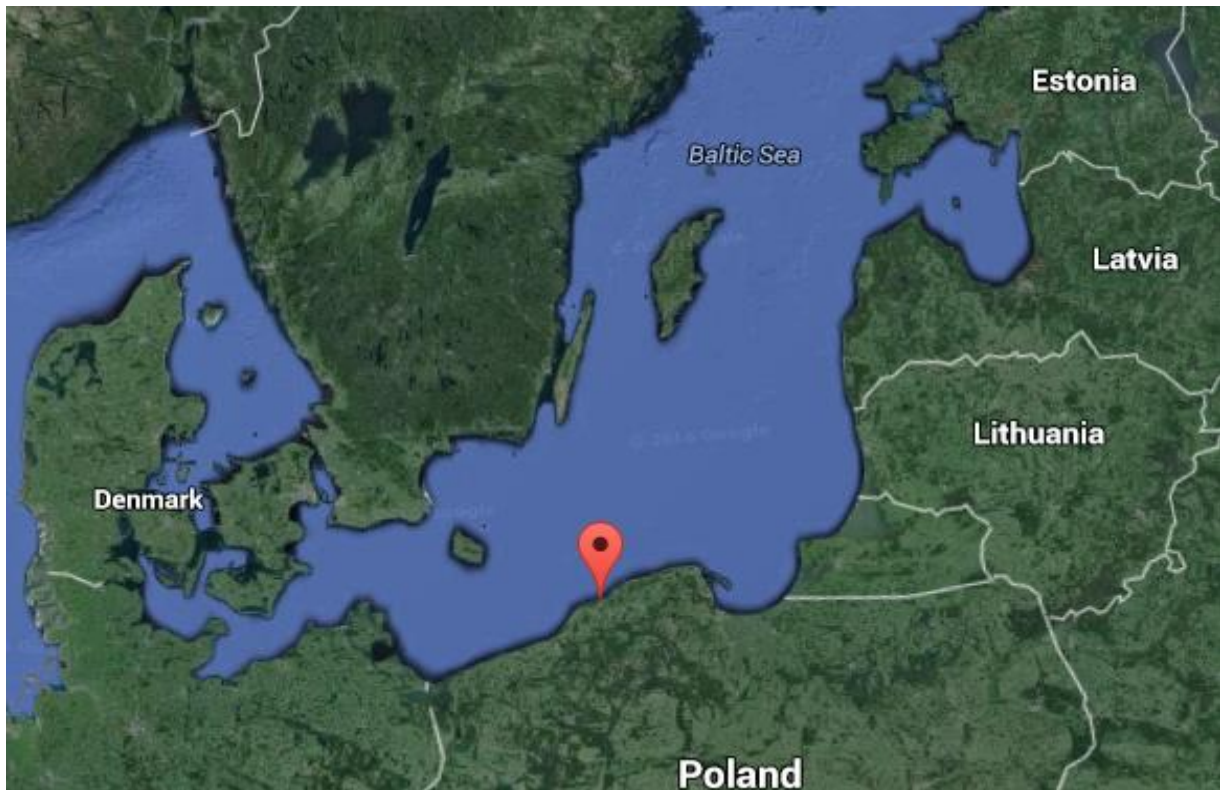


Figure 1 Location – Harbour in Ustka (Source: Google Earth)

The bathymetry of the Baltic Sea in the region is uniform, the bottom is little sloping. Moreover, approximately 45 km from Ustka there is very shallow area (8-20 m) called Słupsk Bank. It is part of the Polish Exclusive Economic Zone and is best known for its gravel deposits, yielding nearly 3,000,000 m³ of gravel during 1985-2003. More information can be found in the report by Uscinowicz (2003). Słupsk Bank is also the site of interest for the Polish government as a proposed location for a new offshore wind farm.

There are two beaches in Ustka. The Eastern Beach and the Western Beach, divided by the river Słupia. The Eastern Beach is more prone to abrasion. The maintenance of that beach, which after the winter storm season becomes very narrow, is one of the considerable expenses of Ustka authorities. The Eastern Beach is signified by high sand cliffs. The Western Beach is flat. Figure 2 shows the coastline of Ustka and the coordinates and breakwater layout of the existing harbour.



Figure 2 Location - Port in Ustka with coordinates (Source: Google Maps)

First information about a Port of Ustka is from the 14th century. Ustka and surrounded area were under the jurisdiction of Duchy of Pomerania. It was a small settlement consisting of a little more than fifty buildings. Despite its small size, Ustka had a strategic meaning for Słupsk. This was because that the shopkeepers and rich tradesmen from Słupsk were developing their businesses using this harbour. The main export commodity was farm products (crops), smoked salmons, local beer but also more important wood and amber products. The most common imported products were salted herring from Sweden, French wine and salt from Kołobrzeg. Ustka returned to the Polish lands after II World War. In 1948 the highest ship traffic was reported. The main export raw material was coal. Many vessels from Scandinavia were sailing there to buy it. In those times the harbour was also known as a place where a renowned shipyard was located. Local shipyard produced rescue boats made of synthetic material and fishing boats that were exported to Mexico, France or even Vietnam. Unfortunately, industrial activity did not last long, and as a result of political change the industry collapsed and fishing became the main activity at the port. More information about history of the Ustka can be found in document prepared by Brzóska et al. (2011).

2.2. Current situation and technical problems

The renovations and modernizations of the existing port have changed its original geometry. Current layout is obtained after works that were conducted in 2004 and 2014. Entering the harbour is possible thanks to the approaching channel with a length of 926 m, width of 60 m at the bottom and the depth of 8 m - see Christow (2007). Port entrance with the width of 40 m allows for entry of yachts at sea state up to 5 (wave heights between 2.5 to 4 meters) Internal harbour basins are sheltered by two concrete breakwaters. The eastern breakwater with a length of 318 m is founded at the depth of 4.4 m and ends with a head which is 15 m long and founded at the depth of 6.0 m. The western breakwater with a length of 416.8 m is

founded at the depths varying from 3.3 to 1.6 m and ends with a head which is 14.8 m long and founded at the depth of 5.5 m. Exterior walls of the abovementioned facilities have energy dissipating layer made of rip-rap and tetrapods. Movement of the vessels inside the harbour is carried out using internal channel with the length of 1250 m, width of 24 m and depth of 5.5 m. This is also the depth of the turning circle with the diameter of 67 m, which allows vessels to turn before berthing. The layout of all the described facilities is presented on Figure 3. More information about navigation in Ustka can be found at Sailing Poland (2016).

Apart from aforementioned facilities of port infrastructure, inside port in Ustka there are basins. Heading from the entrance to the port towards the south firstly one meets the coal basin, with the area of 9 540 m². It is located on the west side of the river and surrounded by five quays: Łabskie, Elbląskie, Puckie, Sopotkie and Helskie. Next to it, a new constructed fishing basin is located. At a distance of approx. 600 m from the entrance to the port on the east side of the river is winter basin, used by fishing vessels. On the opposite side to it, on the west side of the river there is renovation basin situated perpendicular to the river. Its width alters from 20 to 40 meters. The most advanced to the south is sediment basin with the area of 13 240 m². Its depth varies from 6 to 6.5 m. It includes the following quays Swarzewo, Oksywie, Karwia and Kuźnice. In the eastern part there is also a shipyard. Detailed dimensions of port facilities have been presented in document prepared by Bobin (2012).

As it was mentioned before, nowadays the harbour in Ustka handles only fishing boats, sports yachts and tourist ferries. In order to provide development of the city and the whole region it is necessary to modernize existing technical infrastructure of the harbour. At this point it is very important to note what is the technical condition of existing facilities, and also the malfunctions or failures, which occurred recently. The ability of detecting structural defects is very important for every engineer. Basing on the previous experience one can prevent a new design from replicating of the same mistakes, thereby can create a construction that is more durable and resistant to the loads acting on it and, what is not less important, cheaper in exploitation.

Apart from the dimensions of the harbour basins and approaching channels, another factor that makes further port development and handling larger vessels impossible are quays. Based on data from Brzóska et al (2011) it can be stated that the total length of the harbour quays is 2731 m which is insufficient at the current and target port usage. It is worth pointing out, that the quays located near the mouth of the river are also prone to failure and the stability problems because of intense filtration of the overtopping water. During storm surges increased water level is caused by high and long waves entering the harbour and obstructing free water flow from the river which results in the rise of water level.

Report made by Bolt et al. (2015) brings a lot of valuable information on the technical condition of the Pilot quay. At the beginning of 2015 water levels rising up to 5.9 m during a storm were recorded. This resulted in failure of the Pilot quay (item no. 3 in Figure 3) later in February that year. This quay is located between eastern breakwater and Kołobrzeg quay and is a part of an estuary of Słupia river. It is open quay construction with arc shape, founded on wooden piles, reinforced with steel piles with the diameter of 30 and 60 cm and sheet piles G62. The reason for such a diversity are reparation works mentioned before. The whole upper edge is connected by reinforced concrete beam with a trapezoidal shape which is 1.7 m high, 1.2 m wide at the bottom and 0.6 m at the top. In the geotechnical evaluation ordered by Maritime Office in Słupsk it was revealed that assumed design water level of 5.09 m was exceeded repeatedly. Many omissions and faults during renovation works were stated as well.

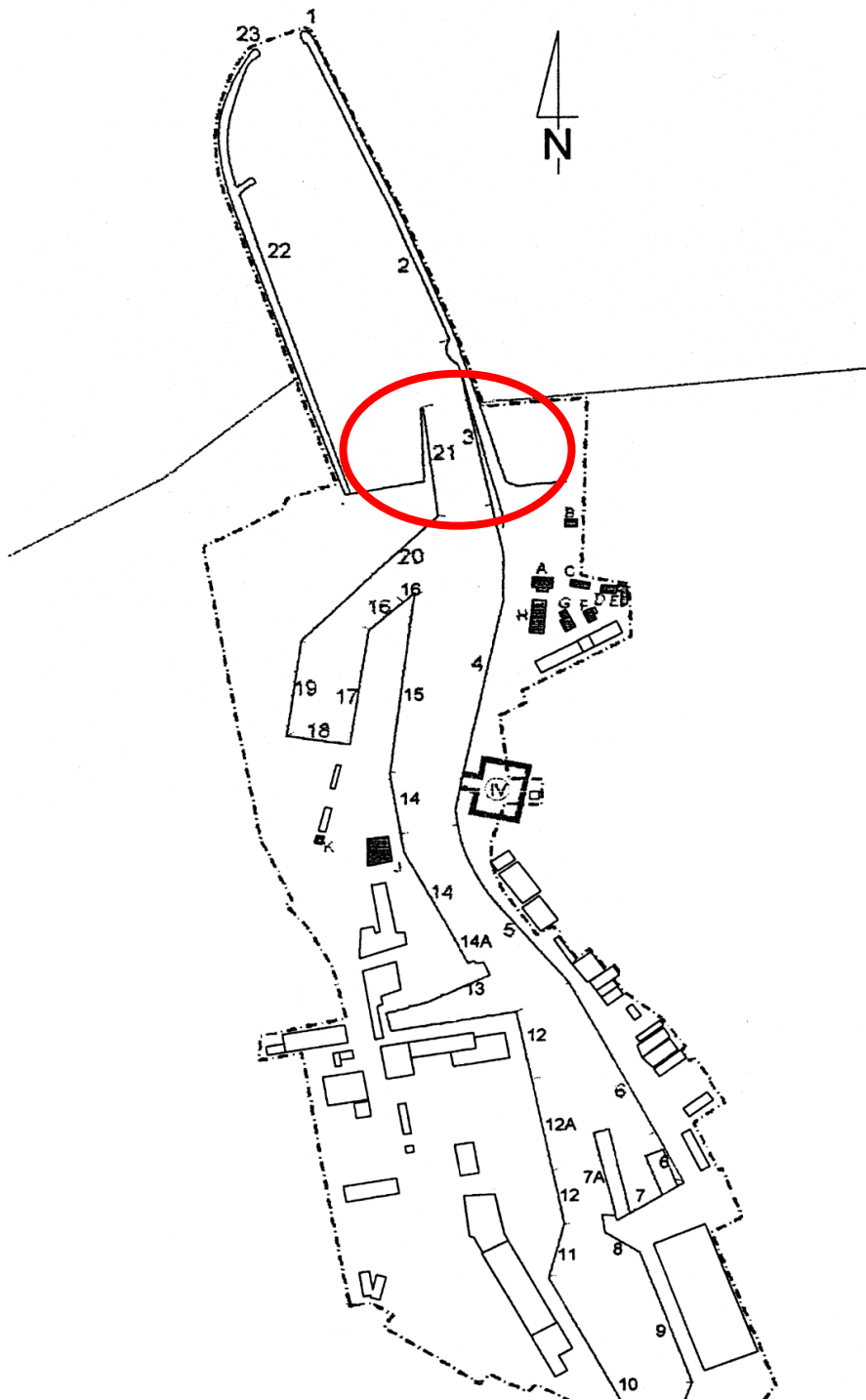


Figure 3 Plan of the current port in Ustka. Pilot Quay marked with red ellipse.

Maritime Office Hydrotechnical objects: 1. Head of the eastern Breakwater (15.0 m); 2. East Breakwater (318.0 m); 3. Pilot Quay (155.5 m); 4. Kołobrzeg Quay (301.0 m); 5. Słupsk Quay (181.0 m); 6. Lębork Quay (151.5 m); 14. Władysławowo Quay (86.5 m); 16. Łeba Quay (41.5 m); 17. Elbląg Quay (111.0 m); 18. Puck Quay (55.2 m); 19. Sopot Quay (98.6 m); 20. Hel Quay (155.4 m); 21. Hel Groyne (99.5 m); 22. West Breakwater (416.8 m); 23. Head of the western Breakwater (14.8 m); Maritime Office Buildings: A. Port Captain Office; B. Lighthouse; C. Bunker; D. Warehouse, Manufactory; E. Garage, Storehouse; F. Warehouse; G. Boiler Room; H. Custom Office; J. Warehouse 53; K. Smithy. Other users: 6. Lębork Quay (Shipyard) 44.0 m; 7. Shipyard – Yacht Quay (66.6 m); 7A. Shipyard - Pier (87.0 m); 8. Shipyard - Swarzewo Quay (78.0 m); 9. Shipyard Oksywo Quay (120.0 m); 10. Karwia Quay (166.0 m); 11. Kuźnice Quay (50.5 m); 12. Rozewie Quay (120.0 m); 12A. Community - Rozewie Quay (95.0 m); 13. Constructing Basin (235.5 m); 14. Army Władysławowo Quay (60.5 m); 14A. Władysławowo Quay (39.0 m); 15. Army - Darłowo Quay (163.0 m); 16. Army - Łeba Quay (13.5 m).

2.3. Demands and planned functions of the new harbour

One of the critical factors that have a significant impact on the location, the geometric parameters of the harbour entrance and also the arrangement of basins and channels is the nature and function the planned harbour. Once the functions are known one can assume what type of vessels will use its service and thus choose the design ship, based on which geometry and layout of the port facilities can be decided. Due to the limited size of ships able to enter the old port (Length of 58.0 m, width of 11.5 m and depth of 4.5 m) and aesthetic qualities it was decided that the old port will handle smaller units, such as fishing boats, sports boats and small tourist ferries.

For the newly designed part of the Port of Ustka three main functions are assumed. These are the following:

- The trade function with a focus on handling general cargo ships. For this purpose, it will be necessary to make a new harbour basin, along with the waterfront, where there will be an area for warehousing and storage of goods, together with the necessary equipment for loading and unloading ships.
- The technical useful function of shelter for ships constructing and servicing the offshore wind farms. At a distance of 16 miles northward of Ustka there is Słupsk Bank which is a shallow area of approximately 1000 km² with the depth varying from 8 to 20 m. An offshore wind farm is to be built there. When this investment will be carried out a place for storing parts of the wind turbines and for mooring ships constructing the farm will be needed. Specialized vessels (such as jack-up heavy lift vessel), even though they are not the largest vessels calling at ports, but because of the unusual width of the hull, draft or limited manoeuvrability must be taken into account when designing the width of the entrance to the port and geometry of the basins.

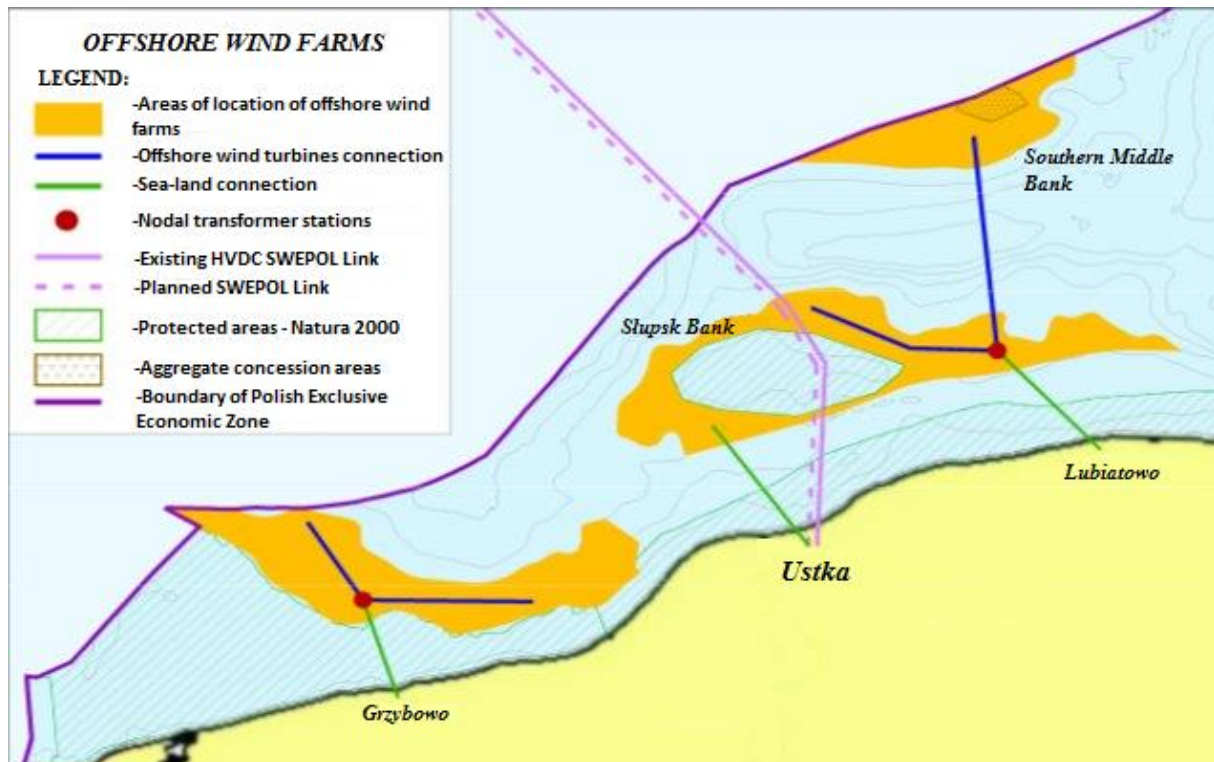


Figure 4 Southern Baltic Sea areas proposed for installation of maritime wind farms (Source: Renewable Energy)

- The military function: because of the close proximity of the military areas and training grounds, military manoeuvres and trainings take place frequently in this region. Unfortunately, due to shallow water and small dimensions of the existing harbour basins ground forces are not able to train together with the navy. After the new harbour is built this will change and will have positive influence on Polish defence forces.

2.4. Proposed breakwater layouts for Ustka new harbour

For the purposes of this Master thesis, Maritime Office in Słupsk presented four suggested concepts of breakwater layout for the new port of Ustka, see Fig. 6-9. In order to improve the protection of the harbour entrance, extension of the old breakwater and reinforcement of the armour layer with additional riprap is proposed. Suggested concepts differ with the location, geometry and way of construction. The three types of construction proposed are:

- a rubble mound breakwater with the width on the top of 11.9 m. Armour layer made of stone is 4.4 m thick. Below there is 2 m thick underlayer and 1.2 m of filter layer. It is protected at the bottom by a toe with a height of 2.5 m,
- a breakwater made of prefabricated caissons filled with soil, with additional wave-absorbing perforated chamber,
- a breakwater made of two sheet pile walls filled with soil and topped off with reinforced beam. From the sea-side breakwater is protected by rock embankment with a slope of 1:1.5 and armoured by accropode blocks.

For this thesis, the third type is chosen for all layout variants (see Figure 5).

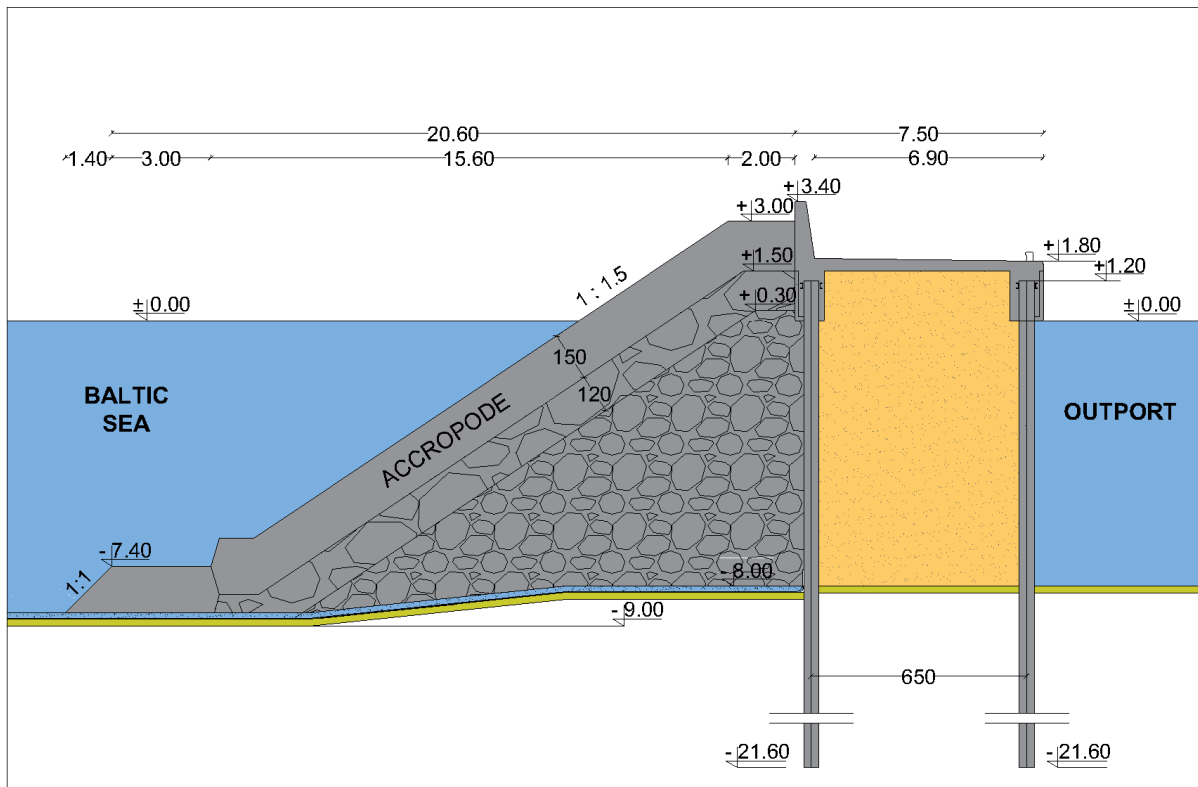


Figure 5 The cross section of the chosen breakwater type. (Source: Maritime Office in Słupsk; Designer: Borodziuk A.)

As it was mentioned in subsection 2.3, new harbour is supposed to have two main functions: military and technical, as a base and storage facility for construction of an offshore wind farm located at the nearby Słupsk Bank. In order to ensure a proper depth, enabling safe manoeuvrability both for military ships and vessels servicing and constructing offshore wind turbines such as heavy jack-up lift ships, whose maximum draft reaches 6.0 m, depth of the new harbour basins is assumed to be 8.0 m. Each of the suggested layouts is described below.

First concept is shown on Figure 6 and involves the realization of a new western Breakwater with a length of 1200 m at a distance of 980 meters from the old one. This would result in the creation of an outport with the area of approximately 480 000 m². Inside there will be a turning wheel and two smaller basins: military and trade, with the width of 100 m and closed, concrete quays with a total length of 1118 m. In addition, between trade basin and old western breakwater, quay with a length of 365 m will be available. In order to shelter the entrance of the old harbour an extension of 50 m of the eastern breakwater is provided and 160m long detached breakwater.

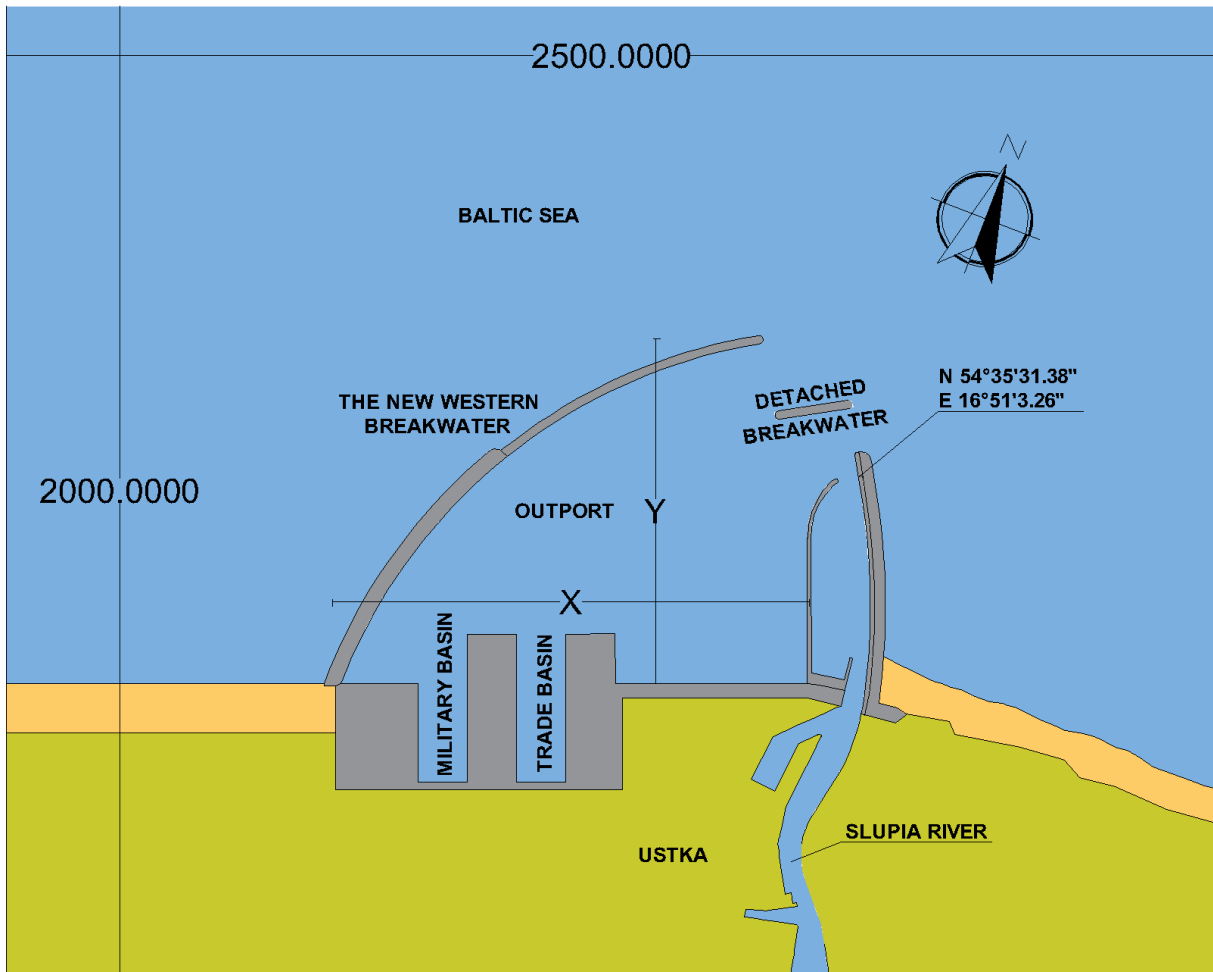


Figure 6 Proposed layout no. 1. (Source: Maritime Office in Slupsk; Designer: Borodziuk A.)

In the proposed layout no. 2 the most important difference is the abandonment of the detached breakwater, which was sheltering the entrance to the old harbour. Its functions will be partially taken over by modified geometry of the western breakwater. The part which is parallel to the shore will be placed 190 closer to the land and extended by 188 m towards east. Described arrangement is presented on Figure 7. This approach will create an outport with an area of 327000 m². The length of quays will be reduced and will amount to 832m. Port entrance will be reduced and equal to 80 metres.

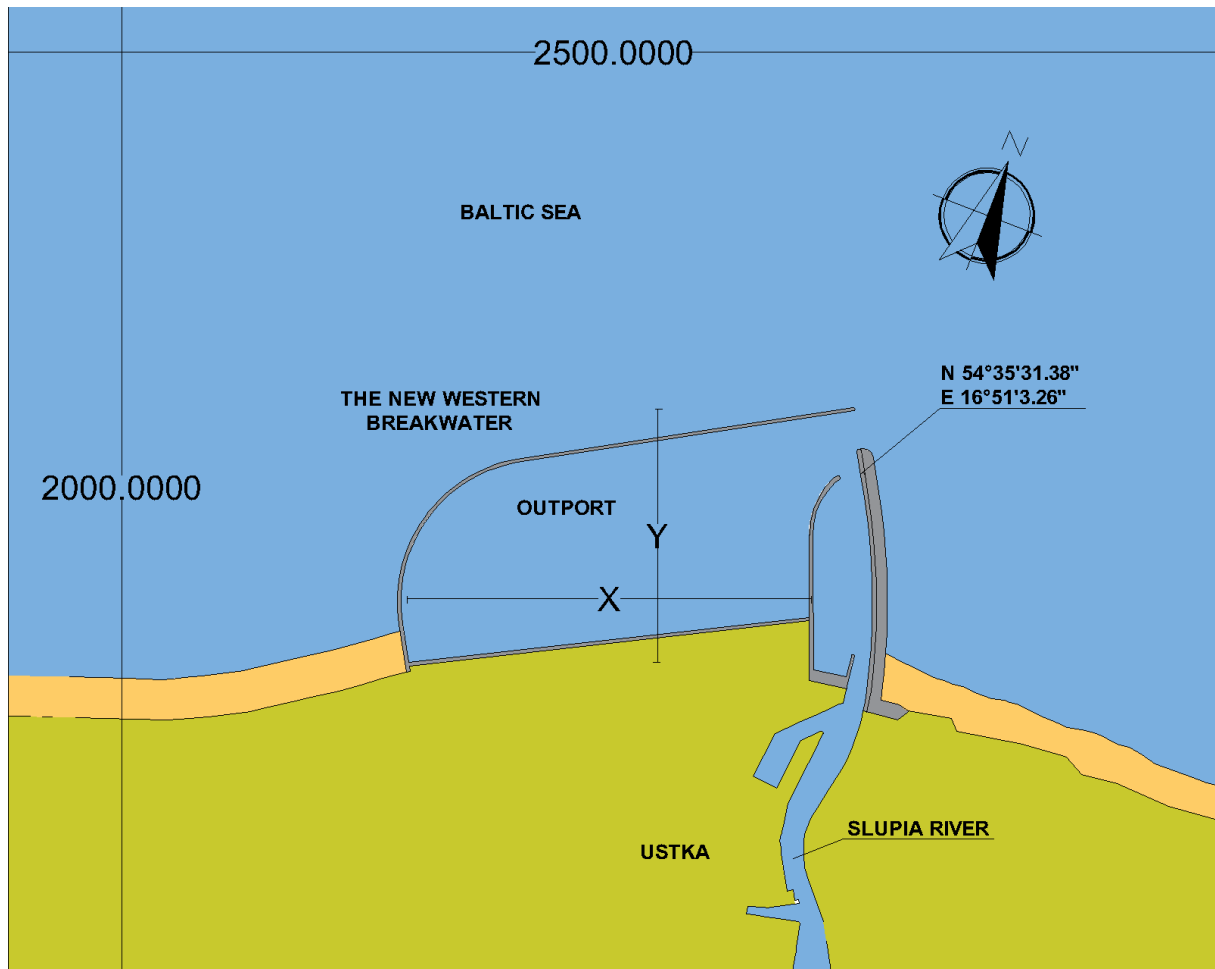


Figure 7 Proposed layout no. 2. (Source: Maritime Office in Słupsk; Designer: Borodziuk A.)

The third concept is only a slight change in the layout no. 2. The distance between the old and the new western breakwater is reduced to 475m and the new breakwater is moved away from the shore line about 20 meters towards the open sea. Thanks to that, the entrance is broadened up to 100 m. Another advantage is the use of natural seabed topography. Moving about 20 meters away from the shoreline results in about 1-1.5m additional depth. This will reduce the amount of dredging works needed. The part of the breakwater parallel to the shore is shorter as well, but still protects the old harbour entrance. With such a geometry, the basin created will be 213 000 m² and the length of available quays will be 470m. Layout no. 3 is presented on Figure 8.

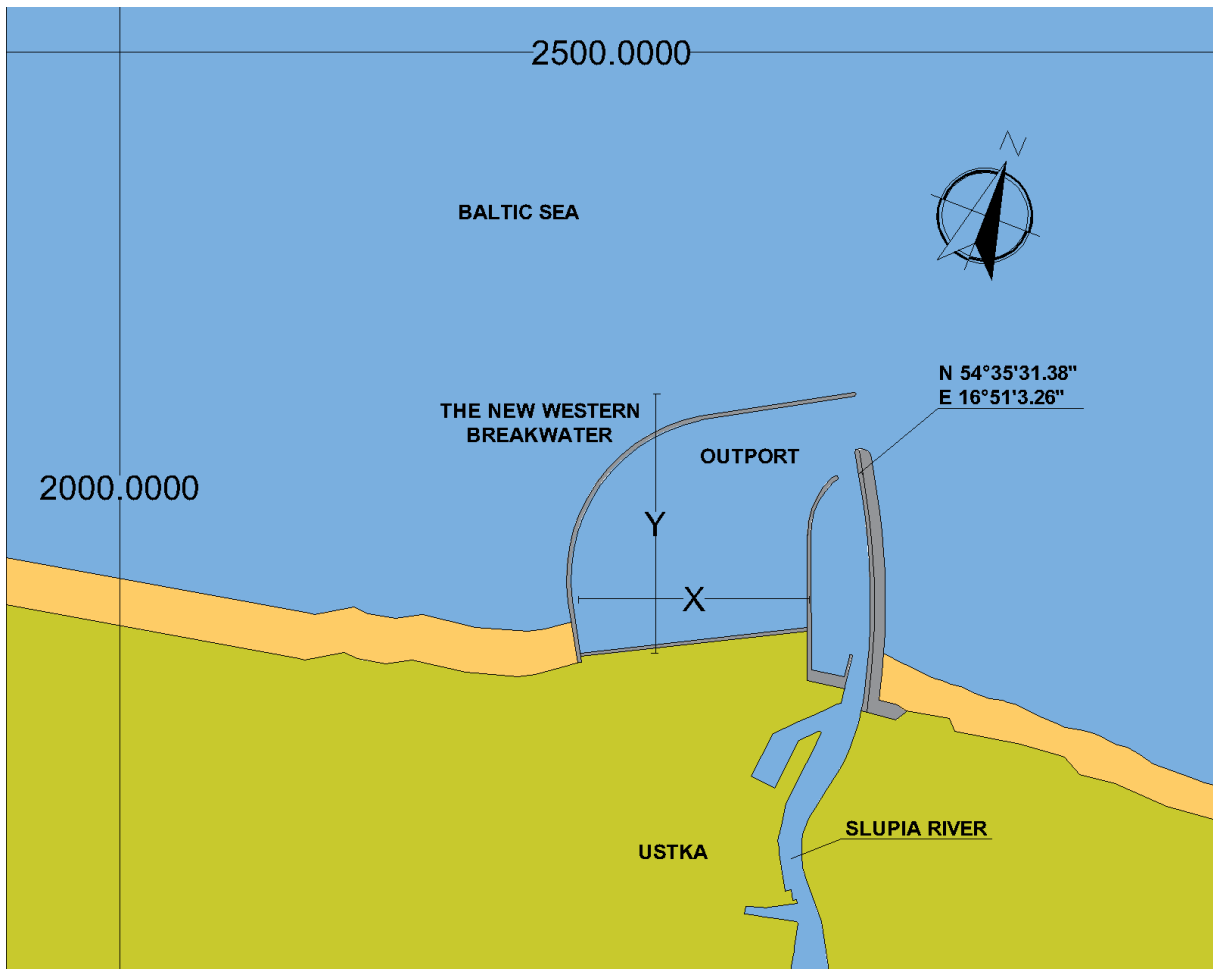


Figure 8 Proposed layout no. 3. (Source: Maritime Office in Słupsk; Designer: Borodziuk A.)

The last proposition is a modification of the third layout. The distance between breakwaters remains the same. The part parallel to shore is 100 metres shorter and 100 metres further into the deep sea, but the idea of the detached breakwater is introduced again. This time it is assumed to be 322 metres long. The harbour entrance will be 90 m wide, and created basin will have 223 000 m². The total length of the quays remains unchanged, and will be equal to 470 m.

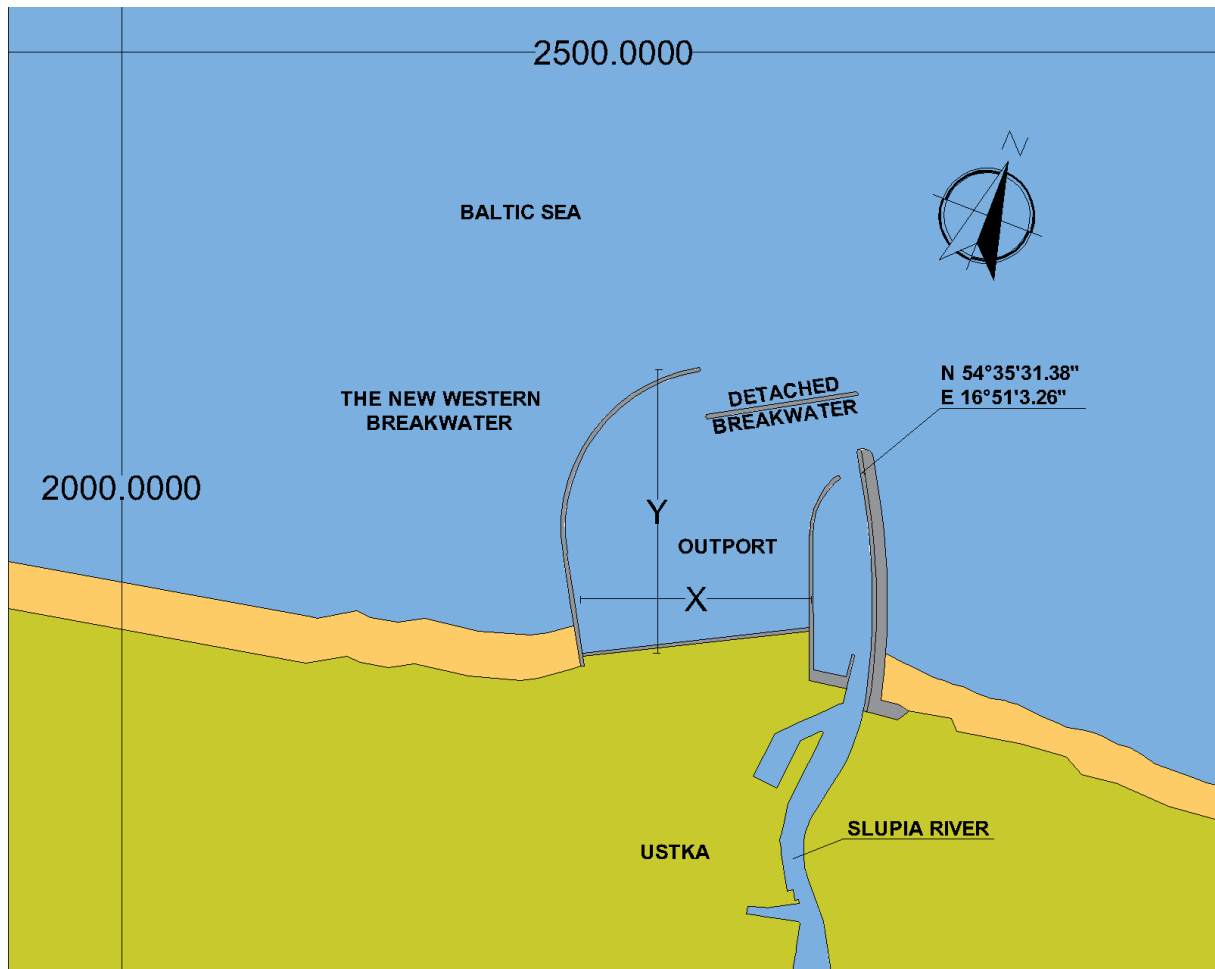


Figure 9 Proposed layout no. 4. (Source: Maritime Office in Słupsk; Designer: Borodziuk A.)

Comparison of the geometrical properties of the layouts described above is shown in the Table 1.

Table 1 The geometrical properties of the proposed layouts.

Layout	Western breakwater		Length of detached breakwater [m]	Outport area [m ²]	Quay length [m]	Entrance width [m]
	X [m]	Y [m]				
1	980	710	160	480 000	1483	143
2	833	520	x	327 000	832	80
3	475	540	x	213 000	470	100
4	475	640	322	223 000	470	90

3. PORT DESIGN

Port is a place, where various processes take place. Each of them requires certain conditions to be satisfied. Port geometry, and layout of the structures has to provide easy manoeuvrability inside the basins and channels and shelter from harsh sea conditions like waves or currents. The wave or wind induced movement of moored ships and boats should be small enough to ensure the safety of the mooring structure and cargo handling. In cases where this is interrupted, the ship expenditure becomes a large waste of money.

Designer responsible for designing new harbour should be aware of all those challenges and propose a layout, that will meet all the above mentioned criteria. Large and massive protective structures such as breakwaters, and wide and vast channels and basins will always fulfil the requirements, but there is one more factor that makes work of the engineers around the world so demanding and difficult. This is of course economic feasibility of the design. In order to please the investor as well as create durable and practical design engineer has to find a reasonable balance between the costs and the efficiency.

The purpose of this chapter is to look into the various factors and their meaning and importance to harbour workability. In order to systematize our research, it was divided into three subsections dealing with technical, environmental and economic aspects respectively.

3.1. Technical requirements

Technical aspects which have to be taken into account can be divided into two groups. One is associated with designing port geometry and layout of the structures that provide sufficient spaces and conditions allowing for a fairly good and uninterrupted operability. Second one deals with preparing appropriate design of the structures, that have to be safe and result in reasonable construction and maintenance costs.

There are several factors that determine the geometry of a harbour. One of the most important factors is navigational safety. To ensure this all the parts of the port, such as channels, entrance, basins should have appropriate dimensions depending on the size of the design ship, which is usually the biggest vessel, or the vessel with some unusual dimensions or navigational requirements. A large number of publications can be found, for example Thoresen (2010), where recommended approach for choosing the geometry of a harbour is discussed.

Channels should be located in such a way, that the impact of the prevailing wind and crossing currents will be reduced to minimum. Areas in which channels are located should be as deep as possible, and should not be exposed to excessive siltation, so that the amount of initial and maintenance dredging is as small as possible. Channel should be straight in best case, and its width should take into account, apart from the beam of the design ship, the allowance for some yawing movement caused by bank suction due to the asymmetrical flow of water round the ship. To counteract this negative phenomena additional bank clearance should be added. In total bottom width of the channel should be 3.6-6 times larger than beam of the design ship for the one-way traffic, and 6.2-9 times larger for two-way traffic inside the channel. When bends are unavoidable, channel should be broadened in the areas of curves, and there should be kept sufficient distance between two consecutive curves.

The entrance should be located on the leeward side of the harbour, or protected by overlapping breakwater. It is recommended, that the width of the entrance is not larger than necessary to provide the possibility of entering and navigating safely. As a rule of thumb the width should be around 0.7-1.0 of the design ship's length (Thoresen 2010).

Harbour basins have to facilitate berthing, turning, anchoring, grounding (in case of emergency), and provide an area for vessels to shelter temporary in case of harsh conditions outside. If the harbour handles both large vessels and small ships, boats or yachts it is reasonable to divide it into two parts. Inner, shallower part should receive smaller units, while all the large ones should be handled within the outer part. Turning area should be located in the centre of designed basin and its diameter depends on the length of the ship, its manoeuvrability and the time that can be spent on each turning manoeuvre. The anchorage areas are used mainly by the smaller ships waiting for their turn to berth or protecting themselves during periods of bad weather. It should be located near the main harbour areas, but away from the main harbour traffic. It was also mentioned in Thoresen (2010), that in case of emergency it is important to provide a grounding area, where damaged vessel can be safely grounded in order to prevent its sinking or for example oil spilling.

One can distinguish four main natural loads that have to be taken into account during designing quay facilities. These are wind, waves, currents and ice. All of those mentioned forces have different characteristics of action, source, and effect. To ensure proper resistance and durability of the construction for whole designed lifetime it has to be considered that they can occur individually or as a combination of each other.

Wind

To classify wind conditions Beaufort scale is commonly used where the wind is divided into twelve levels. Each level corresponds to other scope of wind velocity. Values shown in Table 1 (Huler (2004)) are mean wind velocity. It means the velocity which is recorded at the height of 10 meters above mean sea level as an average of 10-minute-long measurements of the speed and direction.

Table 2 The Beaufort wind scale [Huler (2004)]

Beaufort	Description	Velocity [m/s]
0	Calm	0.0-0.2
1	Light air	0.3-1.5
2	Light breeze	1.6-3.3
3	Gentle breeze	3.4-5.4
4	Moderate breeze	5.5-7.9
5	Fresh breeze	8.0-10.7
6	Strong breeze	10.8-13.8
7	Near gale	13.9-17.1
8	Gale	17.2-20.7
9	Storm gale	20.8-24.4
10	Storm	24.5-28.4
11	Violent storm	28.5-32.6
12	Hurricane	32.7-

Despite the fact, that wind effects on harbour operations are more important than effects of wave, there is not much that can be done to decrease wind speed in harbour area, and only designing appropriate mooring system can provide safety during harsh conditions.

Waves

Classification of waves can be found in a lot of publications. Usually they are divided in terms of two criteria: origin and the place of occurrence as shown below (see Thoresen 2010)

Origin:

- i) **Locally generated wind waves.** Waves generated by wind that is acting at the sea surface surrounding port site or even inside port.
- ii) **Ocean waves (swell).** Waves generated also by blowing wind, but are created in the deep ocean not in close proximity to the harbour. It can happen that at the time the waves reach the port the wind will change direction or even stop blowing and there will be no chance to feel or observe it.
- iii) **Long waves (e.g. seiching).** These are waves with very long period from 30s up to the tidal period 12h 24min. Usually are found in enclosed or semi closed basins, fjords or bays. Can be induced by changing atmospheric pressure along bay.
- iv) **Waves from passing ships.** Created by moving object e.g. sailing ship or launching ship. Can have a significant meaning in areas where high waves are not expected.
- v) **Tsunami.** These are very long waves generated by sudden forcing such as earthquake, volcano eruption or landslides ending up in the ocean.

Place of occurrence:

- a) **Deep-water waves.** Waves with ratio $\frac{d}{L}$ (where d is a water depth and L is a wavelength) is higher than 0.5.
- b) **Intermediate-water waves.** Waves where $\frac{d}{L}$ is lower than 0.5 and higher than 0.05
- c) **Shallow-water waves.** Ratio $\frac{d}{L}$ is lower and equal to 0.05.
- d) **Breaking waves.** These are waves in which the forward crest velocity is higher than the velocity of propagation of the wave itself. Usually it occurs in deep water when $L < 7H$ (where L is a wavelength and H is wave height) and in shallow water when $\frac{d}{H}$ is equal to 1.25.

Fig. 10 below shows basic waves parameters. L means wavelength, H is wave height and d is water depth.

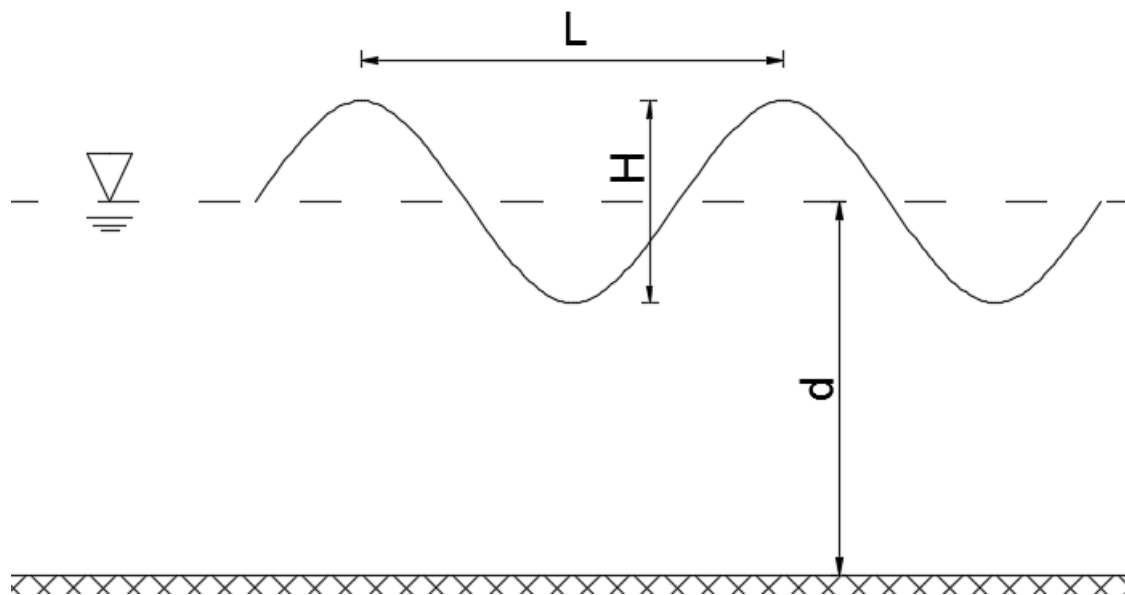


Figure 10 Basic wave parameters.

Three main parameters that define wind-generated waves are length, period and height. All three depend on the fetch – the distance the wind blows over the water surface, velocity and direction of the wind. Wavelength is a distance between two neighbouring wave crests or wave troughs or simple between two particles being in the same phase. Wave period is a time needed for passing successive wave crests through a given point. By wave height, we understand perpendicular distance between wave crest and wave trough. Wave height may be defined in many ways. For example, H_m is an arithmetical mean value of all wave heights that have been recorded during period of time and H_s is a significant wave height that means it is the arithmetical mean value of the highest 1/3 of the waves. It is worth to notice that waves generated in shallow or intermediate water depth are smaller and shorter than waves generated at deep water.

Port designers should consider two types of waves: those generated locally and in the open ocean. There is usually a combination of those two sea states and it is taken as a root of the sum of squared local and ocean wave heights. Even if the breakwater is well-designed, inside port basins both short and long waves can occur. Those two types of waves have different characteristic and result with different impact on moored ships. For example, small ships such as sport yachts, fishing boats or small ferries are vulnerable to waves with short period and in the other hand waves with long period may affect almost all vessels. Here ratio between wavelength and ship length plays an important role. Waves that are longer than the vessel will result with higher movement and forces on mooring system. As it is described in Chapter 4 by Thoresen (2010), waves with period shorter than 6-8s generates acceptable conditions for mooring but much more longer waves – 20s periodic with length in range 5000-8000m will generate high movements of large vessels. This is because this type of waves has similar frequency to the natural ship frequency what can cause resonance phenomena.

Below in Table 2 acceptable and suggested threshold wave heights for cargo handling operations are shown and, for comparison, in Table 3 maximum wave heights for different

types of ships are given. Basing on data from Table 2, for medium cargo ship with displacement less than 50 000 GT (50 000GT is equal to 44 000 dwt see Takahashi et al. 2006), permissible wave is equal to 0.5m, that means it should not cause hazardous movements. But according to Table 3 for similar cargo ship with displacement less than 30 000 GT maximum wave height reaches up to 0.7m. It is easy to see that values showed in table 2 and 3 are different. The reason of that is what is taken as a benchmark: permissible wave height for a vessel or for handling system. Summing up, not only port designers but also people responsible for port operations have to keep in mind that requirements for mooring and loading-unloading system may be different than those for ships.

Table 3 Reference Values of Threshold Wave Height for Cargo Handling Works [OCDI-2002]

Ship size	Threshold wave height for cargo handling works
Small craft (<500 GT)	0.30m
Medium/large ship	0.50m
Very large ship (>50 000 GT)	0.70 – 1.50m

Table 4 Maximum wave heights [Thoresen (2010)].

Ship at berth	H_s at berth
Marinas	0.15m
Fishing boats	0.40m
General cargo (<30 000dwt)	0.70m
Bulk cargo (<30 000dwt)	0.80m
Bulk cargo (30 000-100 000dwt)	0.80 – 1.50m
Oil tankers (<30 000dwt)	1.00m
Oil tankers (30 000- 150 000dwt)	1.00 – 1.70m
Passenger ships	0.70m

There is also one geometrical factor, that can be easily overlooked, and can cause disastrous effects. Every harbour being under certain conditions can exhibit water surface oscillations, that can cause significant damage to moored ships and port structures and, what is more, create undesirable currents inside the harbour. This can be induced by waves of specific periods or atmospheric pressure variations. These phenomena are known as seiches or harbour oscillations, and were investigated in many publications. When designing a new harbour, it is therefore very important to adjust the geometry in a way that will make occurrence of those oscillations so unlikely as possible.

Currents

There are many causes of currents in ports such as river flow, tidal effects, differences in salinity and temperature of water or wind transport of water masses. Prevailing currents can hinder the use of approaching channels and berthing of the ship. Like wind, currents cause additional forces on mooring system. In order to minimize the effect of current berth front panel should be oriented parallel to the main current direction. Since current forces depends also on the clearance beneath the keel additional water depth should be provided in order to avoid large forces on the ship and mooring system.

What is more, current affects not only the manoeuvrability of vessels, but can make it difficult to construct a port structure. High current velocity will make it extremely difficult to drive a sheet pile precisely or for the divers to work properly.

Ice

Ice impact on port activities is not thoroughly investigated, but there are effects that have to be taken into account when designing a port in areas where the temperature drops below the freezing point for a certain period of the year. Ice can seriously impede or even prevent the navigation. Furthermore, it results in both vertical and horizontal forces on the structures. The horizontal forces are mainly due to pressure of drift ice pushed by wind and current. It is worth to notice that thermal expansion of the ice can cause in very high horizontal force especially in closed basins. Vertical forces, on the other hand, arise when firmly frozen structure is subjected to a tidal water level variation. This may be problematic for structures with low deadweight (e.g. wooden piles). In order to prevent structures from freezing installation of the additional equipment, such as compressed-air bubble plant, can be required.

3.2.Environmental aspects

Above few impacts on designed structure caused by nature were listed. However, as well as during performance of land structure or even more during performance of the facilities in the coastal zone one should be aware of the effects of the construction on the environment. Particularly worth noting is the negative influence on the environment because repairing the damage is associated often with enormous costs and sometimes may be even impossible. In this section several processes which the designer should have in mind will be presented.

In close proximity to the coastal area a lot of imperceptible processes take places that have effect on bottom topography and shape of the beach. A good example is a sediment movement caused by current or waves propagation. In case when the shape of the coastline is going to be changed by a structure also those processes will not remain unchanged. Interference and distortion of the natural movement of sediment may result in phenomena such as: blockage of river mouths, shallowing of the port basins and channels or beach erosion. Sawaragi (1995) took time duration of such changes as a criterion and classified erosion in two groups:

- a) Long-time beach erosion that continues for several years. Construction process and the artificial devastation of the natural balance of sediment movement results in beach erosion where longshore sediment transport is important.
- b) Short-time beach erosion that continues for a week. It is caused by a presence of high waves generated by a low pressure system. Brings beach erosion and cross – shore (offshore and onshore) sediment movement.

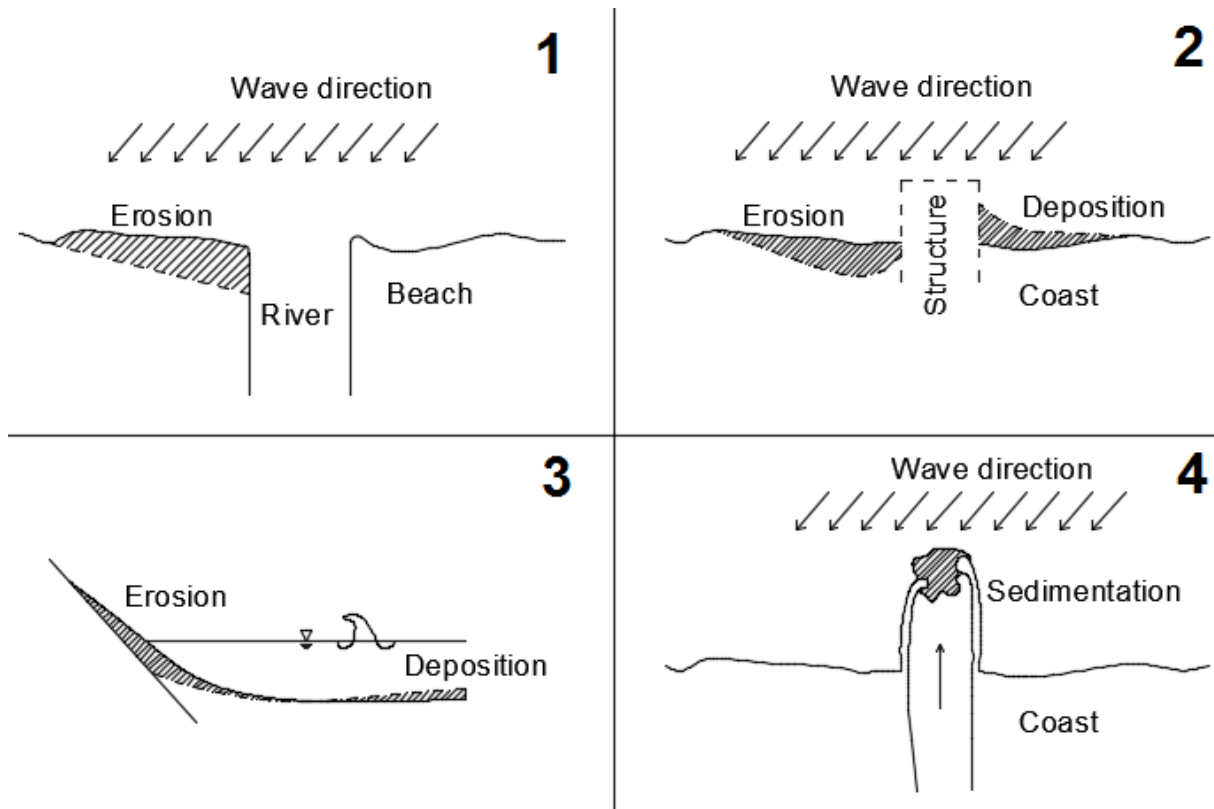


Figure 11 Sediment transport processes on the coastline. [Sawaragi (1995)]

Figure 11 shows processes that take place at the coast. First two depend on a longshore transport, third one shows deformation of the beach depends of cross-shore sediment transport due to high waves. The last one shows possible place of occurrence of high particles movement due to current on the head of breakwater and water flow from the river.

When talking about environmental aspects one aspect cannot be ignored. That is the presence and production of contaminants. It may happen during industrial works in the port that some amount of oil, solvent, chemical, and even heavy metals which pose a high risk of contamination can be released into the water. Moreover, some ports have a special shallow place where damaged and leaking vessels can settle on the bottom to avoid sinking. This operation creates also a risk of contamination. In order to ensure safety and reduce the risk of environmental contamination one should apply the appropriate procedures and regulations, moreover port should have properly designed water drainage system and sewage connected to municipal system or to a dedicated treatment facility.

Industrial activity, sewage and fuel from ship are not only one source of pollution. It is worth to notice that ballast water may be a threat to local fauna and flora. Organisms and different species of fishes transported from another part of the world released in area where are good conditions to procreation can ruin and displace local population of organisms. Also it may

happen that bacteria and pollutions will be transported with ballast water. Usually it has disastrous consequences for the local ecosystem.

There are more kinds and sources of pollutions and the environmental impact e.g. to those generated by ship we can add noise, vibrations and garbage produced during a cruise but it is not the main subject of this treatises. More detailed information were presented by Trozzi and Vaccaro (2000).

3.3.Economy aspects

After technical and environmental aspects, it is time for another very important aspect which is strongly connected to those two. Every time when construction is being designed, economic and financial features have to be taken into account. At this point it is necessary to mention the return period and structure lifetime that have significant influence on the cost. Return period is the average time between two incidents when the wave height exceeds or is equal to designed wave height. For simple technical or small structures, the designed return period should be equal to 50 – 100 years, usually it is 100 years. In case of structures where the consequences of failure are meaningless and human life is not threatened, the designed return period can be shorter (e.g. 25 years). Ratio between costs of construction and durability has to be balanced and deeply discussed because any investor will be willing to pay for it.

Construction and maintenance costs should always be estimated. It may happen that it will be more profitable to design construction that will need regular maintenance or repair work than a resistant and one with high durability. One has to remember that cheaper solution cannot result in decreased safety of personnel and surrounding areas.

Considering financial feasibility, one has to remember about future extension. This can be clarified based on an example of a container terminal. When designing the layout of the port and its basins space must be planned in such a way, that in the future as the demand for new storage and cargo-handling place will grow, the modernization and cessation of work of the whole harbour is not necessary, and construction works can be carried out exclusively in the parts intended for expansion. In the container terminals even appropriate container stack height affects the performance and capacity of the port. The same applies to the selection of cargo handling equipment. Depending on the assumed number of cargo handling operations suitable fleet of lifts and cranes should be selected (fork-lifts, reach-stackers, straddle-carriers, ship-to-shore cranes, RT or RM gantries). In large ports a system to manage the port is also introduced in order to optimize the work of people and machines, which helps to reduce costs, increase productivity, and thus will result in bigger profits.

Since approximately 35 methodical study of the financial feasibility of the project is available. Those studies and computer models which are based on it will not provide exact results but are very helpful for evaluation if project is good and worth for investment or if is not. Estimation of the economic feasibility is based on ratio between annual economic costs of the project and benefits from it. Usually it is prepared for next 20 years of life or even more. For port projects there is a main rule that the costs are high at the beginning and benefits result later. A good overview through economic and financial feasibility was presented by Agerschou et al. (2004).

3.4. Aspects covered in the master thesis

As taking into account all those above mentioned aspects is a challenging task for every consulting group preparing harbour designs it is impossible to investigate them all in one

master thesis. It is necessary to focus on one particular, narrow and detailed scope of factors that influence designed port layout. This master thesis will only focus on the technical aspects in terms of operability of the future Port of Ustka. Since the wave conditions seem to have a significant impact on the operability, it is just the waves inside the harbour basin that will be the subject of this analysis and criterion determining the best layout.

4. NUMERICAL MODELLING OF WAVES

In previous chapter various factors influencing the final layout and geometry of a harbour are mentioned. From all this different things, this master thesis will deal only with the wave climate inside the harbour. In order to make sure, that waves inside the harbour basins are not considerably disturbing operations, numerical modelling tools are widely used. Despite the facts, that well established software packages for wave modelling do exist and engineers have been using them in their work for many years, one cannot use such software packages as the “black box”. A qualified user of these software must know which processes are taken into account, what equations are solved, and what procedure is the software following while calculating the output values. The purpose of the following subsections is to describe briefly, but in sufficient detail, the state-of-the-art of wave modelling as well as give the scientific background of both modules used in this master thesis.

4.1. Wave modelling State-of-the-art

People has been trying for a long time to predict and calculate as accurate as possible how do the waves propagate and change when they reach the coastal zone. It is believed that the first attempt at operational wave forecasting was when the D-day operation (the landing operations on Tuesday, 6 June 1944 of the Allied invasion of Normandy in Operation Overlord during World War II) was prepared in 1944. Since then our knowledge and abilities have evolved a lot. It started with strictly parametric relationship between wind speed and significant wave height. Then, with the development of computers a road to much more complicated and time-consuming calculations was opened. In this way, the wave spectral model (abbreviated later as SW) was introduced and successively improved.

The basis of all SW models is the spectral action balance equation, which is discussed later in this chapter. The various generations of models differ mainly in the way of describing the source and sink terms, such as for example wind input, non-linear wave interactions, energy dissipation. In the first generation those source terms were not properly represented. Wind induced wave generation was described with the empirical equations and the energy dissipation was assumed by setting the universal upper limit for spectra densities. Furthermore, in those models non-linear quadruplet wave-wave interactions were not included. The second generation models tried to account for that by parametrizing these interactions. Nowadays, in the third generation models these relationships are described explicitly, with no restrictions regarding either spectra shapes or energy levels. That makes them much more versatile, but the computational power required to perform calculations is significantly higher.

An important drawback is the fact that all SW models are phase-averaging and compute only the energy of the waves. In cases where one deals with complicated geometry, for example in harbour or when the coastline and the bottom topography are not simple and change rapidly, usually more information about phenomena such as diffraction, refraction, reflection or wave breaking is needed. This kind of output is impossible to get from the ordinary phase-averaging model. In this task models based on Boussinesq equation work better. They are phase-resolving, which means that calculate the wave surface instead of energy spectrum. Despite the fact, that Boussinesq came up with his equations at the end of the nineteenth century, only during the last decades the Boussinesq wave models (BW) became gradually introduced into engineering applications. Only the final modifications allowed for overcoming the main restriction, limiting the applicability of the models only for shallower water and longer waves.

While the original upper limit of kd value (where k is wave number and d water depth) was set as lower or equal to one, currently the simulations for much greater values give accurate results. As the BW models are resolving the water surface, the mesh used while preparing the model has to have much higher resolution. That implies the need of more computational power and causes that BW models are commonly used to simulate waves in smaller scale than SW.

Apart from the two types of models described above, sometimes the construction is really complicated and interaction between water and structure or between water and air is important. CFD (Computational Fluid Dynamics) models can be then of great use. It was widely used in aircraft industry and now is more and more used in marine civil engineering. It is based on Navier-Stokes equations and gives us almost the full insight into water behaviour. It is also the most demanding among the all mentioned models.

All models described in this subsection are constantly being developed and give us more and more reliable and accurate output. Depending on the case, different model or combination of models can be used. In the case selected for this master thesis a combination of SW and BW models is used.

4.2. Theoretical background of the numerical models used in this master thesis

4.2.1. Spectral Wave model

As it is described by the developer: “MIKE 21 SW is a state-of-the-art third generation spectral wind-wave model developed by DHI. The model simulates the growth, decay and transformation of wind-generated waves and swells in offshore and coastal areas.” (DHI, MIKE 21 Spectral Waves FM, Short description). The most essential knowledge about this type of models together with some basic equations are discussed below.

There are two different formulations available when using MIKE 21 SW. On the one hand is the fully spectral formulation, which is based on the wave action conservation equation, and the other option is directional decoupled parametric formulation where that equation is parametrized in the frequency domain by introducing zeroth and first moments of wave action spectrum. Equations can be expressed in either Cartesian coordinates or polar-spherical, depending on the size of the area.

We have decided to focus only on the Cartesian formulation of the equations, as they can be easily transformed into polar-spherical ones, so there is no need to describe both versions in this master thesis. All equations, with more detailed explanations can be found in User Manual of the software, scientific documentation of the software, and in other references (e.g. Hasselmann (1974) and Hasselmann (1985) or Eldeberky (1996)).

The main equation used in spectral wave model is the action balance equation, which reads:

$$\frac{\partial}{\partial t} N + \frac{\partial}{\partial x} c_x N + \frac{\partial}{\partial y} c_y N + \frac{\partial}{\partial \sigma} c_\sigma N + \frac{\partial}{\partial \theta} c_\theta N = \frac{S}{\sigma} \quad (4.1)$$

where $N(x, y, \sigma, \theta, t)$ is the action density spectrum defined as a function of frequency σ , coordinates x and y , direction θ , time t , and is related to energy density spectrum by

$$N = \frac{E}{\sigma} \quad (4.2)$$

$$\sigma = \sqrt{gk \cdot \tanh kd} = \omega - \vec{k} \cdot \vec{U} \quad (4.3)$$

σ is the relative angular frequency, ω is the angular frequency, \vec{k} is the wave vector, \vec{U} is the current velocity vector, g is acceleration of gravity and d is the water depth.

Left side of the Eq. 4.1 consists of five different terms. From left to right respectively they describe the local rate of change in the spectrum regarding to time, coordinates (x and y), frequency and direction. Except of the first one, each one is connected to the corresponding propagation velocity ($c_x, c_y, c_\sigma, c_\theta$).

Right side of the equation represents the source term in terms of energy density. There are many components that can be taken into account while describing the source terms, such as wind induced wave generation, energy transfer caused by non-linear wave-wave interaction, dissipation of the energy caused by whitecapping, friction and depth-induced breaking.

The wind input source term is given by

$$S_{in}(f, \theta) = \max(\alpha, \gamma) E(f, \theta) \quad (4.4)$$

where α is responsible for the linear growth and γ for the non-linear growth. There are a lot of factors, that have influence on both α and γ . The most important one is the wind velocity. Most commonly used linear model is the one proposed by Ris et al. (1994), whereas nonlinear model by Janssen (1991) is preferred. They are described very precisely in the MIKE 21 SW Scientific Documentation.

Another very important phenomena, especially in deep water, are quadruplet wave-wave interactions. This is very complex phenomenon, and solving it exactly, using three-dimensional, non-linear Boltzmann integral is too computational demanding, so the discrete interaction approximation (DIA) developed by Hasselmann et al. (1985) is used. It was discovered, that energy exchange occurs, when following resonance conditions are met:

$$\begin{aligned} \vec{k}_1 + \vec{k}_2 &= \vec{k}_3 + \vec{k}_4 \\ \omega_1 + \omega_2 &= \omega_3 + \omega_4 \end{aligned} \quad (4.5)$$

\vec{k}_i are wave number vectors ($i=1,2,3,4$), and ω_i are frequencies associated with wave numbers through dispersion relation.

When waves come to shallow water triad-wave interactions are becoming more important. The energy transfer between interacting wave modes occurs. In MIKE 21 SW an approach proposed by Eldeberky and Battjes (1995, 1996) is used to model this.

The most crucial process, governing the dissipation of the energy in the coastal zone is depth-induced breaking. When waves propagate towards shore, they are becoming higher and steeper with the decreasing water depth. When limit value of the wave height/water depth is

reached they break and dissipate part of the energy. To take this into account, well tested model proposed by Battjes and Janssen (1978) is implemented.

Apart from breaking, energy is dissipated through bottom friction as well. It also affects some other coastal processes as shoaling or refraction. The rate of dissipation is given by:

$$S_{bot}(f, \theta) = -(C_f + f_c \frac{\bar{u} \cdot \bar{k}}{k}) \cdot \frac{k}{\sinh(2kd)} \cdot E(f, \theta) \quad (4.6)$$

C_f is a friction coefficient, f_c is a friction coefficient for current, k is the wave number, u is current velocity and d is water depth.

The last factor, which dissipates the energy is whitecapping. The model proposed by Komen et al. (1994) is used, which allows the proper balance between wind input and dissipation at high frequencies.

4.2.2. Boussinesq Wave model

Boussinesq Wave (BW) model, being state-of-the-art numerical tool for the analysis of port, harbour and coastal areas was used successfully in numerous researches and consists of two modules:

- 2DH Boussinesq wave module, which covers two dimensional space, and is used in port and harbour modelling
- 1DH Boussinesq wave module, which model one dimensional space and is mainly used to coastal areas modelling

Due to the character of the master thesis, as it is dealing with modelling of the harbour, only 2DH Boussinesq wave module will be described below.

Two horizontal space co-ordinates module is capable of reproducing most interesting wave phenomena, which occurs in harbours and ports such as: shoaling, refraction, diffraction, wave breaking, reflection or non-linear wave interactions. The advantage of the software are also well described phenomena of generation and release of low-frequency oscillations, such important for harbour oscillations and seiches.

2DH Boussinesq module solves enhanced Boussinesq equations in two horizontal dimensions and in terms of free surface elevation (ξ) and depth-integrated velocity components (P , Q)

The equations read as follows:

Continuity equation:

$$n \frac{\partial \xi}{\partial t} + \frac{\partial P}{\partial x} + \frac{\partial Q}{\partial y} = 0 \quad (4.7)$$

X-momentum:

$$n \frac{\partial P}{\partial t} + \frac{\partial}{\partial x} \left(\frac{P^2}{h} \right) + \frac{\partial}{\partial y} \left(\frac{PQ}{h} \right) + \frac{\partial R_{xx}}{\partial x} + \frac{\partial R_{xy}}{\partial y} + F_x \quad (4.8)$$

$$n^2 gh \frac{\partial \xi}{\partial x} + n^2 P \left[\alpha + \beta \frac{\sqrt{P^2 + Q^2}}{h} \right] + \frac{gP \sqrt{P^2 + Q^2}}{h^2 C^2} + n \Psi_1 = 0$$

Y-momentum:

$$\begin{aligned}
& n \frac{\partial Q}{\partial t} + \frac{\partial}{\partial y} \left(\frac{Q^2}{h} \right) + \frac{\partial}{\partial x} \left(\frac{PQ}{h} \right) + \frac{\partial R_{yy}}{\partial y} + \frac{\partial R_{xy}}{\partial x} + F_y \\
& n^2 gh \frac{\partial \xi}{\partial y} + n^2 Q \left[\alpha + \beta \frac{\sqrt{P^2 + Q^2}}{h} \right] + \frac{gQ \sqrt{P^2 + Q^2}}{h^2 C^2} + n \Psi_2 = 0
\end{aligned} \tag{4.9}$$

Ψ_1 and Ψ_2 are dispersion terms derived as:

$$\begin{aligned}
\Psi_1 \equiv & - \left(B + \frac{1}{3} \right) d^2 P_{xxt} + Q_{xyt} - nBgd^3 \xi_{xxx} + \xi_{xyy} \\
& - dd_x \left(\frac{1}{3} P_{xt} + \frac{1}{6} Q_{yt} + nBgd \ 2\xi_{xx} + \xi_{yy} \right) \\
& - dd_y \left(\frac{1}{6} Q_{xt} + nBgd \xi_{xy} \right)
\end{aligned} \tag{4.10}$$

$$\begin{aligned}
\Psi_1 \equiv & - \left(B + \frac{1}{3} \right) d^2 Q_{yyt} + P_{xyt} - nBgd^3 \xi_{yyy} + \xi_{xxy} \\
& - dd_y \left(\frac{1}{3} Q_{yt} + \frac{1}{6} P_{xt} + nBgd \ 2\xi_{yy} + \xi_{xx} \right) \\
& - dd_x \left(\frac{1}{6} P_{yt} + nBgd \xi_{xy} \right)
\end{aligned} \tag{4.11}$$

Where subscripts x, y, t mean derivatives with respect to x, y direction and time respectively.

F_x, F_y are horizontal stress terms:

$$\begin{aligned}
F_x &= - \left(\frac{\partial}{\partial x} \left(\nu_t \frac{\partial P}{\partial x} \right) + \frac{\partial}{\partial y} \left(\nu_t \left(\frac{\partial P}{\partial y} + \frac{\partial Q}{\partial x} \right) \right) \right) \\
F_y &= - \left(\frac{\partial}{\partial y} \left(\nu_t \frac{\partial Q}{\partial y} \right) + \frac{\partial}{\partial x} \left(\nu_t \left(\frac{\partial Q}{\partial x} + \frac{\partial P}{\partial y} \right) \right) \right)
\end{aligned} \tag{4.12}$$

Where ν_t is the horizontal eddy viscosity.

R_{xx}, R_{yy}, R_{xy} account for the excess momentum caused by non-uniform velocity distribution due to the presence of surface roller, and are denoted as:

$$\begin{aligned}
R_{xx} &= \frac{\delta}{1 + \delta/d} \left(c_x - \frac{P}{d} \right)^2 \\
R_{xy} &= \frac{\delta}{1 + \delta/d} \left(c_x - \frac{P}{d} \right) \left(c_y - \frac{Q}{d} \right) \\
R_{yy} &= \frac{\delta}{1 + \delta/d} \left(c_y - \frac{Q}{d} \right)^2
\end{aligned} \tag{4.13}$$

Here δ is the thickness of the roller surface and c_x, c_y are components of roller celerity.

Below other symbols used in the aforementioned equations are listed:

B – Boussinesq dispersion coefficient (-)

h – total water depth ($=d+\zeta$)

d – still water depth (m)

g – gravitational acceleration (m/s^2)

n – porosity (-)

C – Chezy resistance number ($m^{0.5}/s$)

α – resistance coefficient for laminar flow in porous media (-)

β – resistance coefficient for turbulent flow in porous media (-)

ζ – water surface elevation above datum (m)

There is one shortcoming of the original Boussinesq equations. They can be used properly only when dealing with shallow water, where ratio of water depth to wavelength (h/L_0) is smaller than 0.22. This criterion is often too sharp for small waves entering the harbour. In order to solve this problem enhanced Boussinesq Equations were introduced by Madsen and Sørensen. The limit value is then increased up to 0.5-0.85, so that the application range is extended into deeper water/smaller waves.

5. NUMERICAL MODEL FOR WAVES IN THE NEW USTKA HARBOUR

5.1. Approach

Numerical model presented in the master thesis was done using MIKE, a powerful and well known commercial software developed by a Danish group DHI. It consists of the several modules and cover almost every part of the complex process of preparation of model and running simulations. In our master thesis, two different types of models will be prepared and calculated. Firstly, because of the lack of the initial data and large distances between sites providing measurements needed, the MIKE 21 SW FM module will be used. This is the spectral wave model with which uses flexible mesh. The purpose of using this tool is to obtain reliable input data in the near proximity of our site of interest. In order to investigate how do the tides and currents affect the wave climate in proximity of Ustka two different Spectral Wave models were prepared. One assuming constant water level and neglecting currents and second one where those phenomena are taken into account. Information about tides and current were prepared using MIKE 21 HD. The procedure of the preparation of the model and results from MIKE 21 HD are also shortly presented in this chapter (Subsection 5.2.4). Afterwards, wave spectra calculated by spectral wave module are to be used as an input in the second step of our work. This is the part were another module, MIKE 21 BW is employed. As the face-resolving, Boussinesq wave module, MIKE 21 BW is supposed to give us more detailed insight into the various processes that take place in the harbour basins and around the structures. After calculating and checking every given breakwater layout, the best design can be chosen.

5.2. SW model

5.2.1. Domain Description

The present model is designated to calculate the wave generation by wind, and transformation and propagation of both sea and swell waves while approaching the shoreline. The model domain is about 400 km x 250 km with a maximum water depth of approximately 150 m. Bathymetry and land geometry data were obtained from MIKE C-MAP software, which contains good resolution bathymetry data for the entire world, and allows for extraction of data for different locations. After loading the data into MIKE Mesh Generator mesh was generated and improved by refining and smoothing. Final mesh consists of 25968 grid cells of maximum angle of 30° and maximum area equal to 5 km². Original mesh was smoothed 100 times. After that bathymetry data was interpolated to all the grid points. Prepared bathymetry of the whole area is shown in Figure 12, whereas Figure 13 presents a close up on the bathymetry and created mesh in the vicinity of the area of interest.

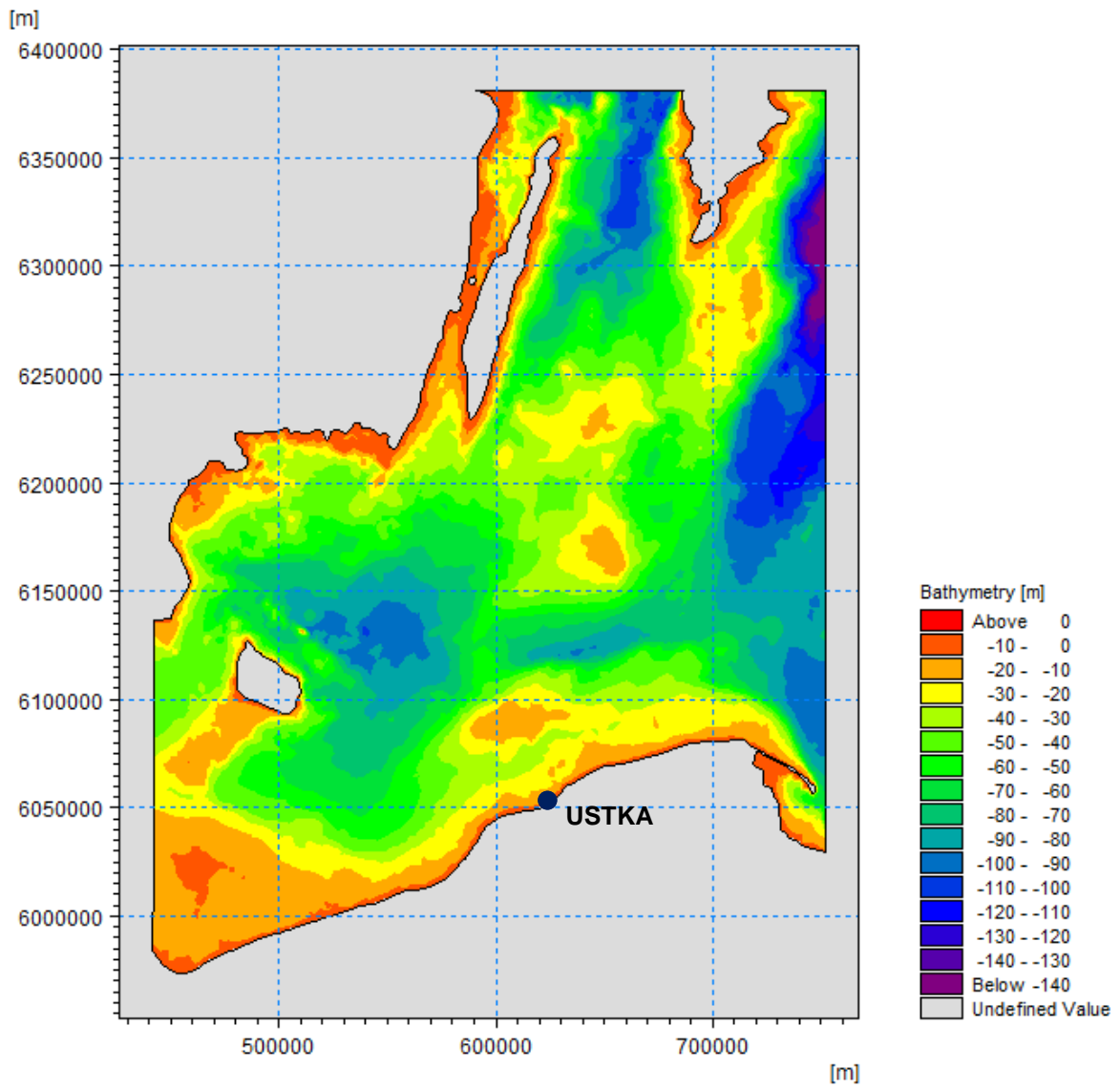


Figure 12 Bathymetry of Baltic Sea generated by Mike Zero software.

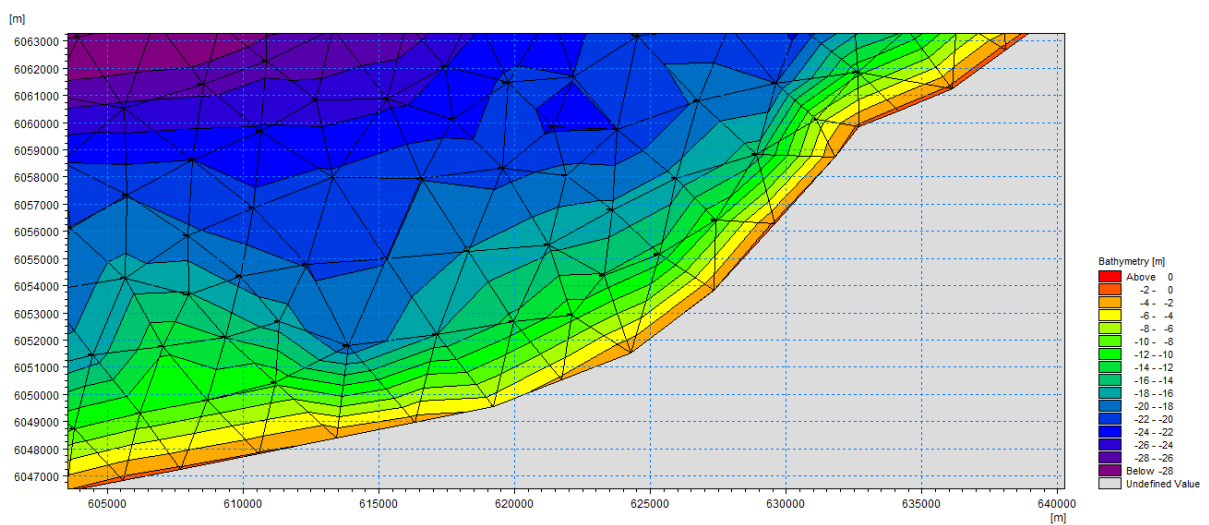


Figure 13 The view on the generated mesh. Zoomed into local area of interest. Prepared using Mike Zero Software

5.2.2. Boundary Conditions

Besides properly defined domain of the numerical model and setting correct water level, another very important factor during setting a model is to define proper boundary conditions. It has a significant influence on accuracy and accordance with real values. Poland does not have measuring buoys that can provide data useful as an input to the model prepared in this master thesis. Therefore, data from Swedish and German measuring buoys were applied. SMHI (Swedish Meteorological and Hydrological Institute) provided data from Sodra Ostersjon and Knolls Grund probe and data from FIN02 WR probe was obtained from German Federal Waterways and Shipping Administration (WSV), and forwarded by the German Federal Institute of Hydrology (BfG). Locations of those measuring devices are shown in Figure 14. The period of time that is most valuable for this simulation begins at 00:00:00 6th of January 2015 and lasts till 23:00:00 28th of February 2015. The choice was made based on the data from local meteorological station and Jakusik (2006) research results where is stated that January and February are months when conditions at the sea are roughest and wind blows from north-east, north and north-west, which results in the highest waves in the proximity of Ustka coastline. What is more, it was mentioned in Chapter 2 point 2 that in January 2015 a storm surge took place that resulted in quay stability problem.

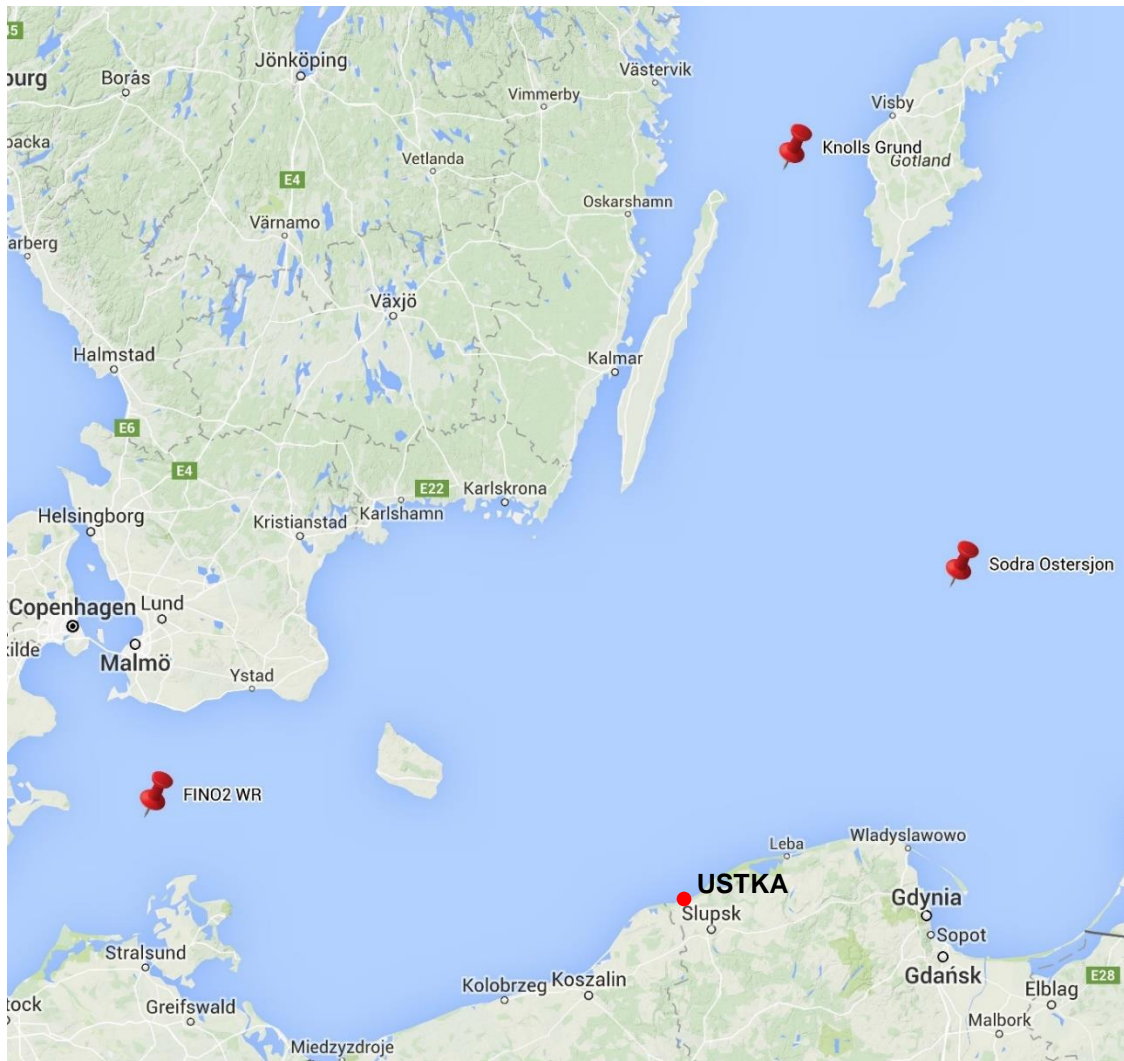


Figure 14 Position of the measuring buoys (Source: Google Maps)

Localization of the measuring buoys designated the size and layout of the model's boundaries. There are three different open boundaries on the north, east and west of the domain. The locations of those boundaries are indicated on Figure 15. For the northern, eastern and western boundaries data from Knolls Grund buoy, Sodra Osterson buoy and FIN02 WR buoy was applied respectively.

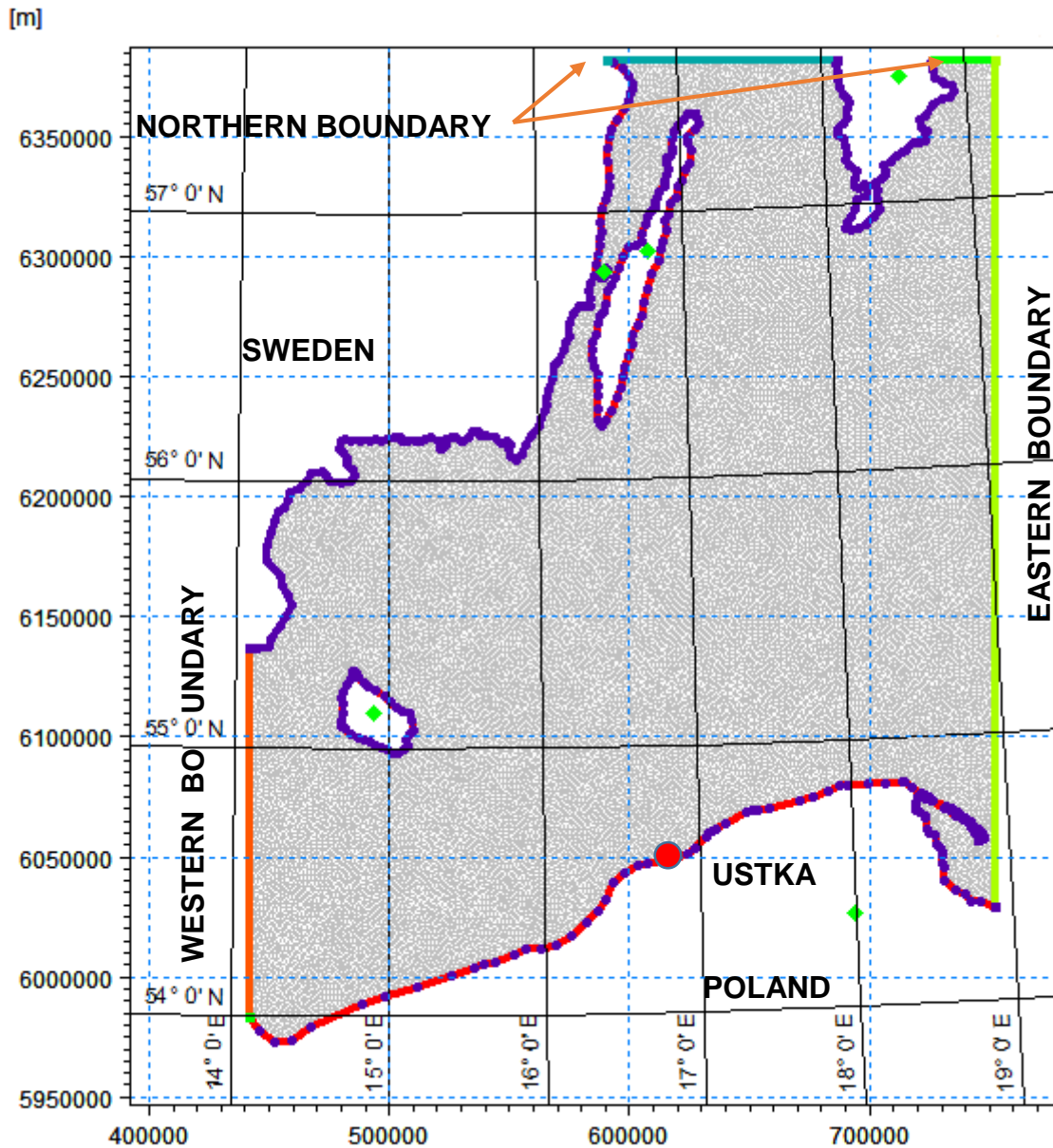


Figure 15 Northern, Eastern and Western boundaries of the defined domain

Below time series of wave height, wave period, direction and spreading factor from described buoys are shown (Figure 16-18). The time step in the provided data was equal to one hour.

Input file should consist of four parameters, which are significant wave height, peak period, mean wave direction and directional spreading index (Version 1) or directional standard deviation (Version 2). The first three of them were obtained from wave rider buoys, while the last one had to be assumed based on the experience and type of the sea state. It is usually assumed, that the directional spreading index is typically within the interval 2-8 for wind

waves and larger than 10 for swell. Because in the present case a mix of a wind sea and swell is expected, the directional spreading index was set equal to 9 in all three wave inputs.

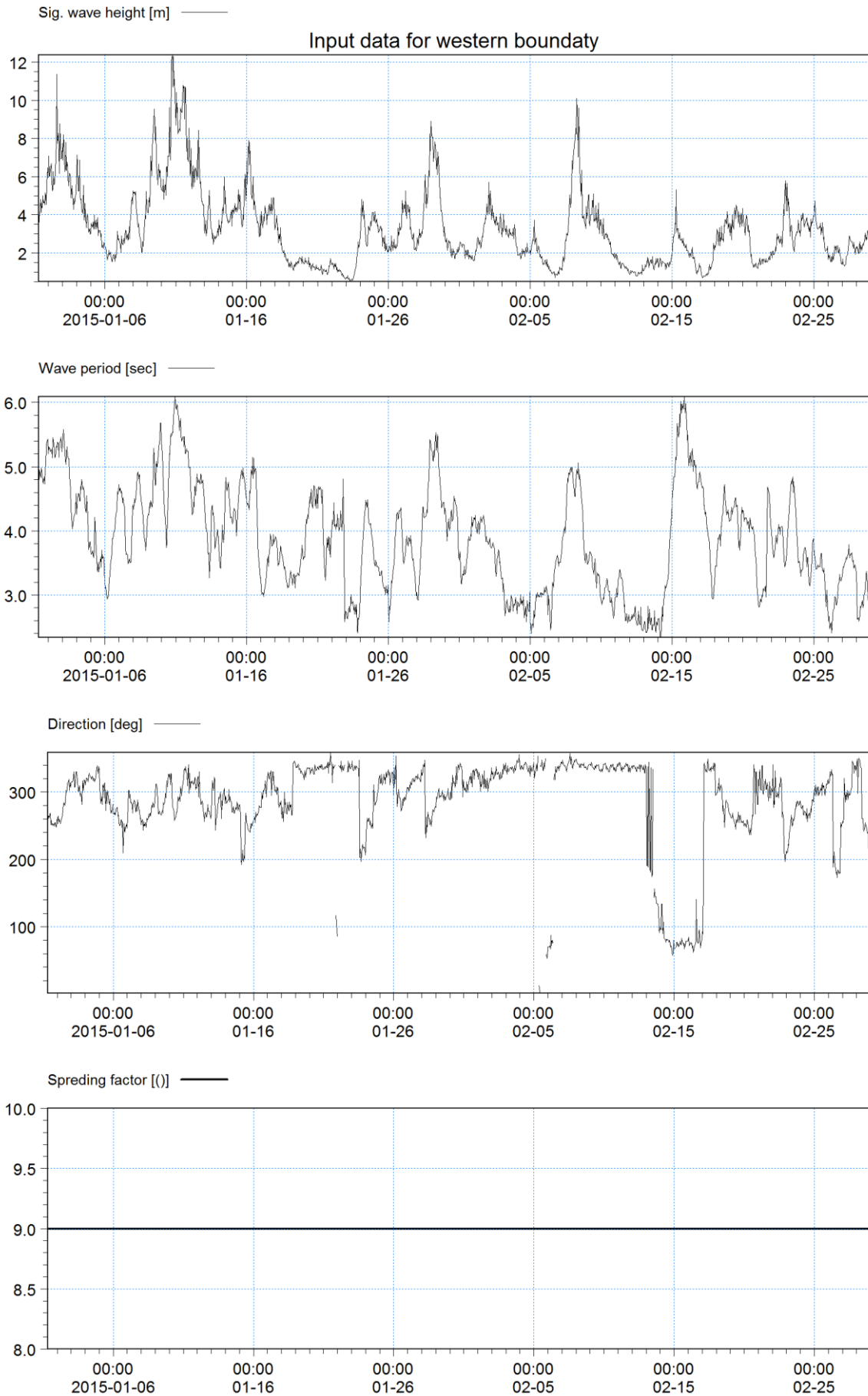


Figure 16 Plot of the input data from FinO2 WR Buoy –Western boundary

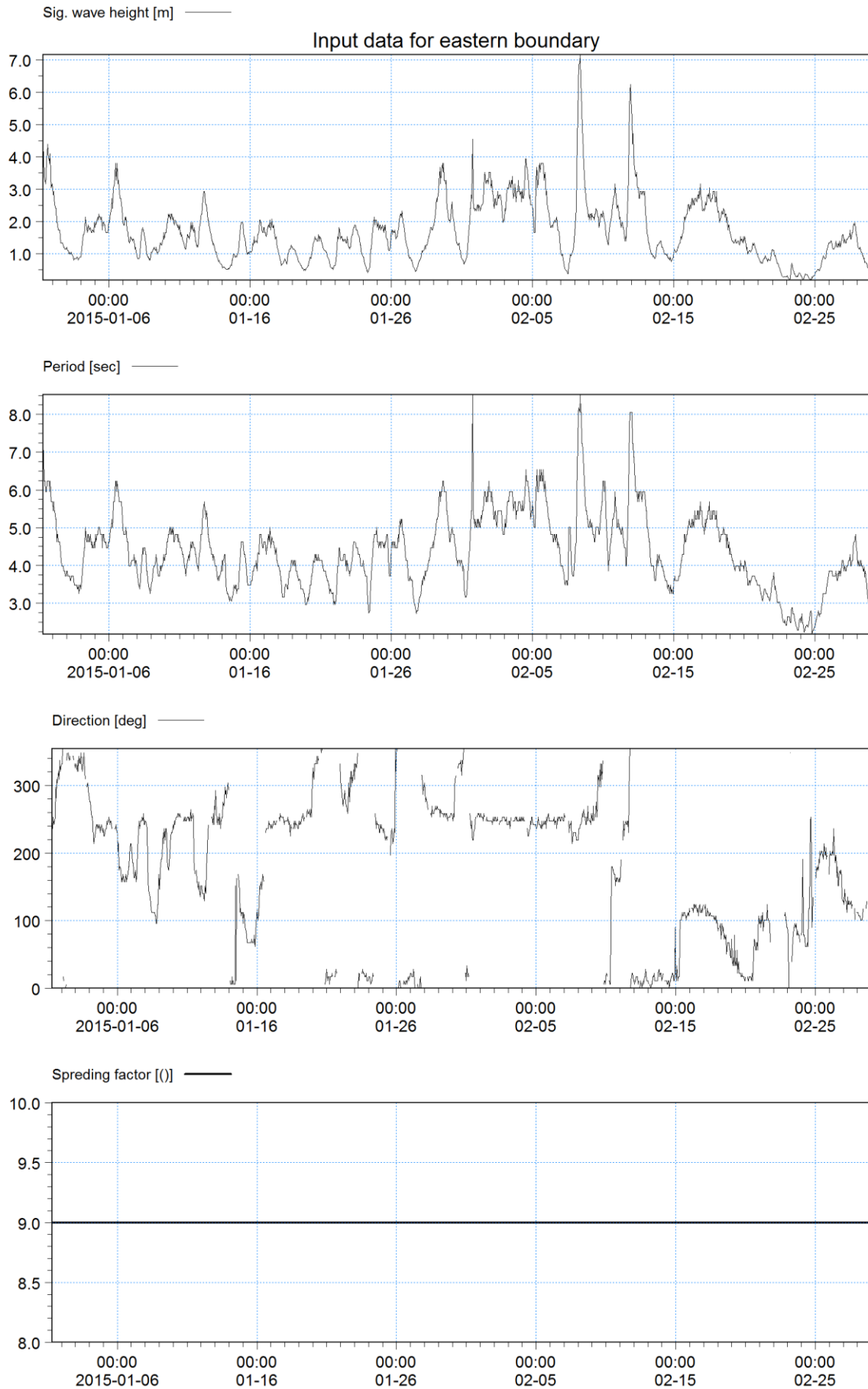


Figure 17 Plot of the input data from Sodra Ostersjon Buoy – Eastern boundary

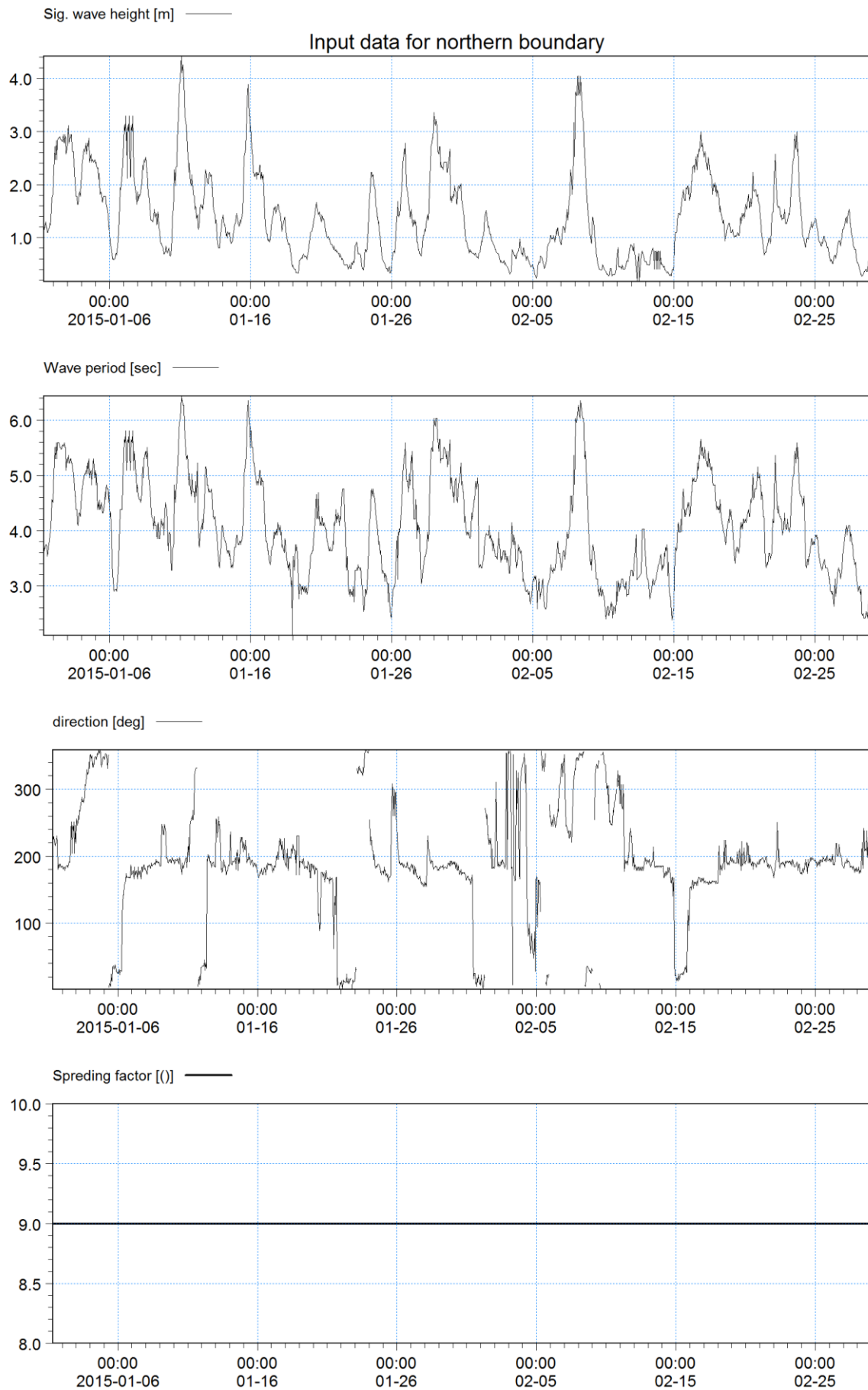


Figure 18 Plot of the input data from Knolls Grund Buoy – Northern boundary

5.2.3. Wind forcing

As there is no measured wind data for the period of the simulation wind data used as an input was extracted from ECMWF database. Global atmospheric reanalysis data, ERA-Interim, was used. It is publicly available in the form of resolved wind velocity components in the x and y direction, at a 0.125° resolution and an interval of 6 hours. Figure 19 shows an example view of the wind velocity for the area.

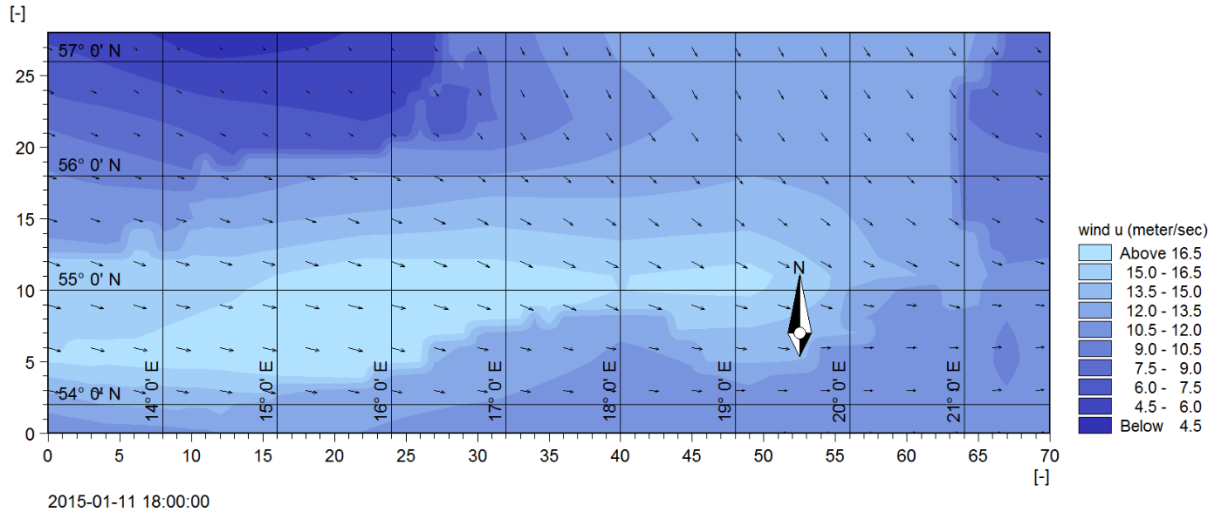


Figure 19 Wind velocity contour plan over the area (Source: ECMWF)

East and North velocity component is not the only way of providing data by meteorological institutes. It may happen that one receives a resultant value of the wind velocity together with its direction θ , which is defined as an angle between north direction and velocity vector. In order to calculate resultant vector of the velocity and its direction from east and north velocity component, root of the sum of the squared x and y is needed (Eq. 5.1) and arc tang (Eq. 5.2).

$$V = \sqrt{x^2 + y^2} \quad (5.1)$$

$$\theta = \tan^{-1} \frac{x}{y} \quad (5.2)$$

Relationship between those vectors is shown in Figure 20 below.

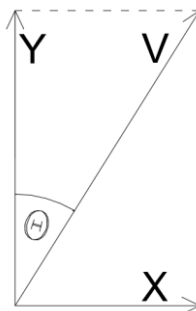


Figure 20 Relationship between x and y velocity component.

In order to investigate the correlation between the ECMWF reanalysis data and the real observations the wind speed and directions extracted for the area of Ustka from the ECMWF

database is compared with the data from Ustka meteorological station, publicly available at NOAA database. For comparison time series of resultant wind speed and direction for a point closest to Ustka was extracted from dfs2 - grid series file type. Rose plots and comparison of the time series created in MIKE Plot Composer tool are shown below (Figures 21 - 23).

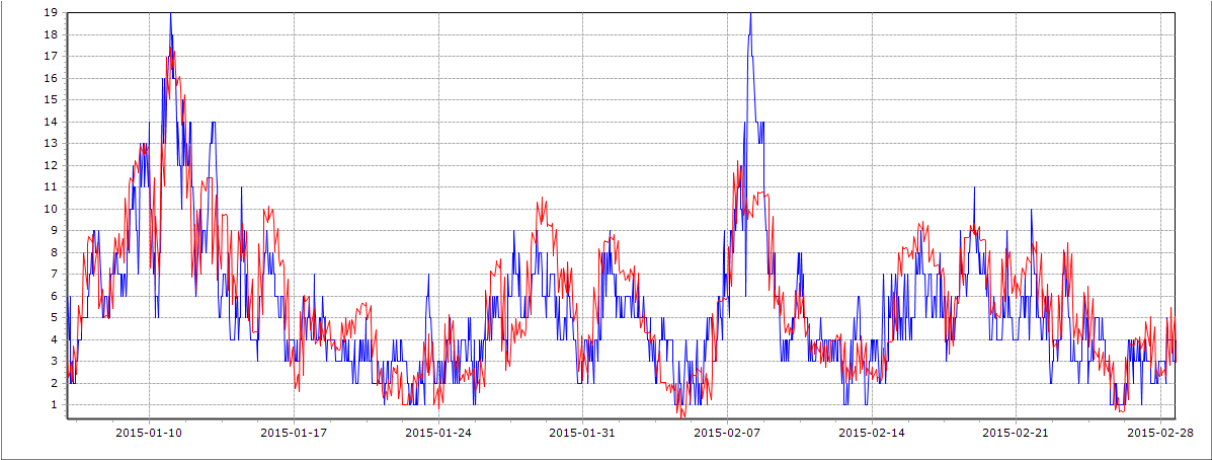


Figure 21 The comparison of the mean wind speed from Ustka measurements (blue) and ECMWF data (red). (Generated by: Mike Zero by DHI)

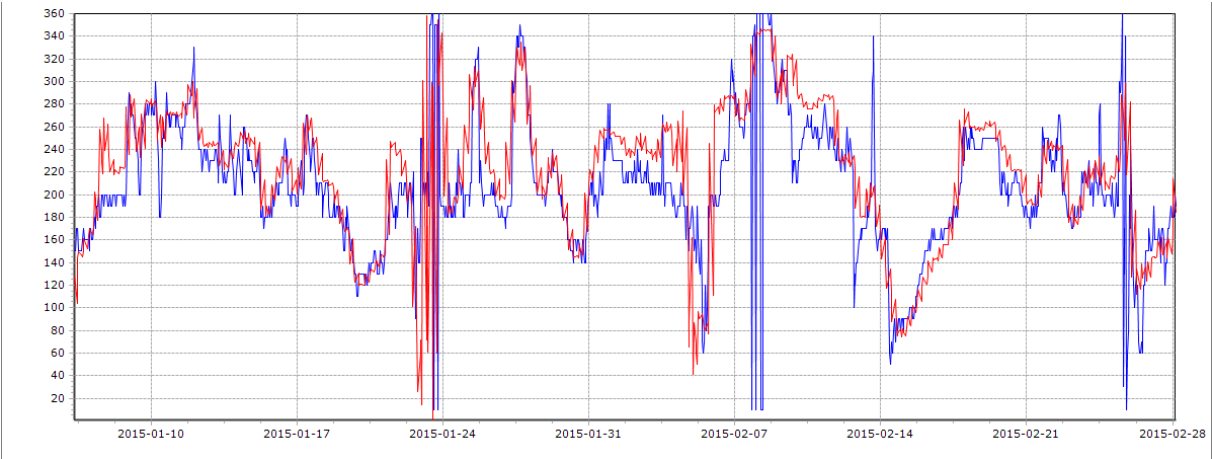


Figure 22 The comparison of the mean wind direction from Ustka measurements (blue) and ECMWF data (red). (Generated by: Mike Zero by DHI)

It is seen that both datasets are very consistent with each other in terms of wind speed and direction. Comparison done using MIKE 21 Time Series Comparator revealed that the index of agreement for the wind speed was over 0.90, whereas for the direction data it was almost 0.83. This is better than expected and allows to assume that wind field over whole domain resembles very well real conditions.

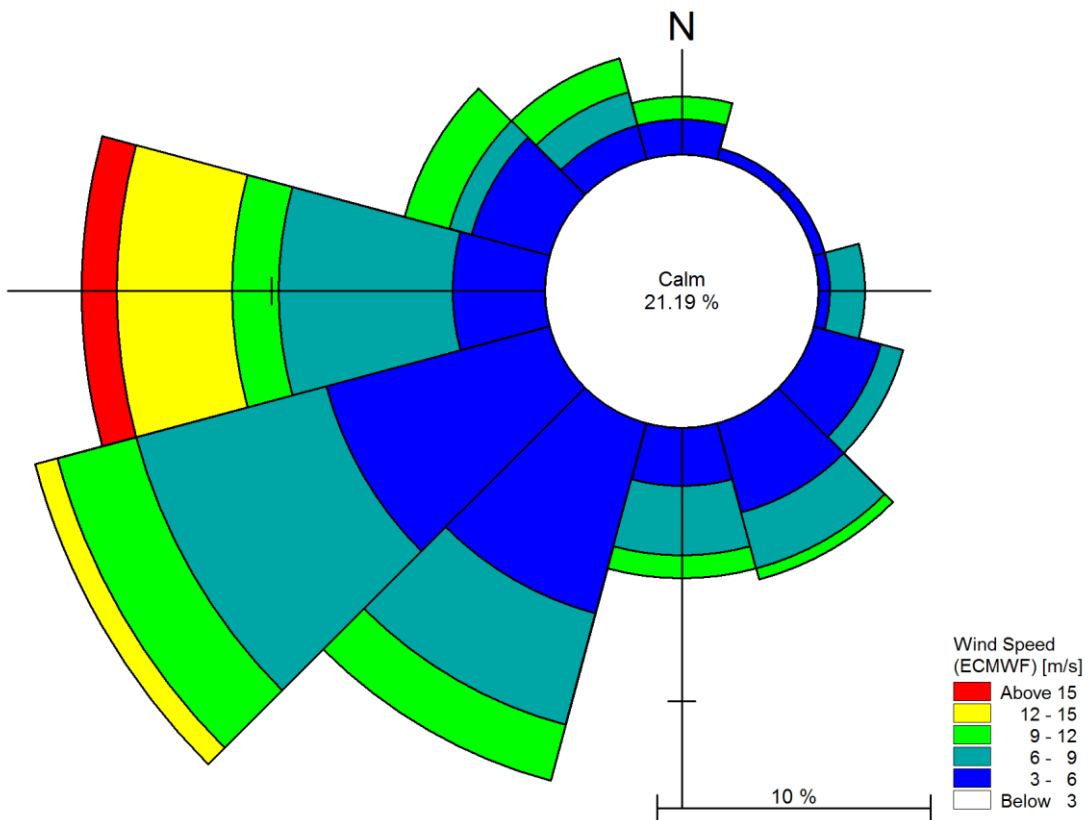
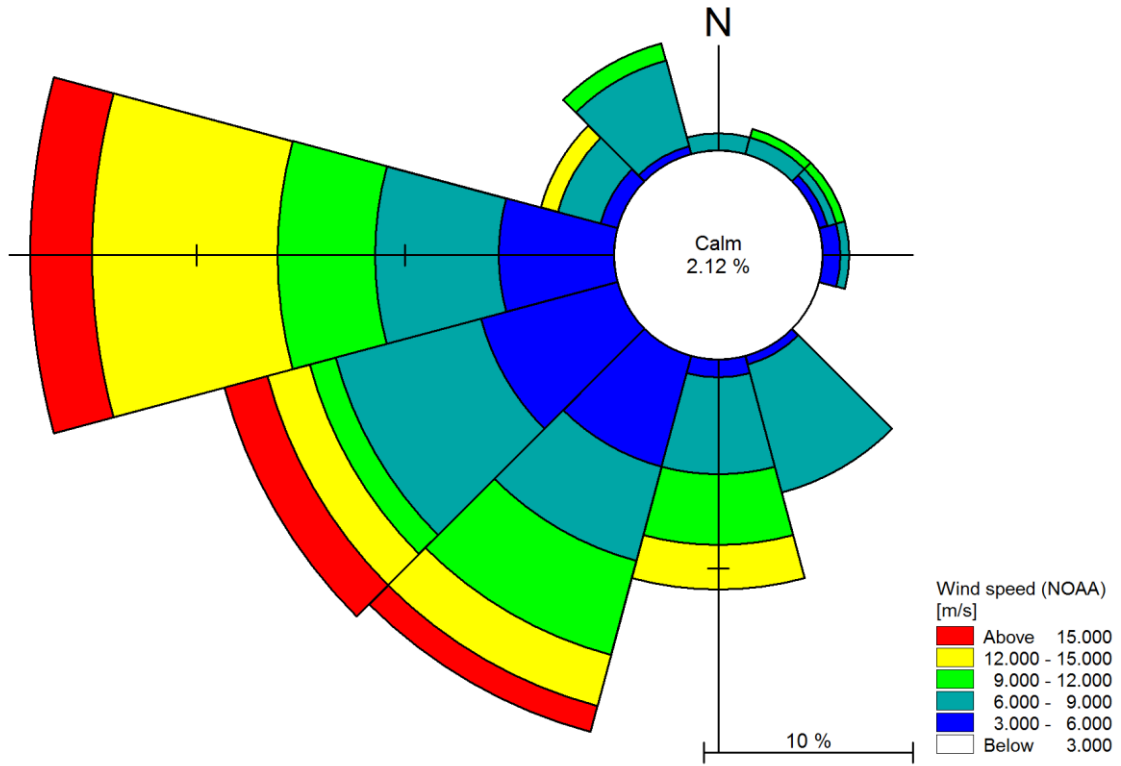


Figure 23 The rose plots of the mean wind speed for Ustka from ECMWF (on the bottom) model and NOAA (top). (Generated by: Mike Zero by DHI)

5.2.4. Water level

In order to provide as realistic as possible conditions it was important to give input regarding changes of water levels and current velocities over the whole domain. Centres of high pressure will cause lowering of sea level, and the low-pressure centres will cause raising. In Norway, changes in pressure may cause fluctuations that reach up to 1 meter. Unlike the North Sea, the Baltic Sea is not a place where centres of low pressure are formed directly, so it is foreseen that the fluctuations in sea level caused by the pressure difference will be smaller. To verify if the currents and tides have significant meaning for results two SW simulation were performed.

5.2.4.1. SW with constant water level

This model assumes that waver level at the boundaries is constant and current and tide influence is neglected. Only wind forcing over entire domain is taken into calculations.

5.2.4.2. SW with varying water level

To include varying water level in the SW model, hydrodynamic simulation was done using MIKE FM HD module. Beside the wind forcing described above, grid series of pressure changes over entire domain were obtained from ECMWF database and used in the HD simulation, see Fig. 24. All those parameters combined allow for including water level changes induced by storm surge in the analysis. Like wind velocities, pressure data was obtained with the resolution of 0.125° . As a boundary conditions water level recording from German buoy FINO2 on western boundary and Swedish buoy VISBY (57.64° N, 18.29° E) on northern one were used. For eastern boundary a constant value was assumed equal to 0.33 m (mean value of water level at the neighbouring Northern boundary) due to fact that Sodra Osterson Buoy (located at Eastern boundary) does not record water level fluctuations. Below are presented time series of water level at those boundaries.

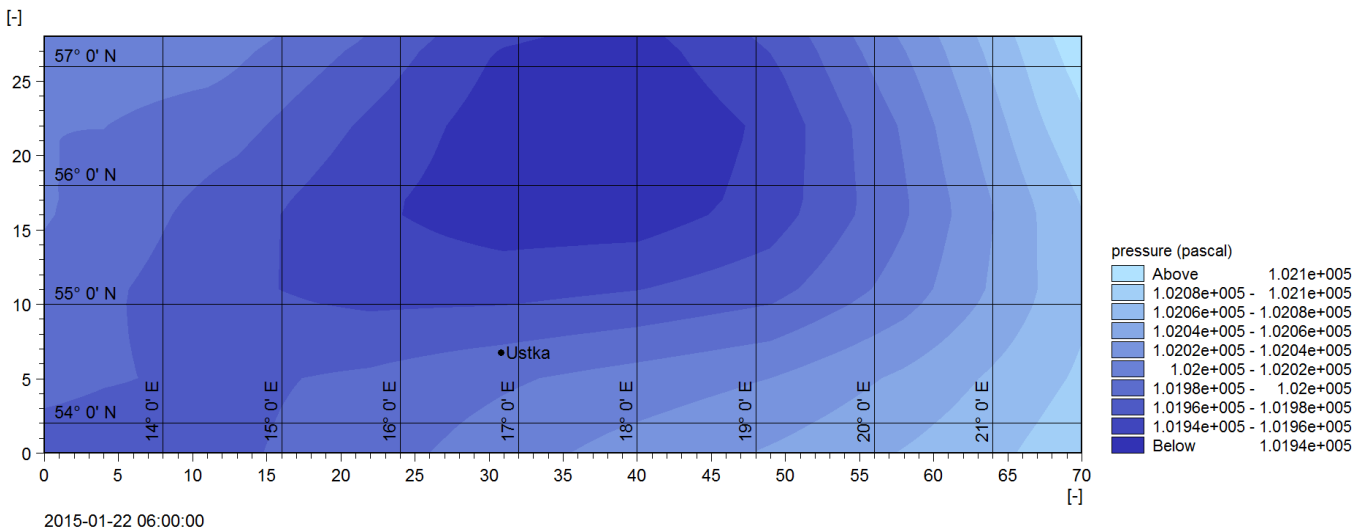


Figure 24 Pressure snapshot over the area (Source: ECMWF)

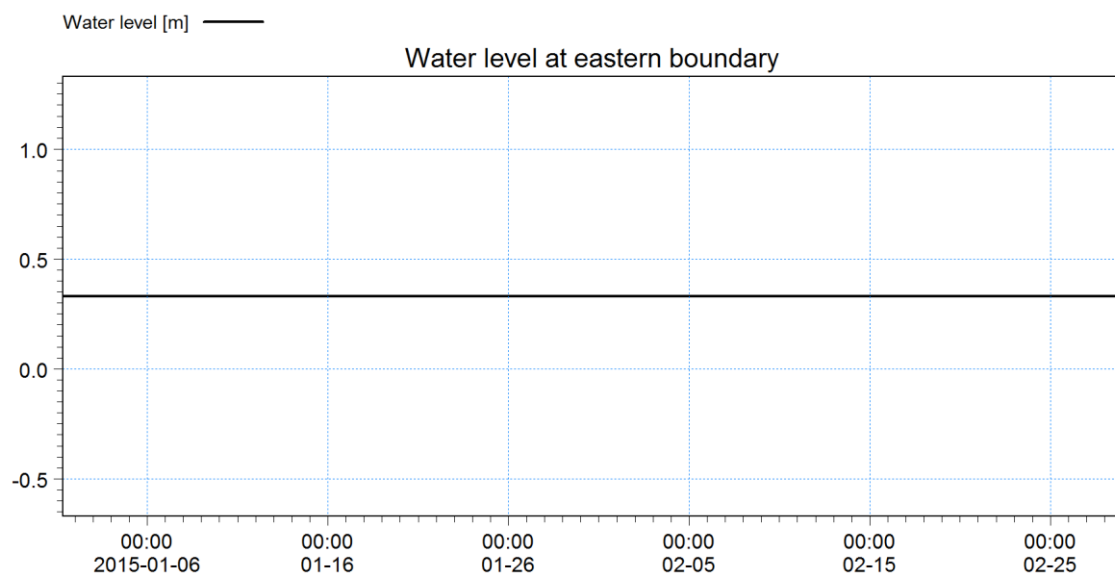
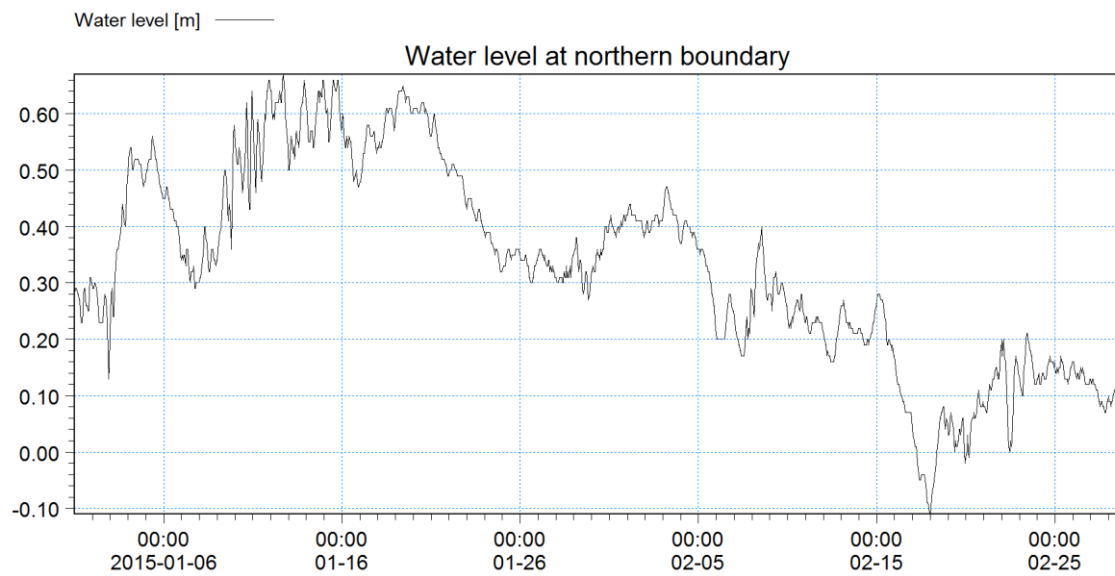
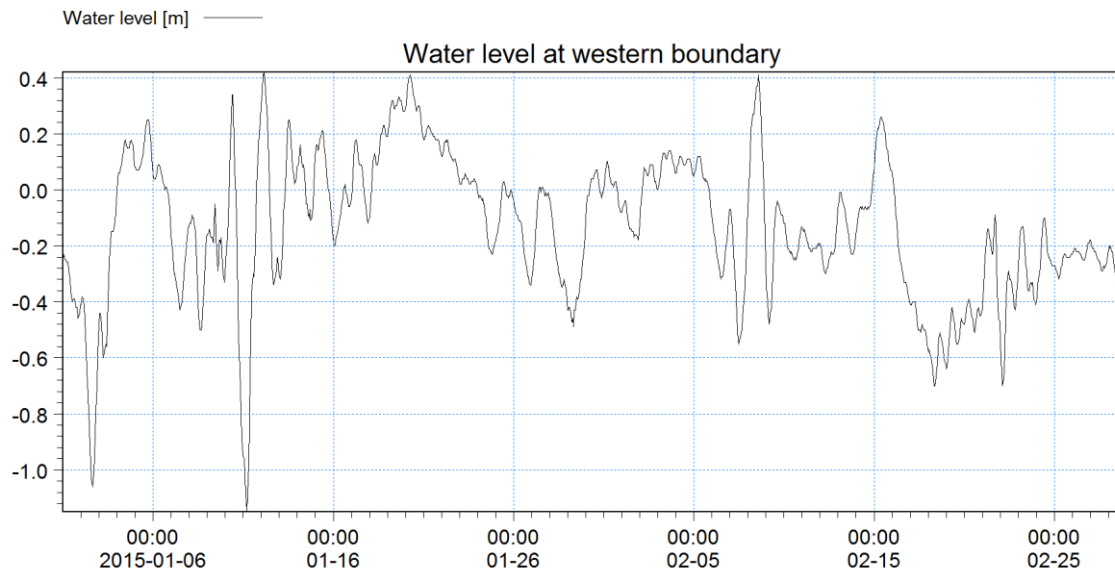


Figure 25 Water level at western, northern and eastern boundary respectively. Generated by Mike Zero Plot Composer.

MIKE FM HD was run using low-order, fast algorithms, with parameters of the algorithm kept as default. Effect of depth correction, ice coverage, precipitation, evaporation, infiltration and wave radiation was neglected. Setting regarding flood and dry, density changes and impact of Coriolis forcing were also kept as default. Eddy viscosity was modelled using Smagorinsky formulation with constant value of 0.28. To include effects of bed resistance, constant Manning number equal to 32 m^{1/3}/s was introduced to the model. All parameters and input data are summarized in the Table 5 below:

Table 5 Specification of the Hydrodynamic model (HD)

Parameter	Value
Mesh and Bathymetry	13404 Nodes, MIKE C-MAP described in 5.2.1
Simulation Period	2015-01-06 00:00 – 2015-02-28 18:00 (53 days)
Time Step Interval	3600s (1 hour)
No. of Time Steps	1290
Solution Technique	Low order, fast algorithm Minimum time step: 0.01s Maximum time: 120s Critical CFL number: 0.8
Depth	No depth correction
Flood and dry	Standard Flood and Dry Drying depth: 0.01m Flooding depth: 0.05m Wetting depth: 0.1m
Density	Barotropic
Eddy viscosity	Smagorinsky formulation Constant value: 0.28
Bed resistance	Type: Manning number Constant value: 32 m ^{1/3} /s
Coriolis forcing	Varying in domain
Wing forcing	Varying in time and domain Input from global model (ECMWF): wind velocity in u and v direction and pressure described in point 5.2.3 above Neutral pressure: 1013 hPa Soft start: 7200 s Format: .dfs2 Wind friction: varying with wind speed
Ice coverage	No Ice coverage
Tidal potential	Not included
Precipitation-Evaporation	No precipitation No evaporation
Infiltration	No infiltration
Wave radiation	No wave radiation
Structures	No structures
Initial conditions	Constant Surface elevation: 0.017 m U: 0 m/s

	V: 0 m/s
Boundary conditions	<u>Northern Boundary - Specified level:</u> Data from: SMHI Visby buoy Content: surface elevation Format: .dfs0 <u>Western Boundary – Specified level:</u> Data from: FinO2 WR buoy Content: surface elevation Format: .dfs0
Result File	Area series Format: .dfsu Projection: UTM-33 <u>Basic variables:</u> Surface elevation Still water depth Total water depth U velocity V velocity
CPU Simulation Time	About 43 minutes with a 2 x 2.5 GHz PC, 12 GB DDR RAM

5.2.5. Summary of all input data and parameters used

The SW was run in fully spectral formulations with instationary time formulation. It means that the directional-frequency wave action spectrum is the dependent variable. Logarithmic type of discretization was used without separation of wind-sea and swell. Ice coverage was neglected, while variation of water-level and current were neglected only in one run (SW without HD). Wind forcing was set up as a varying in time and domain. All the boundary conditions and wind forcing were applied with soft start of 7200 seconds with linear interpolation. Geographical space discretization was made using low order, fast algorithm technique. Wave energy transfer was included with quadruplet wave interaction.

Effects such as diffraction, wave breaking and white capping were kept at default values, and bottom friction was included using Nikuradse roughness. There were no structures added in SW model. JONSWAP fetch formula was chosen for calculating wind generated waves. To include influence of the current and changing water level, results from HD model were used as an input to describe those phenomena. The summary of all input parameter is presented in Table 6 below.

Table 6 Specification of the SW model + HD

Parameter	Value
Mesh and Bathymetry	13404 Nodes, MIKE C-MAP described in 5.2.1
Simulation Period	2015-01-06 00:00 – 2015-02-28 18:00 (53 days)
Time Step Interval	3600s (1 hour)
No. of Time Steps	1290
Solution Technique	Low order, fast algorithm Minimum time step: 0.01s Maximum time stop: 30s
Spectral Discretization	Logarithmic

	<p>Number of frequencies: 25 Minimum frequency: 0.055Hz Frequency factor: 1.1</p>
Water Level Conditions	<p>1st simulation: no water level variation. 2nd simulation: from MIKE HD Model Specify water level variation Varying in time and domain Content: Surface elevation Soft start: 7200s Format: .dfsu</p>
Current Conditions	<p>1st simulation: no current variation 2nd simulation: from MIKE HD Model Specify current variation Varying in time and domain Content: U and V velocity component Soft start: 7200s</p>
Wind	<p>From global model (ECMWF) wind velocity at u and v direction described in point 5.2.3 above Soft start: 7200 s Format: .dfs2</p>
Initial Conditions	<p>JONSWAP fetch growth expression Maximum fetch length: 100km Maximum peak frequency: 0.4Hz Maximum Philips constant: 0.0081 Shape parameter, =0.07 Shape parameter, =0.09 Peakness parameter: 3.3</p>
Bottom Friction	<p>Nikuradse roughness Constant value 0.04m</p>
North Boundary	<p>Data from Knolls Grund buoy (Figure 16) Wave parameters: version 1 Content: wave height, wave period, wave direction Format: .dfs0</p>
East Boundary	<p>Data from Sodra Osterson buoy (Figure 17) Wave parameters: version 1 Content: wave height, wave period, wave direction Format: .dfs0</p>
West Boundary	<p>Data from Fin02 WR buoy (Figure 18) Wave parameters: version 1 Content: wave height, wave period, wave direction Format: .dfs0</p>
Result File	<p>Area series Format: .dfsu Projection: UTM-33 <u>Wave parameters divided into wind sea, swell and total result:</u></p>

	Significant wave height Maximum wave height Peak wave period Wave period T_{01} Wave period T_{02} Wave period T_{m10} Peak wave direction Mean wave direction Directional standard deviation Wave velocity components Radiation stresses Particle velocities Wave power
CPU Simulation Time	Circa 46 hours with a 2 x 2.5 GHz PC, 12 GB DDR RAM

5.3. BW model

5.3.1. Domain Description

Model presented in this section is designed to determine waves conditions inside harbour basin. The initial size of the domain was chosen to 2500x2000m that provides sufficient space to observe interaction between approaching waves and the whole breakwater. First step is to define model, calculate required time of simulation and find the upper limits. It can be done using Mike 21 BW Model Setup Planner. In the beginning one should know the wave parameters: significant wave height, peak period, main direction and also maximum water depth. In this case those parameters were taken from Spectral Wave simulation (see Chapter 6 point 2, Table 8) and have the following values: $H_{sig}=2.5m$, $T_p=9.8s$, $\theta=310.17^\circ$, $d_{max}=12m$, $d_{min}=5m$.

Define your model

- SI units for lengths (m)
- US units for length (ft)

Max. water depth	<input type="text" value="13"/>
Min. water depth	<input type="text" value="5"/>
Model extent in X-direction	<input type="text" value="2490"/>
Model extent in Y-direction	<input type="text" value="1995"/>
Percentage of water points (%)	<input type="text" value="50"/>
Max. distance for waves to propagate	<input type="text" value="1600"/>
Time required for calculation of statistics (minutes prototype time)	<input type="text" value="20"/>
Computational points per CPU second ²⁾	<input type="text" value="100000"/>
Spectral peak period (s)	<input type="text" value="9.8"/>
<input checked="" type="radio"/> Exclude wave breaking/moving shoreline	
<input type="radio"/> Include wave breaking/moving shoreline	

Calculate simulation period

A: Total simulation time

Total time required for simulation (minutes prototype time) ³⁾

Reset and clear all

Figure 26 Dialog window from Setup Planner, part 1. Source: Mike 21 by DHI.

Calculate and check/evaluate T_{min} , Δx and Δt ¹⁾

B: Calculate default upper limits

Upper limits	Classical eq.	Enhanced eq.
Min. wave period, T_{min} (s)	5.91	4
Max. spatial resolution, Δx	5.34	3.17
Max. time step, Δt (s)	0.492	0.114

C: Update upper limits using T_{min} and check/evaluation

Own suggestion		
Min. wave period, T_{min} (s)	5.91	4
Spatial resolution ⁴⁾ , Δx	5.34	1.5
Time step, Δt (s)	0.492	0.1
Check/evaluation of selected T_{min}, Δx and Δt		
Max. ratio h/L_0 for T_{min}	0.2198	0.4798
Max. ratio h/L_0 for T_p	0.0333	0.0333
Min. ratio $L/\Delta x$ for T_{min}	7.0080	14.810
Min. ratio $L/\Delta x$ for T_p	12.409	44.178
Ratio $T/\Delta t$ for T_{min}	12.012	40
Ratio $T/\Delta t$ for T_p	19.918	98
Max. Courant Number	1.0001	0.7236
Estimated CPU time (hours)	0.6964	43.276
Estimated RAM (MB)	21.754	204.97

Figure 27 Dialog window from Setup Planner, part 2. Source: Mike 21 by DHI.

Figures 26 and 27 show dialog window from Setup Planner. At first part the data such as maximal and minimal water depth, size of the domain and peak period are needed to calculate total required time for the simulation. Required time means the time needed for the first wave to reach the structures and the time required for calculation of wave statistics. Time of the first wave can be calculated manually using Eq. (5.3) – Eq. (5.6) and wave table. The time calculated manually is equal to 3.2 min when the one obtained from the software 3.49 min. The difference is due to the fact that software takes into calculation a changing water depth while in manual calculations constant depth of 12 meters was assumed. Below some formulas are presented that can be used to calculate the time needed for wave to propagate from generation line to the farthest point of the domain, where t_{fw} - time of the first wave, a – distance from generation line to the point of interest, C_g – group velocity, C – phase velocity, n – ratio between C and C_g taken from wave table, λ - wave length, T_p – peak period, d – water depth and x – interpolated value from wave table.

$$t_{fw} = \frac{a}{C_g} \quad (5.3)$$

$$C_g = nC \quad (5.4)$$

$$C = \frac{\lambda}{T_p} \quad (5.5)$$

$$\lambda = \frac{d}{x} \quad (5.6)$$

Second part refers to the upper limits of simulation. It means that minimum wave period, grid size (spatial resolution) and time step will be chosen to prevent numerical instability. According to data presented at Figure 27 enhanced equation were chosen with minimum wave period equal to 4s, grid size 1.5m and time step 0.1s.

Due to the high requirements of the computing power wave breaking was excluded from this simulation. To reduce the effects of this assumption, minimum water depth of 5 m was selected. This should allow waves up to 4 meters to propagate without breaking. The results of SW model shown that a maximum wave of 4.6 m (see Chapter 6 point 2, Table 7) is expected. This means that some wave breaking will occur even with minimum water depth of 5 m.

The bathymetry and layout of the new harbour was created using MIKE Zero – Bathymetry Editor. It resembles a spreadsheet in which each cell corresponds to one domain cell. The final model consists of 1660x1330 cells and each cell is 1.5x1.5m what gives a domain of 2490m width and 1995m height. During creating process, it is important to set different values at the edges between land or structures and water. The open boundaries should also be closed. In the next step this operation allows to create sponge and porous layers along those values. Figure 28 shows general view of the created bathymetry. It is easy to see that the minimum depth was set to 5 meters.

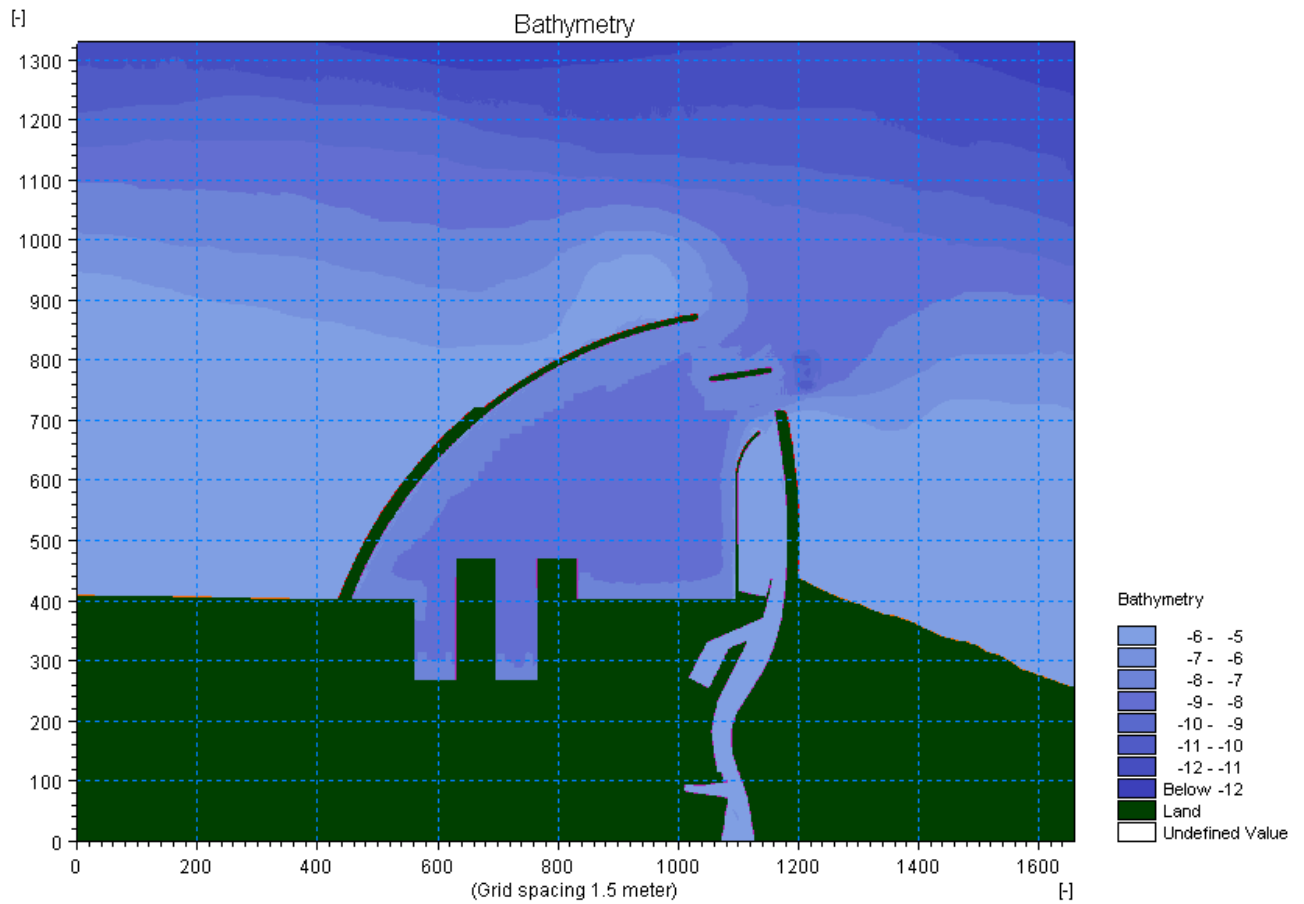


Figure 28 General view of the created bathymetry. Generated by Mike Zero software.

Figure 29 and 30 shows zoomed area where the new breakwater is connected with the coast. Below is presented legend that is necessary for proper reading of the Figure 30.

The legend of the edges values:

- 10 - land value (green),
- 8 - edge between water and breakwater which is covered with rip-rap layer (red),
- 7 - edge between water and breakwater with concrete, reflective walls (purple),
- 5 - edge between water and boundary where sponge layer is placed (orange).

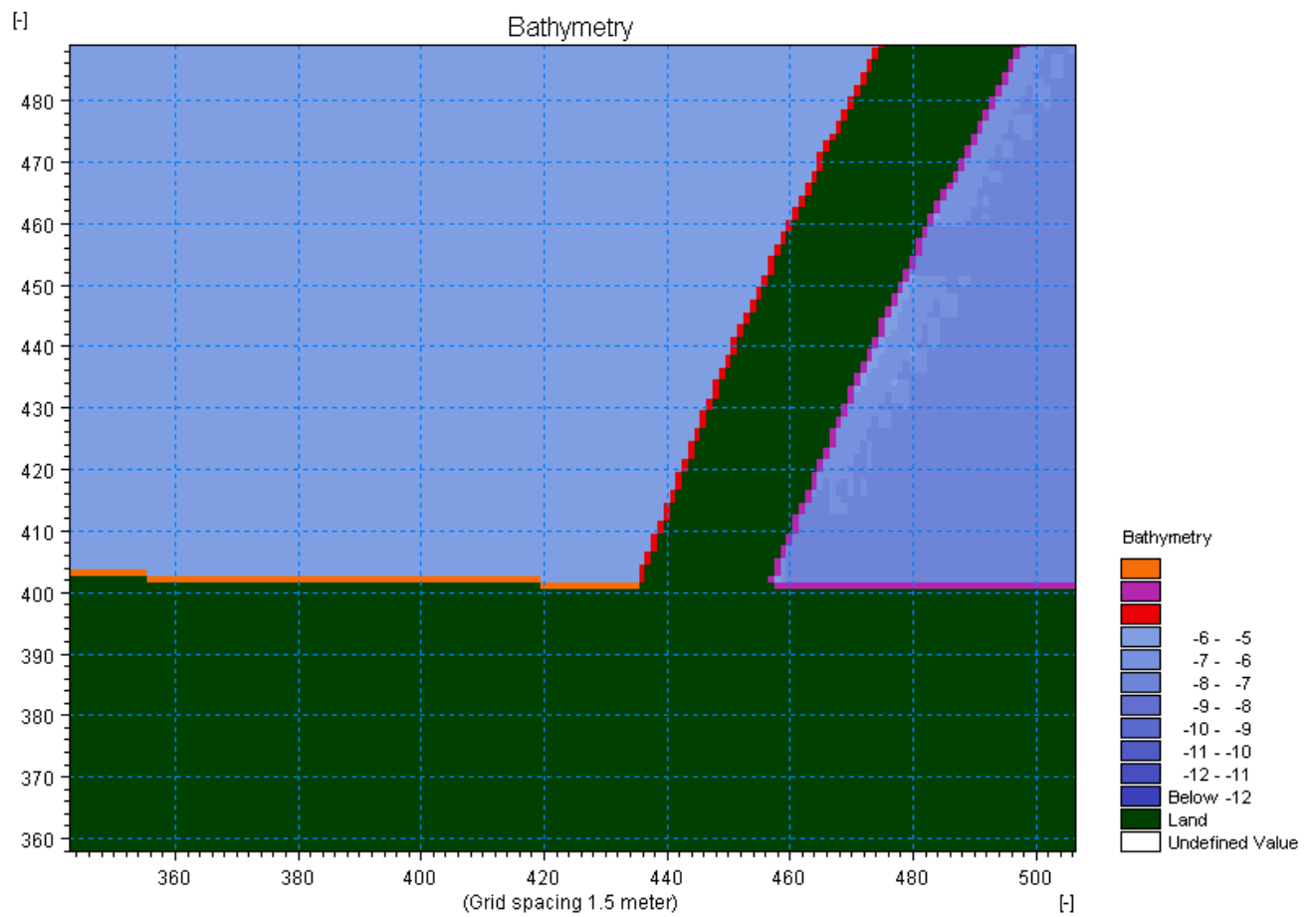


Figure 29 View of the breakwater joint with coast. Different edge values. Generated by Mike Zero software.

	430	431	432	433	434	435	436	437	438
426	-5	-5	-5	-5	-5	-5	-5	-5	-5
425	-5	-5	-5	-5	-5	-5	-5	-5	-5
424	-5	-5	-5	-5	-5	-5	-5	-5	-5
423	-5	-5	-5	-5	-5	-5	-5	-5	-5
422	-5	-5	-5	-5	-5	-5	-5	-5	-5
421	-5	-5	-5	-5	-5	-5	-5	-5	-5
420	-5	-5	-5	-5	-5	-5	-5	-5	-5
419	-5	-5	-5	-5	-5	-5	-5	-5	-5
418	-5	-5	-5	-5	-5	-5	-5	-5	-5
417	-5	-5	-5	-5	-5	-5	-5	-5	-5
416	-5	-5	-5	-5	-5	-5	-5	-5	-5
415	-5	-5	-5	-5	-5	-5	-5	-5	-5
414	-5	-5	-5	-5	-5	-5	-5	-5	-5
413	-5	-5	-5	-5	-5	-5	-5	-5	-5
412	-5	-5	-5	-5	-5	-5	-5	-5	-5
411	-5	-5	-5	-5	-5	-5	-5	-5	-5
410	-5	-5	-5	-5	-5	-5	-5	-5	-5
409	-5	-5	-5	-5	-5	-5	-5	-5	8
408	-5	-5	-5	-5	-5	-5	-5	-5	8
407	-5	-5	-5	-5	-5	-5	-5	-5	8
406	-5	-5	-5	-5	-5	-5	-5	8	10
405	-5	-5	-5	-5	-5	-5	-5	8	10
404	-5	-5	-5	-5	-5	-5	8	10	10
403	-5	-5	-5	-5	-5	-5	8	10	10
402	-5	-5	-5	-5	-5	-5	8	10	10
401	5	5	5	5	5	5	10	10	10
400	10	10	10	10	10	10	10	10	10
399	10	10	10	10	10	10	10	10	10
398	10	10	10	10	10	10	10	10	10
397	10	10	10	10	10	10	10	10	10
396	10	10	10	10	10	10	10	10	10
395	10	10	10	10	10	10	10	10	10
394	10	10	10	10	10	10	10	10	10
393	10	10	10	10	10	10	10	10	10
392	10	10	10	10	10	10	10	10	10

Figure 30 Dialog window from Bathymetry Grid Editor, view on a place where breakwater connects with the coast. Generated by Mike Zero Bathymetry Editor.

Figures 31 and 32 show visualization of the first layout. All presented concepts of the new breakwater layout at Chapter 2 point 4 were made in the same way. Their final shapes are shown at the end of this section.

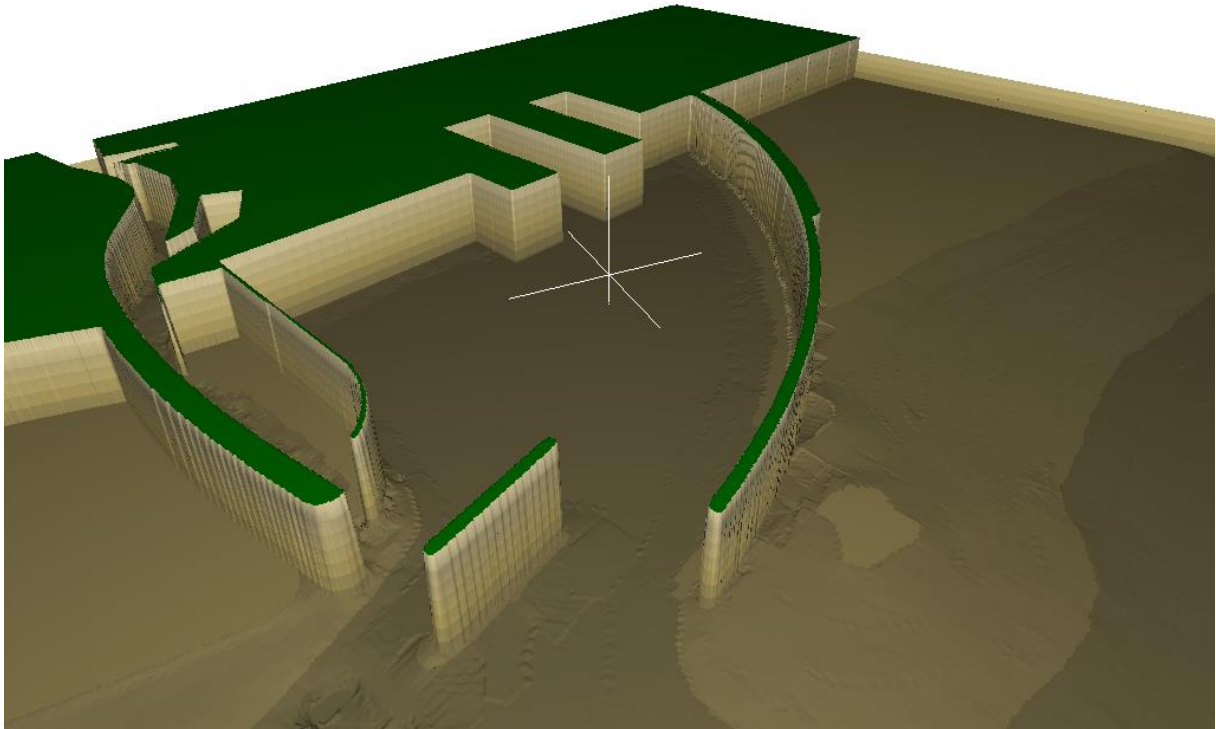


Figure 31 Visualization of the first concept. View from the north-east. Generated by Mike Animator Plus.

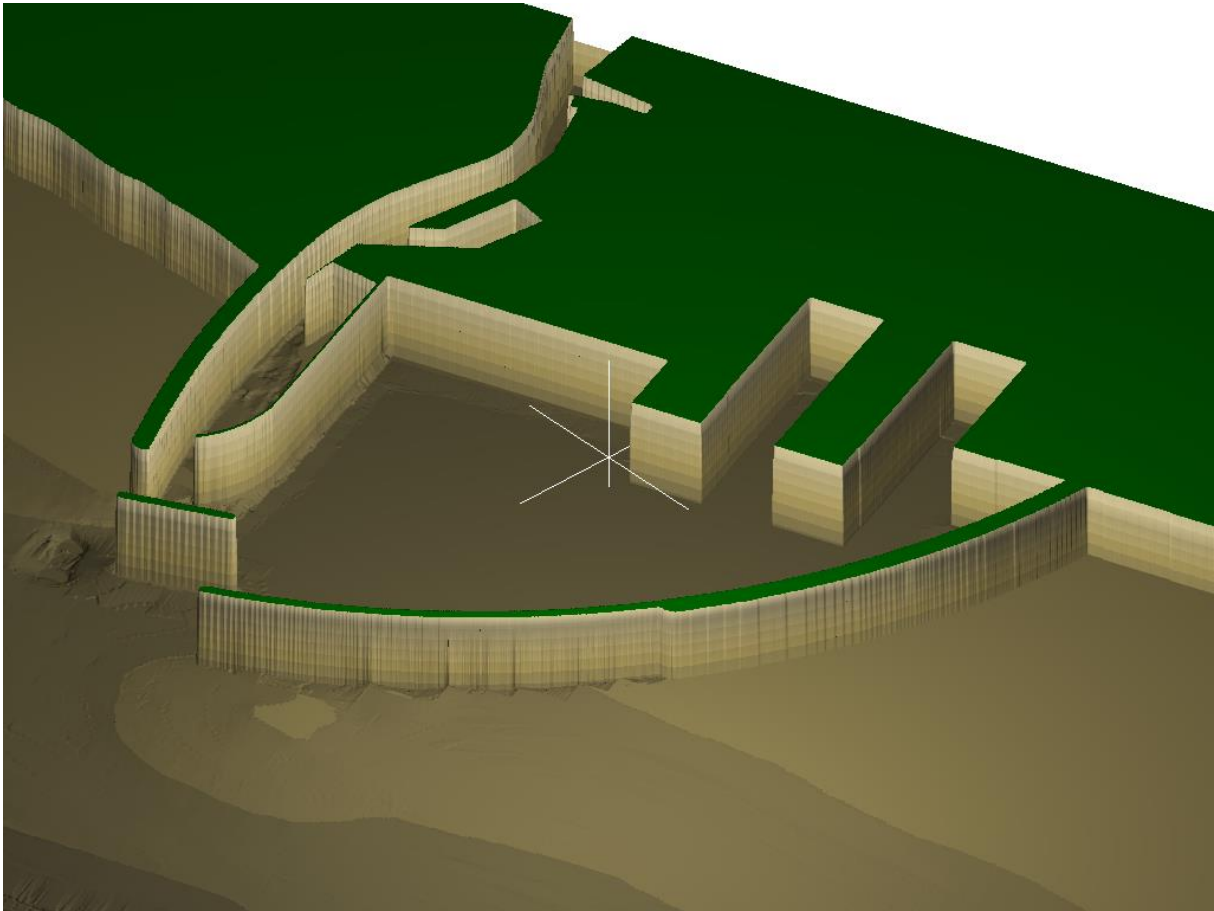


Figure 32 Visualization of the first concept. View from the north-west. Generated by Mike Animator Plus.

After properly defined bathymetry sponge and porous layers were made using Mike Zero Toolbox. It is an easy process that depends on assigning proper reflection value to the edge values described above. Thus for rip-rap layer 85% of reflection was assumed and for concrete reflective walls 99% of reflection was set in order to avoid numerical instabilities caused by total reflection. Sponge layer was made similarly but with a small exception. Based on user guide Mike 21 BW (2016) appropriate absorption of the wave occurs when thickness of the sponge layer (artificial beach) is equal to one or two wave lengths. Deep water wave with peak period 9.8s according to Eq. (5.7) has length 149.8m. Dividing it by resolution equal to 1.5m gives 99.86 grid points of sponge (layers). Figure 33 shows a table from Mike Zero Toolbox user guide with suggested values for sponge layer. According to those values and also to ensure numerical stability 200 layers was applied with base value 'a' equal to 10 and power value 'r' set to 0.95.

$$\lambda = 1.56 \cdot T^2 \quad (5.7)$$

Such a number of layers ensures that the wave dissipates gradually with propagation in the sponge.

Table 25.1 Recommended values for sponge layer coefficients

N_{sponge}	a	r
10	5	0.5
20	7	0.7
50	10	0.85
100	10	0.92
200	10	0.95

Figure 33 Recommended values for sponge layer coefficients. Source: Mike Toolbox user guide.

Next two Figures 34 and 35 shows visualization of created sponge layer (orange) and porosity respectively.

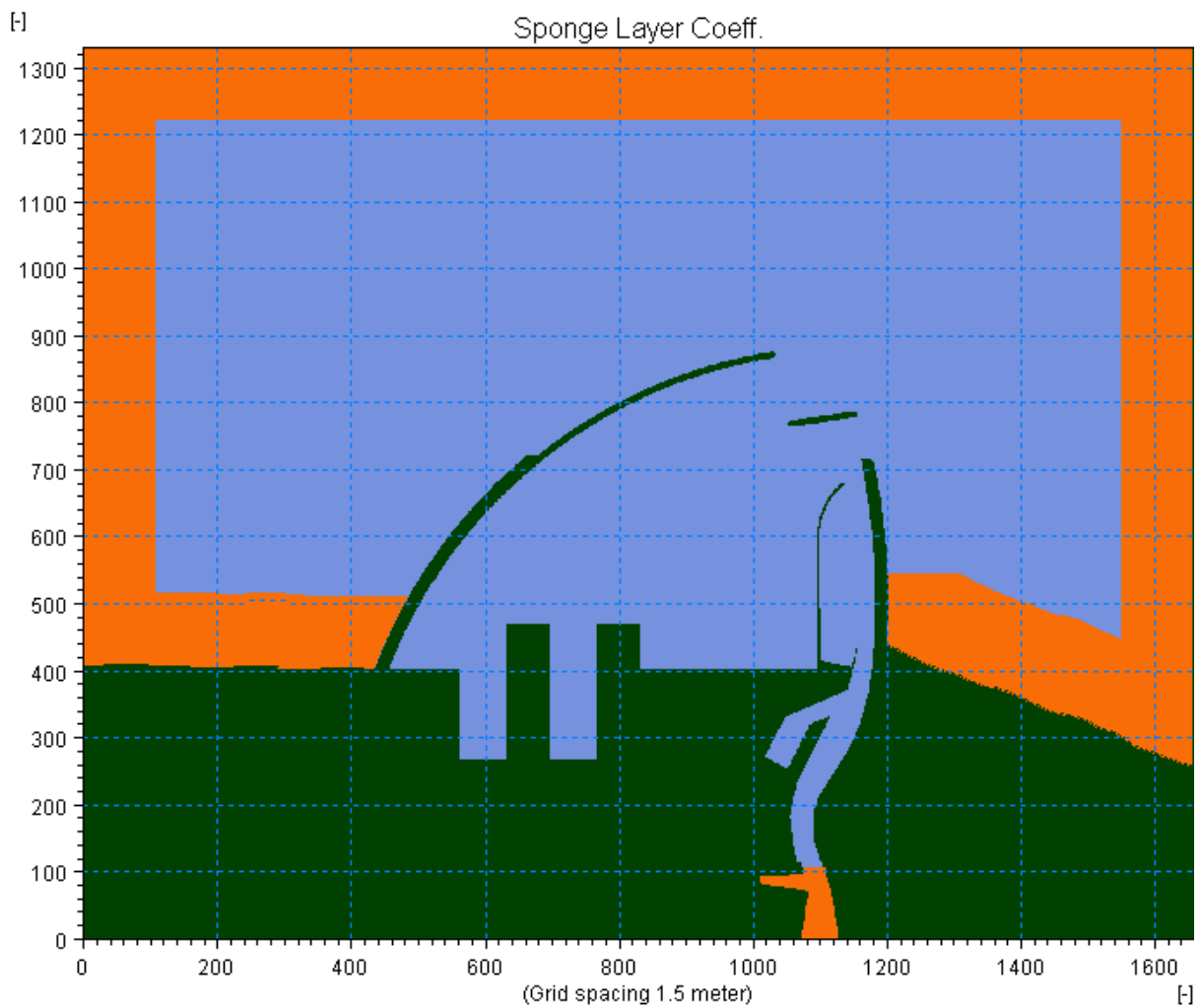


Figure 34 Visualization of the sponge layer. Generated by Mike Zero software.

Colour red symbolized rip-rap layer with dissipation factor equal to 15% and purple colour symbolize concrete walls with 1% dissipation factor as described before.

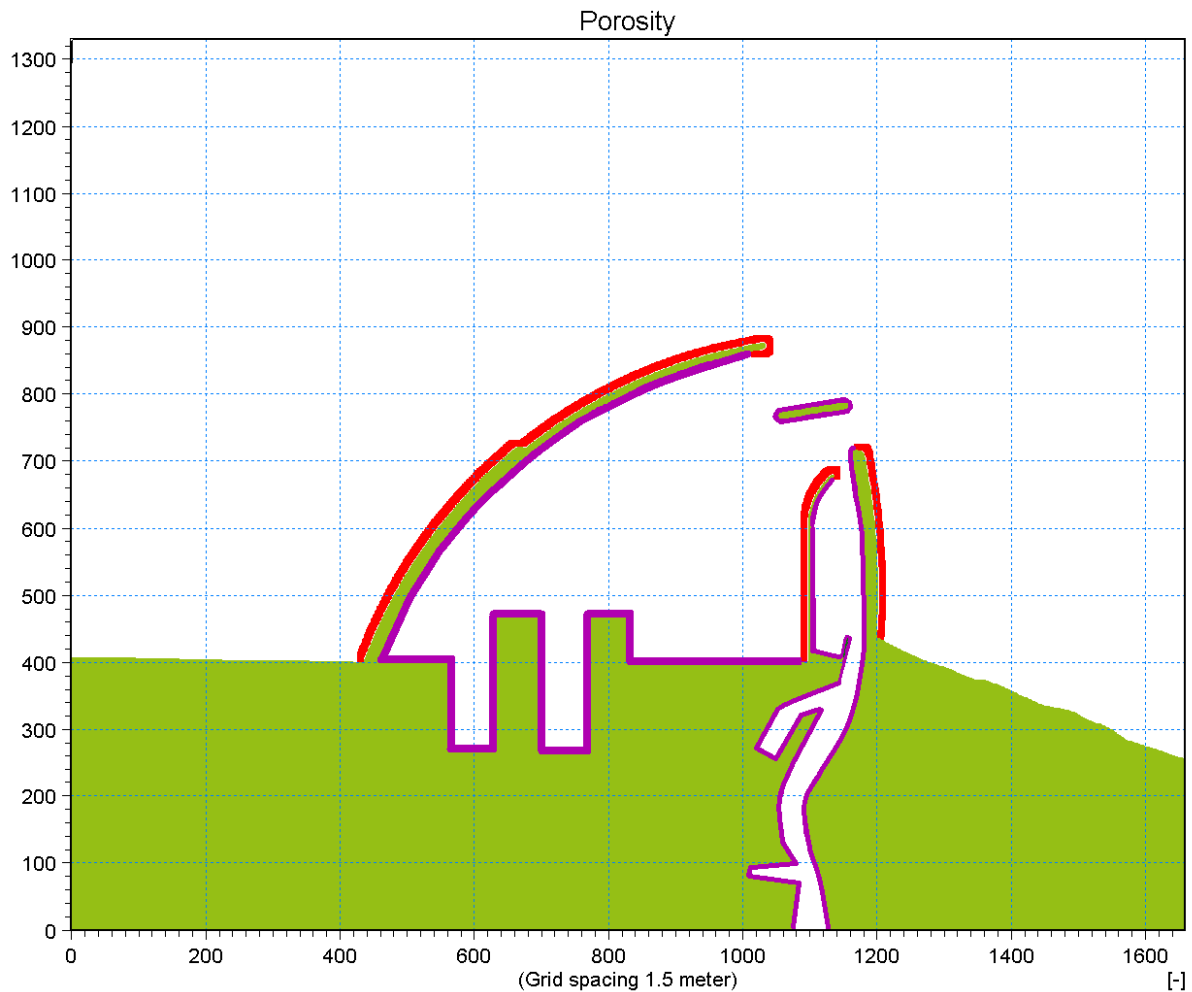


Figure 35 Visualization of the porosity layer. Generated by Mike Zero software.

5.3.2. Boundary Conditions

As it was mentioned before, results from Spectral Wave model were used as an input to Boussinesq Wave model. Based on them the main wave direction from where the highest waves come from is assumed northwest (308.91° clockwise from north), the significant wave height is equal to 2.5m and peak period 9.8s. It was found that with the proposed shapes of breakwater, highest waves from the northwest may not cause unfavourable conditions in the harbour basin. Therefore, it was decided to make an additional simulation of waves propagating from the northeast with the following parameters: significant wave height 1.07m peak period 7.7s. and direction 30.67° (clockwise from the north). These values were also obtained from the SW simulation.

To properly setup the above mentioned boundary conditions Random Wave Generator from Mike 21 Toolbox was used (Figure 36). It creates internal generation line (forcing line) with JONSWAP spectrum that reproduce realistic conditions for developing storm. The advantage of using generation line is that can be placed in the front of the sponge layer to absorb waves leaving the model. What is more, the position of the line should be parallel to X or Y-axis and the water depth should be the most constant as possible.

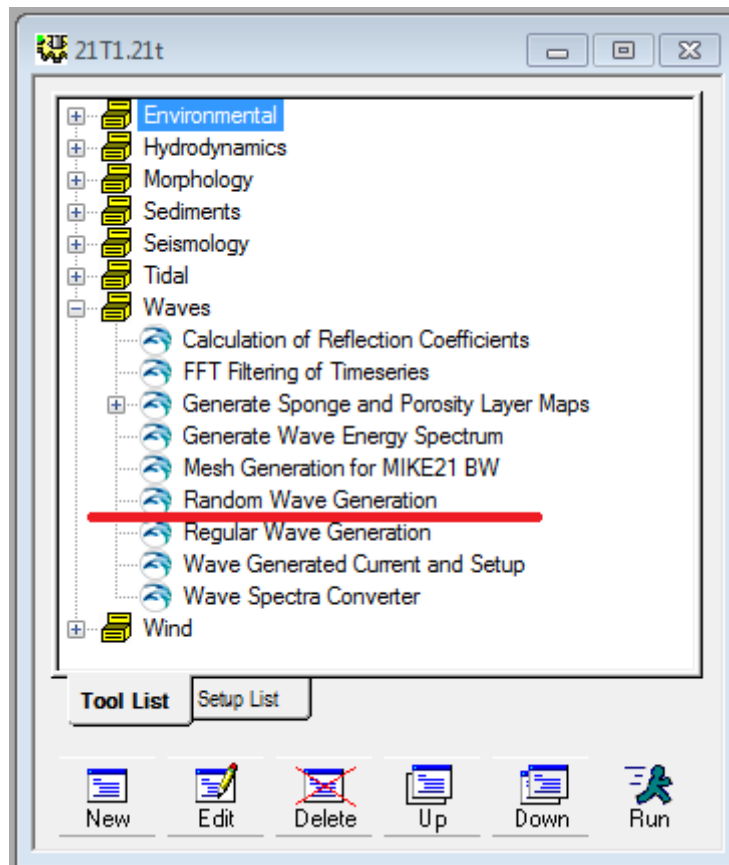


Figure 36 Mike Zero - Random Wave Generator.

For the purpose of simulation of waves from northwest one generation line was used on the northern boundary (black line, see Fig. 37). Due to size of domain and probability that one line will not generate enough waves that enter into harbour basin for waves coming from northeast two generation lines were used on northern and eastern boundary (black and white line).

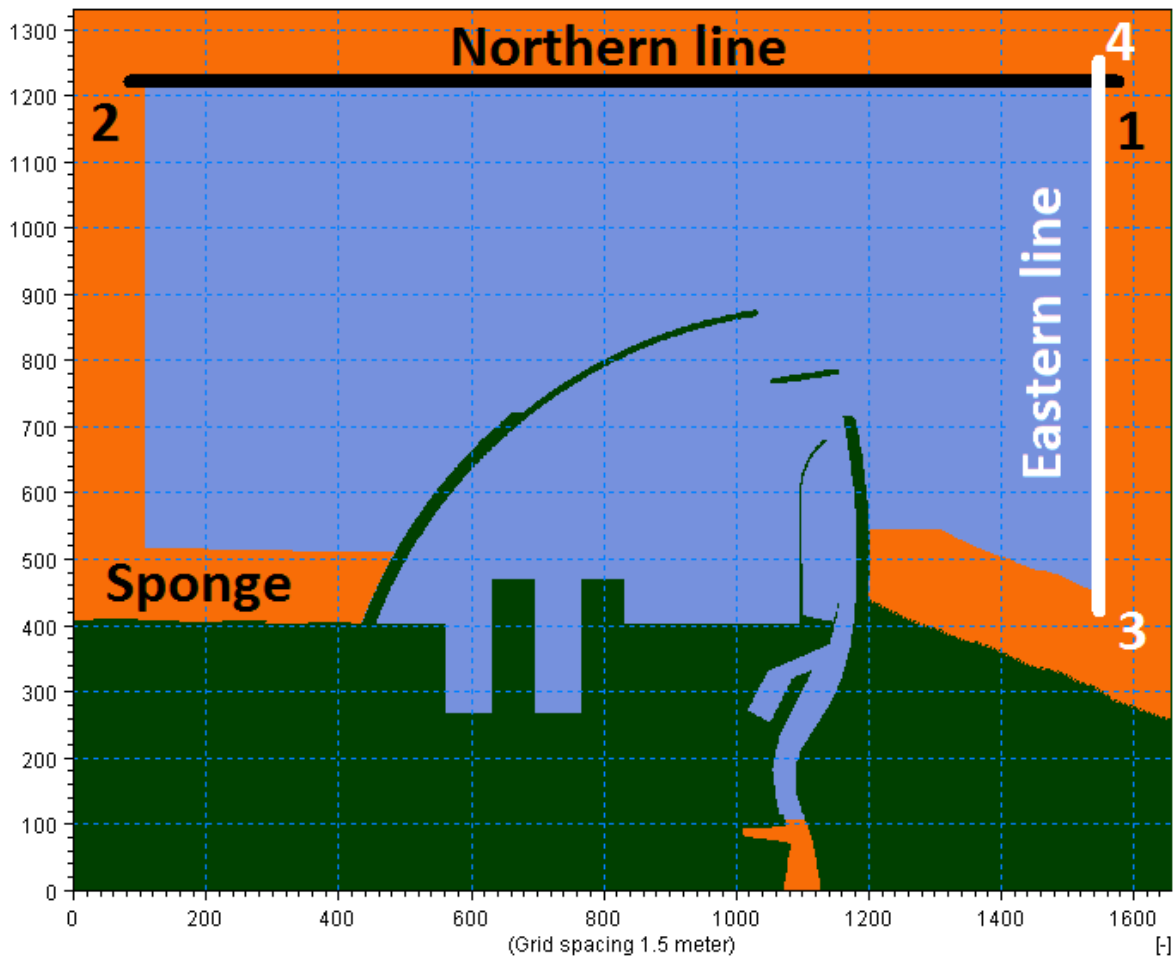


Figure 37 Position of the generating lines. Created by Mike Zero software.

Figure 37, shown above, presents position of mentioned generation lines. As recommended in the Mike 21 BW manual for the placing of generation lines points 1 and 3 were set as a starting points, and 2 and 3 set as ending points of northern and eastern generation line respectively. In order to obtain stable and not deformed solution lines have been "nested" inside sponge layer (i.e. starting and ending points are inside sponge layer instead of being placed at the edge between water and sponge). During setting model one should keep in mind to properly define the angle of propagation. Figure 38 shows right convention.

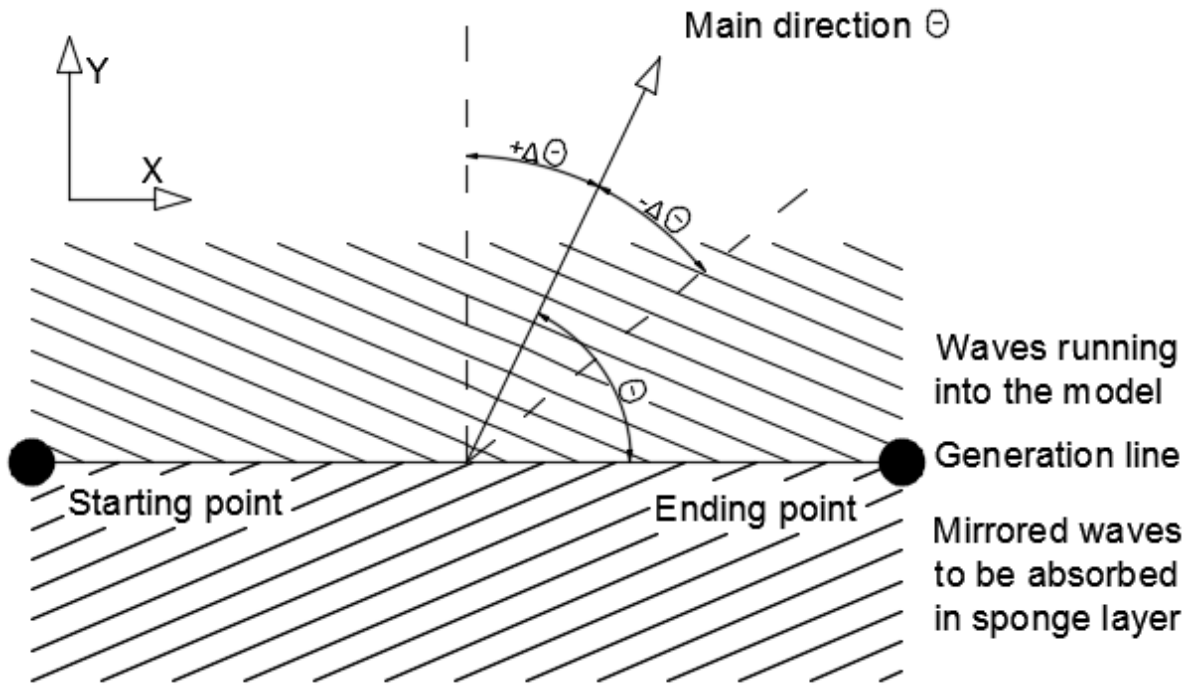


Figure 38 Angle convention. Source: Mike 21 BW User Guide.

To benchmark the results, simulation with regular wave was run. In this case generation line was made at the northern boundary using Mike 21 Toolbox Regular Wave Generator. Summary of all parameters relating to generating lines are presented below in Table 7.

Table 7 Summary of prepared generation lines

Regular Wave Generator	
Waves from north	
Parameter	Value
Number of lines	1
Location	Northern boundary: Starting point: (1159, 1228) cell; (1740, 1843.5) m End point: (100, 1228) cell; (151.5, 1843.5) m
Type of wave	One-dimensional
Theory	Boussinesq Order: 1
Dispersion parameter	Default value: 0.067
Wave characteristic	H=1 m T=9.8 s Depth=10 m
Discretisation parameters	No. of time steps: 15 000 $t_s=0.1$ s Simulation period: 25 min.
Random Wave Generator	
Waves from northwest	
Number of lines	1
Location	Northern boundary:

	Starting point: (1558, 1128) cell; (2338.5, 1693.5) m End point: (101, 1228) cell; (153, 1693.5) m
Type of frequency spectrum	Jonswap, defined by H_s , T_p , and γ $H_s=2.5$ m $T_p=9.8$ s Shape parameter (default value): $\gamma: 3.3$ $\sigma_a: 0.07$ $\sigma_b: 0.09$
Type of wave	Directional
Initial random number	100
Water depth	$d=10$ m
Smallest wave period	4 s
Grid spacing	1.5x1.5 m
Rescale truncated spectrum	Enclosed
Second order correction	Neglected
Discretisation parameters	No. of time steps: 15 000 $t_s=0.1$ s Simulation period: 25 min.
Convention of angles	Scientific / BW
Type of directional distribution	\cos^n (dir-main dir.)
Spreading parameters	Main direction: 308.91° (clockwise from north) Max deviation from main dir.: 30 Power of cosine: $n=8$
Waves from northeast	
Number of lines	2
Location	1. Northern boundary: Starting point: (1558, 1128) cell; (2338.5, 1693.5) m End point: (101, 1228) cell; (153, 1693.5) m 2. Eastern boundary Starting point: (1458, 600) cell; (2188.5, 901.5) m End point: (1458, 1228) cell; (2188.5, 1693.5) m
Type of frequency spectrum	Jonswap, defined by H_s , T_p , and γ $H_s=1.07$ m $T_p=7.7$ s Shape parameter (default value): $\gamma: 3.3$ $\sigma_a: 0.07$ $\sigma_b: 0.09$
Type of wave	Unidirectional (due to two generation lines)
Initial random number	100
Water depth	$d=10$ m
Smallest wave period	4 s
Grid spacing	1.5x1.5
Rescale truncated spectrum	Enclosed

Second order correction	Neglected
Discretisation parameters	No. of time steps: 15 000 t _s =0.1 s Simulation period: 25 min.
Convention of angles	Scientific / BW
Type of directional distribution	cos ⁿ (dir-main dir.)
Spreading parameters	Main direction: 1. Northern boundary: 30.4° (clockwise from north) 2. Eastern boundary: 30.4° (clockwise from north) Max deviation from main dir.: 5 Power of cosine: n=8

Type of wave used in simulation of north-eastern waves was chosen as unidirectional. It is a recommended operation when two generation lines are used to ensure phase and direction compliance. Time step, simulation period and the smallest wave period were set according to values obtained from Setup Planner and were described in the beginning of Chapter 5.3.

5.3.3. Summary of all input data and parameters

Below are presented bathymetry files of the other three layouts. To find right setup of those models and check if bathymetry data works well with sponge and porosity layer simulation with regular wave was performed. The simplest discretisation type was used – Simple upwind differencing with time-extrapolation factor 0.7. It is an alternative discretisation method for high resolution models with grid spacing 1-2 m. The simple upwind scheme is the most dissipative scheme but still is much less than the dumping caused when backward time centering of the cross-terms is used. Time extrapolation factor less than 1 result in artificial dissipation of waves propagating with an angle to the grid. It is helpful to reduce high frequency noise and avoid blow-up model. Values less than 0.5 should not be often used and value equal to 0 for a whole domain should only be used as a last resort. Final simulations of random waves propagated from northeast and northwest were performed basing on more accurate type of discretization – Central differencing with simple upwinding at steep gradients and near land with time-extrapolation factor set to 0.9.

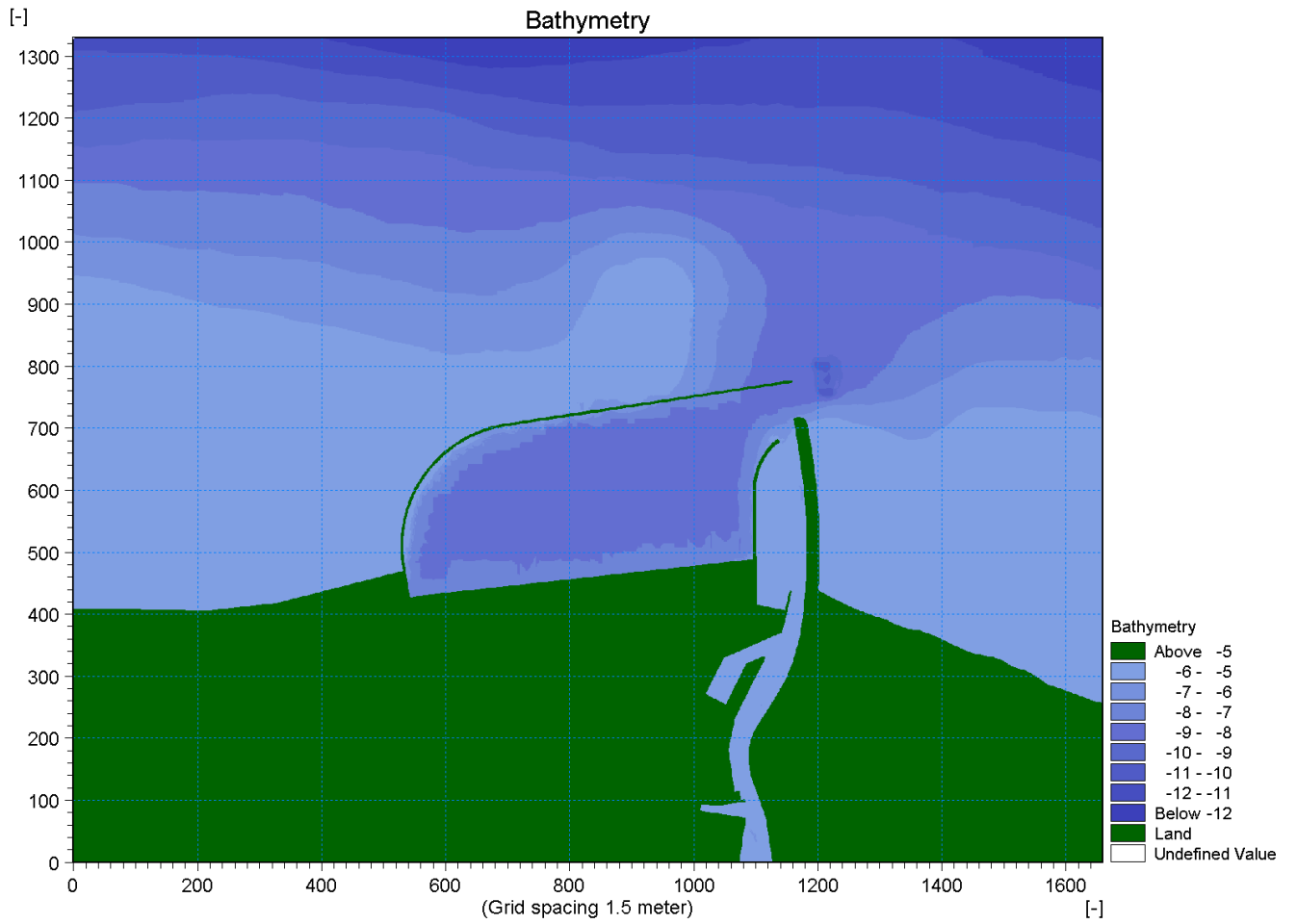


Figure 39 Bathymetry of concept no 2 with marked results points. Generated by Mike Zero software.

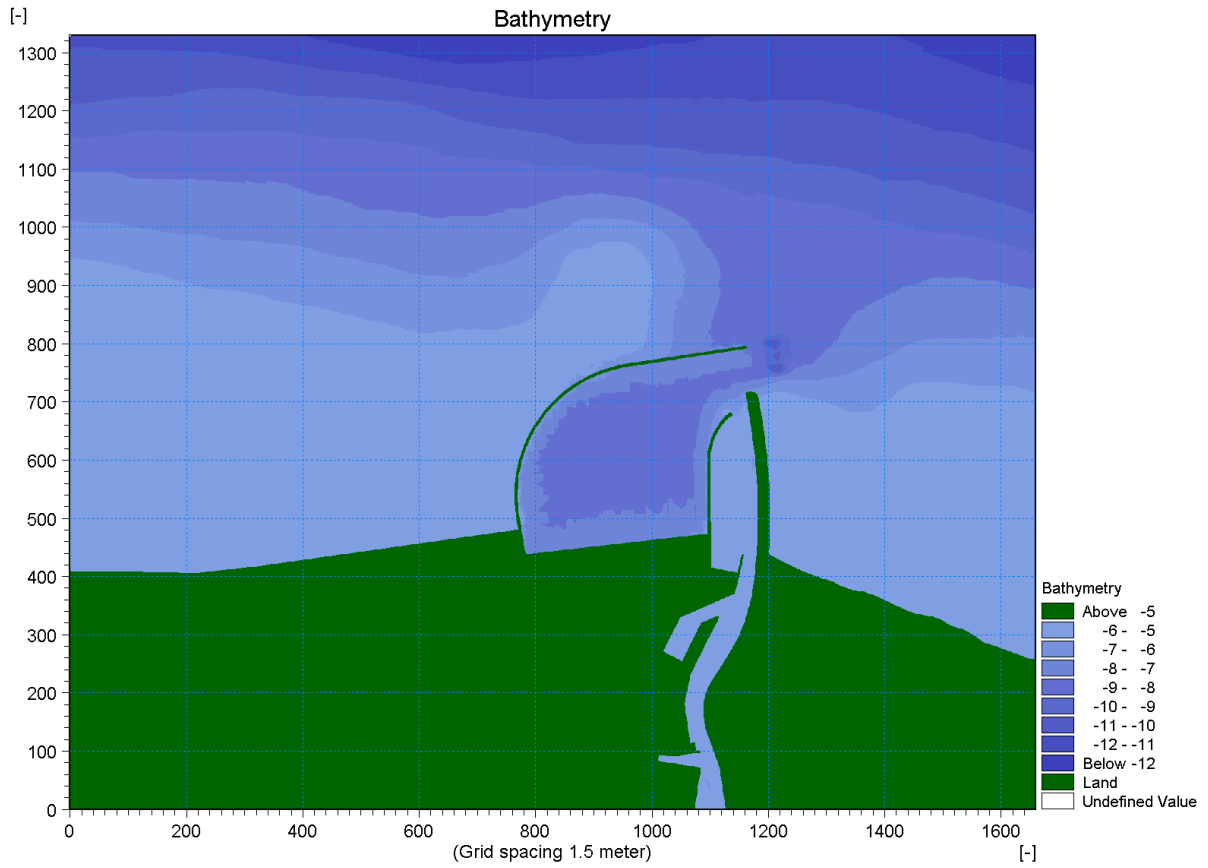


Figure 40 Bathymetry of concept no 3 with marked results points. Generated by Mike Zero software.

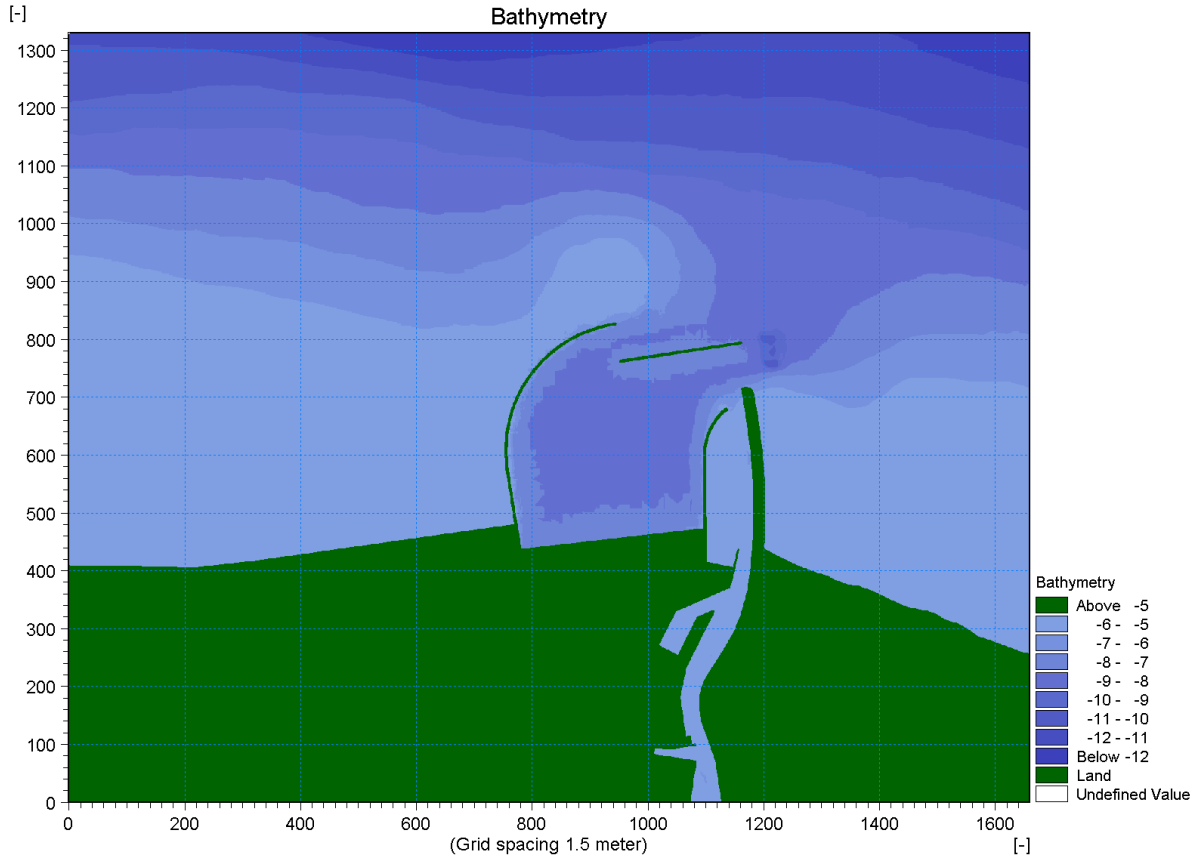


Figure 41 Bathymetry of concept no 4 with marked results points. Generated by Mike Zero software.

Below are placed three tables (Table 8-10) that contain summary of the final setup of prepared simulations.

Table 8 Final setup of simulation of regular wave.

Trial Simulation of Regular Waves	
Waves from north	
Basic Parameter	Value
Module Selection	2D Boussinesq Wave Module;
Bathymetry	Default selection – Cold Start, Concept 1 (Fig. 28);
Type of Equation	Deep Water Terms – Included; Linear dispersion factor – default value: 0.0667;
Numerical Parameters	<u>Type of discretisation:</u> Simple upwind differencing Time-extrapolation factor 0.7 <u>Depth dependent time extrapolation:</u> For depth greater than: 8 Time-extrapolation factor: 0.7
Boundary	Number of open boundaries: 0
Simulation Period	No of time steps: 15 000 Time step interval: 0.1 Simulation start time: 11.01.2015 03:00:00 Simulation end time: 11.01.2015 03:25:00
Calibration parameter	Value
Bathymetric Parameters	Land value: 10
Surface Elevation	Constant value: 0
Internal Wave Generation	Number of lines: 1 First point: (1159, 1228) Last point: (100, 1228) Type of wave: One-dimensional Theta=90 (relative to generation line; the angle shows from where the waves come from)
Bottom Friction	Excluded
Eddy Viscosity	
Filtering	
Wave Breaking	
Moving Shoreline	
Porosity	As described above (Fig. 35) <u>Porosity layer Parameters (default values):</u> Laminar resistance coef.: 1000 Turbulent resistance coef.: 2.8 Characteristic unit diameter: 0.2
Sponge	As described above (Fig. 34)
Output Parameters	Value
Deterministic Parameters	<u>Grid points</u> File type: .dfs2

	<p>Content: surface elevation, water level, flux.</p> <p><u>Time series of surface elevation at specified points:</u></p> <p>P1 (1140, 710) – Entrance to the old harbour;</p> <p>P2 (850, 630) – Central point inside the new basin;</p> <p>P3 (734, 405) – Central point of the new small basin;</p> <p>P4 (1140, 340) – Entrance to Coal Basin;</p> <p>P5 (1095, 780) – Entrance to the new harbour.</p>
--	---

Table 9 Final setup of simulation of random waves from northwest.

Simulation of Random Waves	
Waves from northwest	
Basic Parameter	Value
Module Selection	2D Boussinesq Wave Module;
Bathymetry	Default selection – Cold Start, Concept 1 (Fig. 28), Concept 2 (Fig. 39), Concept 3 (Fig. 40), Concept 4 (Fig. 41)
Type of Equation	Deep Water Terms – Included; Linear dispersion factor – default value: 0.0667;
Numerical Parameters	<u>Type of discretisation:</u> Central differencing with simple upwinding at steep gradients and near land Time-extrapolation factor: 0.9 <u>Depth dependent time extrapolation:</u> For depth greater than: 6 Time-extrapolation factor: 0.8
Boundary	Number of open boundaries: 0
Simulation Period	No of time steps: 15 000 Time step interval: 0.1 Simulation start time: 11.01.2015 03:00:00 Simulation end time: 11.01.2015 03:25:00
Calibration parameter	Value
Bathymetric Parameters	Land value: 10
Surface Elevation	Constant value: 0
Internal Wave Generation	Number of lines: 1 First point: (1558, 1128) Last point: (101, 1128) Type of wave: Directional Theta=308.91° (clockwise from north; from where the waves come from)
Bottom Friction	Excluded
Eddy Viscosity	
Filtering	
Wave Breaking	

Moving Shoreline	
Porosity	As described above (Fig. 35) <u>Porosity layer Parameters (default values):</u> Laminar resistance coef.: 1000 Turbulent resistance coef.: 2.8 Characteristic unit diameter: 0.2
Sponge	As described above (Fig. 34)
Output Parameters	Value
Deterministic Parameters	<u>Grid points</u> File type: .dfs2 Obtained value every 150 time steps (15 s) Content: surface elevation, water level, flux. <u>Time series of surface elevation at specified points:</u> P1 (790, 795) – Centre point of the new break water; P2 (1140, 710) – Entrance to old harbour, P3 (850, 630) – Central point inside the new basin; P4 (734, 405) – Point near the new quay; P5 (1140, 340) – Entrance to Coal Basin; P6 (1095, 780) – Entrance to the new harbour.

Table 10 Final setup of simulation of random waves from northeast.

Simulation of Random Waves	
Waves from northeast	
Basic Parameter	Value
Module Selection	2D Boussinesq Wave Module;
Bathymetry	Default selection – Cold Start, Concept 1 (Fig. 28), Concept 2 (Fig. 39), Concept 3 (Fig. 40), Concept 4 (Fig. 41)
Type of Equation	Deep Water Terms – Included; Linear dispersion factor – default value: 0.0667;
Numerical Parameters	<u>Type of discretisation:</u> Central differencing with simple upwinding at steep gradients and near land Time-extrapolation factor: 0.9 <u>Depth dependent time extrapolation:</u> For depth greater than: 6 Time-extrapolation factor: 0.8
Boundary	Number of open boundaries: 0
Simulation Period	No of time steps: 15 000 Time step interval: 0.1 Simulation start time: 11.01.2015 03:00:00 Simulation end time: 11.01.2015 03:25:00
Calibration parameter	Value

Bathymetric Parameters	Land value: 10
Surface Elevation	Constant value: 0
Internal Wave Generation	<p>Number of lines: 2</p> <p><u>1. Northern line:</u> First point: (1458, 1128) Last point: (101, 1128) Type of wave: Directional Theta=30.4° (clockwise from north; from where the waves come from).</p> <p><u>2. Eastern line:</u> First point: (1458, 600) Last point: (1458, 1128) Type of wave: Directional Theta=30.4° (clockwise from north; from where the waves come from).</p>
Bottom Friction	Excluded
Eddy Viscosity	
Filtering	
Wave Breaking	
Moving Shoreline	
Porosity	<p>As described above (Fig. 35)</p> <p><u>Porosity layer Parameters (default values):</u> Laminar resistance coef.: 1000 Turbulent resistance coef.: 2.8 Characteristic unit diameter: 0.2</p>
Sponge	As described above (Fig. 34)
Output Parameters	Value
Deterministic Parameters	<p><u>Grid points</u> File type: .dfs2 Obtained value every 150 time steps (15 s) Content: surface elevation, water level, flux.</p> <p><u>Time series of surface elevation at specified points:</u> P1 (790, 795) – Centre point of the new break water; P2 (1140, 710) – Entrance to old harbour, P3 (850, 630) – Central point inside the new basin; P4 (734, 405) – Central point of the new small basin; P5 (1140, 340) – Entrance to Coal Basin; P6 (1095, 780) – Entrance to the new harbour.</p>

6. RESULTS AND DISCUSSION

In this chapter results from simulations described in Chapter 5 are presented. The first part contains results from Spectral Wave Model without including water level conditions and currents. Afterwards results from the model involving tides and currents are presented. In the next subsection there is a discussion and comparison of the results from Spectral Wave Model in which changing of the surface elevation and influence of the current were taken into account. Here it is pointed which kind of waves play significant role in creation of the sea state. Next part of this chapter consists of results from Boussinesq Wave Model Simulations where different breakwater layouts were checked. At the end there is a comparison of the calculated wave conditions inside the four proposed breakwater layouts.

6.1. Spectral Wave Model

The following section contains plotted results of MIKE 21 SW calculations. Figures 42, 43 and 44 show significant wave heights and peak periods of calculated wave spectra for the whole domain respectively. The vectors on Figures 42 and 45 indicate the direction of wave propagation.

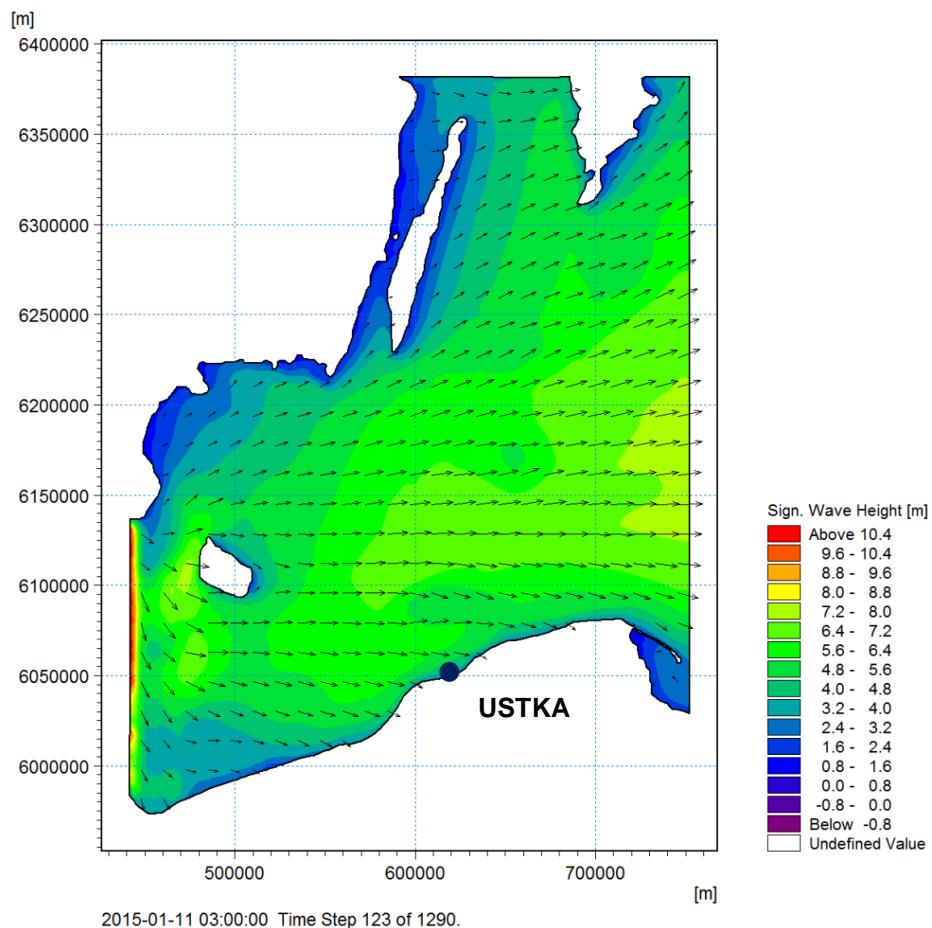


Figure 42 Model domain showing significant wave height and wave vectors.

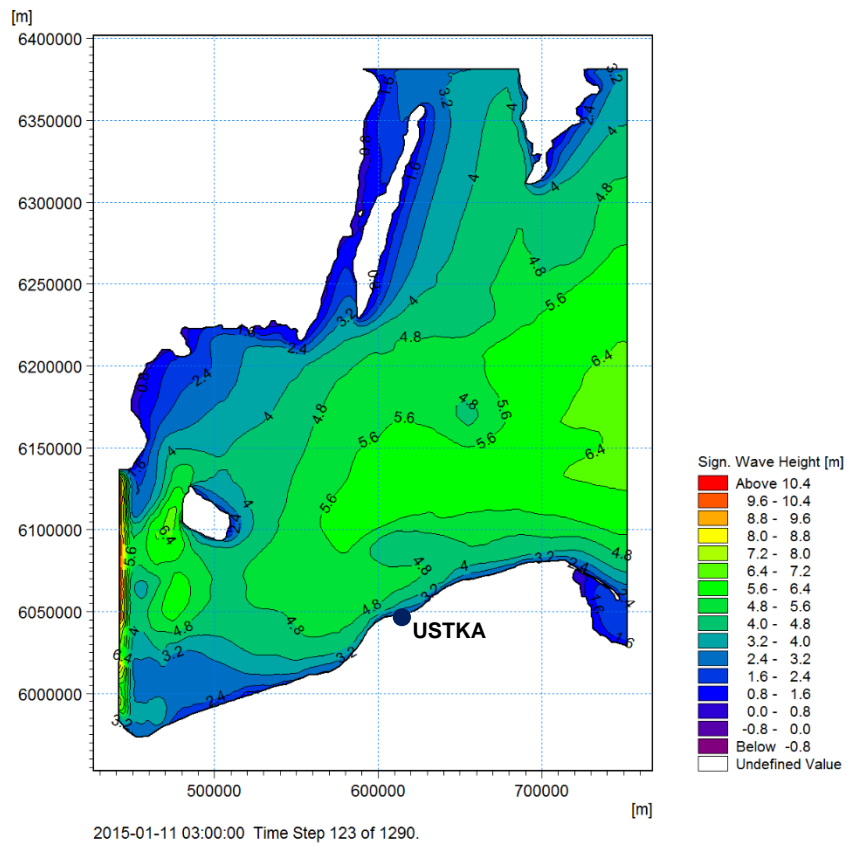


Figure 43 Model domain showing isolines with significant wave height.

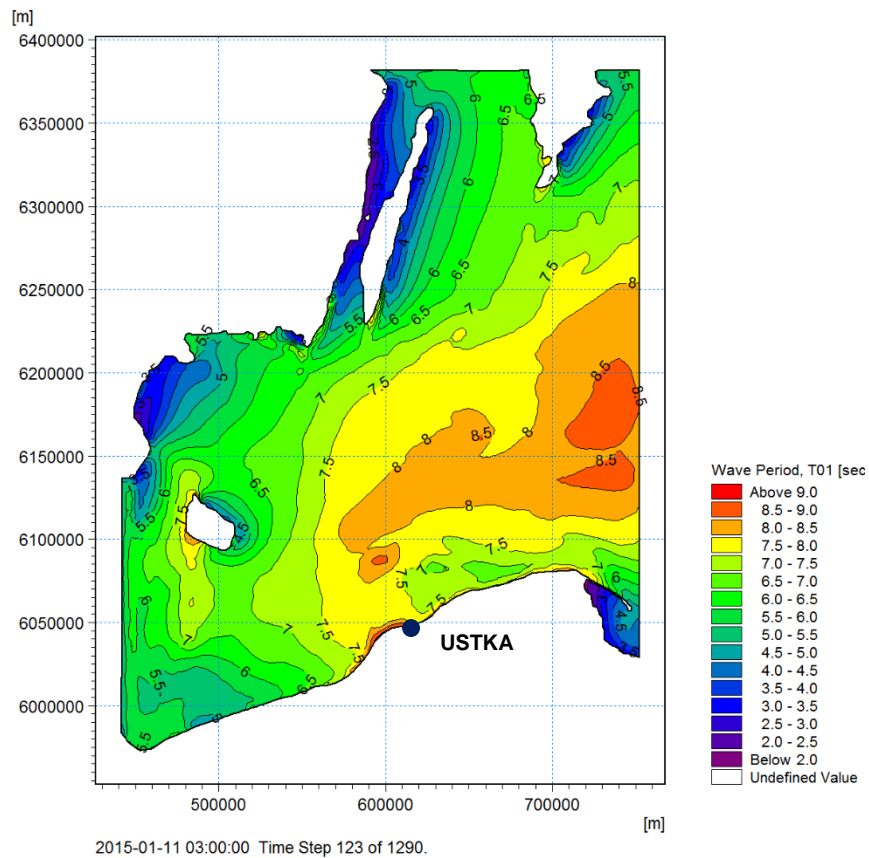


Figure 44 Model domain showing wave period T_{01} .

Next three figures (Figures 45,46,47) present the close-up to the area of interest and also give the information about significant wave height and period.

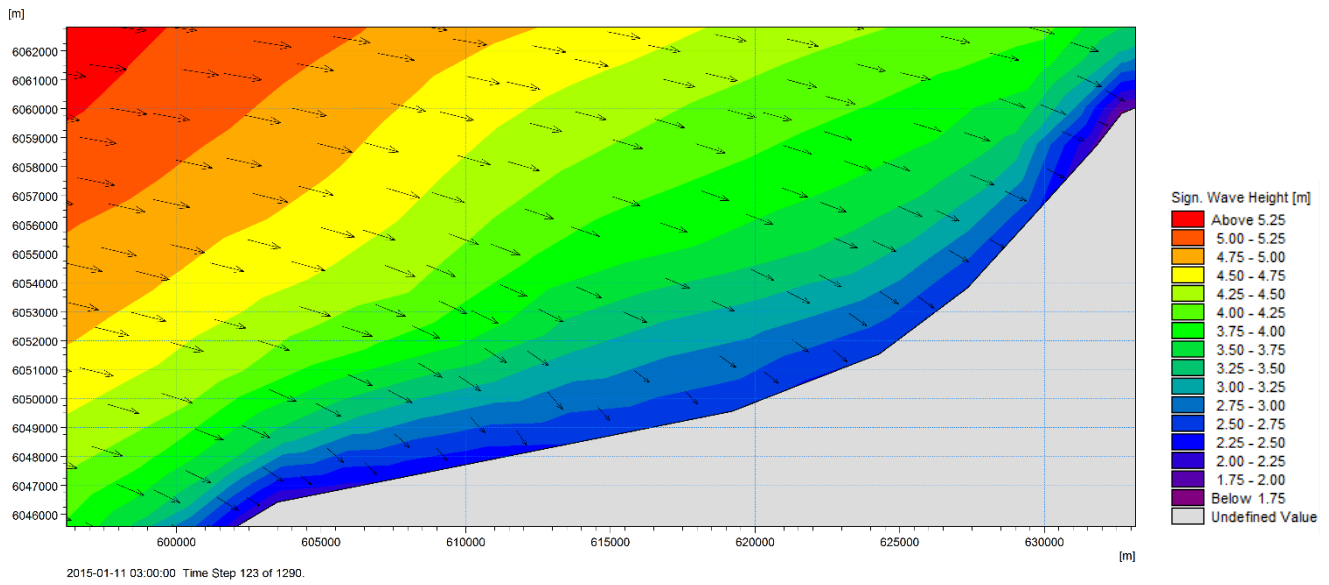


Figure 45 Plot of the area of interest showing significant wave height and wave vectors. Wave refraction can be easily seen.

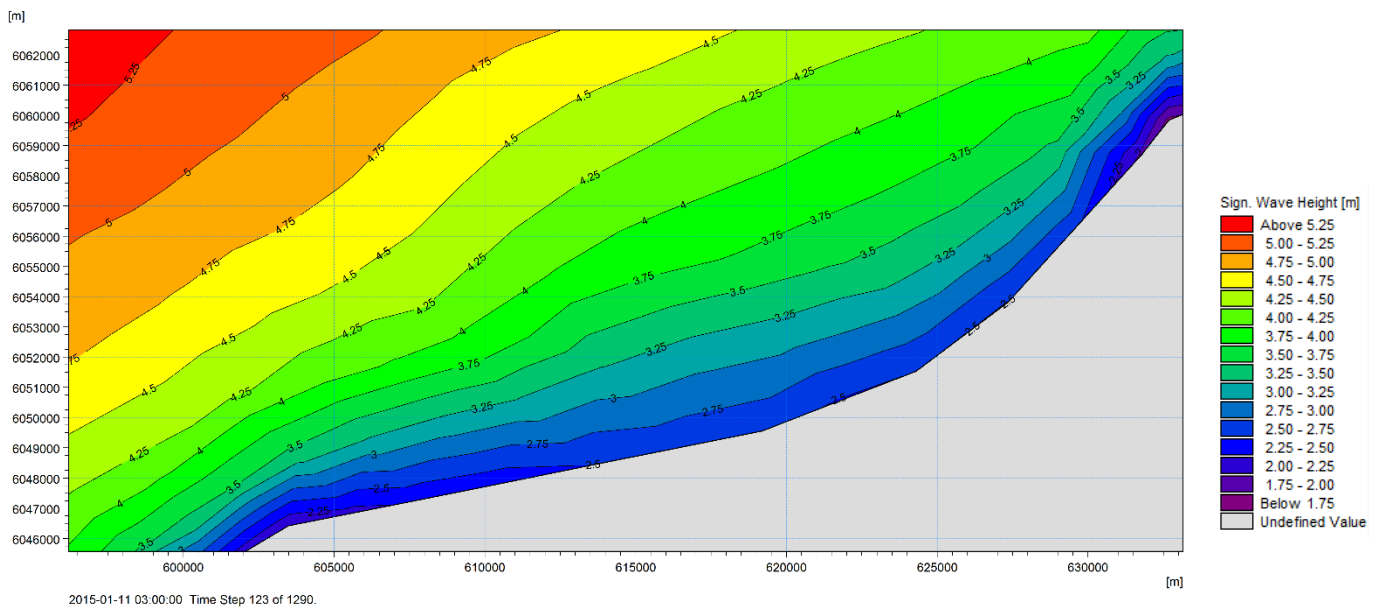


Figure 46 Plot of the area of interest showing significant wave height (isolines).

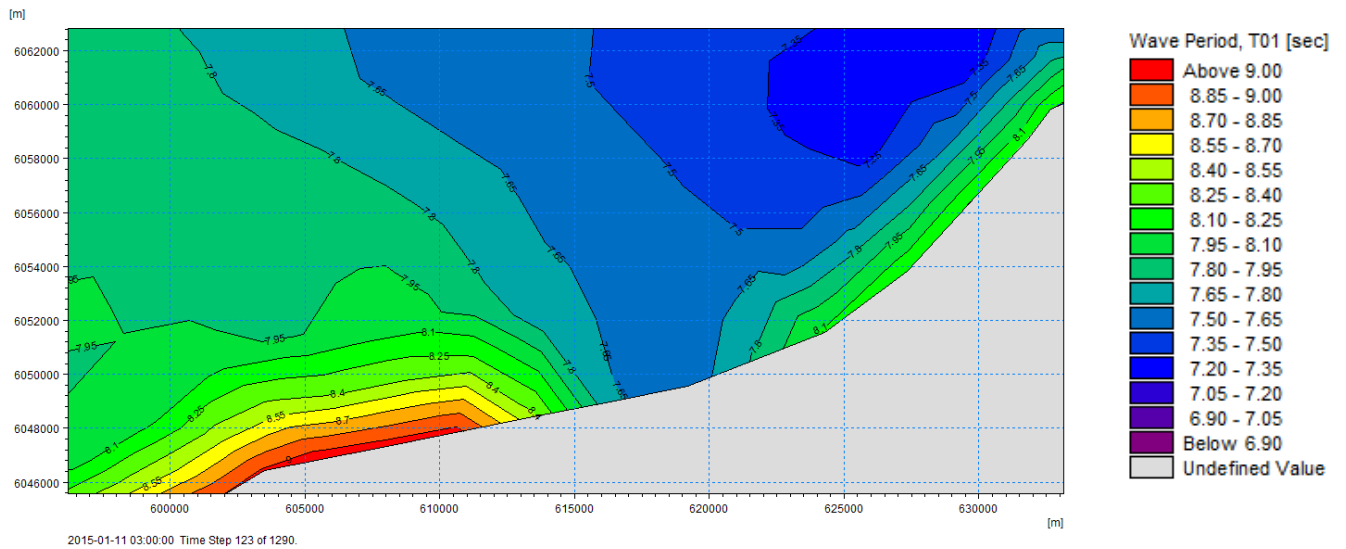


Figure 47 Plot of the area of interest showing wave period T_{01}

Near the harbour in Ustka during simulation period significant wave height vary from 0.1 m and up to 2.5 m, and wave period T_{01} changes from 1.8 to 6.8 seconds. These variations are shown in the time series of the point located at coordinates of the head of eastern breakwater. The two time series are presented on Figures 48 and 49.

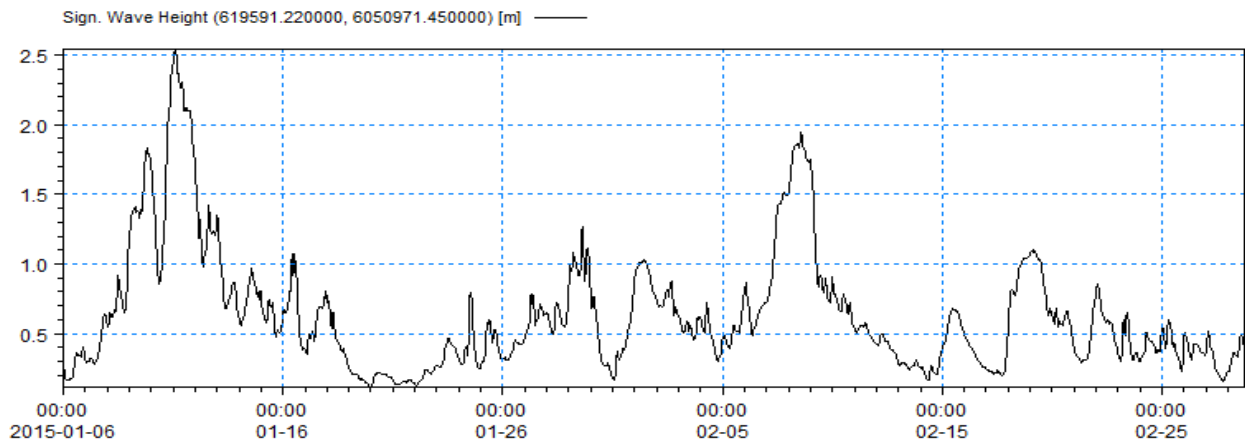


Figure 48 Time series showing significant wave height at the location of the head of the eastern breakwater

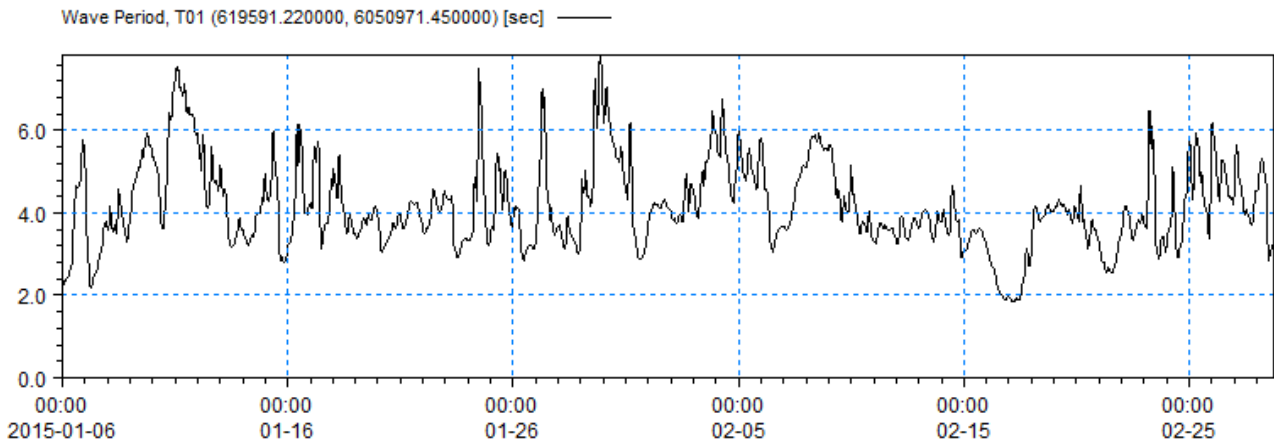


Figure 49 Time series showing wave period T_{01} at the location of the head of the eastern breakwater

6.2. Spectral Wave Model + HD

The following section contains plotted results of MIKE 21 SW+ Hydrodynamic calculations. Figures 50, 52 and 52 show significant wave heights and periods of calculated wave spectra for the whole domain. The vectors on Figures 50 and 53 indicate the direction of wave propagation.

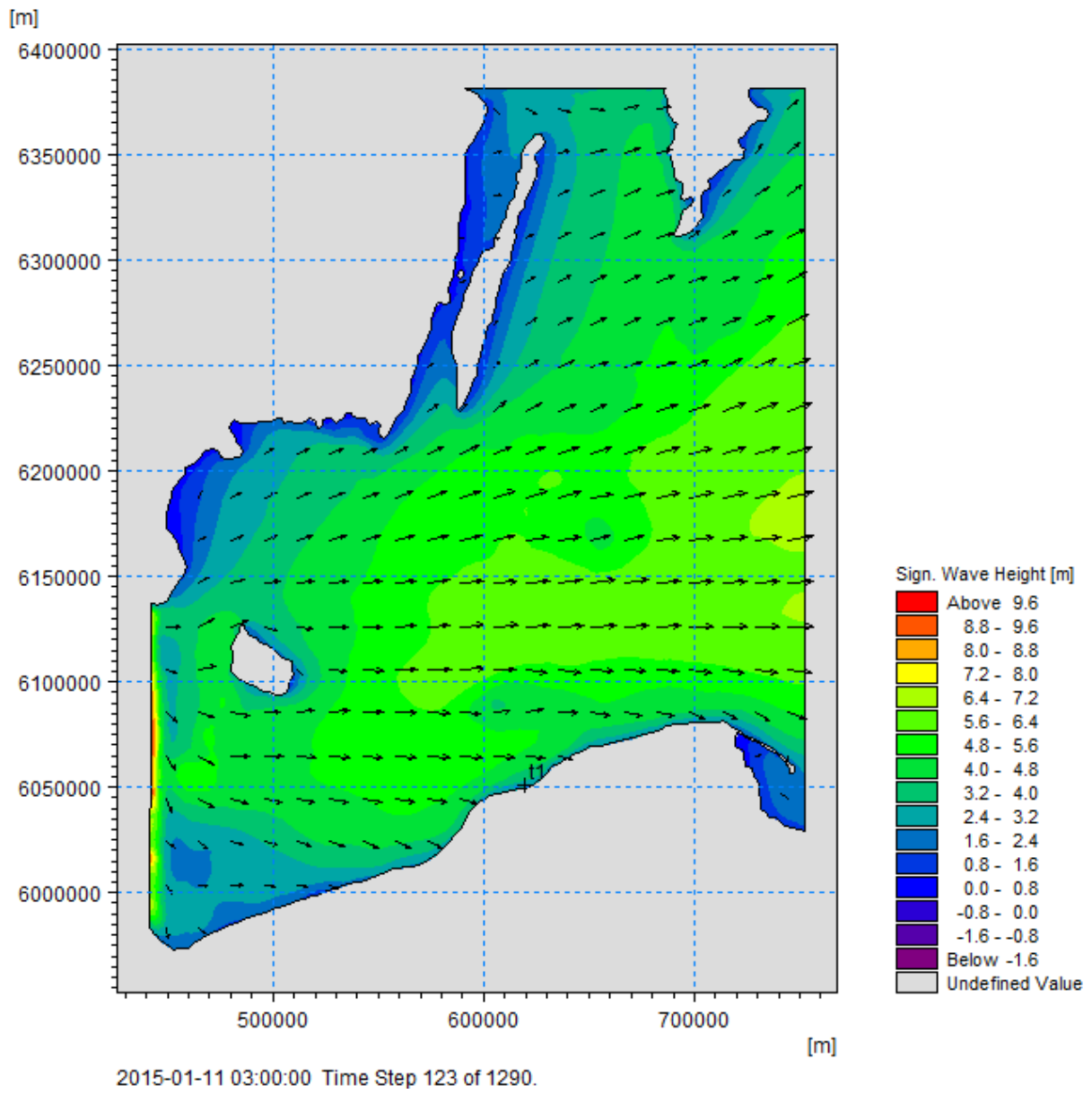


Figure 50 Model domain showing significant wave height and wave vectors.

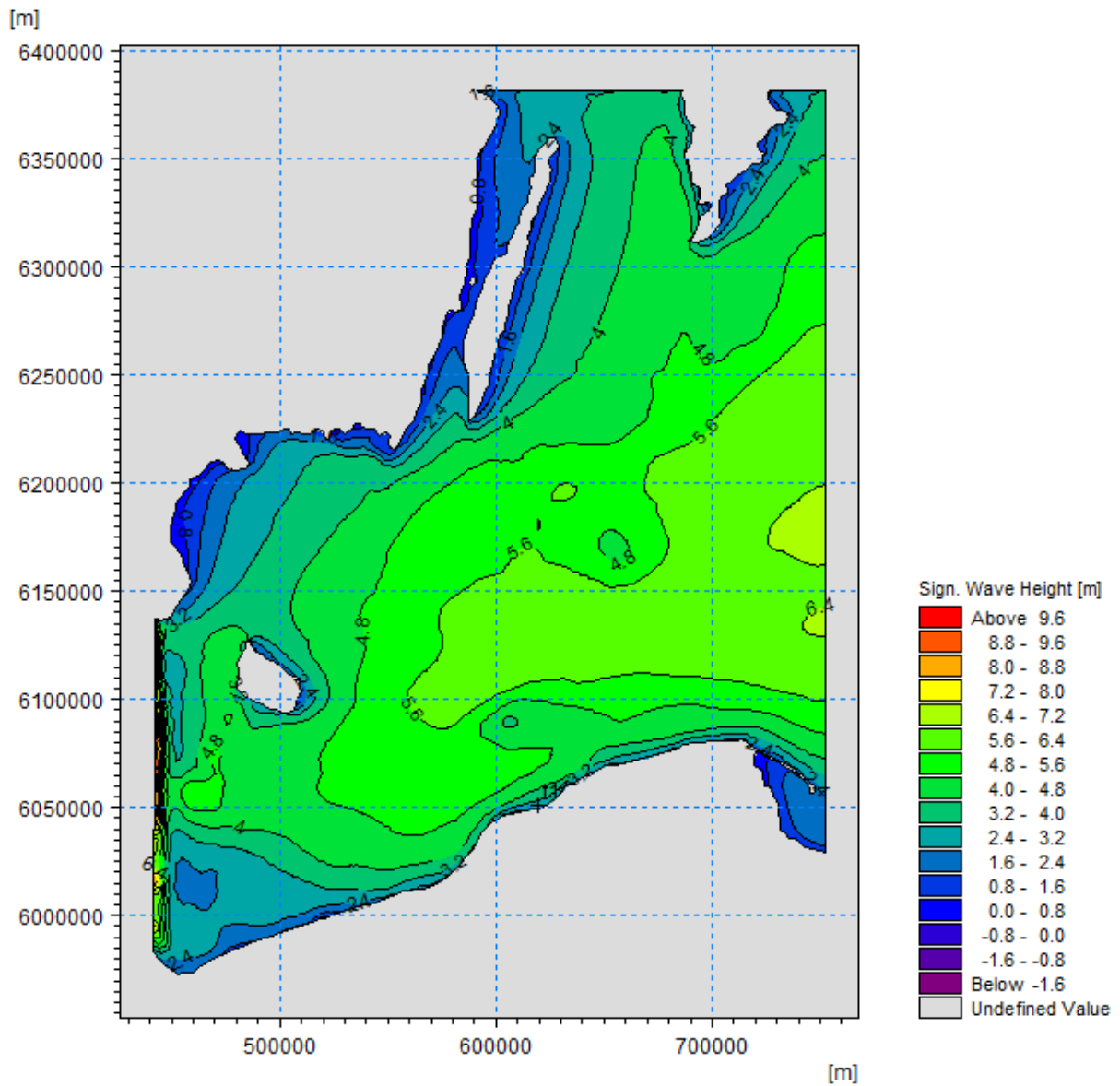


Figure 51 Model domain showing isolines with significant wave height.

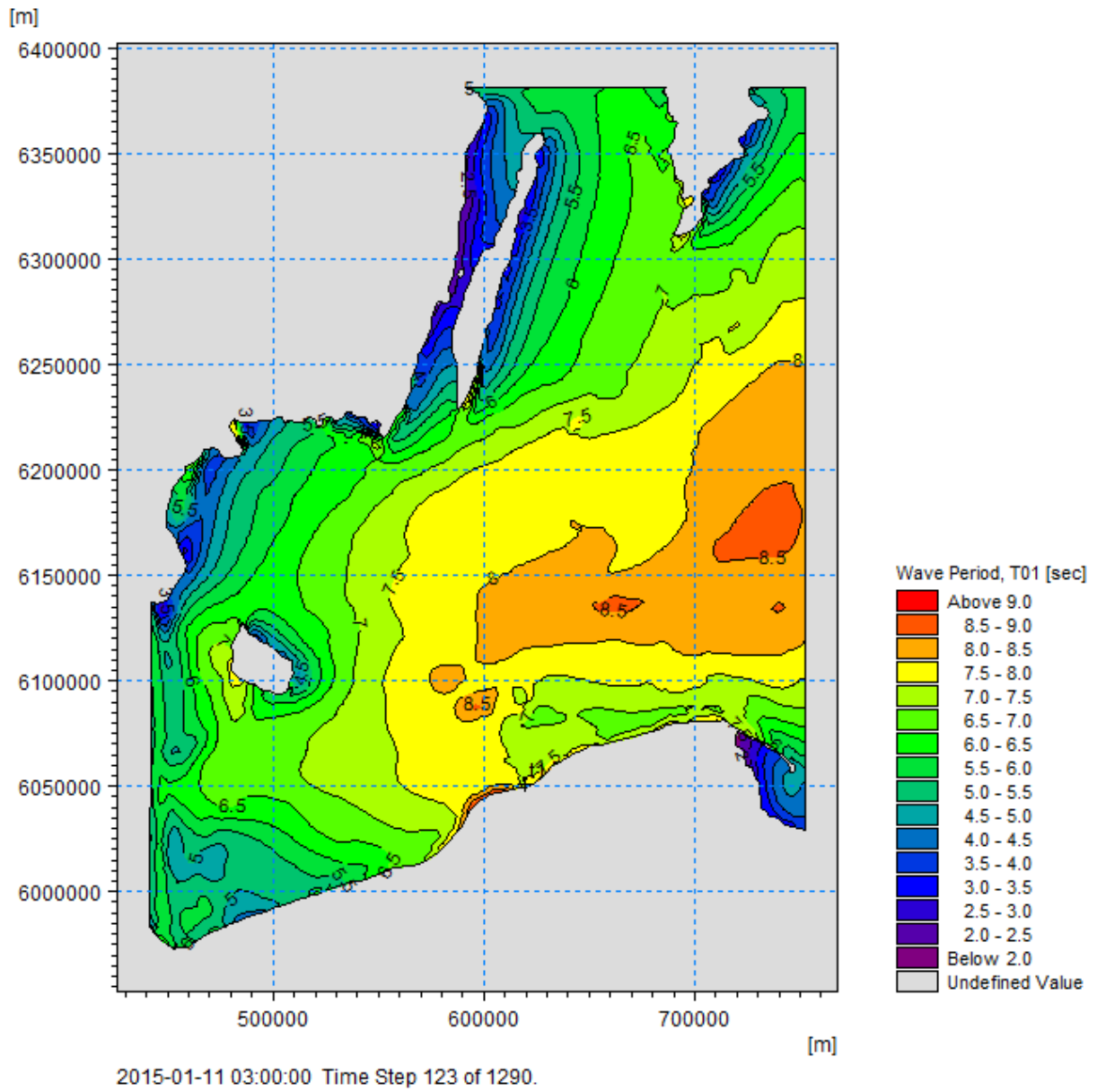


Figure 52 Model domain showing wave period T_{01} .

Next three figures (Figures 53, 54, 55) present the close-up to the area of interest and also give the information about significant wave height and period.

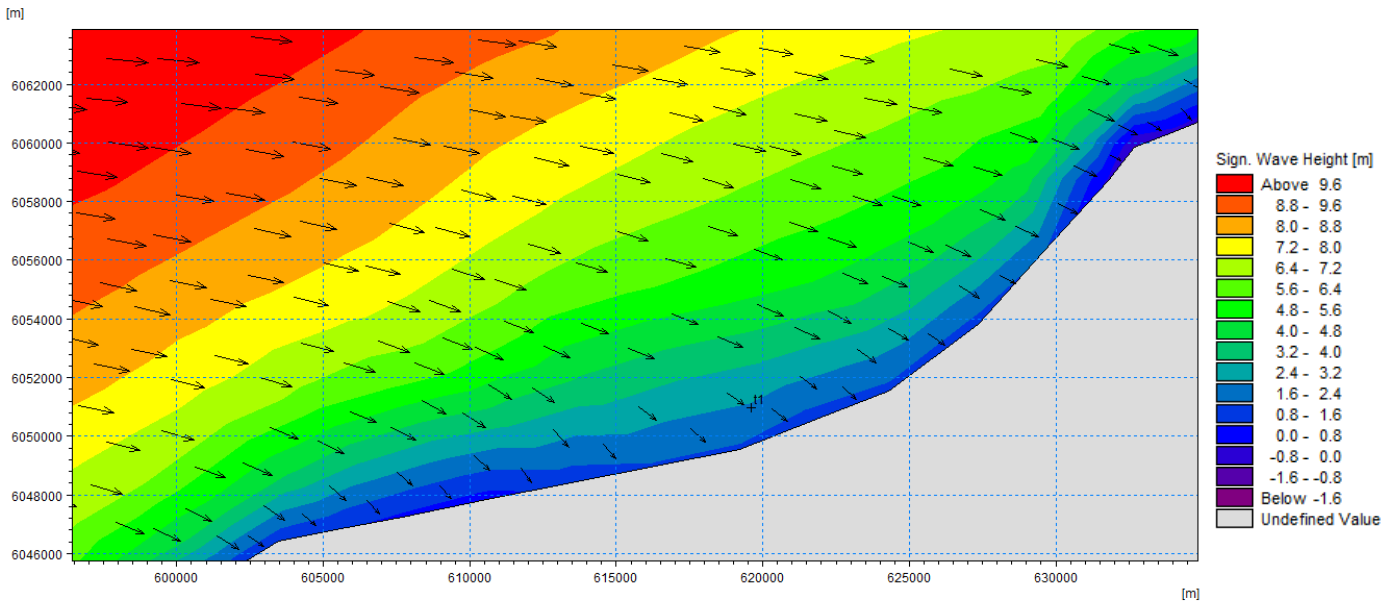


Figure 53 Plot of the area of interest showing significant wave height and wave vectors. Wave refraction can be easily seen.

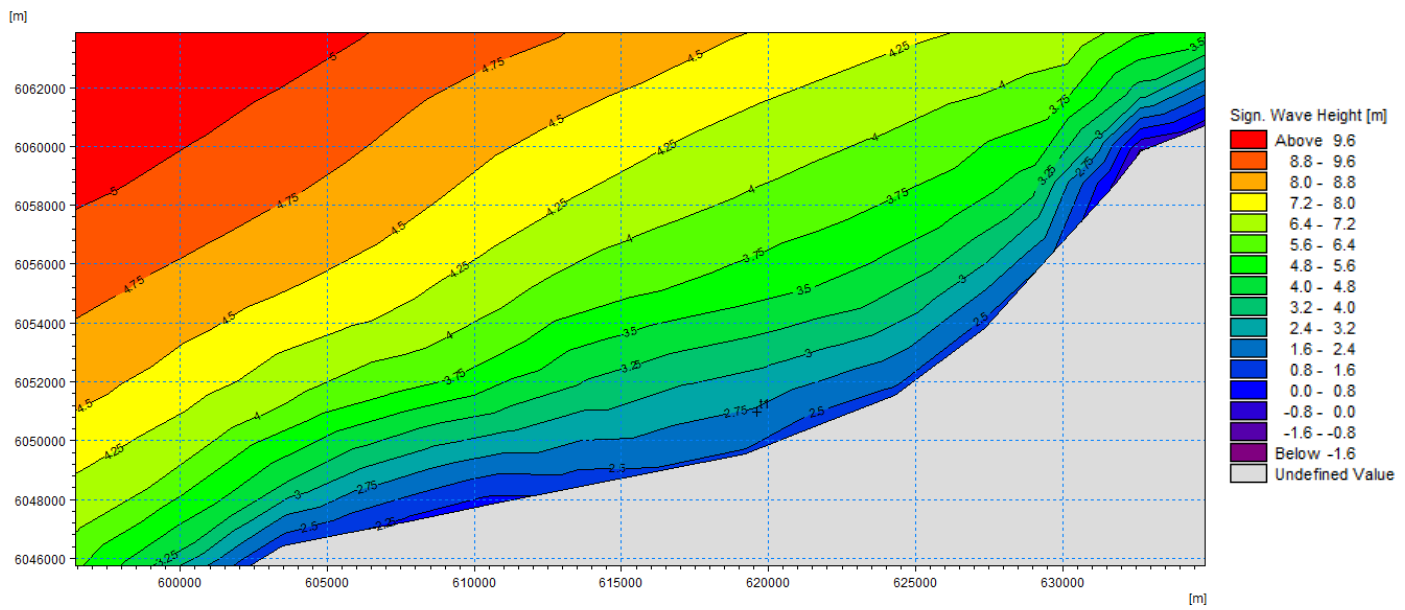


Figure 54 Plot of the area of interest showing significant wave height (isolines).

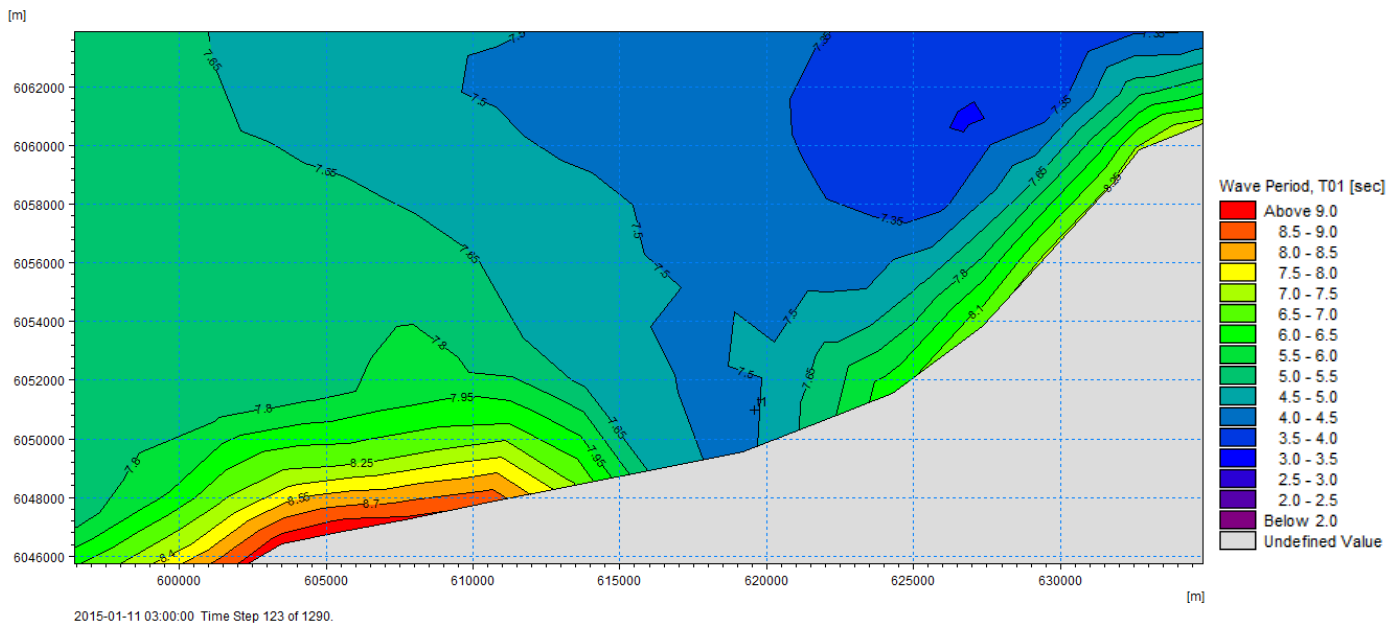


Figure 55 Plot of the area of interest showing wave period T_{01}

Near the harbour in Ustka during simulation period significant wave height vary from 0.1 m and up to 2.5 m, and wave period T_{01} changes from 1.8 to 7.8 seconds. These variations are shown in the time series of the point located at coordinates of the head of eastern breakwater. The two time series are presented on Figures 56 and 57.

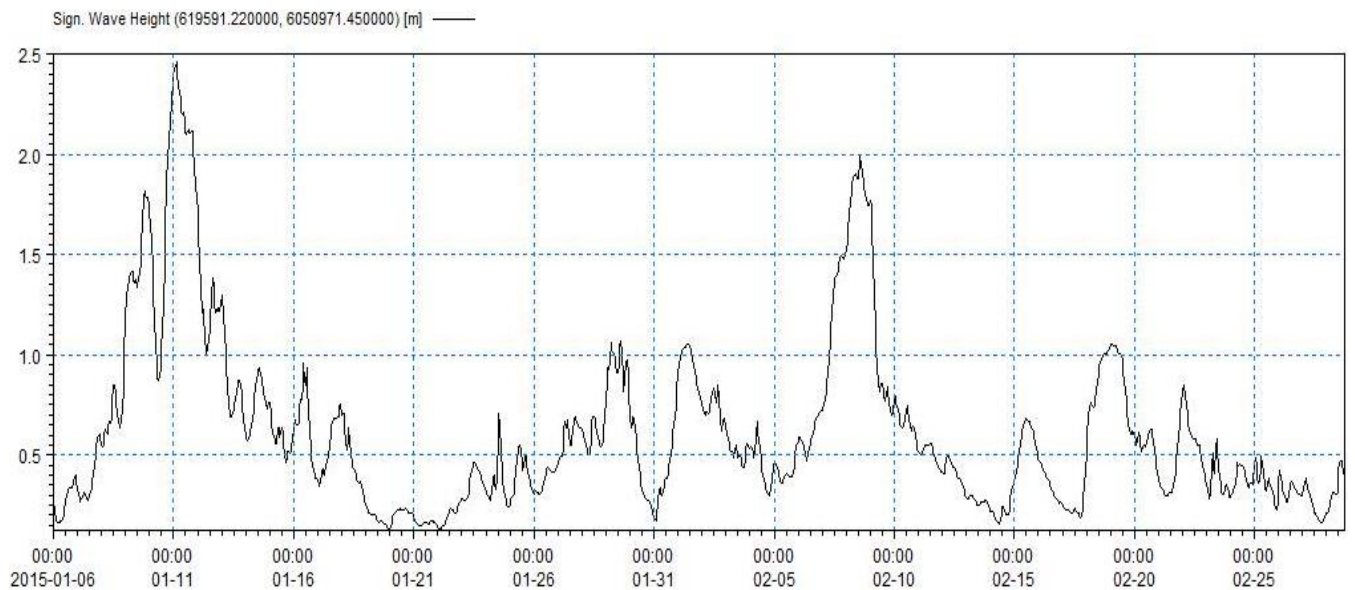


Figure 56 Time series showing significant wave height at the location of the head of the eastern breakwater

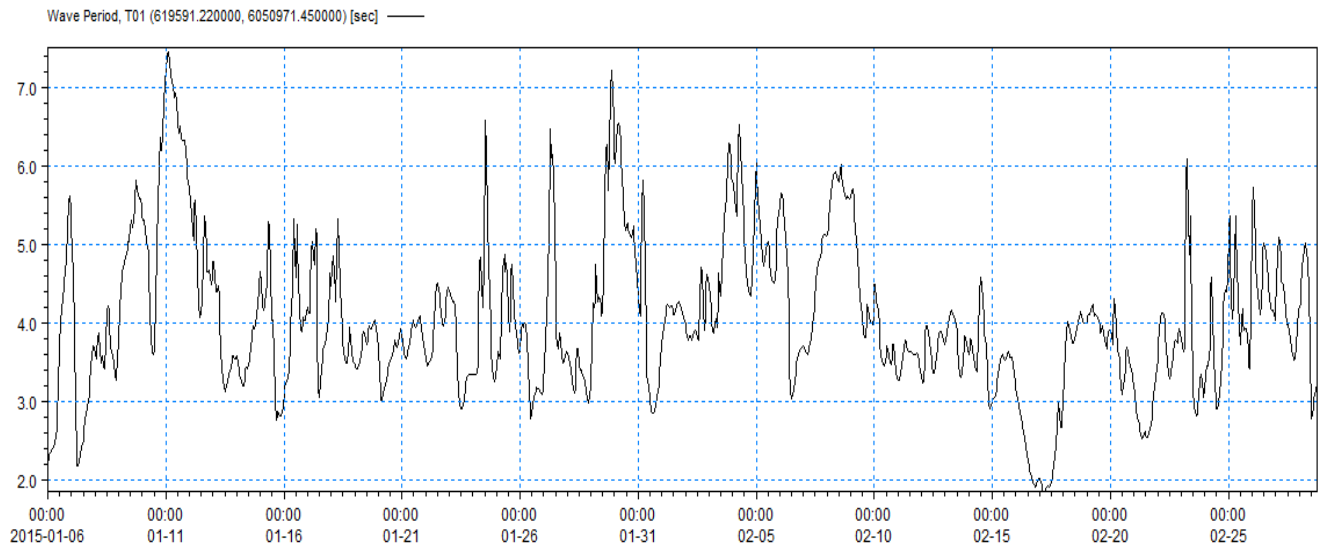


Figure 57 Time series showing wave period T_{01} at the location of the head of the eastern breakwater

Table 7 placed below contains summarized results from SW and SW+HD simulations at the location of the head of the eastern breakwater. Results were divided into three groups depends of the source of origin. Presented values are from 11th of January 2015 when the highest wave approached to the breakwater. All values are from this time. Peak wave period corresponds to the maximum wave height. The total maximum wave height is equal to 4.84m for Spectral Wave simulation and 4.69m for Spectral Wave + Hydrodynamic simulation. Differences between those two models are not so meaningful. Significant wave height in SW+HD is 0.1m lower than in SW model, also wave period is 0.1s shorter. Waves generated by wind in SW model are slightly higher and longer than those from SW+HD model. Adding tidal and current variations does not affect much calculated wave parameters, as predicted.

Table 11 Summary of the results obtained in SW simulation.in at the location of the head of the eastern breakwater

Model	Spectral Wave			Spectral Wave + HD		
Time of occurrence	11-01-2015 03:00:00			11-01-2015 03:00:00		
Origin	Wind	Swell	Total	Wind	Swell	Total
Sig. wave height [m]	2.38	0.90	2.54	2.31	0.83	2.46
Wave period T_{01} [s]	7.39	8.81	7.54	7.30	8.73	7.44
Max. wave height [m]	4.54	1.69	4.84	4.42	1.57	4.69
Peak wave period [s]	9.80	10.15	9.85	9.75	10.20	9.80
Mean wave direction [°]	305.57	343.26	310.17	304.60	342.80	308.91

The time series of water level changes caused by tides, currents and pressure variations for Ustka site is shown below in Figure 58.

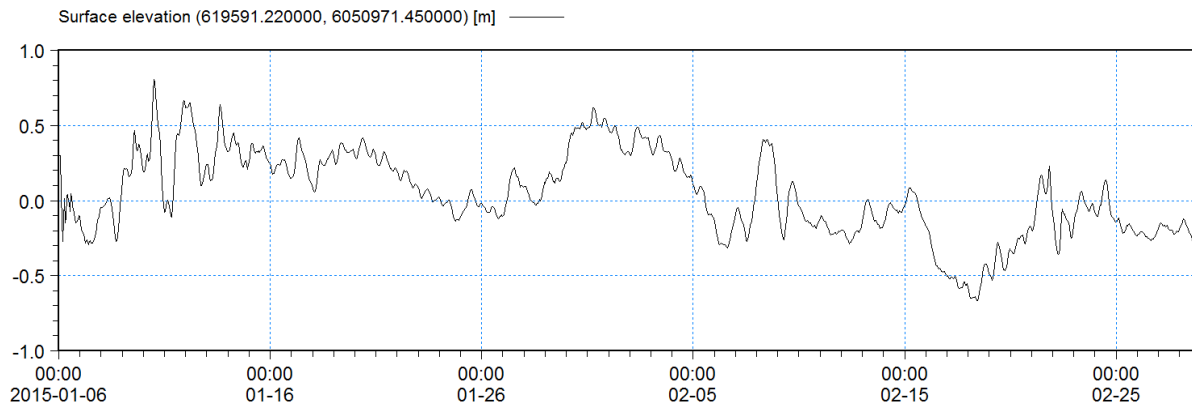


Figure 58 Time series of the surface elevation caused by tides and currents. Generated by Mike Zero.

This time series shows that the surface elevation reaches maximum of 0.8 m which is not large compared to the water depth that is approximately around 8 m at this point. Thus it is not supposed to cause significant changes in wave conditions. Below time series showing the speed of the current at this location is presented.

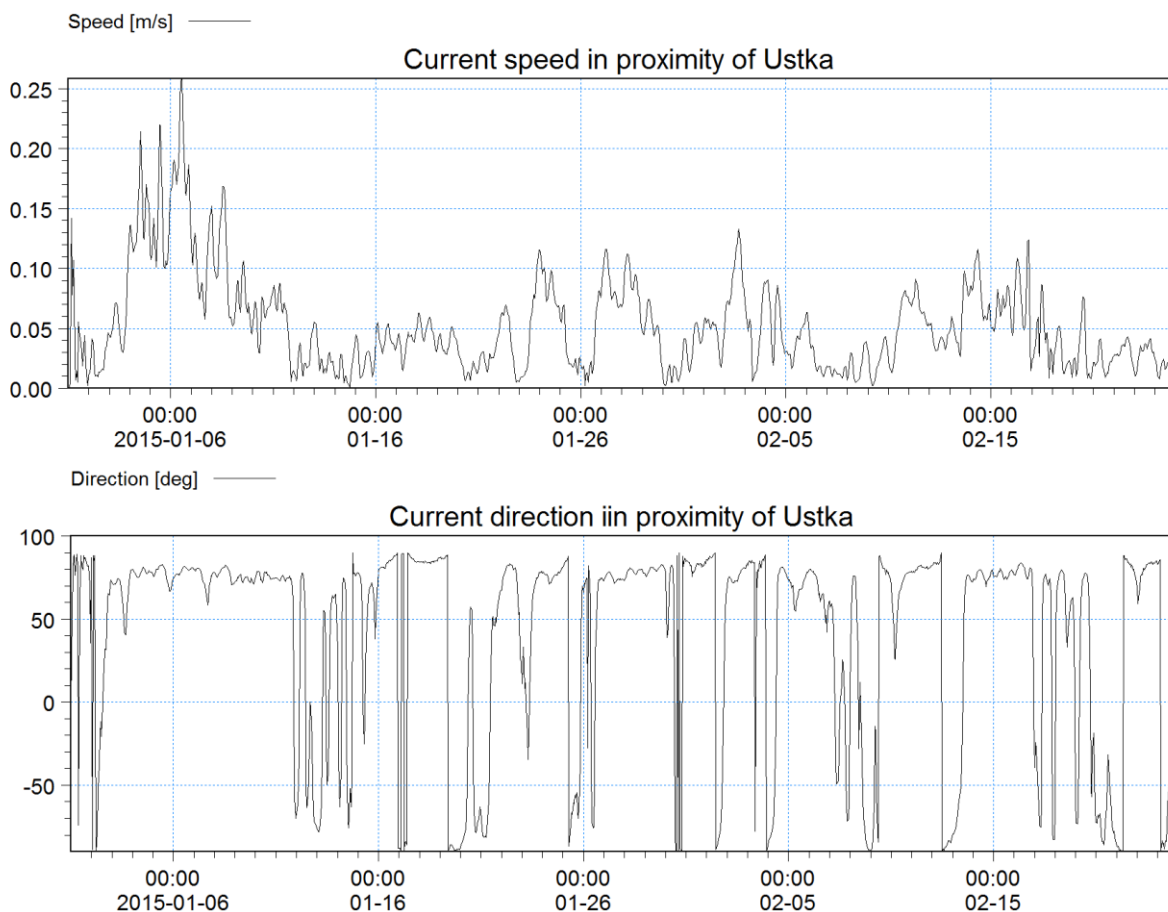


Figure 59 Plot of the speed and direction of the current in proximity of Ustka. Generated by Mike Zero.

In order to visualize how small are the differences between those two models time series of significant wave heights are compared below in Figure 59. Red line shows values for SW model with hydrodynamic analysis and blue shows values for SW model without input about tides and currents. Waves coming into the harbour have significant height of approximately 2.5 m and reach maximum value of 4.8 m. That values are much lower than rough estimate

for breaking wave height which is governed by ratio $H/d=0.8$, where H is wave height at breaking point and d is water depth (8.0 in point from where values are taken, 8.8m when tides are taken into account). From that wave breaking height can be estimated as 6.4-7.04 m. Sometimes high tides allow for higher waves to enter the harbour before they break. This does not happen in this case, as waves are much smaller than breaking height. That is why including tides and currents does not cause much changes.

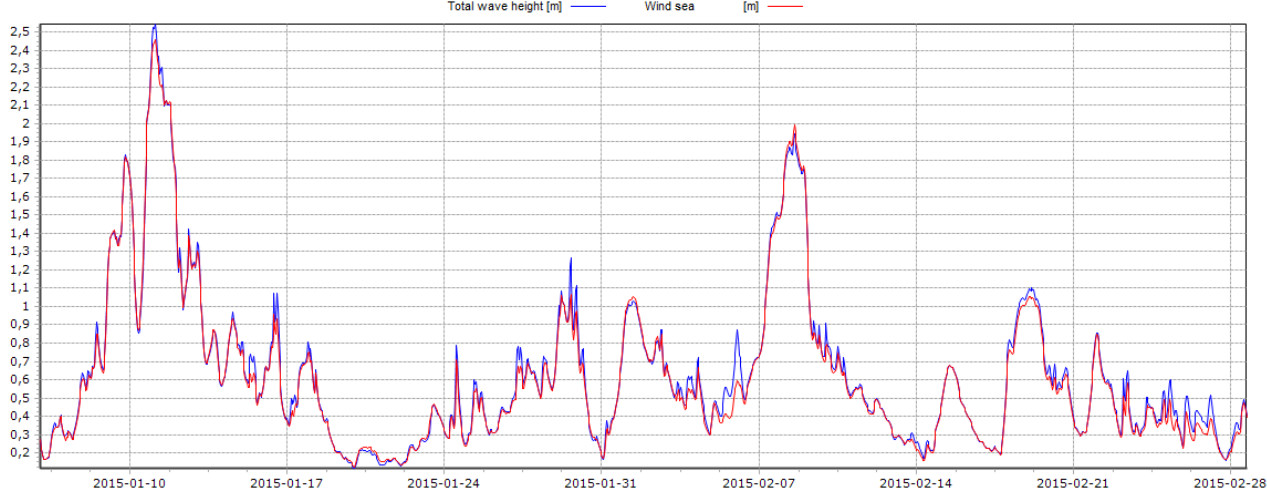


Figure 60 Time series showing comparison of significant wave height at the location of the head of the eastern breakwater. Red line shows SW+HD output and blue one shows output from SW without HD

For a better understanding of the nature of generated waves they were divided into the sea swell and wind. Fig. 60 and 61 present the relationship between the swell, wind sea and the resultant sea state, which is composed by these two terms. It is clear from the figures, that extreme sea state is almost totally governed by waves locally generated by wind, whereas during relatively calmer periods it is swell that mostly affect the sea state.

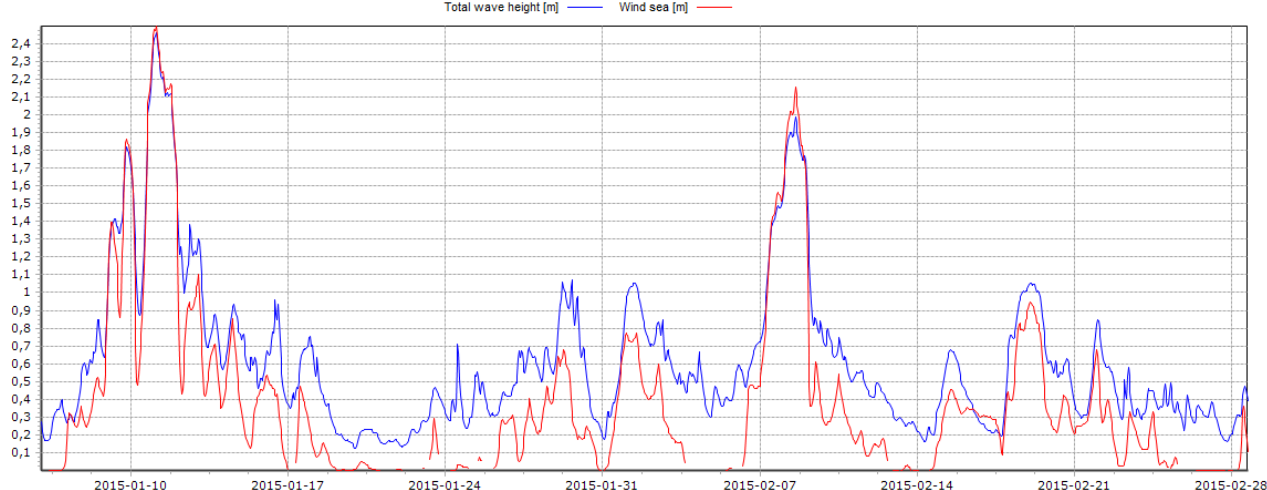


Figure 61 The comparison of total wave height (blue) and wave height for wind sea (red).(Generated by: Mike Zero by DHI)

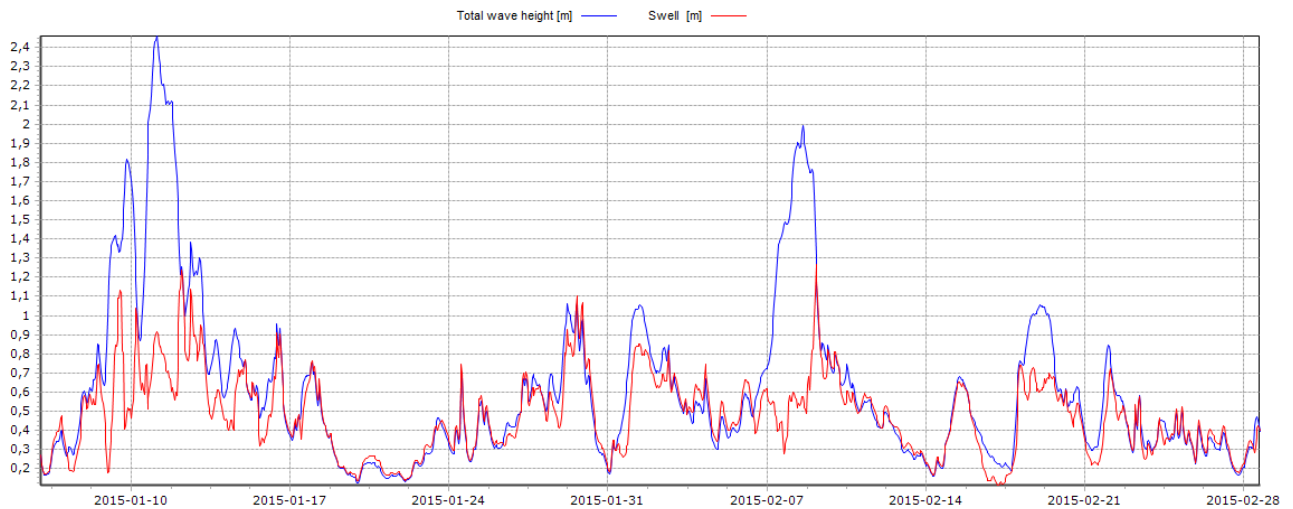


Figure 62 The comparison of total wave height (blue) and wave height for swell (red). (Generated by: Mike Zero by DHI)

According to Czajewski (1988) during wind of 7-8 in Beaufort scale waves can reach height of 3-4 metres, occasionally reaching up to 7 metres. Such a sea state (Beaufort numbers 7-9) took place during the simulation. After analysis of wind and atmospheric pressure data used in the model it can be told that on the 10th January from the 12.00, due to low-pressure centre passing over the Baltic sea, wind speed grown from 18 m/s to the maximum of 21 m/s at 00:00 on the 11th January and decayed to 16.5 m/s during the same day. What is more, Papińska (2000) found, using WAM4 model, that the main direction of wave propagation for polish coast is East to South-East, which is in very good consistence with wave direction obtained (see Figure 63), and that the maximum value of the significant wave height can reach up to 5.94 m (1998-1999). Data presented in more detail in the references and mentioned above refers mainly to the area of southern Baltic sea in general, not precisely to the area in proximity to Ustka. Nevertheless, by comparing them with the results of the simulation it can be concluded that the calculated wave heights lie within the specified ranges. According to Jakusik (2006), the average wave period in the stormy season is 5.2 sec. The given value is little higher than obtained 4.1 s. This may be due to the fact that the simulation was made for the stormiest months - January and February, whereas the whole storm season lasts from October to March. The obtained values from the SW + HD simulation are slightly smaller than those without considering the influence of hydrodynamic processes. At the same time, compared with data from the literature, it can be assumed that they better reflect the actual situation. Therefore, they are used to carry out Boussinesq wave model simulation.

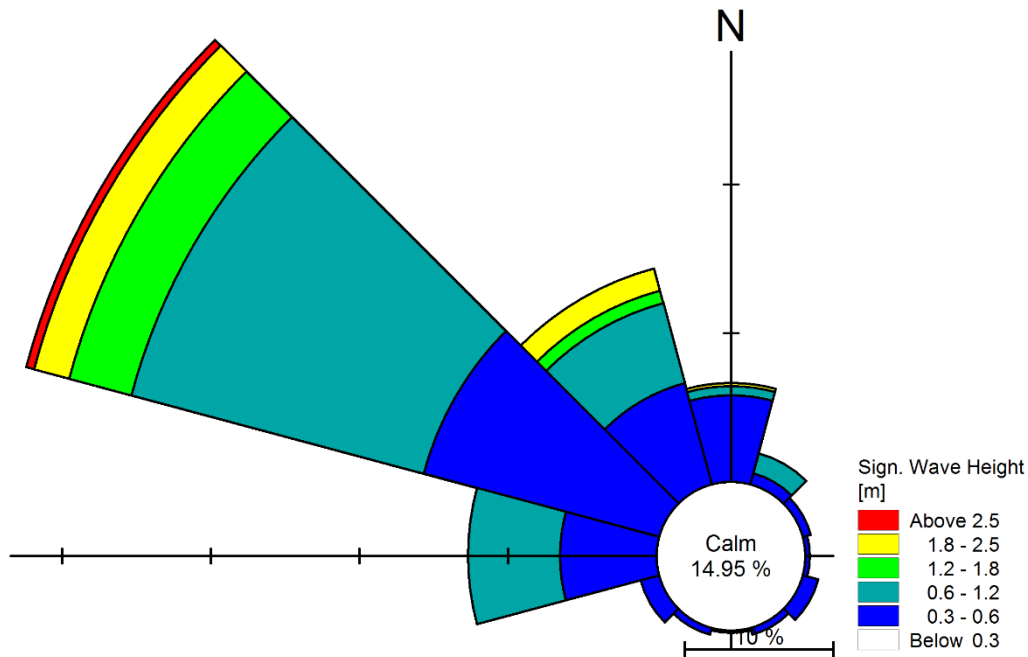


Figure 63 The rose plot of the significant wave height at the proximity of Ustka (Generated by: Mike Zero by DHI)

6.3. Boussinesq Wave Model

The following section contains plotted results of MIKE 21 BW calculations for each proposed harbour layout. At the beginning, the results for the first layout with regular waves coming from the north will be presented and shortly discussed. It was prepared in order to test the model parameters and bathymetry. Afterwards the output for the four concepts will be shown, in two versions of wave direction (north-west and north-east) for each layout. Then the most important parameters will be presented in a table, compared and discussed briefly.

6.3.1. Regular waves

As it was written before, a wave model with regular waves was prepared only in order to benchmark the setup parameters, assumptions and input data of the BW model. Figure 64 presents the first step of the simulation. Figure 65 shows fully developed wave conditions. It can be easily seen that regular waves propagating into the harbour from the north are partially reflected by structure. Wave energy is well dissipated by sponge layers on the boundaries and along the beach. Wave diffraction can be also observed.

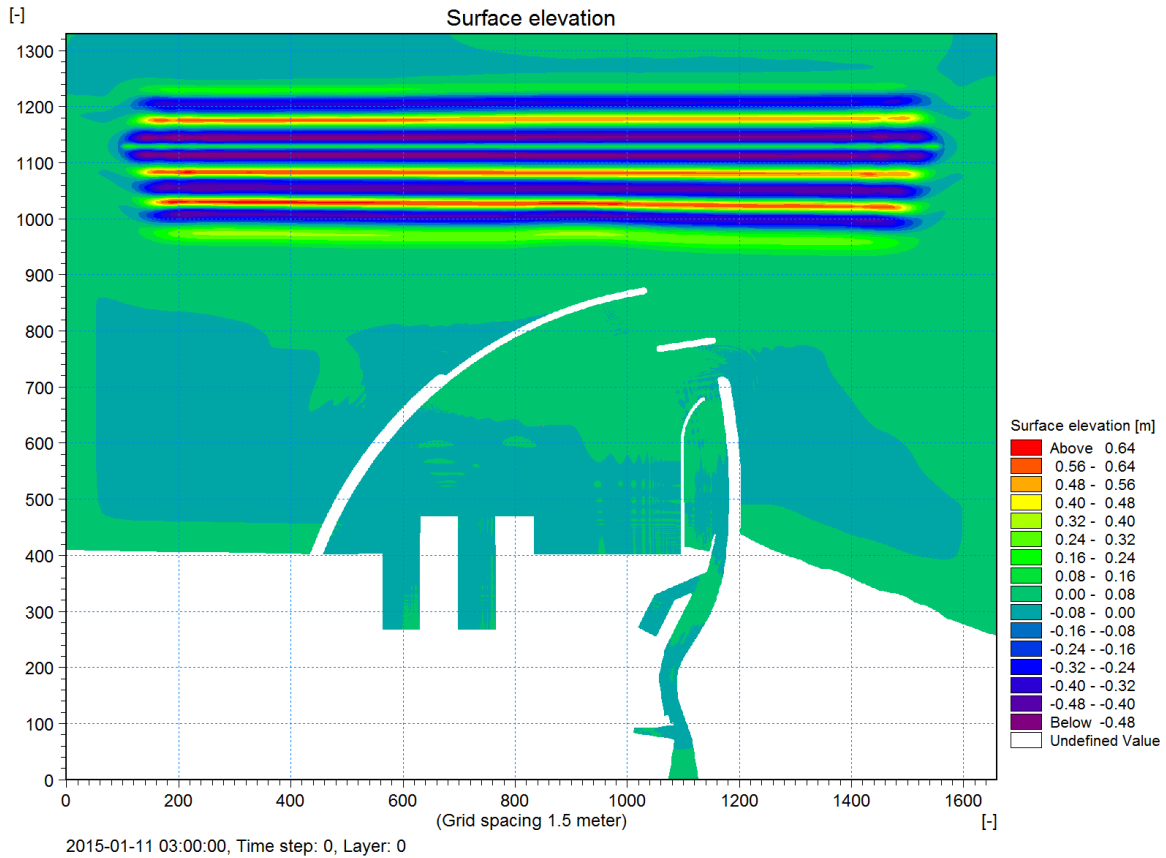


Figure 64 First layout, regular waves: Snapshot of the waves at the beginning of the simulation.

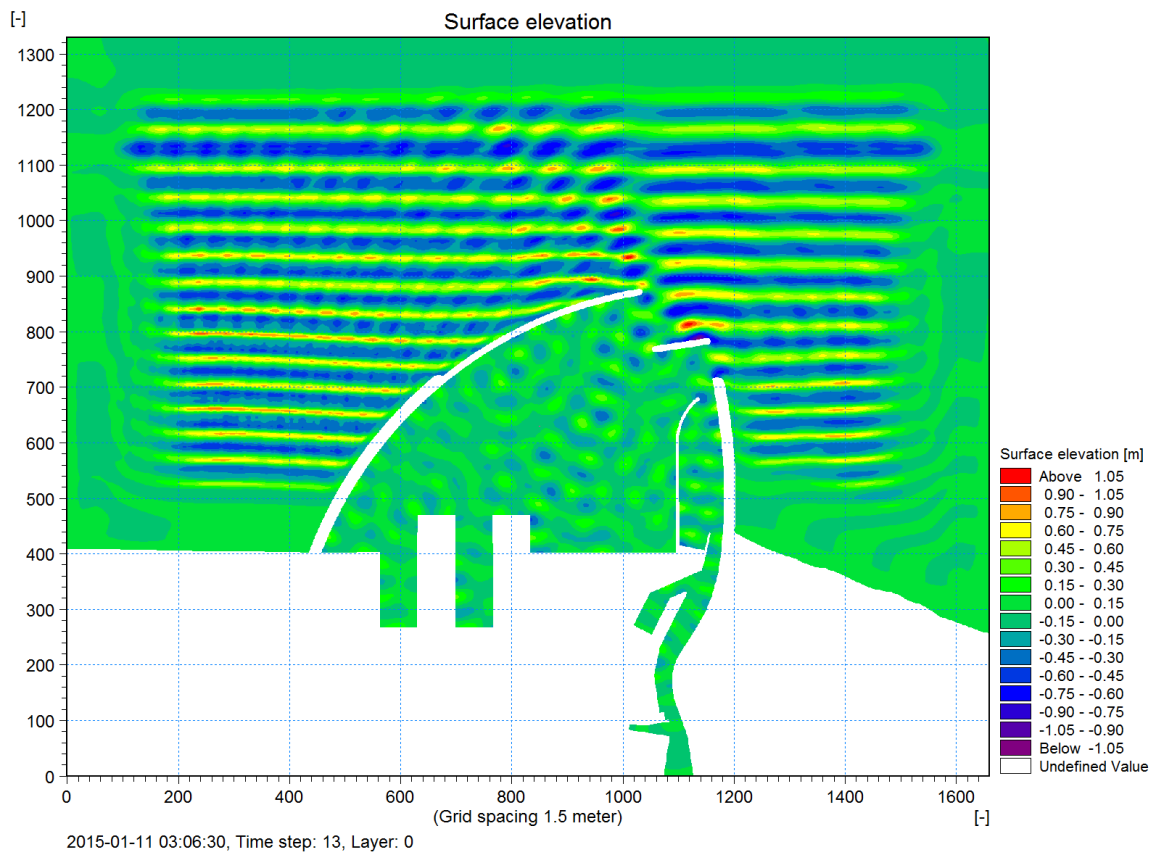


Figure 65 First layout, regular waves: Snapshot of propagating waves at the time of the occurrence of the highest waves at the harbour entrance.

Below in figure 66 two examples of the time series are presented. At the top we can see waves at the detached breakwater (point 6 in Figure 67). Below a time series of a surface elevation for the centre of the new harbour basin (point 3 in Figure 67) is shown. It has much smaller amplitude and is more irregular and shifted in time compared to the first series.

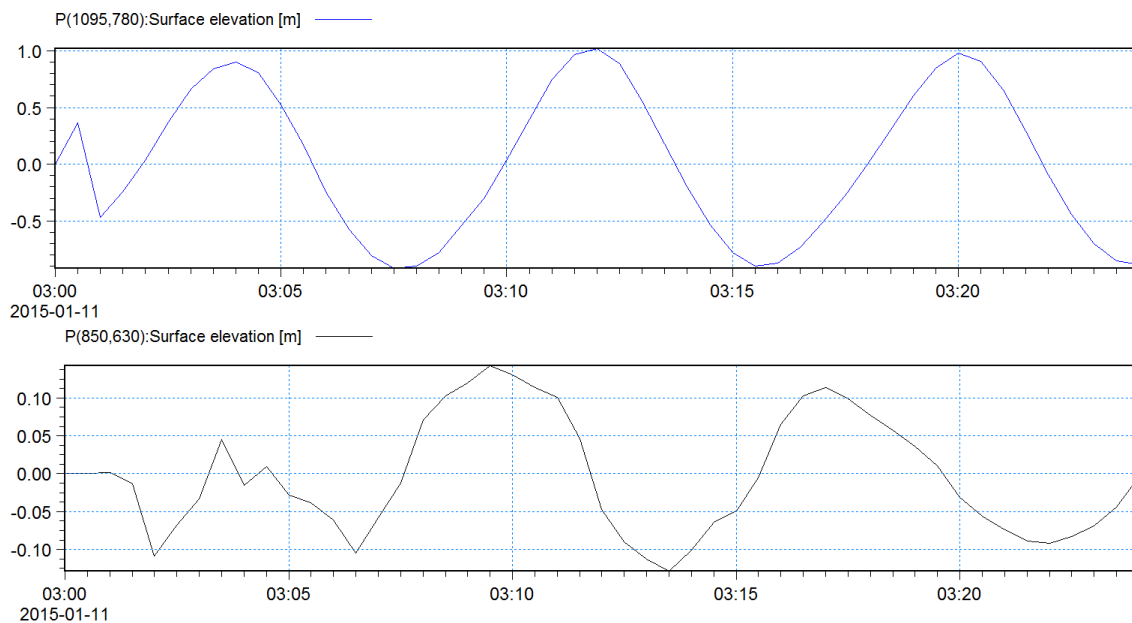


Figure 66 Time series of surface elevation for regular wave conditions at the detached breakwater (top) and centre of new harbour basin (bottom).

6.3.2. Random waves

Every layout was tested against two different main random wave directions. Firstly, the main direction obtained from SW simulation (waves coming from north-west) was used. It can be easily predicted, that proposed breakwater layouts shelter the harbour quite well from the wave incoming from north-west. In order to check much disturbance can be caused by waves coming from most unfavourable direction (north-east) this variation was also checked, but for different wave parameters (also obtained from SW for this direction). In this case two wave-generating lines were used, as described in Chapter 5.3.2.

For each combination of layout and wave direction a set of figures is presented below. At first a situational plan of each proposed breakwater layout is presented, with the indication of the points from where time series and wave parameters will be compared later. These are:

- Point 1: In the middle point of the new breakwater;
- Point 2: In the entrance to the old harbour;
- Point 3: In the central point of the new basin;
- Point 4: In the proximity to the new quay in the new basin;
- Point 5: In the entrance to the Coal basin in the old harbour;
- Point 6: In the entrance to the new basin.

Next a set of time series of wave heights at these point is presented in order to give some more detailed information about the wave parameters. Afterwards two figures, one at the start of wave generation and second one at the time of the occurrence of maximum wave at one determined point, will present the wave generation and propagation process. At the end an additional 3D visualisation is shown.

6.3.2.1. First layout

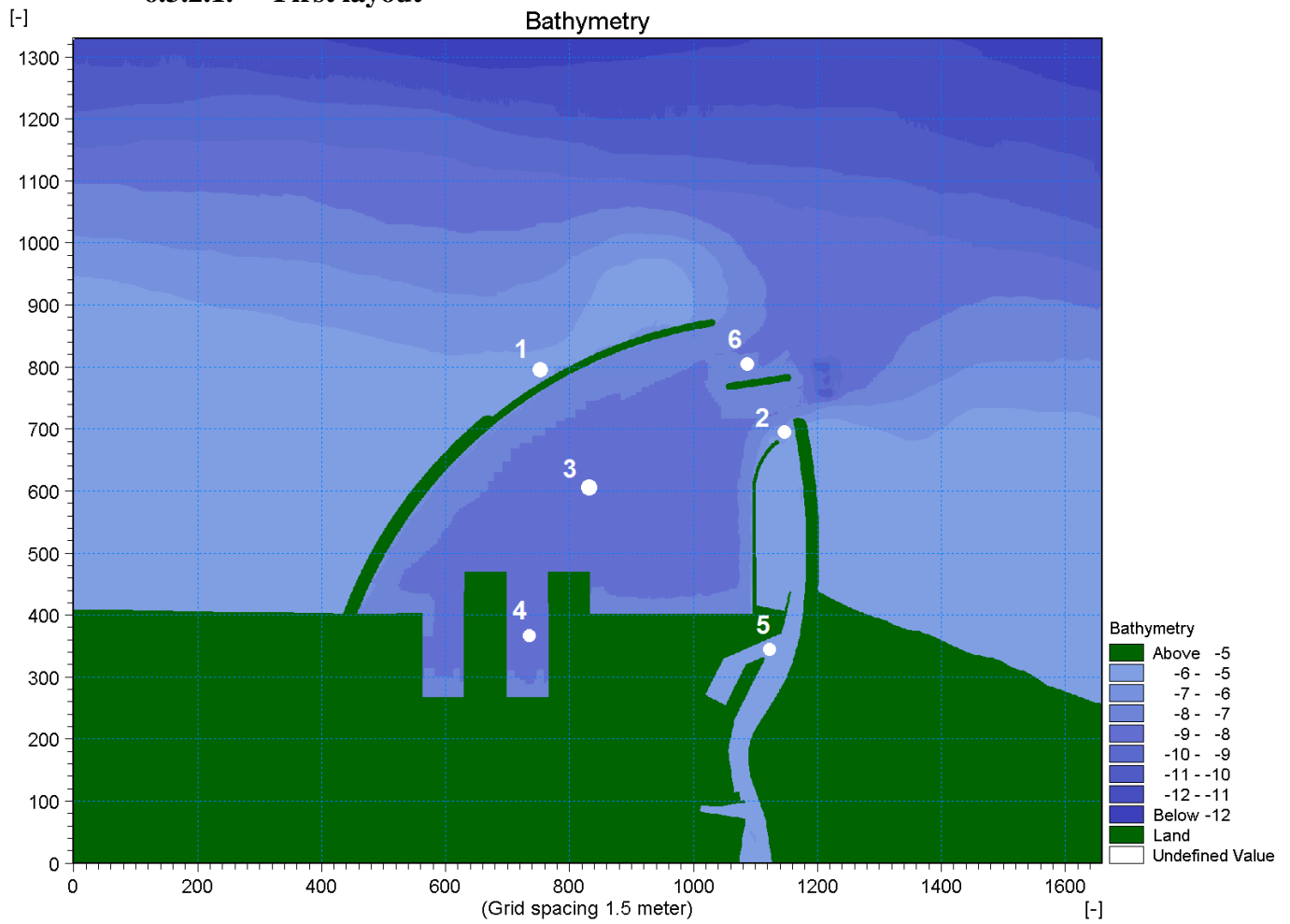


Figure 67 First concept with marked points of interest. Generated by Mike Zero.

Random waves from north-west:

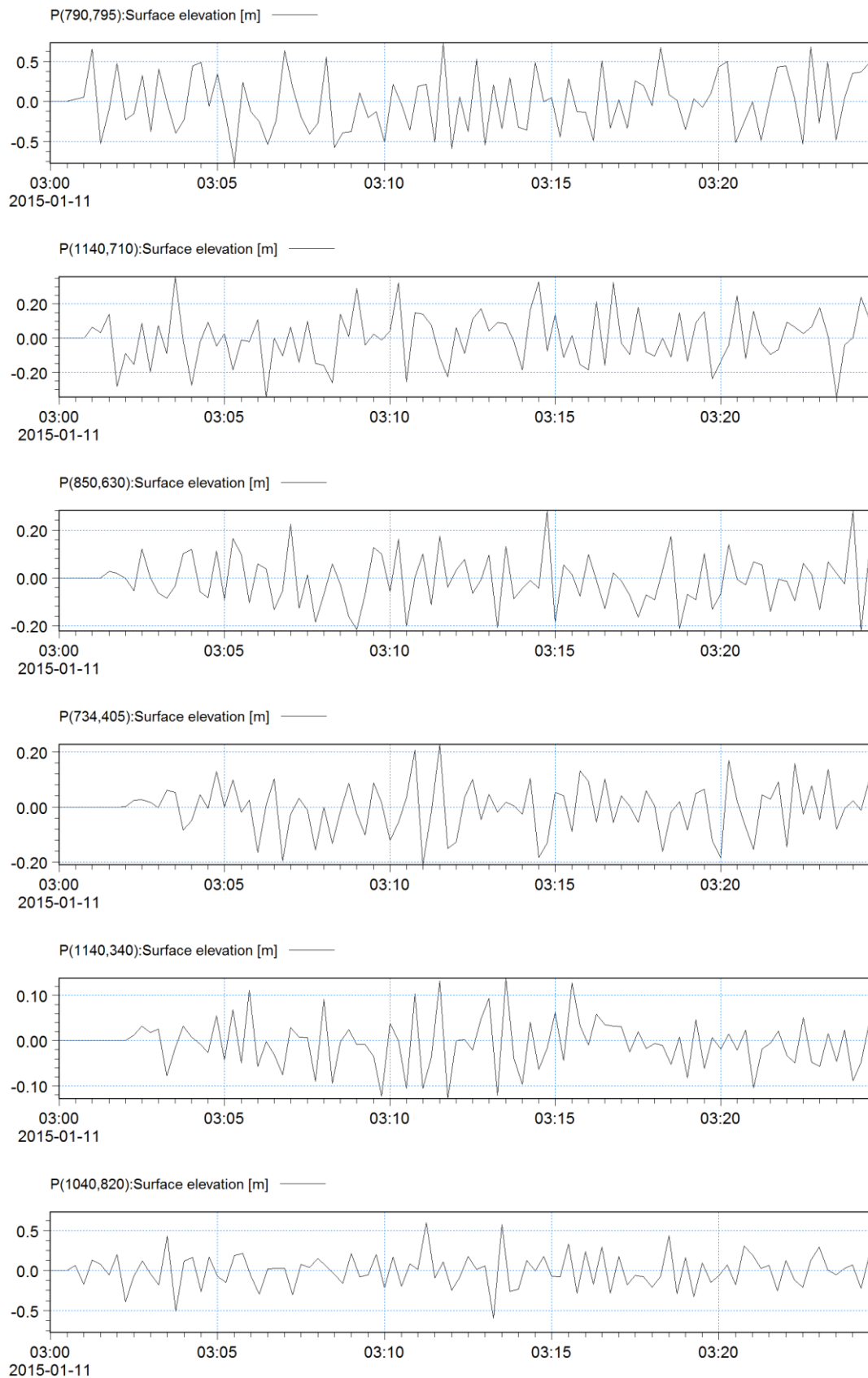


Figure 68 First layout, random waves from north-west: Plot of the time series for point 1-6 from Figure 67, from the top to the bottom respectively

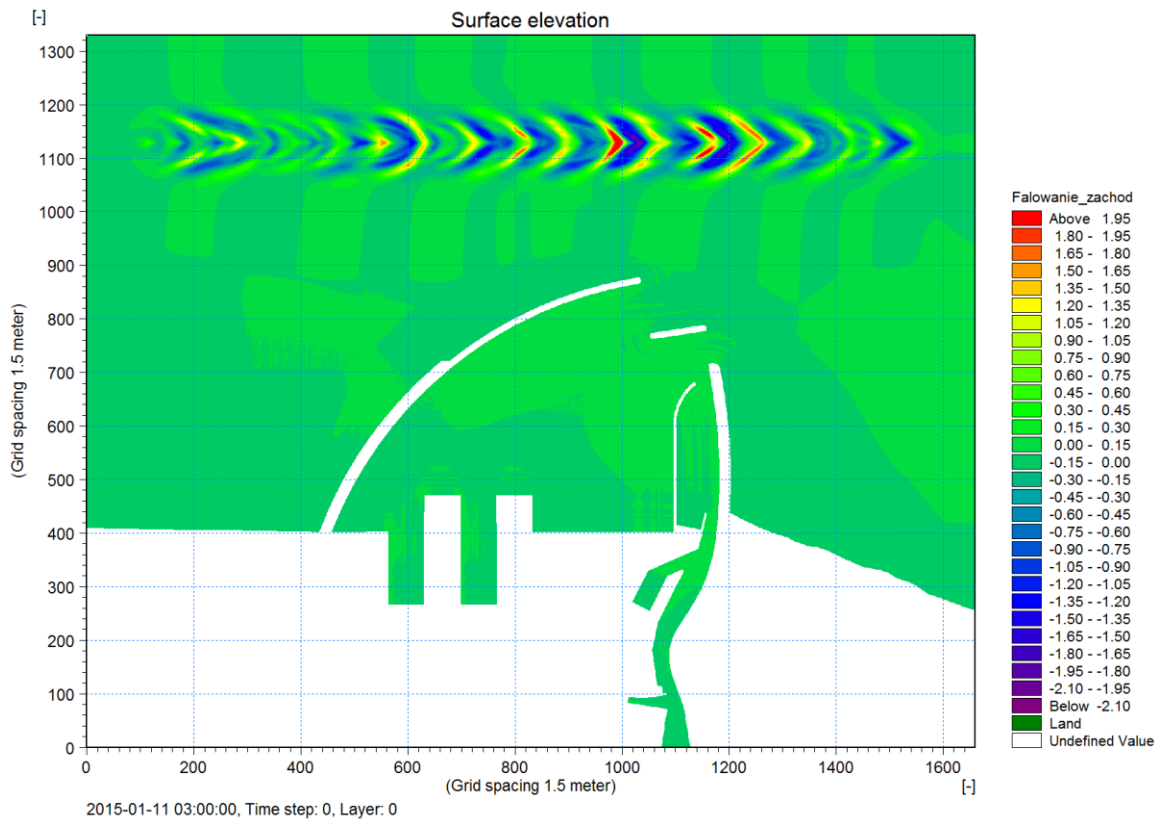


Figure 69 First layout, random waves from north-west: Snapshot of the waves at the beginning of the simulation.

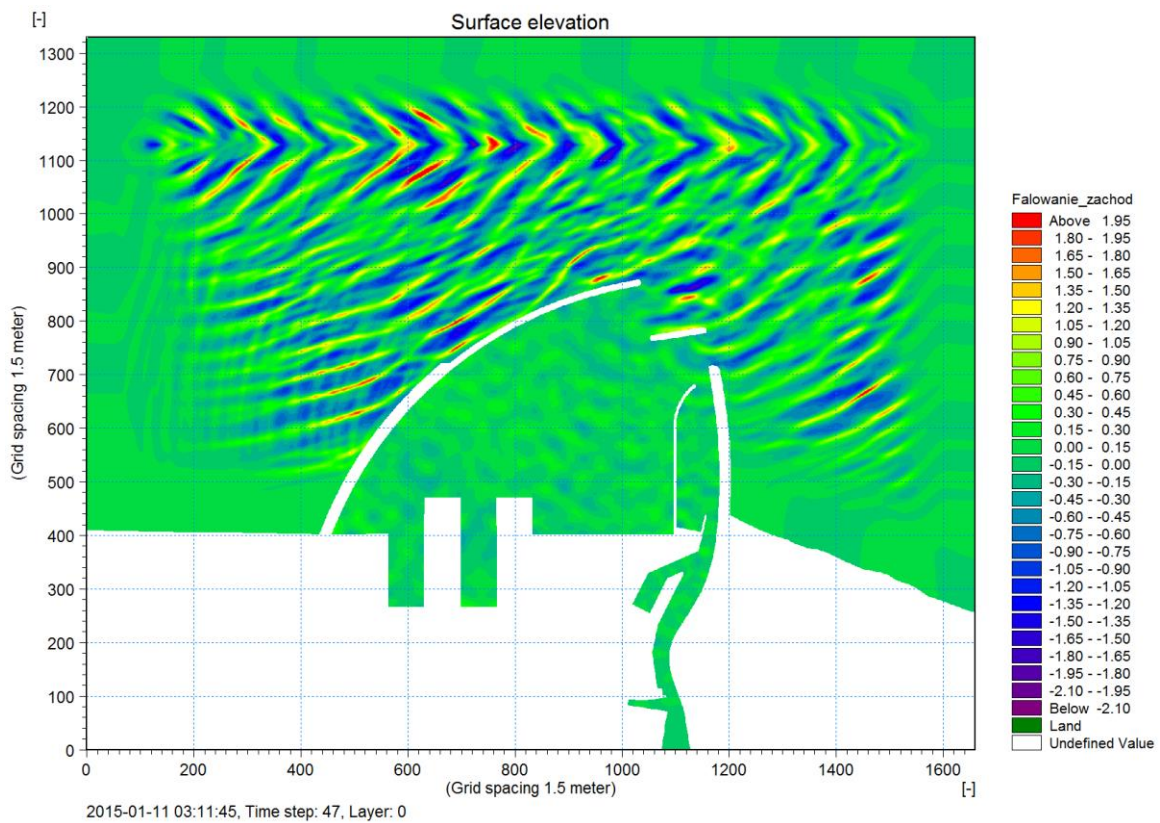


Figure 70 First layout, random waves from north-west: Snapshot of propagating waves at the time of the occurrence of the highest waves at the harbour entrance.

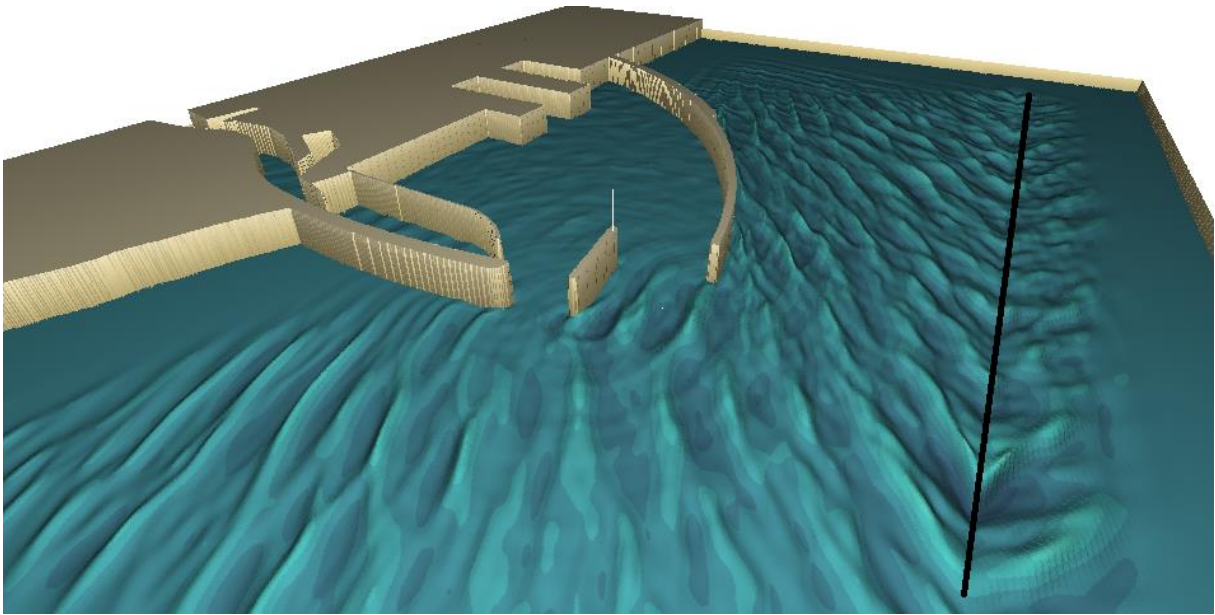


Figure 71 Visualisation of the first layout. Snapshot taken at 47th time step when the highest wave occurs at the harbour entrance. Black line symbolize generation line.

Random waves from north-west:

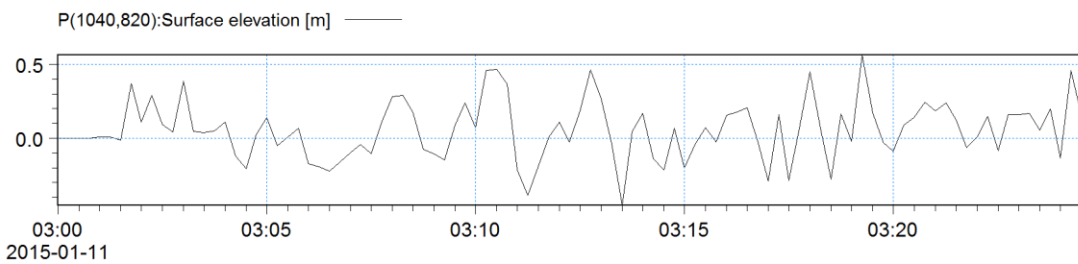
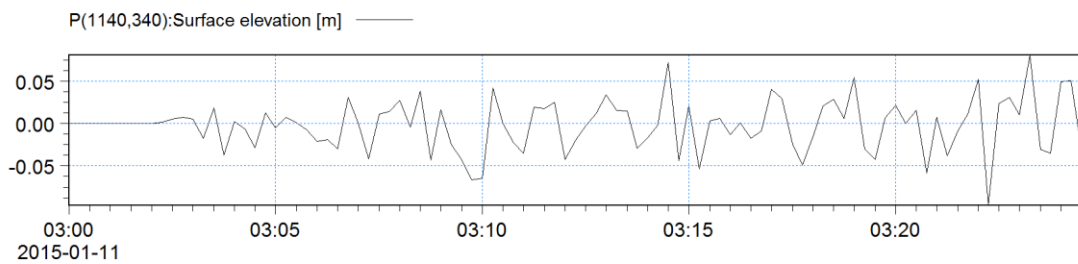
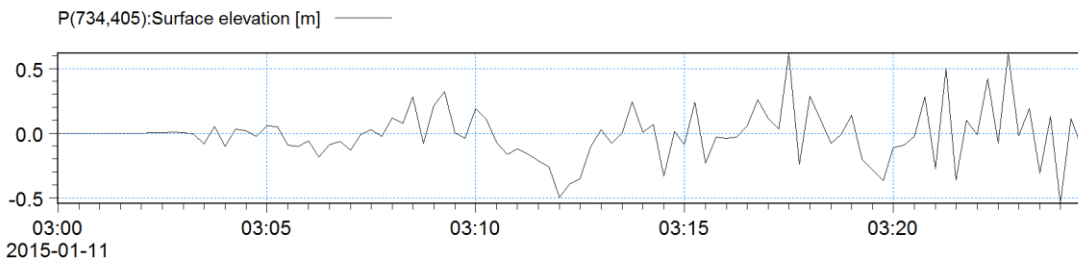
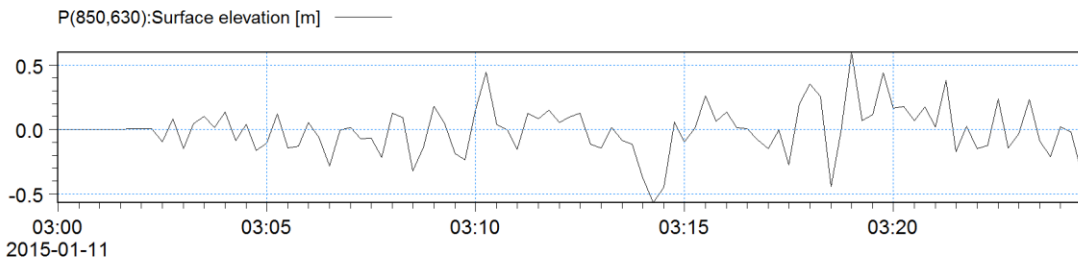
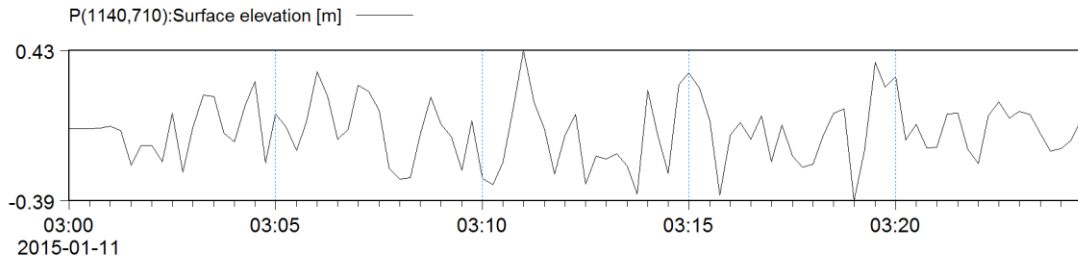
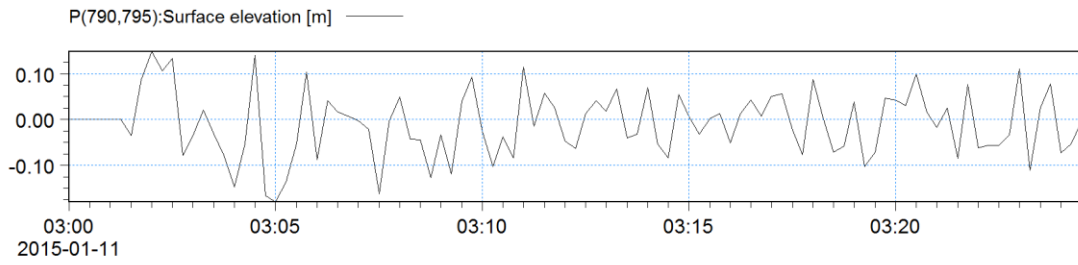


Figure 72 First layout, random waves from north-east: Plot of the time series for point 1-6 from Figure 67, from the top to the bottom respectively

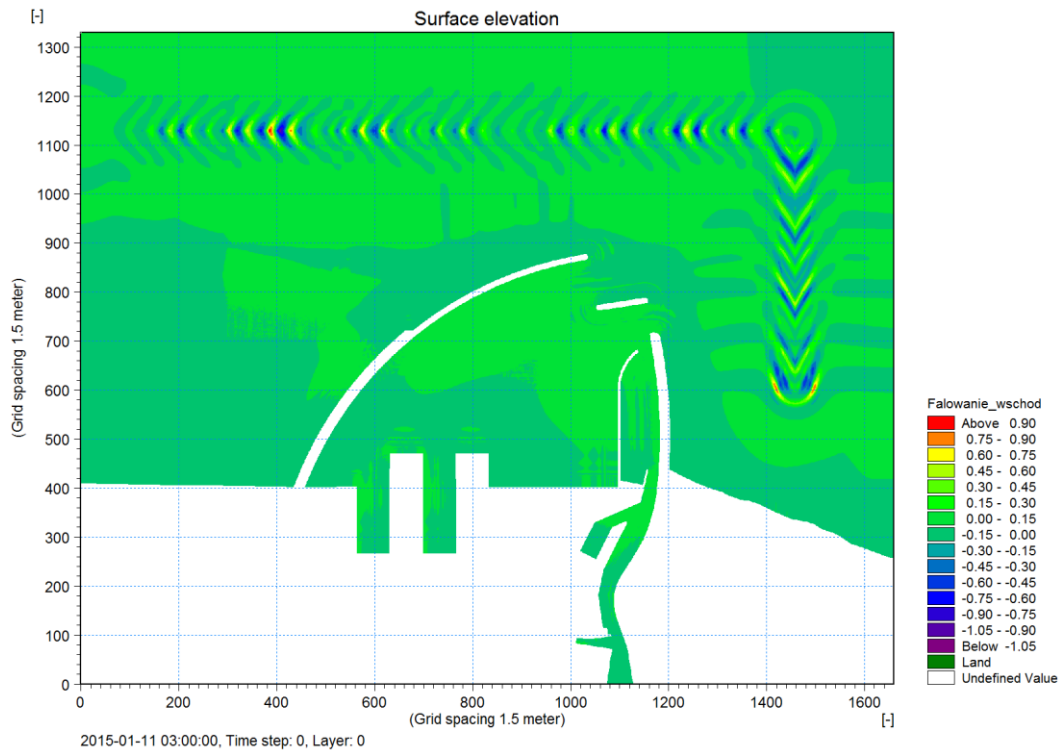


Figure 73 First layout, random waves from north-east: Snapshot of the waves at the beginning of the simulation.

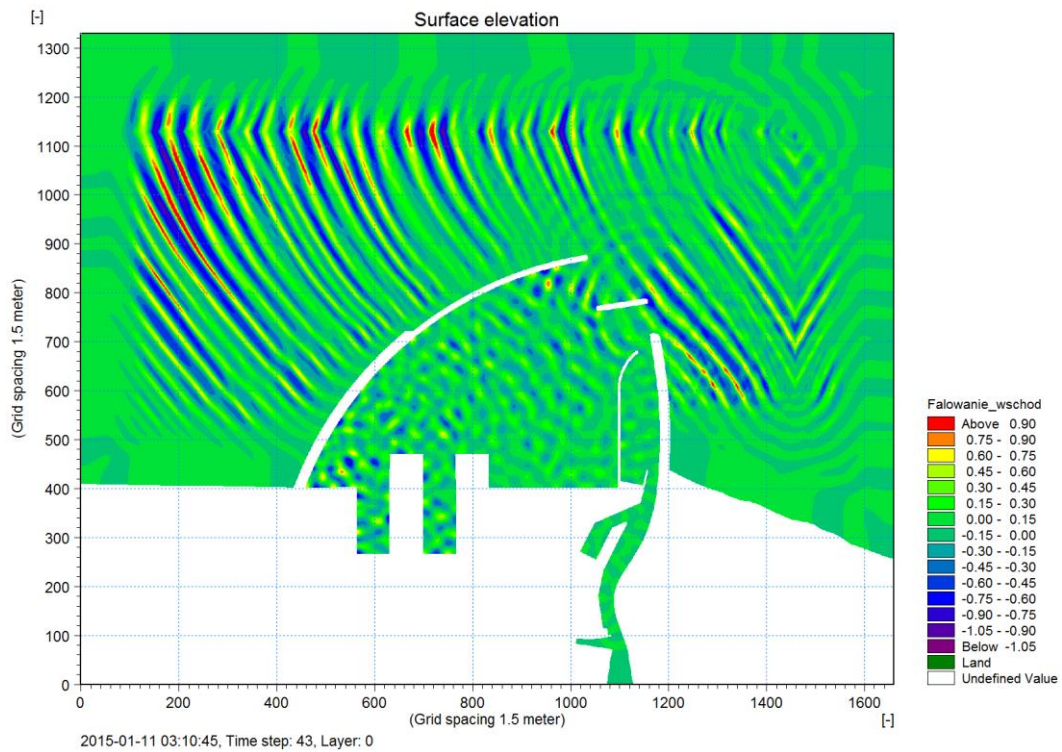


Figure 74 First layout, random waves from north-east: Snapshot of propagating waves at the time of the occurrence of the highest waves inside new harbour basin.

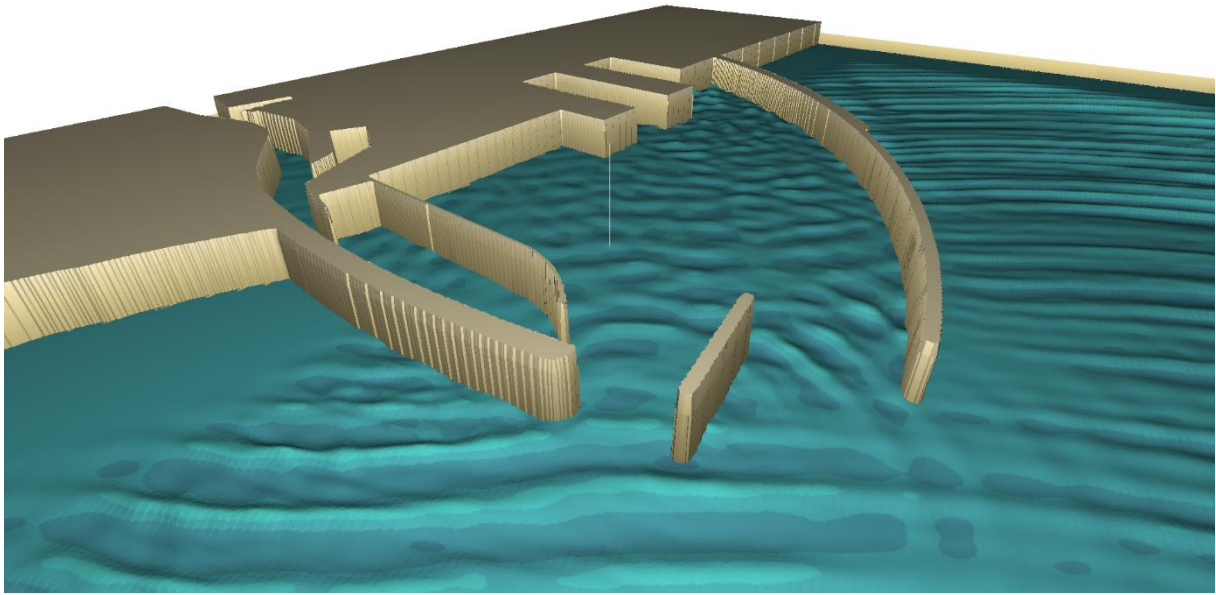


Figure 75 Visualization corresponds to Fig. 74. Snapshot taken at 43th time step. Waves are propagating from north-east.

As it can be seen in Figures 74 and 65, due to reflection of the wave inside the harbour basin an irregular wave pattern was formed with a plenty of places where wave heights reach significant values.

6.3.2.2. Second layout

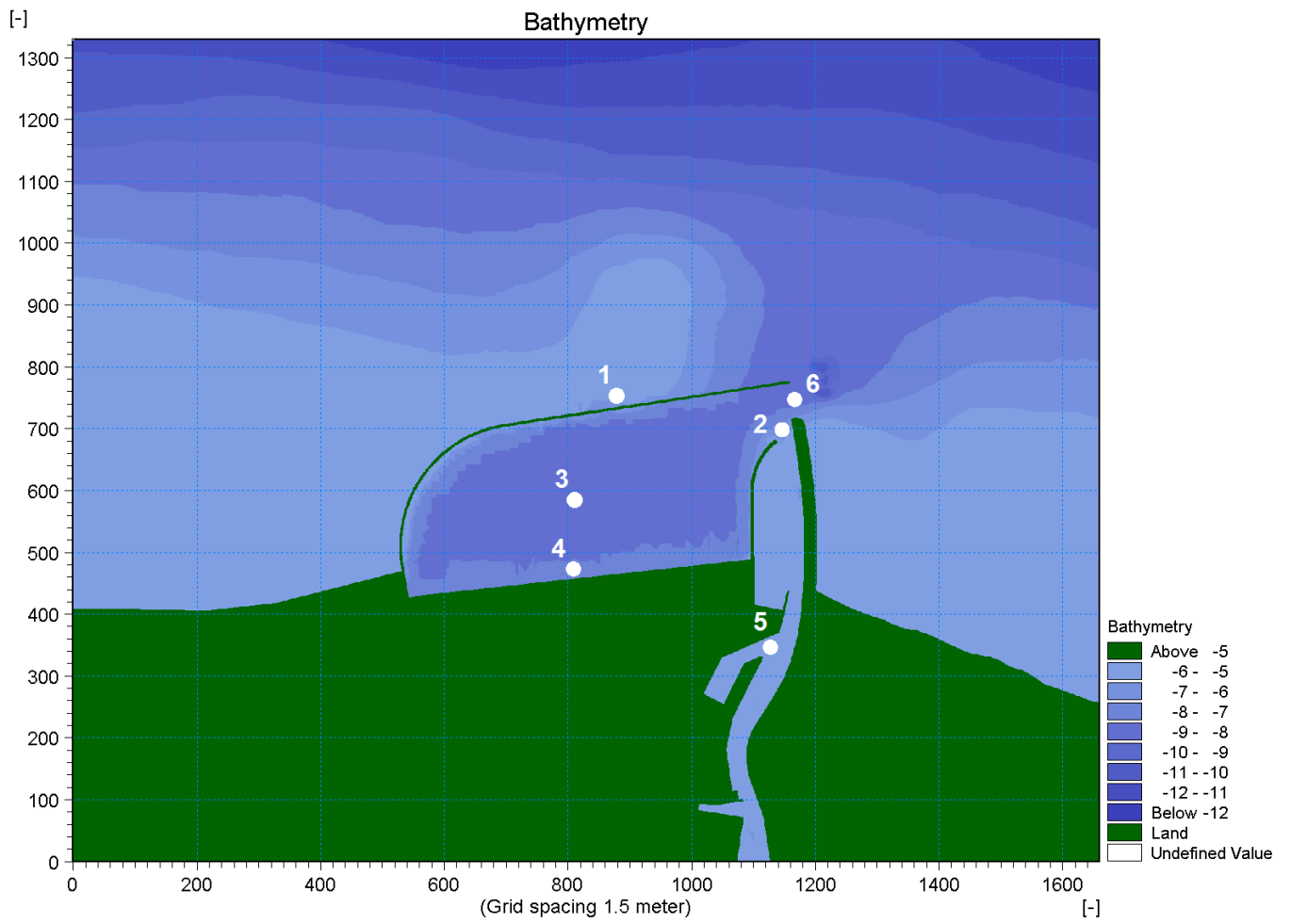


Figure 76 Second concept with marked points of interest. Generated by Mike Zero.

Random waves from north-west:

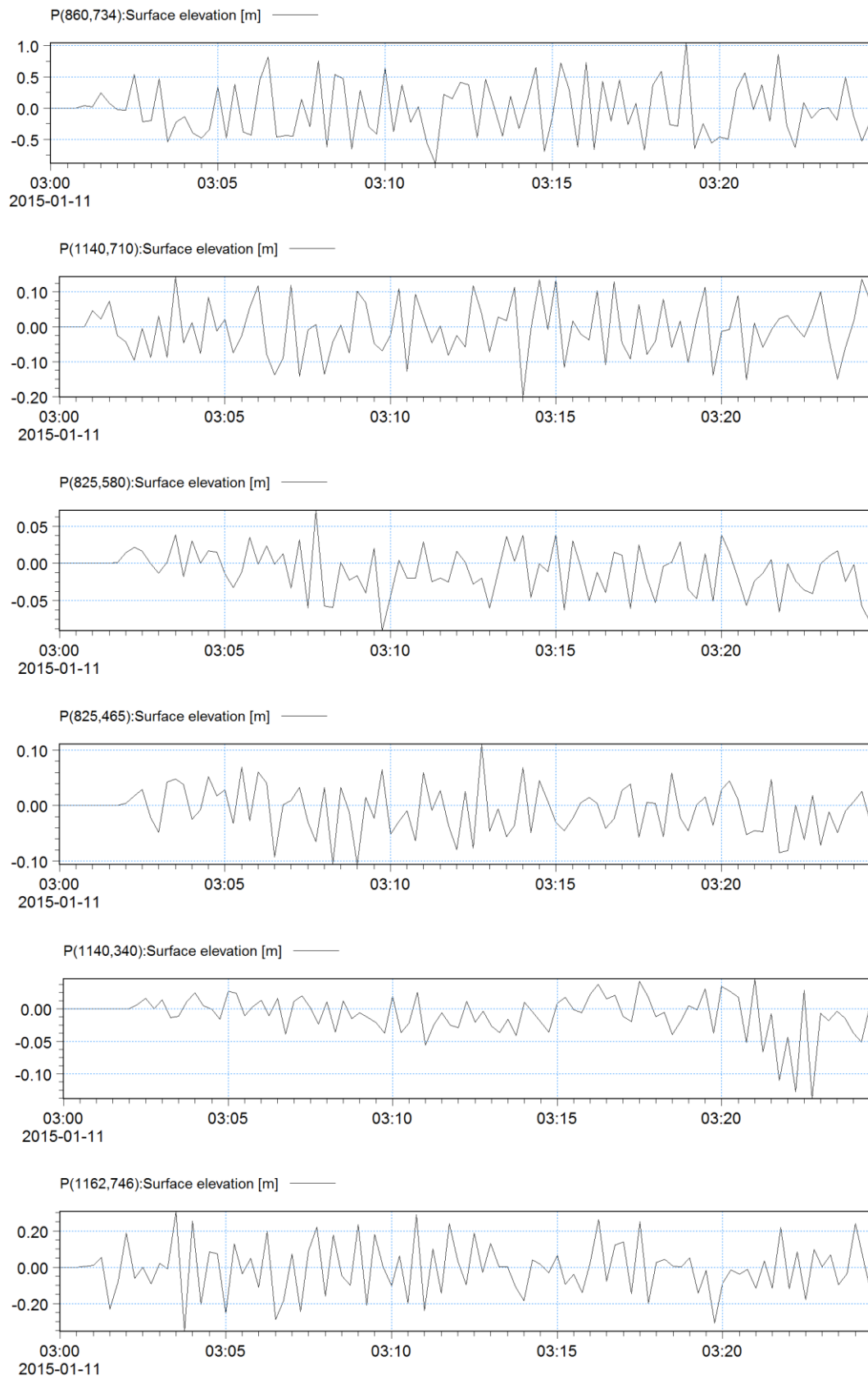


Figure 77 Second layout, random waves from north-west: Plot of the time series for point 1-6 from Figure 76, from the top to the bottom respectively

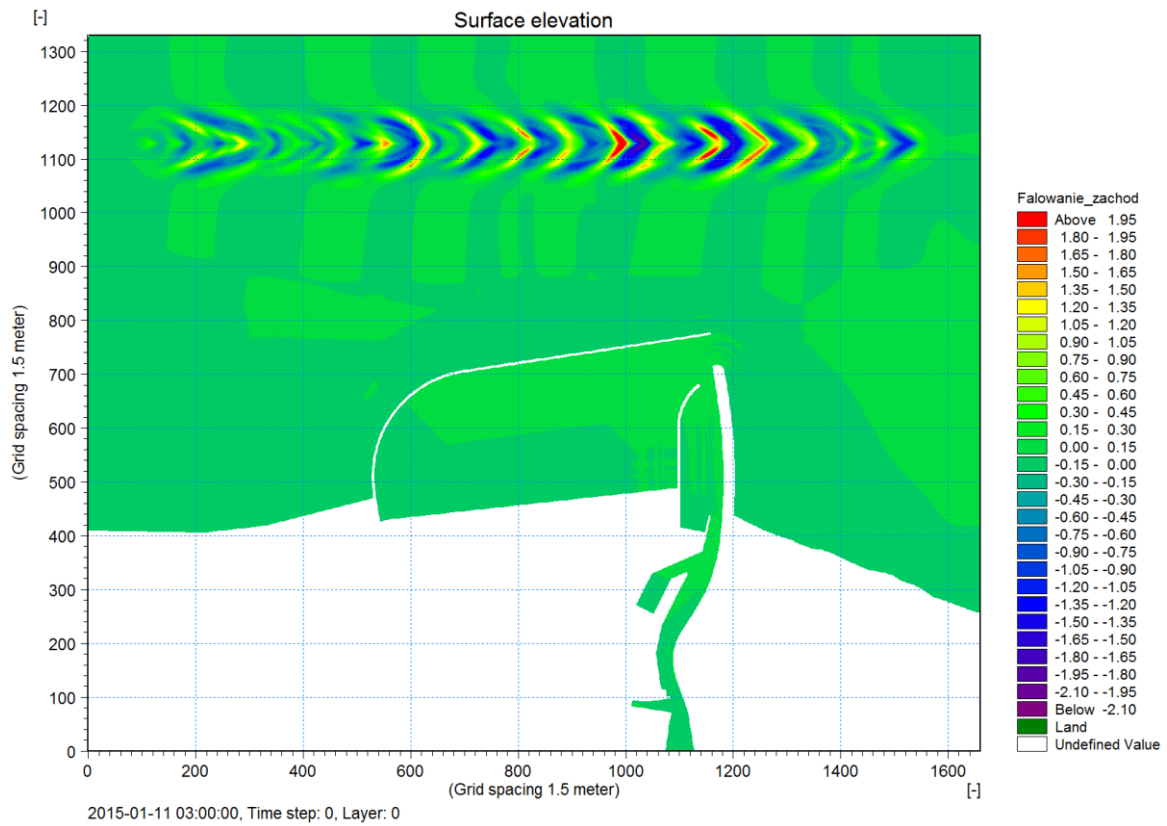


Figure 78 Snapshot of the second layout, random waves from north-west: Plot of the waves at the beginning of the simulation.

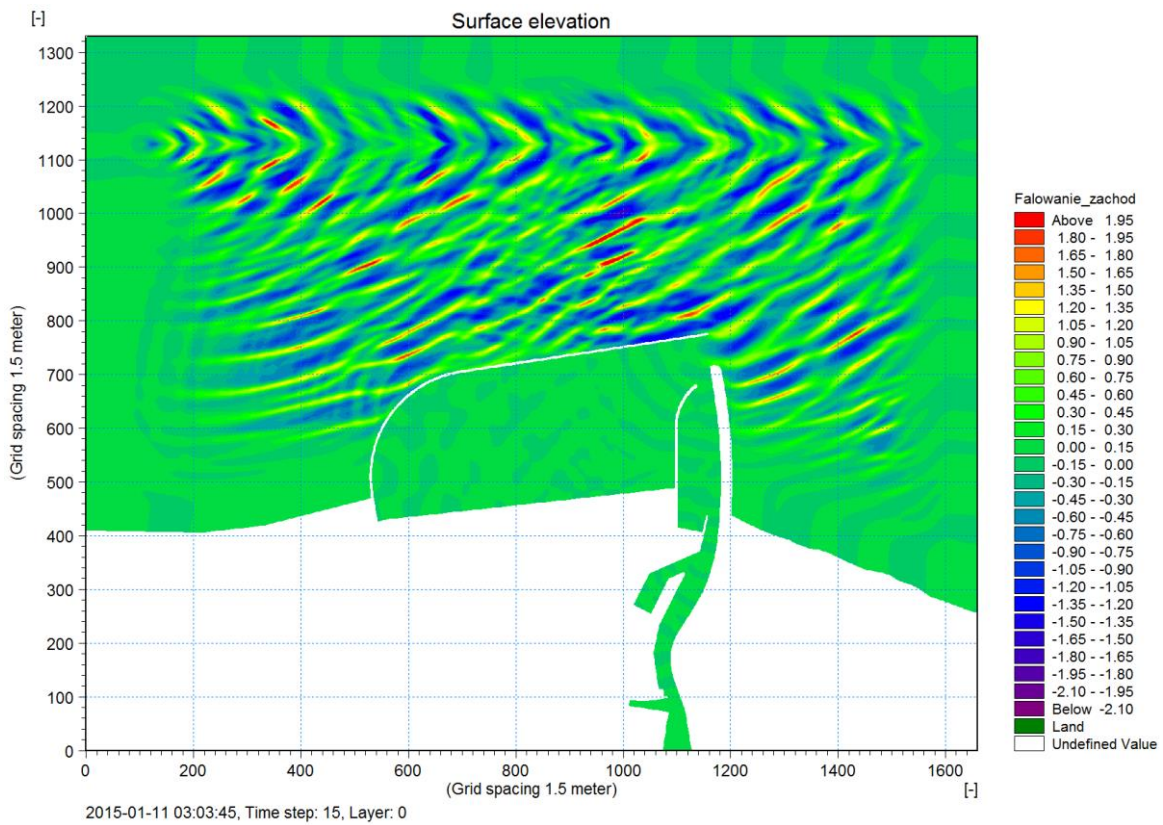


Figure 79 Snapshot of the second layout, random waves from north-west: Propagating waves at the time of the occurrence of the highest waves at the harbour entrance.

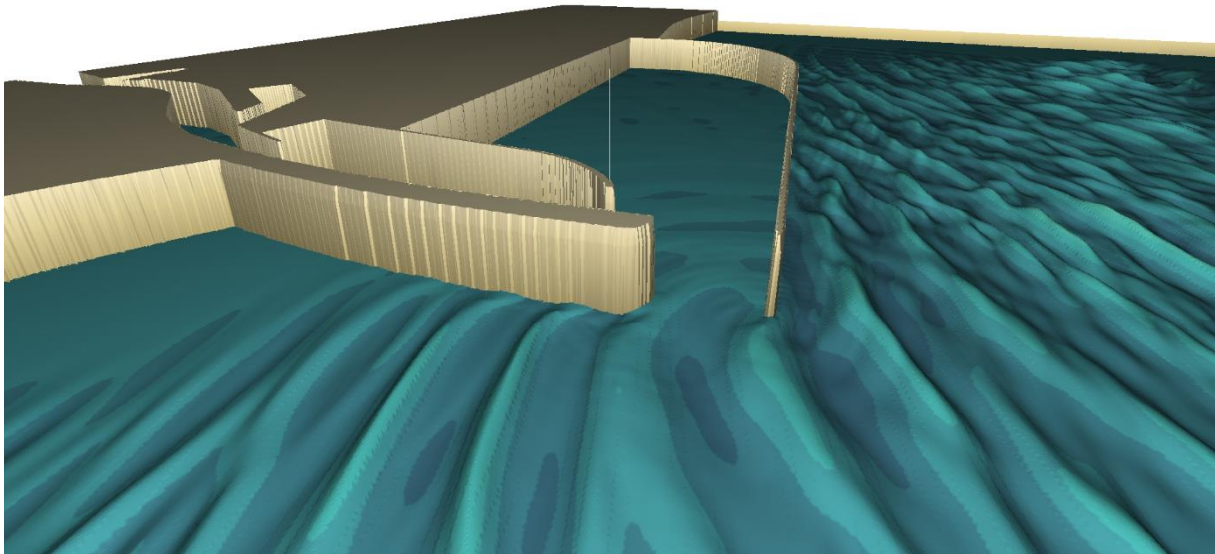


Figure 80 Visualization corresponds to Fig. 77. Snapshot taken at 15th time step. Waves are propagating from north-west.

At Figure 79 one can observe reflected waves from the breakwater also phenomena such as diffraction can be observed e.g. at the entrance to the harbour. With current direction of wave propagation, the breakwater successfully prevents the penetration of waves into the basins. The highest wave that passed next to it was around 1.3 m high and results with small wave at the entrance circa 0.3 m height.

Random waves from north-east:

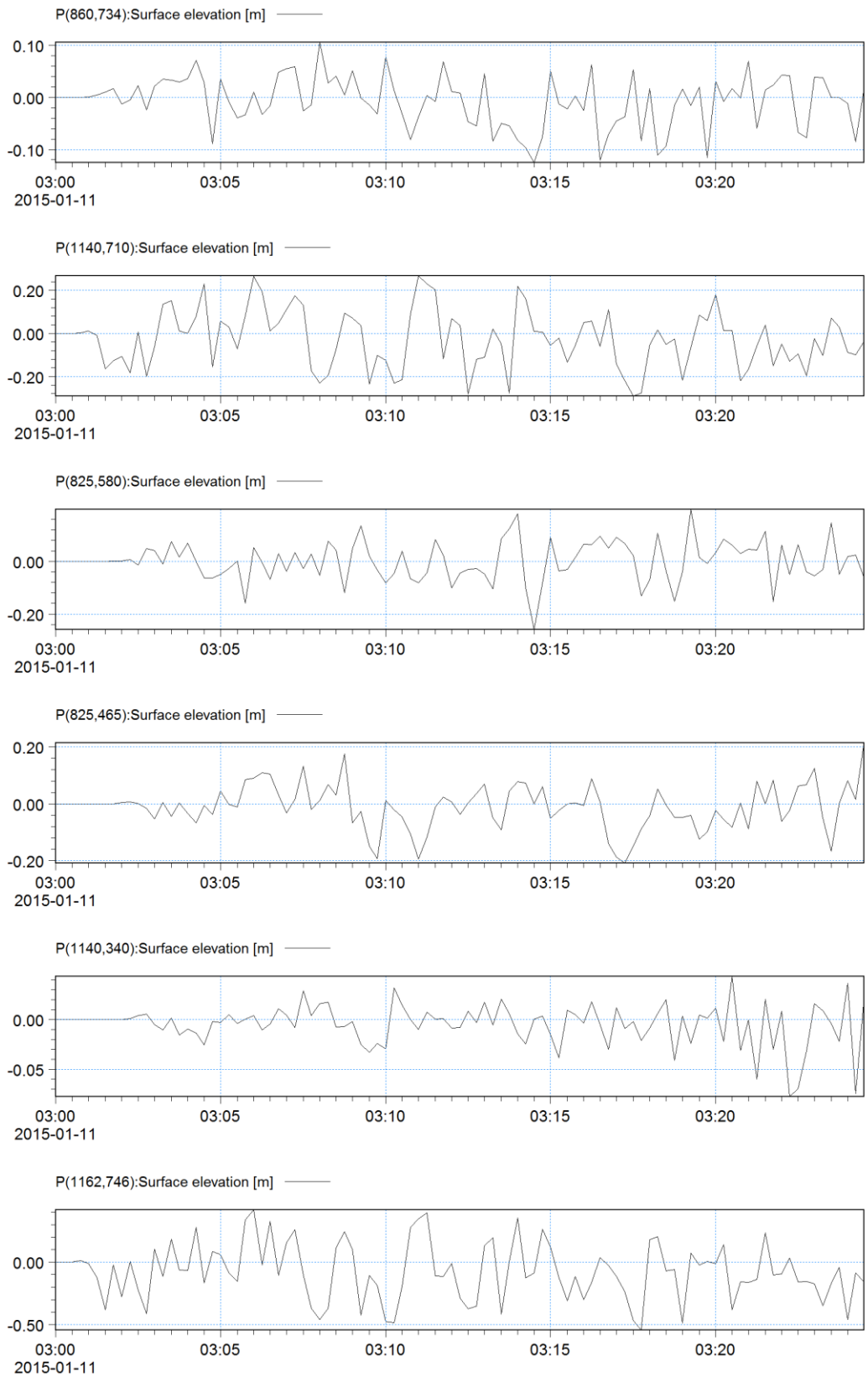


Figure 81 Second layout, random waves from north-east: Plot of the time series for points 1-6 from Figure 76, from the top to the bottom respectively

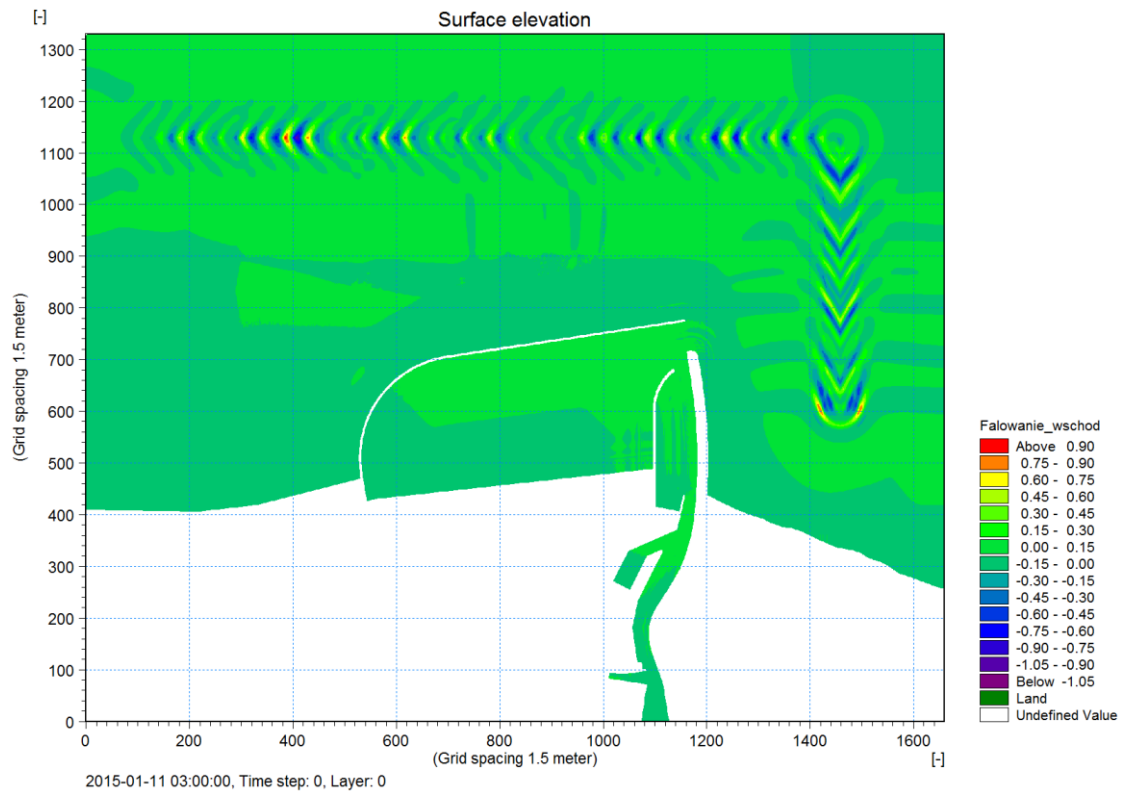


Figure 82 Snapshot of the second layout, random waves from north-east: Plot of the waves at the beginning of the simulation.

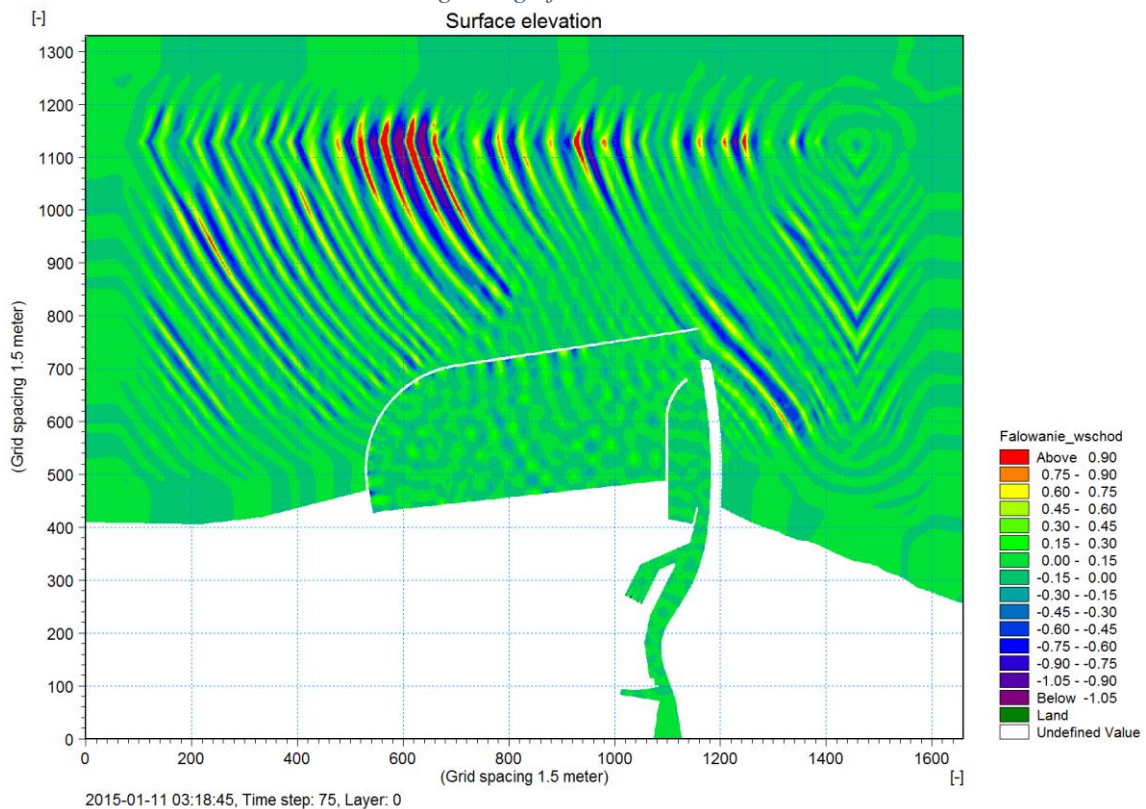


Figure 83 Snapshot of the second layout, random waves from north-east: snapshot of propagating waves at the time of the occurrence of the highest waves at the harbour entrance.

In Figure 83 an interesting phenomenon can be noticed. Waves that are entering the harbour are diffracted at the entrance and then their height tend to rise slightly as they are propagating along the new western breakwater. Below, figure 84 shows closer view on the area.

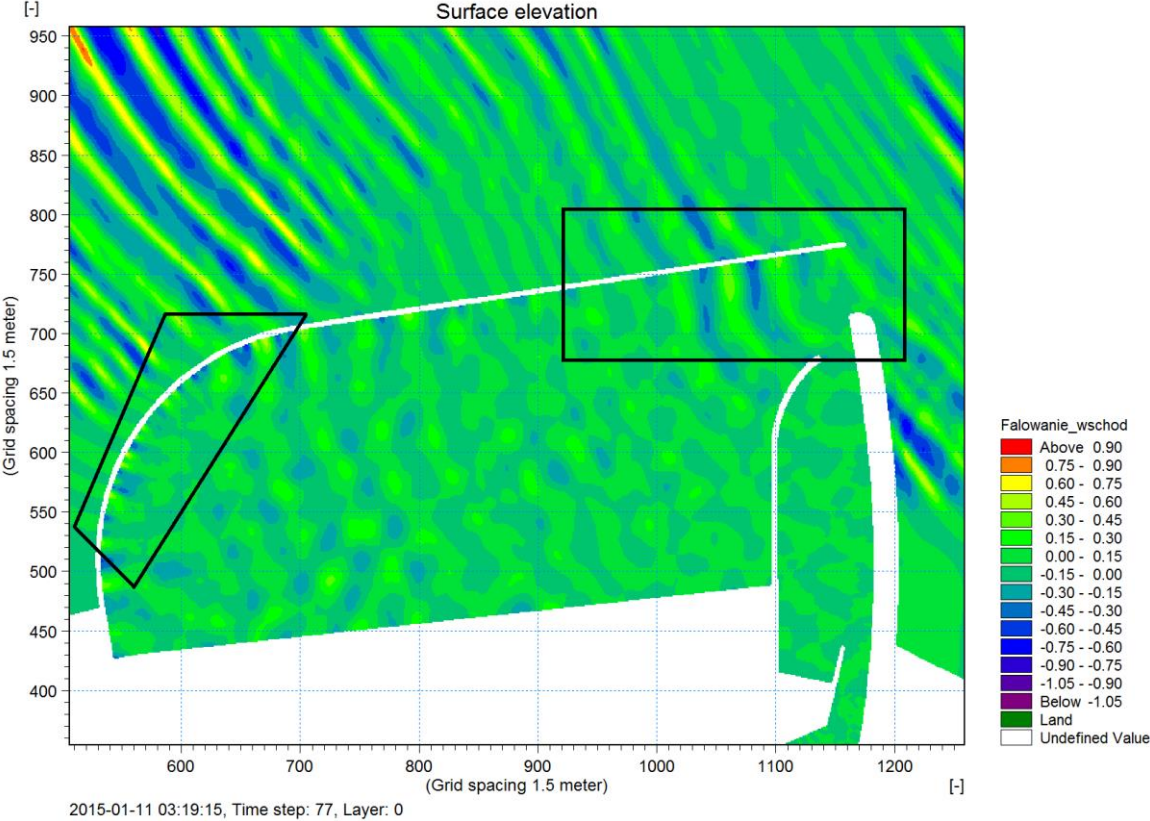


Figure 84 Close-up on the breakwaters showing raising wave heights along the structure

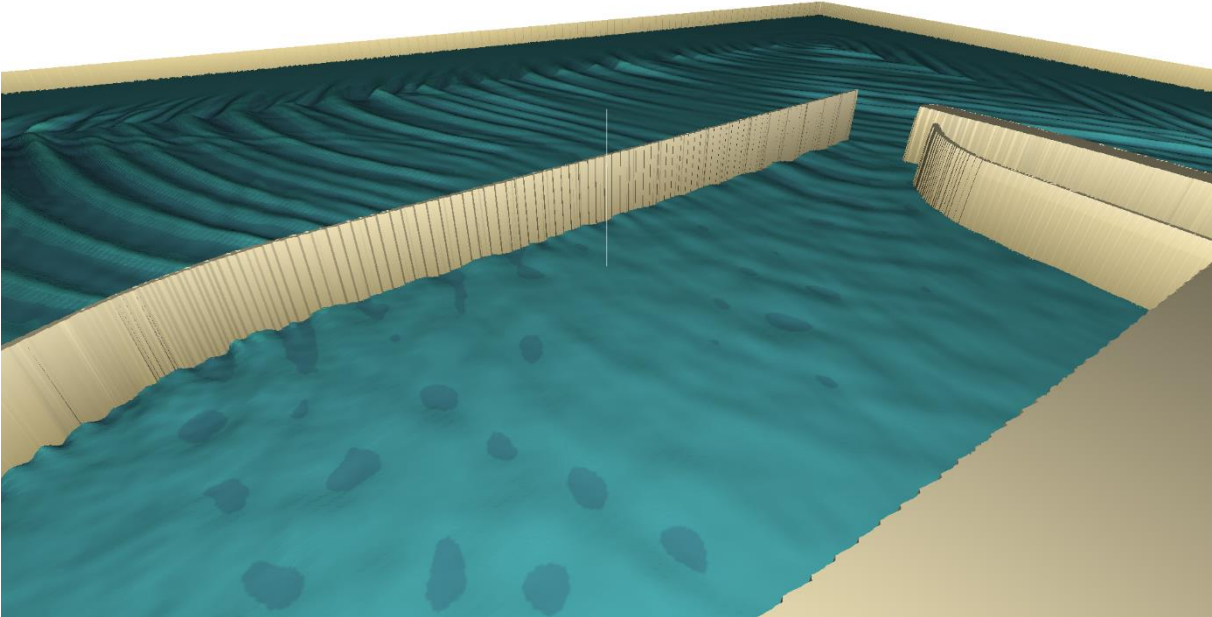


Figure 85 Visualization of the second layout. Snapshot of the 77th time step.

6.3.2.3. Third layout

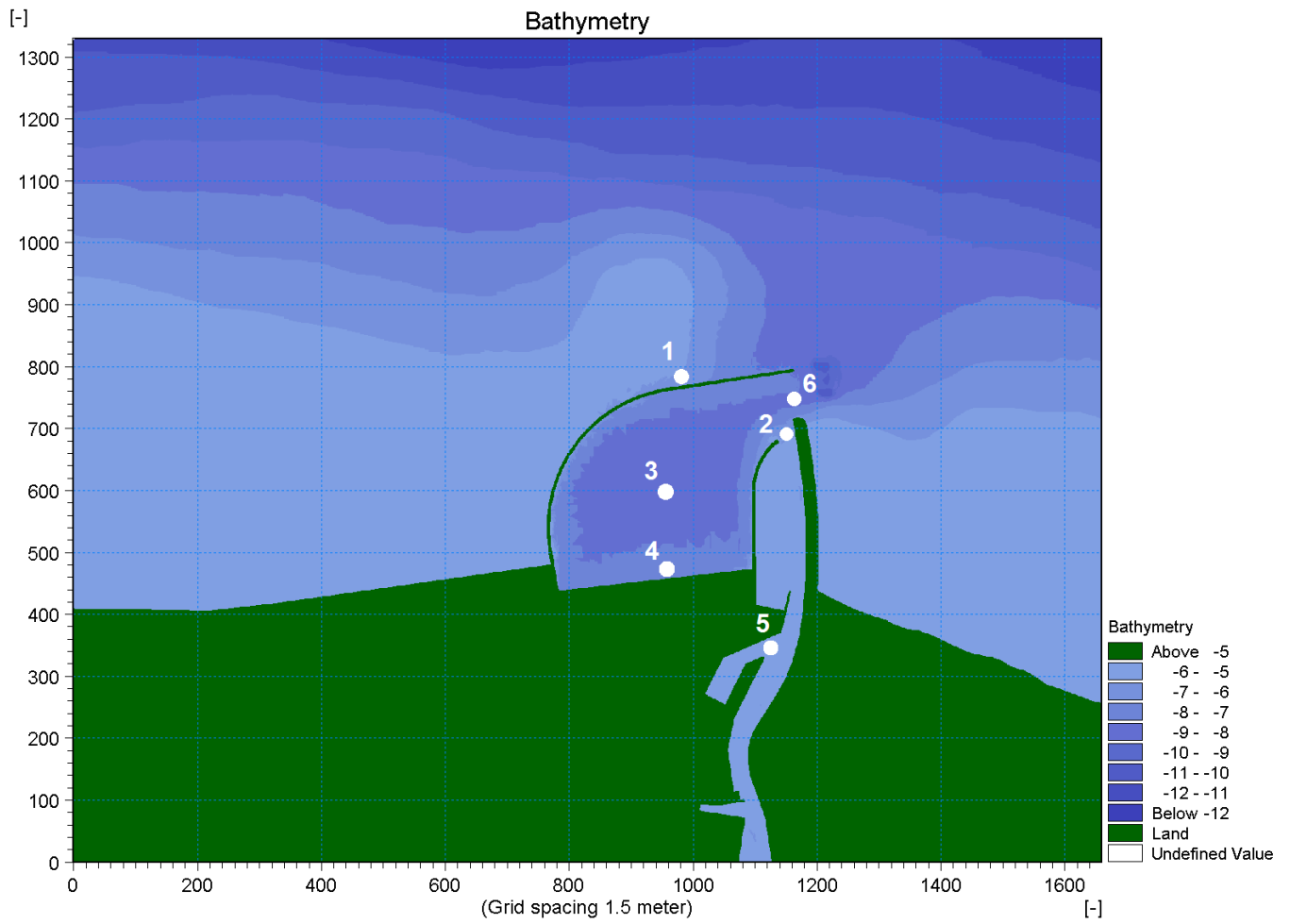


Figure 86 Third concept with marked points of interest. Generated by Mike Zero.

Random waves from north-west:

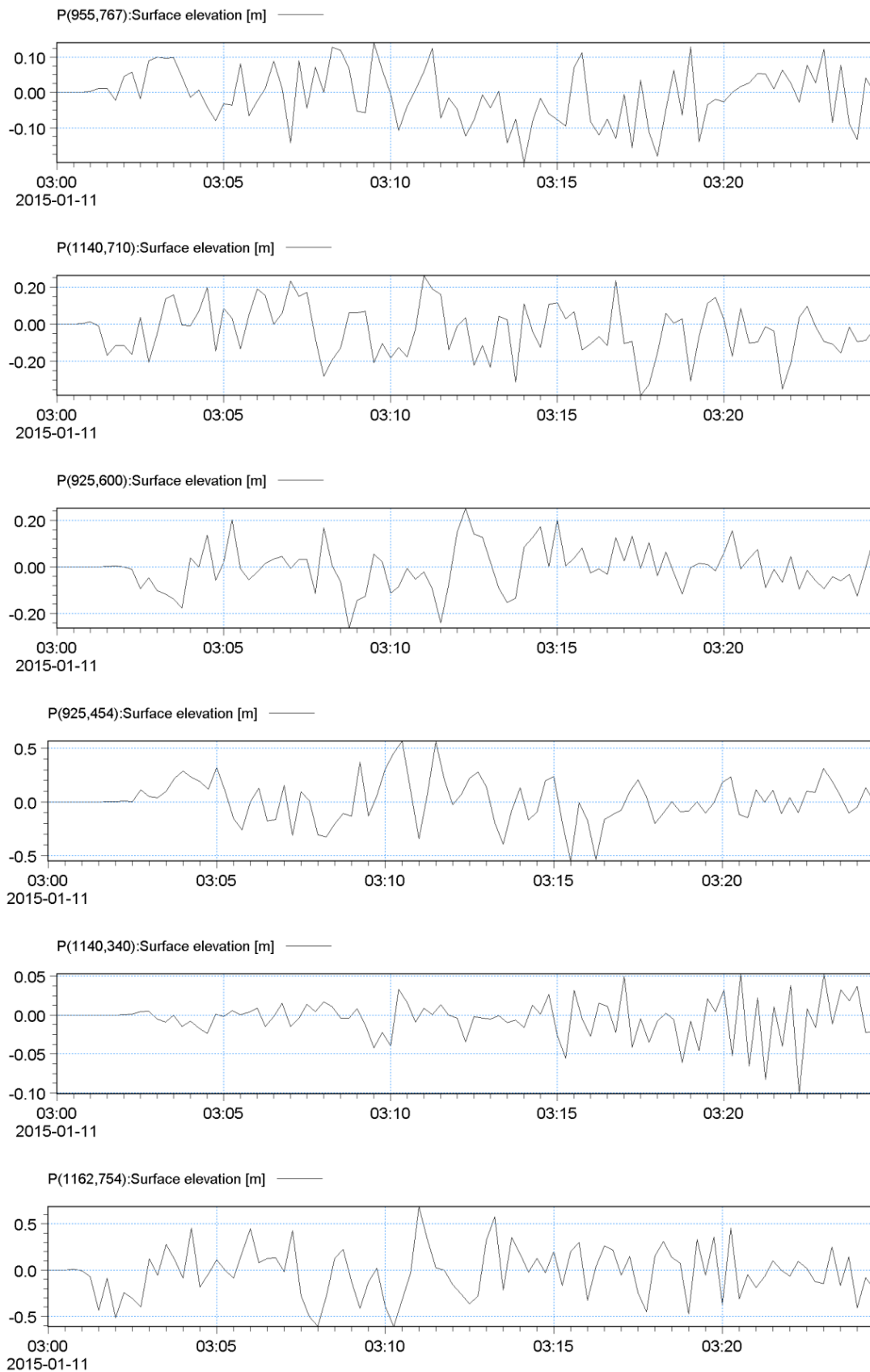


Figure 87 Third layout, random waves from north-west: Plot of the time series for points 1-6 from Figure 86, from the top to the bottom respectively.

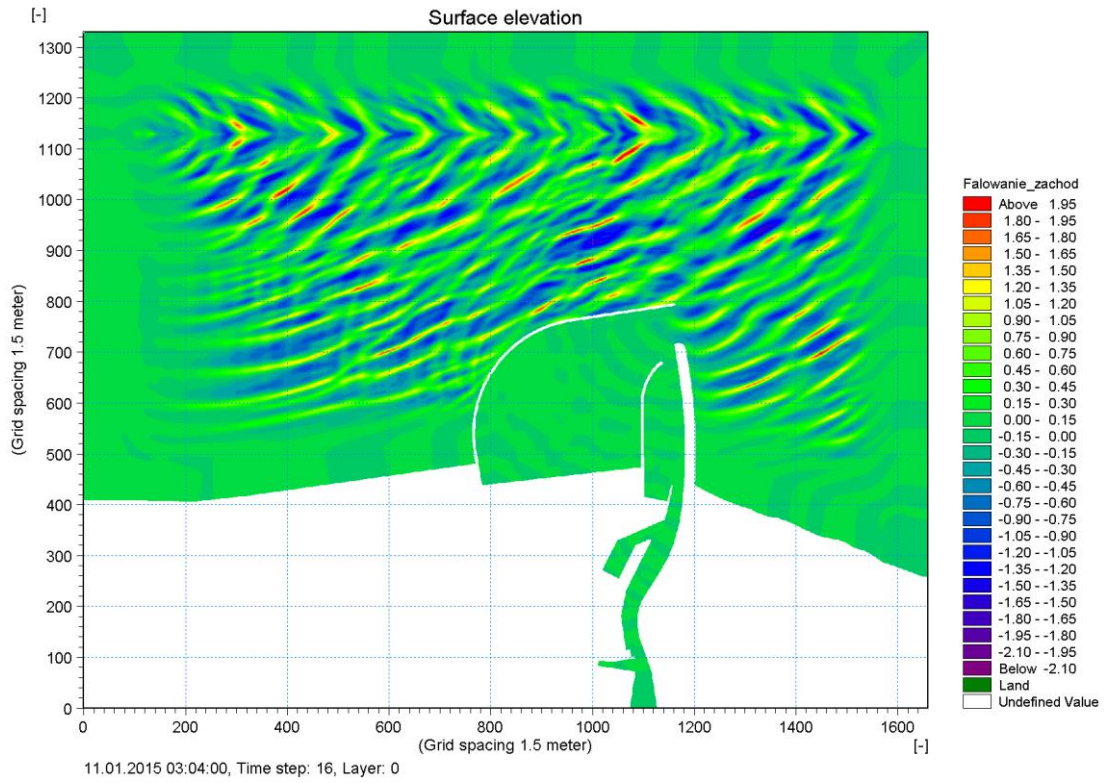


Figure 88 Snapshot of the third layout, random waves from north-west: Snapshot of the waves at the beginning of the simulation.

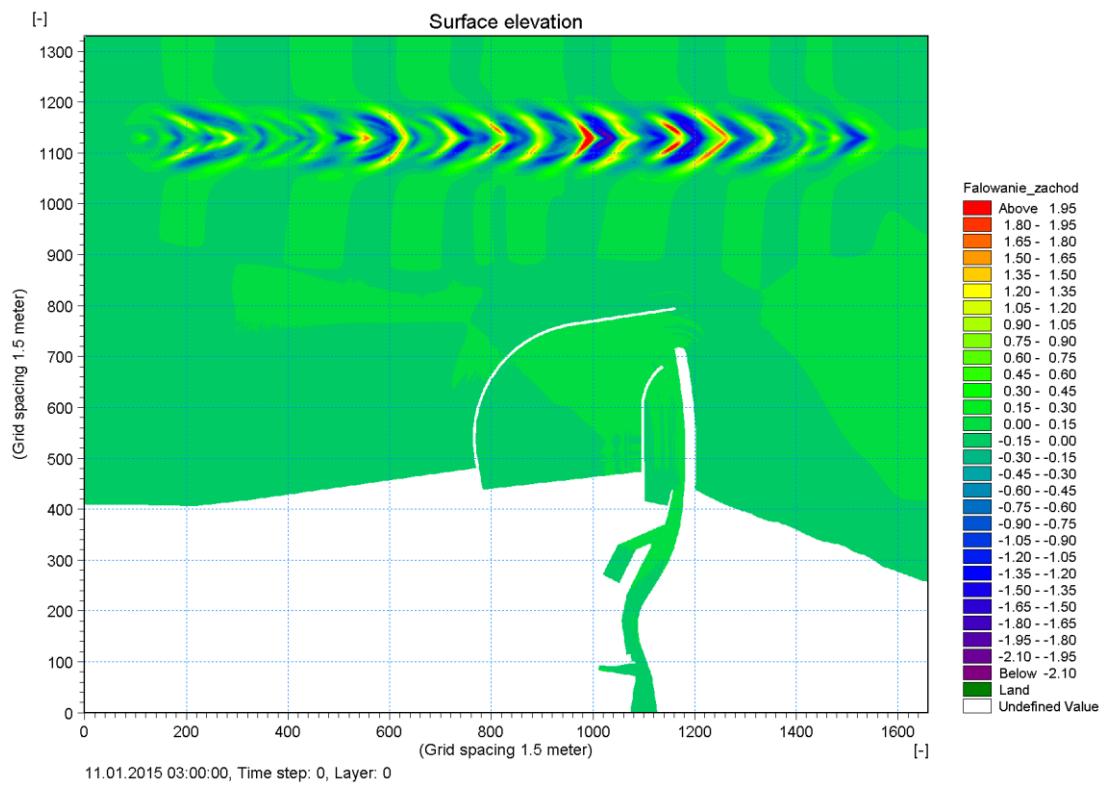


Figure 89 Snapshot of the third layout, random waves from north-west: Plot of propagating waves at the time of the occurrence of the highest waves at the harbour entrance.

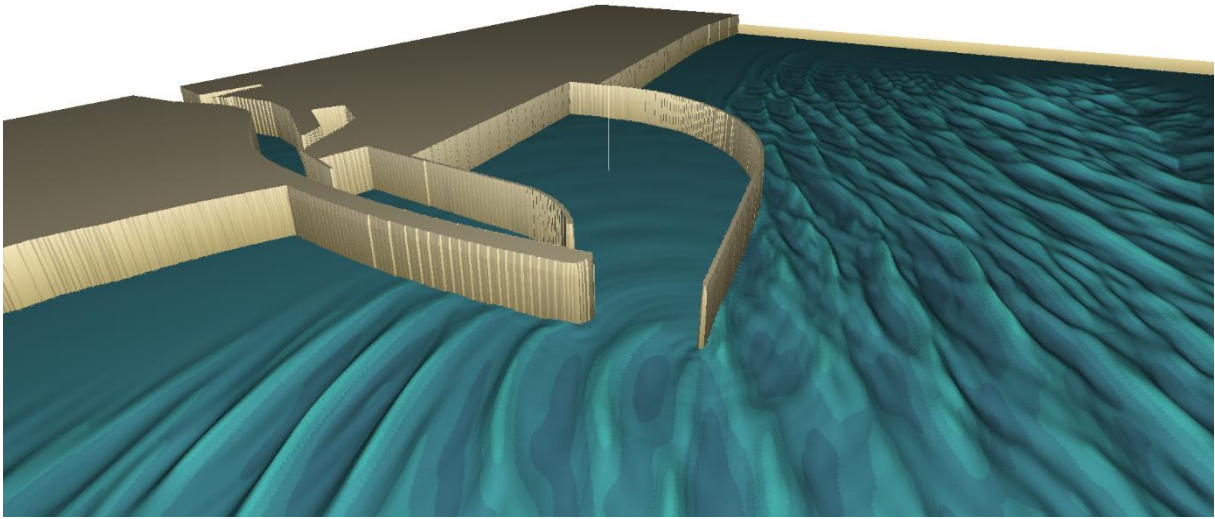


Figure 90 Visualization of the third layout. Snapshot of the 16th time step when the highest wave occurs at the entrance to the harbour.

Random waves from north-east:

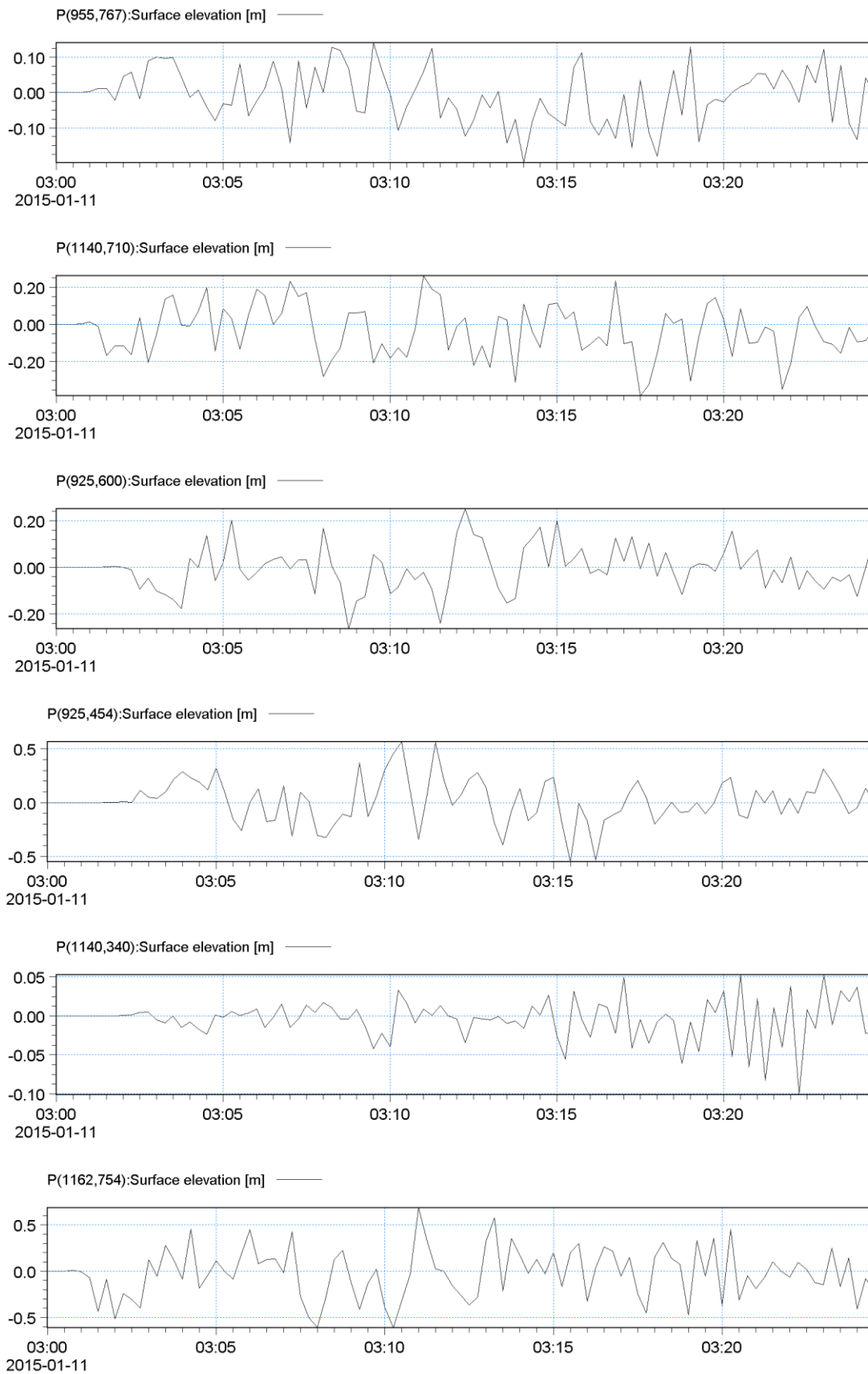


Figure 91 Third layout, random waves from north-east: Plot of the time series for points 1-6 from Figure 86, from the top to the bottom respectively

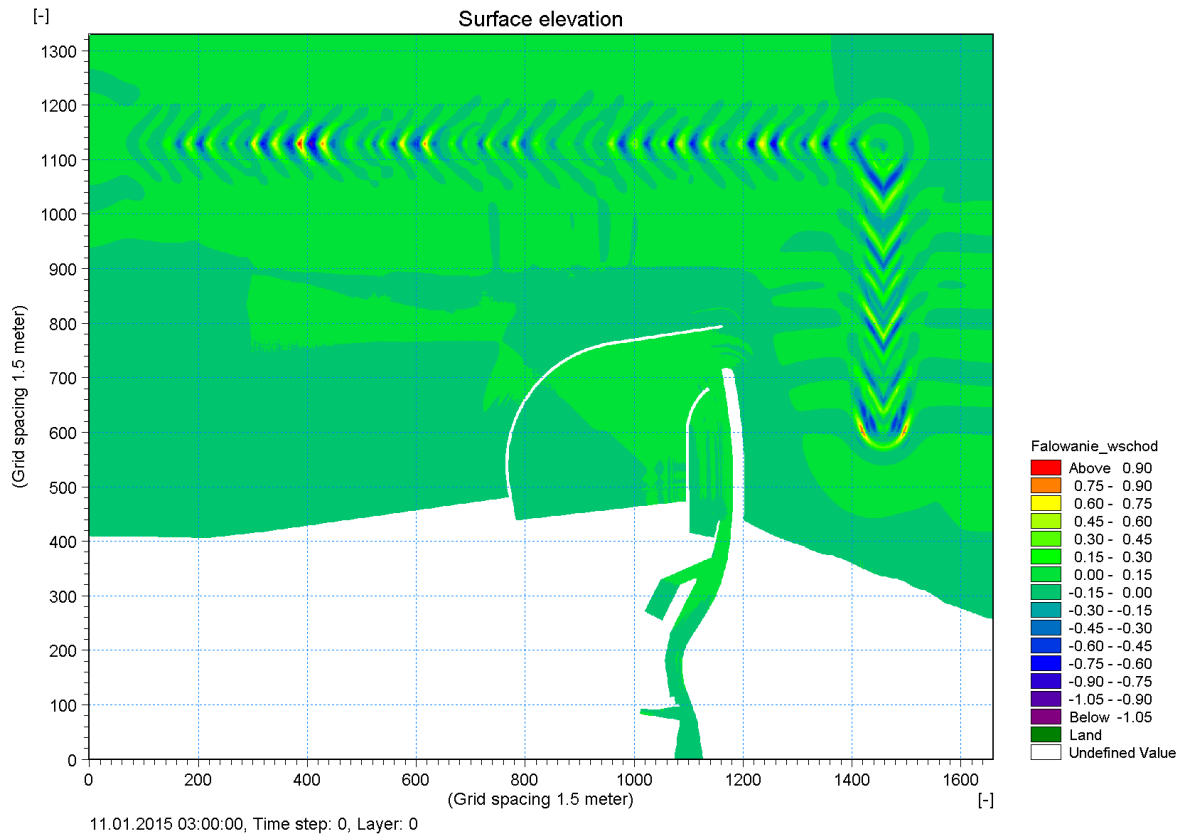


Figure 92 Snapshot of the third layout, random waves from north-east: snapshot of the waves at the beginning of the simulation.

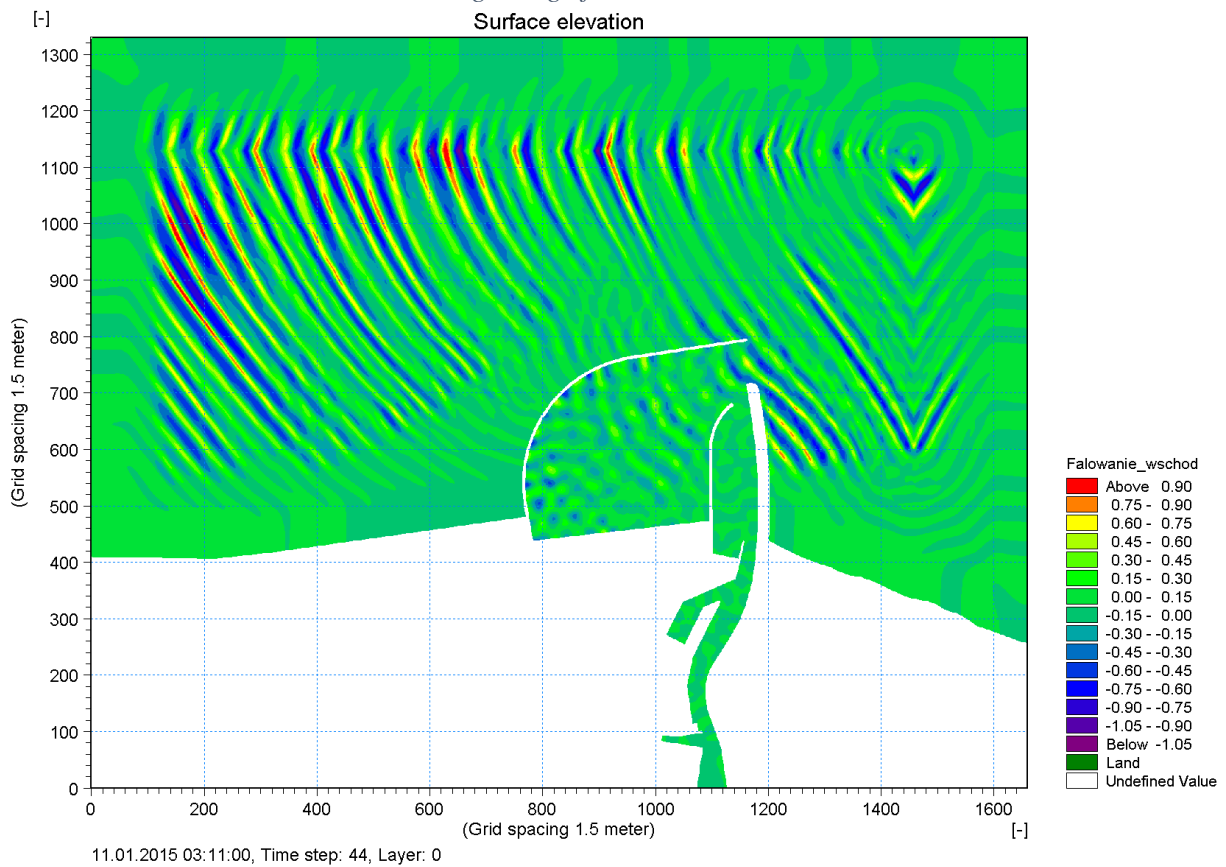


Figure 93 Snapshot of the third layout, random waves from north-east: snapshot of propagating waves at the time of the occurrence of the highest waves at the harbour entrance.

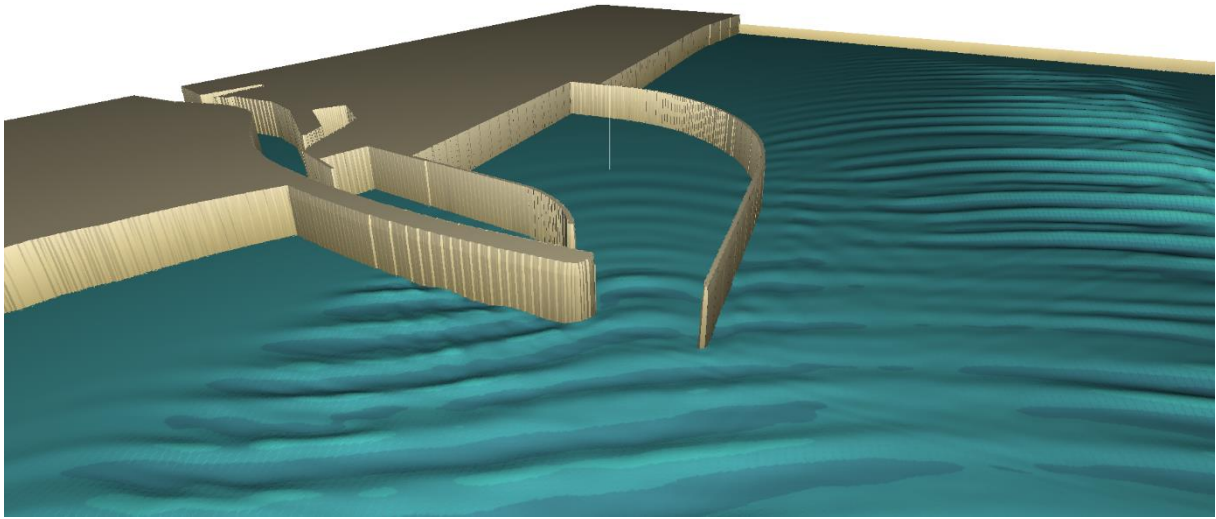


Figure 94 Visualisation of the third layout. Snapshot of the 9th time step. Waves propagating from north-east. First waves entered into the new basin.

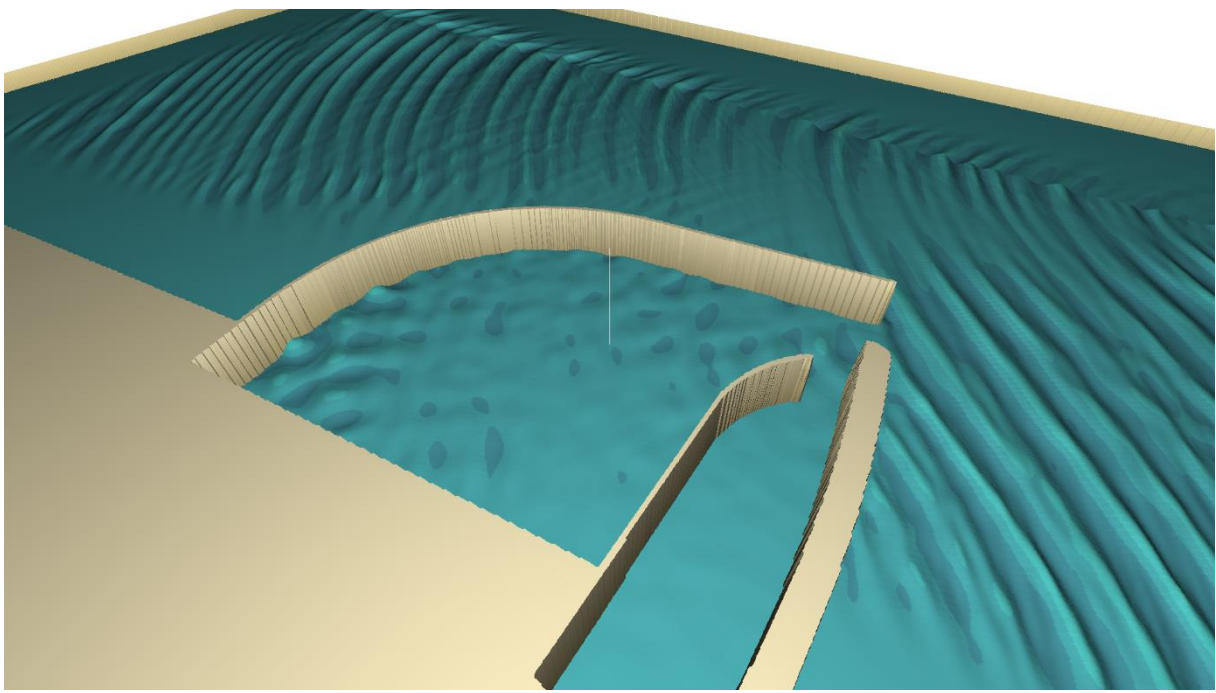


Figure 95 Visualisation of the third layout. Snapshot of the 39th time step. Reflected waves creates standing wave at the corner of the new basin.

6.3.2.4. Fourth layout

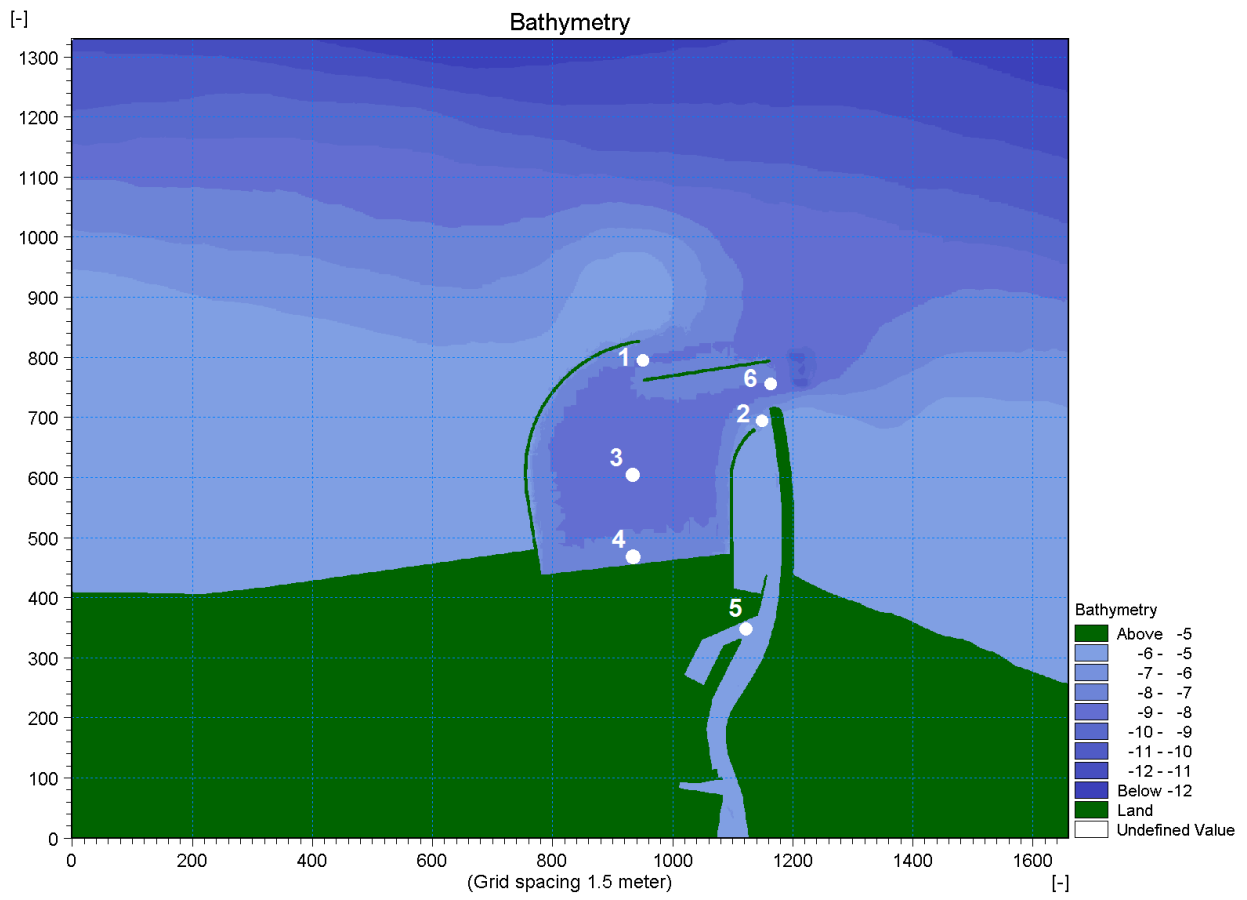


Figure 96 Fourth concept with marked points of interest. Generated by Mike Zero.

Random waves from north-west:

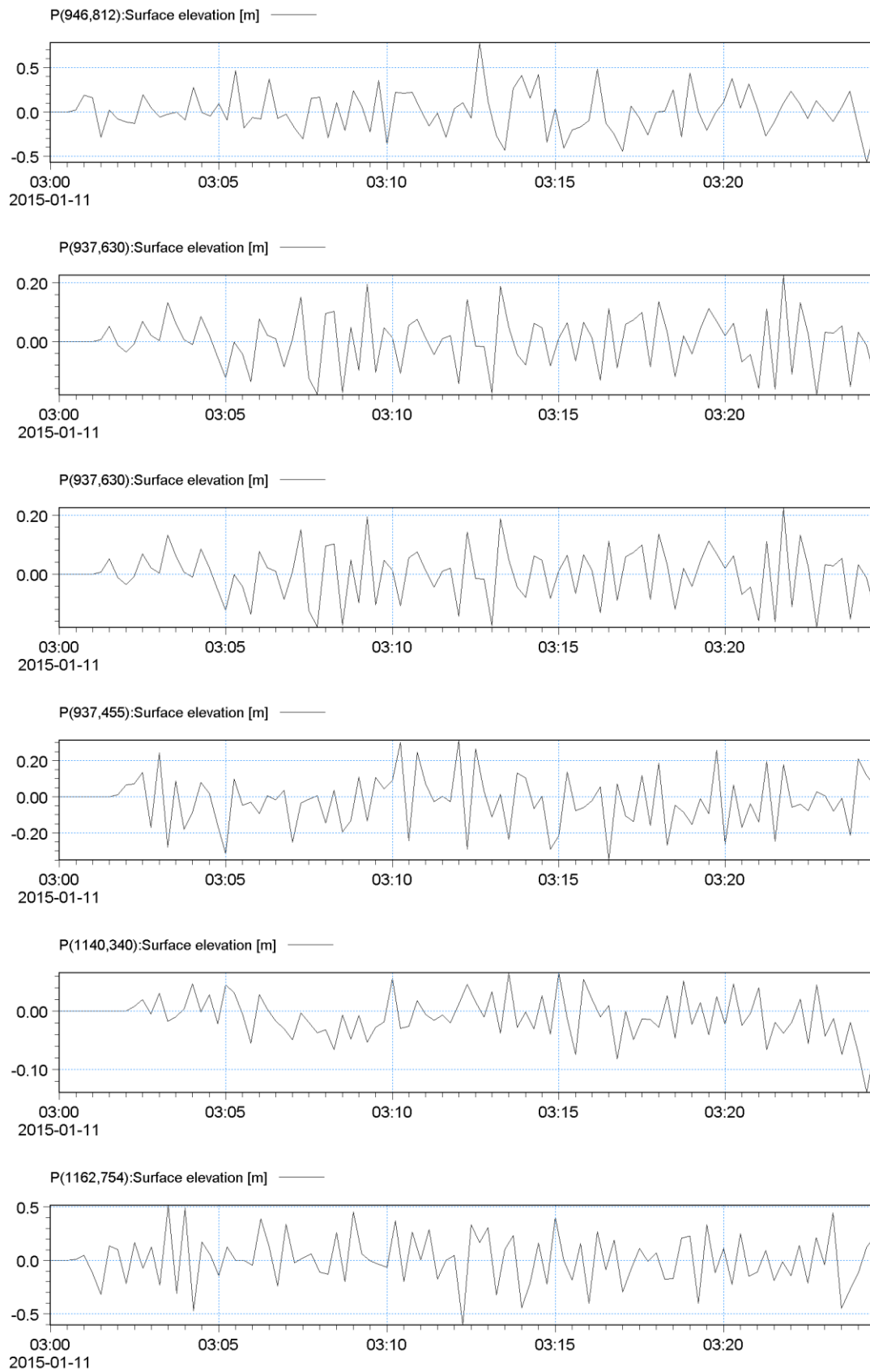


Figure 97 Fourth layout, random waves from north-west: Plot of the time series for points 1-6 from Figure 96, from the top to the bottom respectively

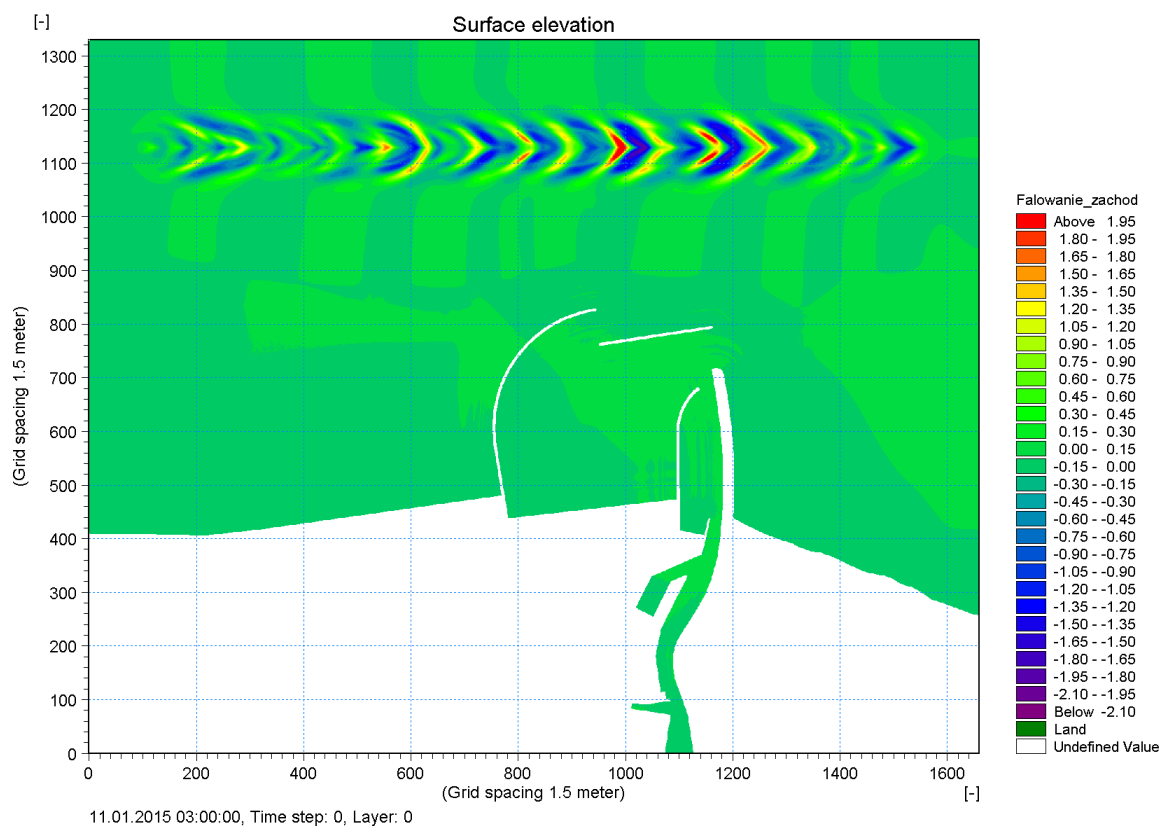


Figure 98 Snapshot of the fourth layout, random waves from north-west: snapshot of the waves at the beginning of the simulation.

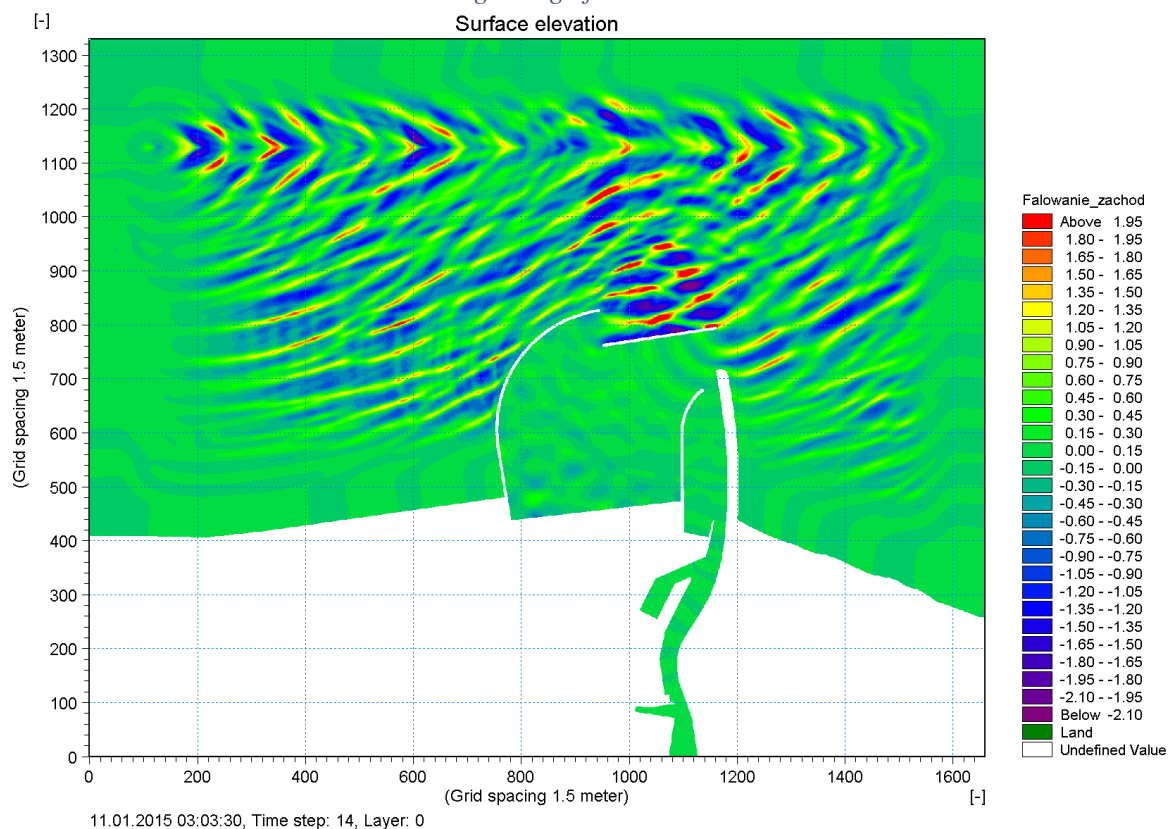


Figure 99 Snapshot of the fourth layout, random waves from north-west: snapshot of propagating waves at the time of the occurrence of the highest waves at the harbour entrance.

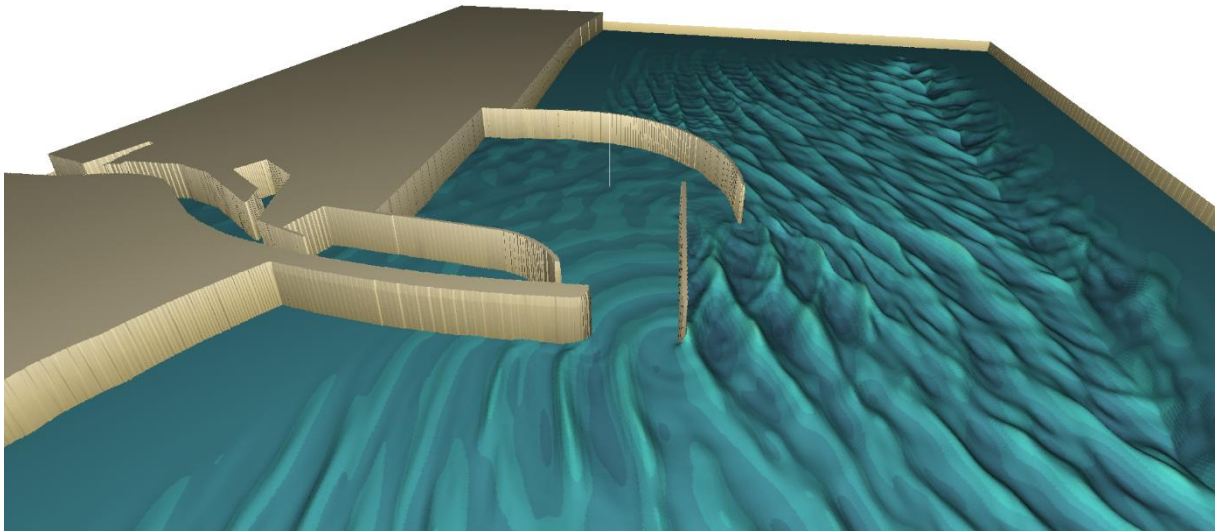


Figure 100 Visualisation of the fourth layout, waves from north-west.. Snapshot of the 14th time step shows standing wave.

As it can be seen on Figures 99 and 100, waves coming from the north-west are propagating almost parallel towards the detached breakwater, and are reflected by it. Thus very high standing wave is created at the entrance to the harbour.

Random waves from north-east:

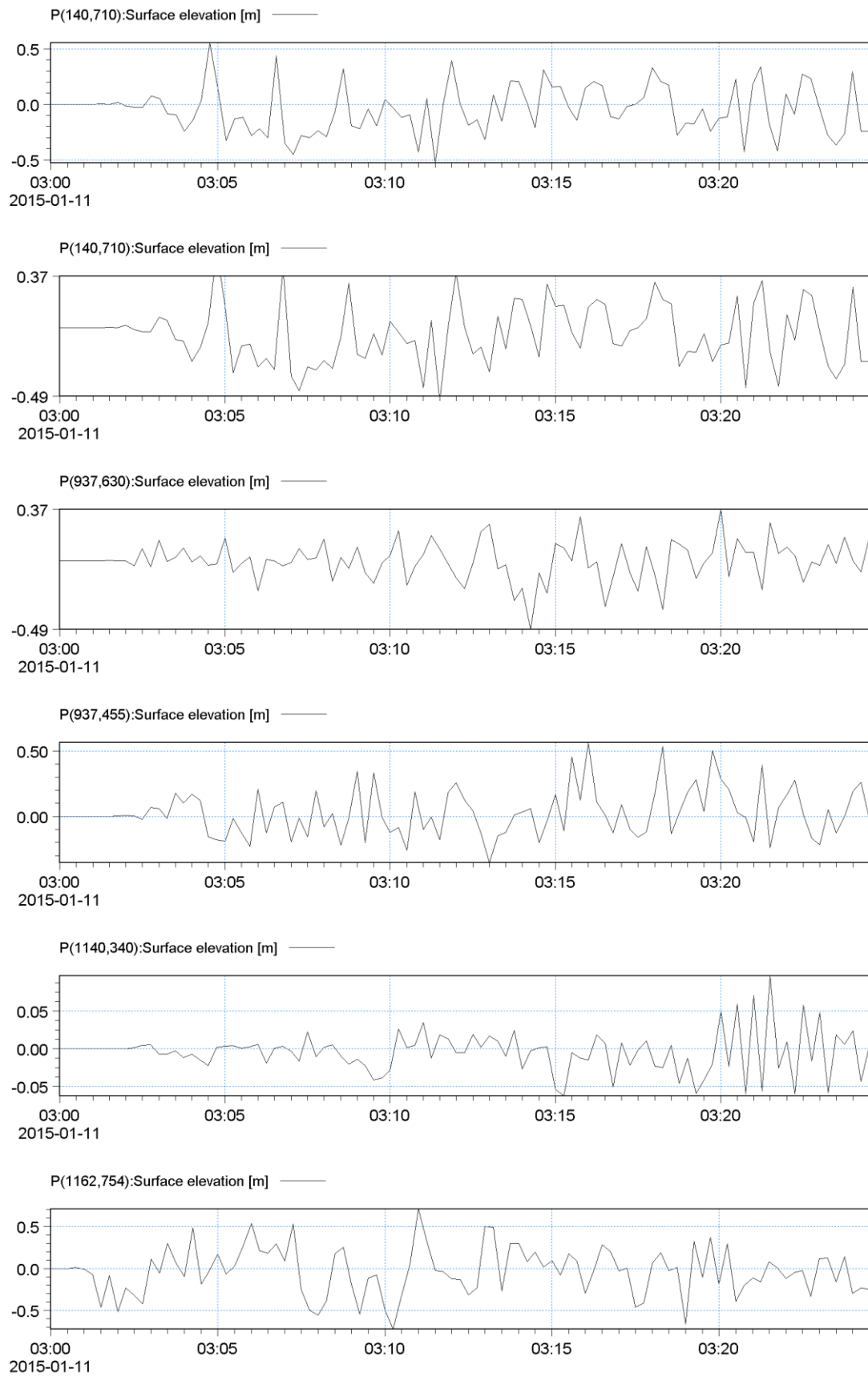


Figure 101 Fourth layout, random waves from north-east: Plot of the time series for points 1-6 from Figure 96, from the top to the bottom respectively

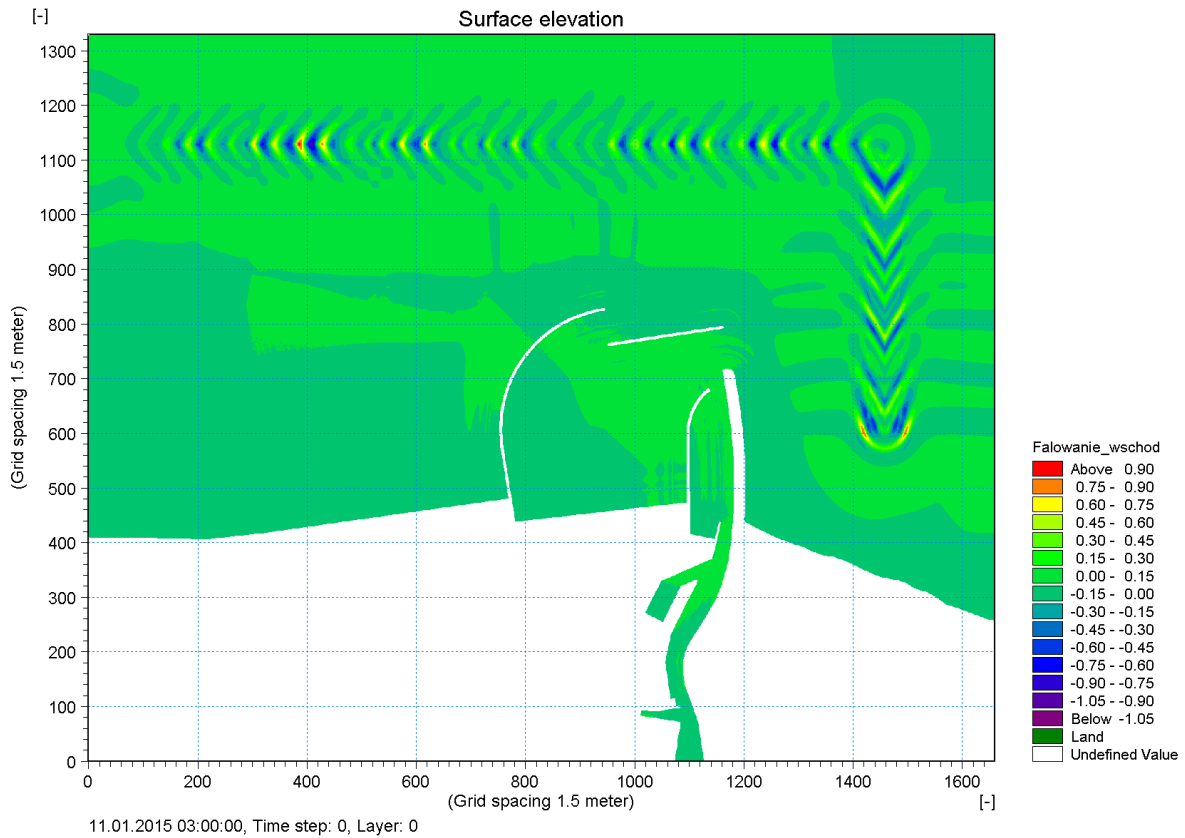


Figure 102 Snapshot of the fourth layout, random waves from north-east: snapshot of the waves at the beginning of the simulation.

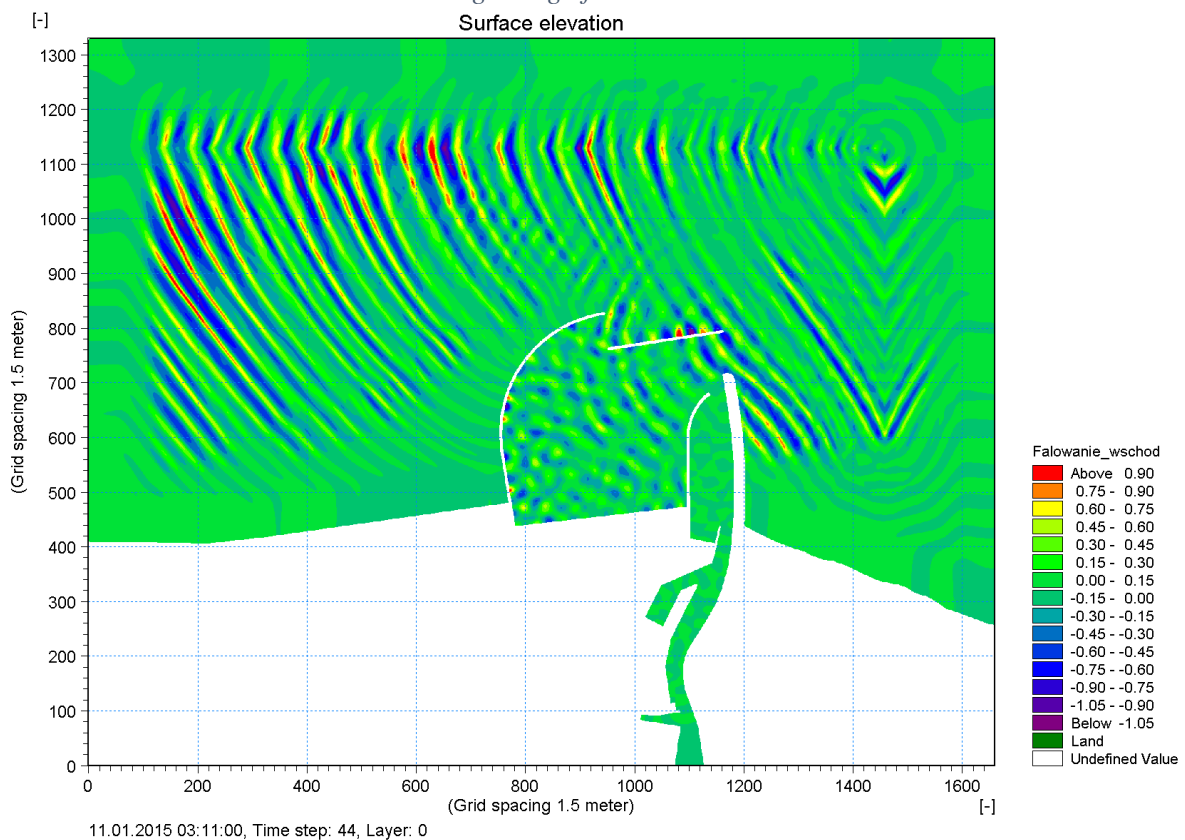


Figure 103 Snapshot of the fourth layout, random waves from north-east: snapshot of propagating waves at the time of the occurrence of the highest waves at the harbour entrance.

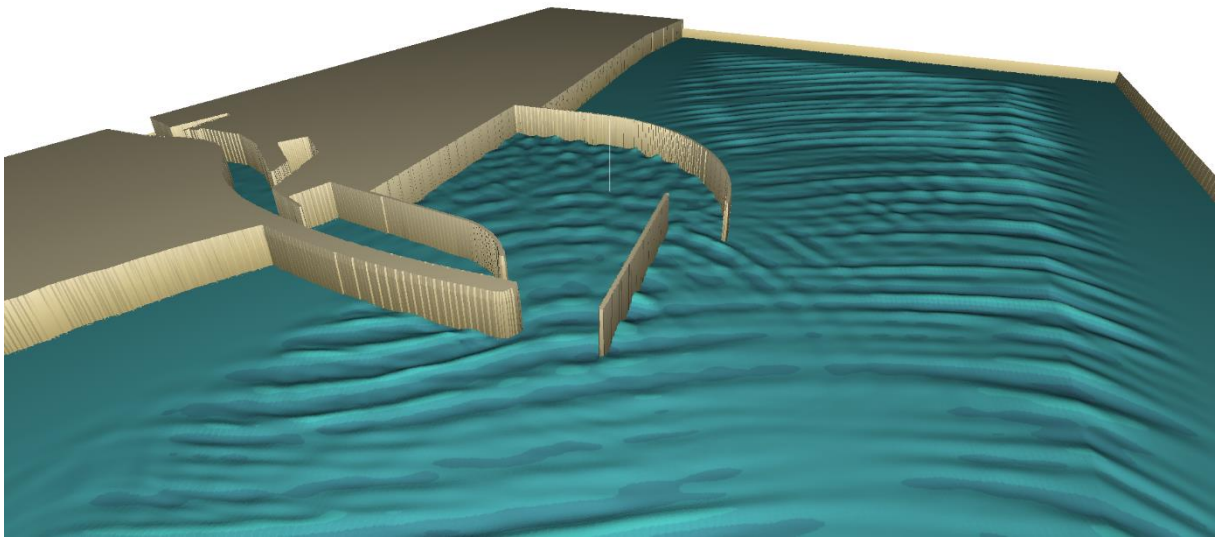


Figure 104 Visualisation of the fourth layout., random waves from north-east: snapshot of propagating waves at the time of the occurrence of the highest waves at the harbour entrance.

In this case again the incoming waves are reflected by the detached breakwater but, as they are propagating much more along, the area of high, standing wave is much smaller than the one formed by waves coming from north-west.

6.4. Comparison and discussion of the results

Figures 105-118 show compared time series for all four proposed harbour layouts at all 6 previously determined points for both wave directions (Figure 105 and 106 for waves from north-west, and figures 107 and 108 for waves coming from north-east). As it can be seen all layouts show some similarities, but have some significant differences as well. All layouts protect the basins from waves coming from north-east, which is the main direction of waves in this area. In all cases at point 5 the waves tend to grow slowly and only at the end of time series the largest waves occur. This is because point 5 is located far from the generation line and is well sheltered, so waves need some time to affect the water surface at that point.

All proposed breakwater layouts create harbour entrances of different width, which affects the wave climate a lot. For layouts 1 and 4, which have two entrances separated by a detached breakwater waves can propagate into the harbour basins more easily than in cases 2 and 3, which have only one narrow entrance.

Wave heights have different values at the different locations inside the harbour, from the approximately 0.08 m inside the old harbour up to over 1.0 m at the detached breakwater (See Figure 96, p.102). Despite the fact, that in the variant with waves coming from north-east imposed waves were significantly smaller ($H_s=1.03$ m instead 2.5 m for waves form north-west) the wave heights obtained at different points of the harbour are not so much smaller when compared to the previous variant. This is caused by the less favourable direction of wave propagation. Such direction of propagation makes it difficult to shelter the basins from the impact of incoming waves.

Maximum wave heights obtained from BW simulation are summarized in Table 12 and 13. In addition, mean wave periods T_{01} are given in Table 14 and 15 for points 3,4,5, that is for the points which are located inside the harbour. In order to obtain information about wave periods Linear Spectral Analysis was used. As it can be easily seen in both variants of approaching wave directions the best results are given by the proposed layout 2. It provides the smaller waves in every point for waves coming from north-east and wave climate provide during wave incoming from north-west should also guarantee undisturbed berthing and cargo handling inside harbour. The worst solution seems to be layout 4. In almost every point obtained wave height exceed the threshold values of safe wave heights for yachts or small fishing boats (*q.v.* Tables 3 and 4 in Chapter 3.1).

Despite the fact that waves obtained in layout have quite large mean wave period (4.5 – 9.5 seconds), that can influence both small and larger vessels, the wave height are small enough to assume, that it will not affect port operations.

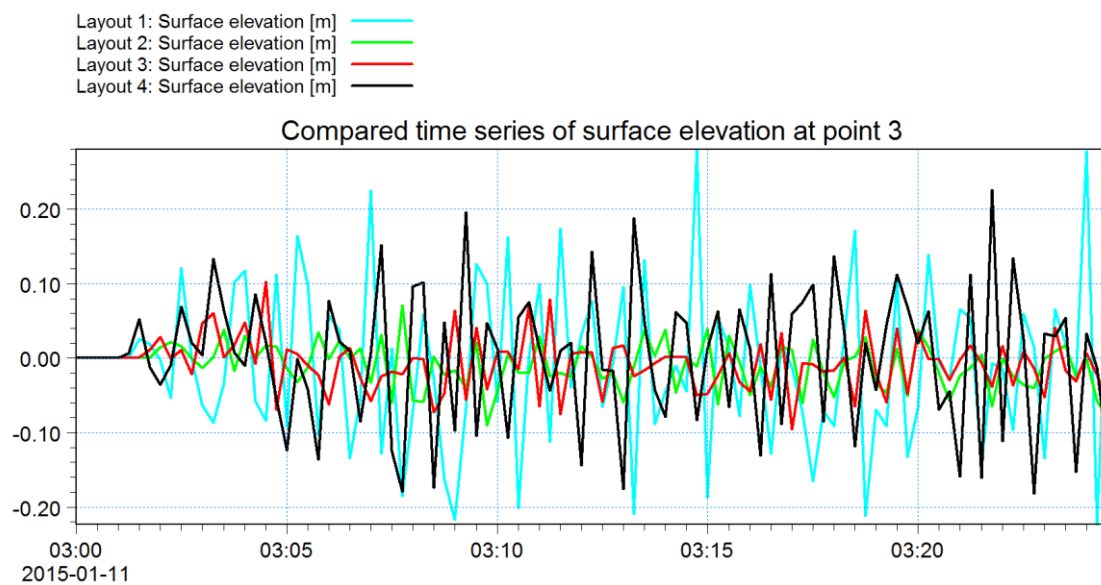
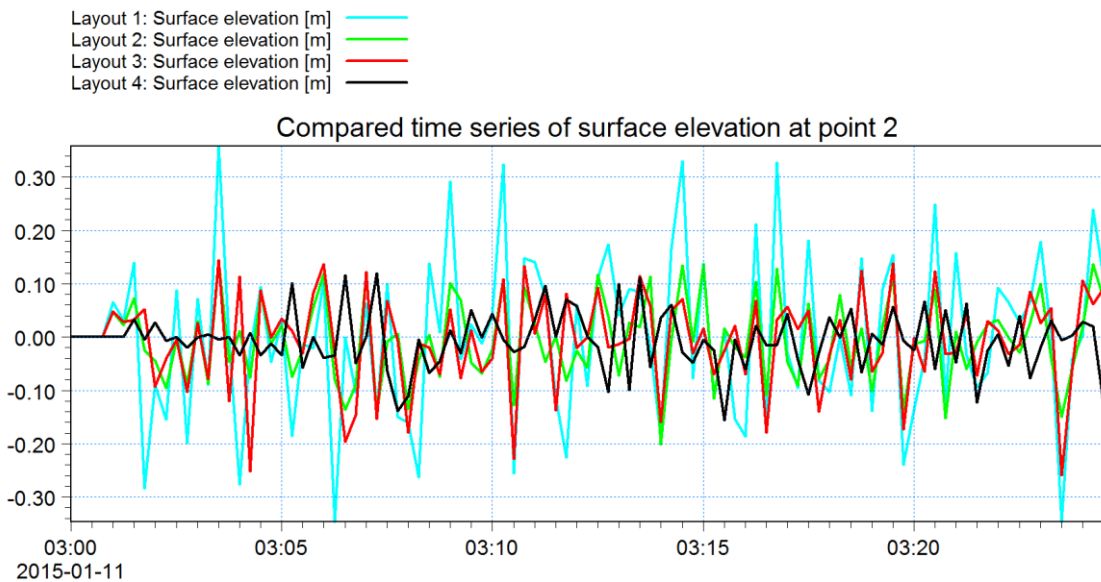
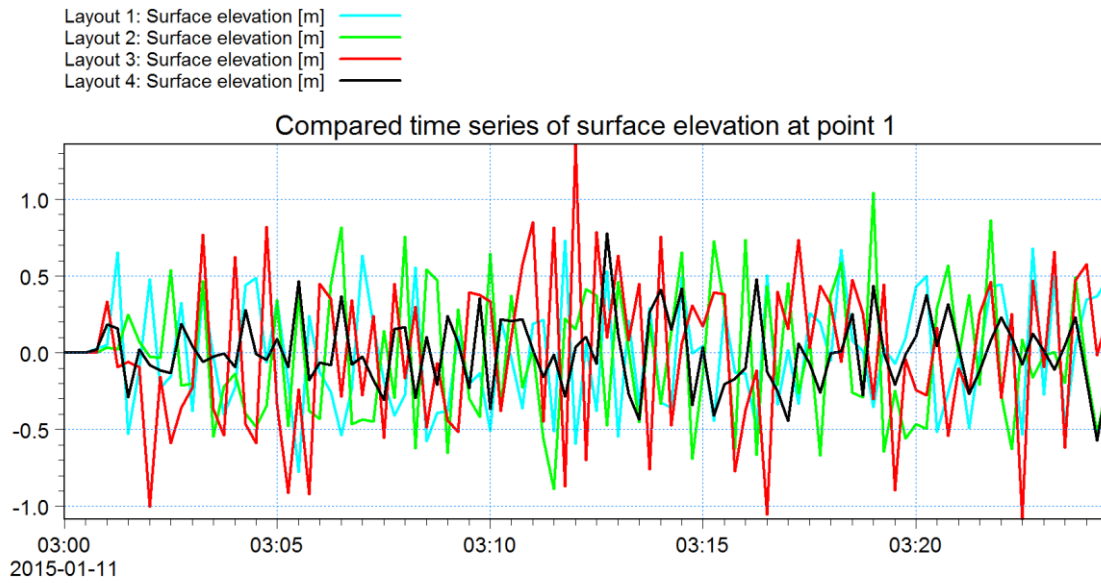


Figure 105 Compared wave height time series for waves coming from north-west (Points 1-3)

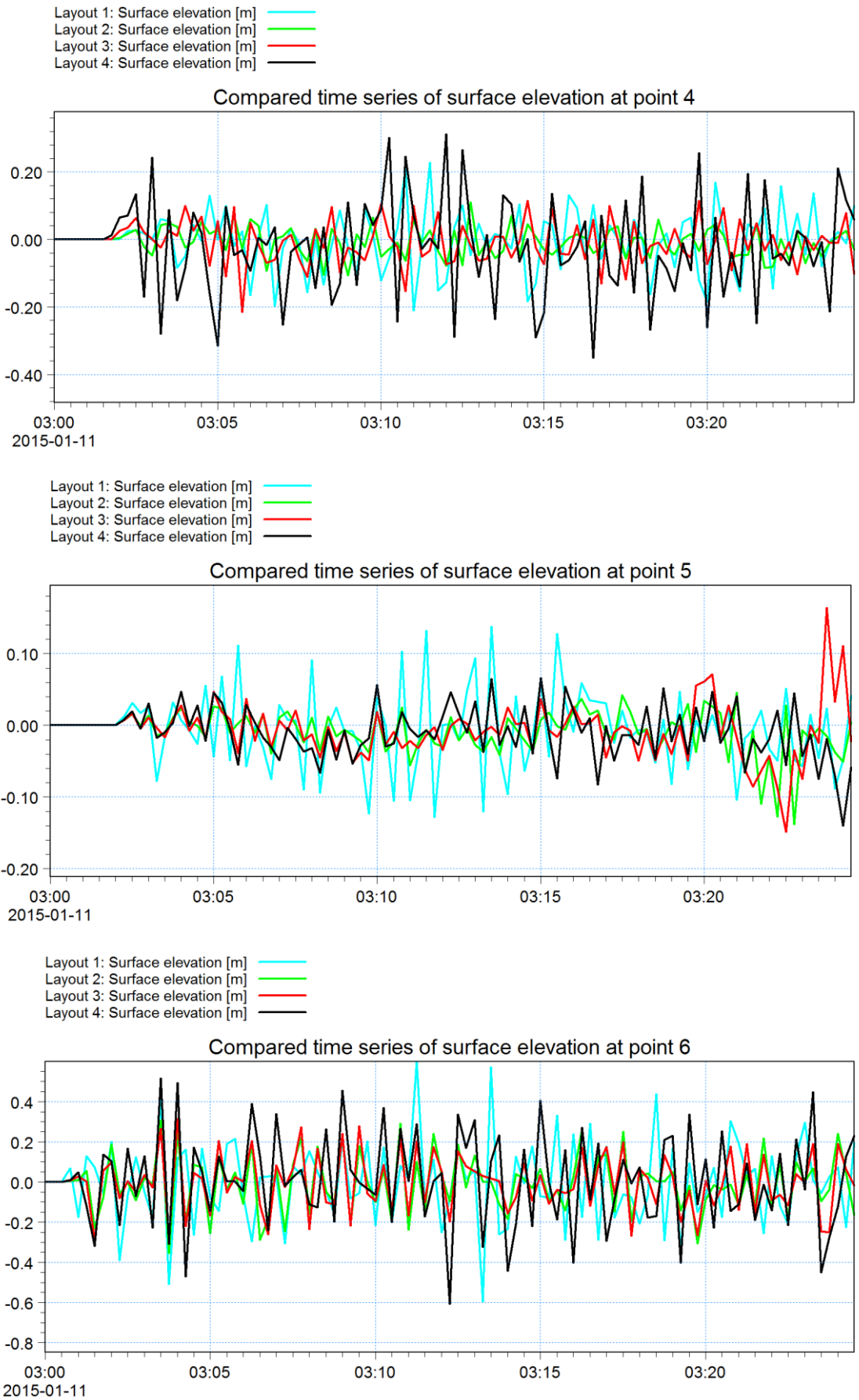


Figure 106 Compared wave height time series for waves coming from north-west (Points 4-6)

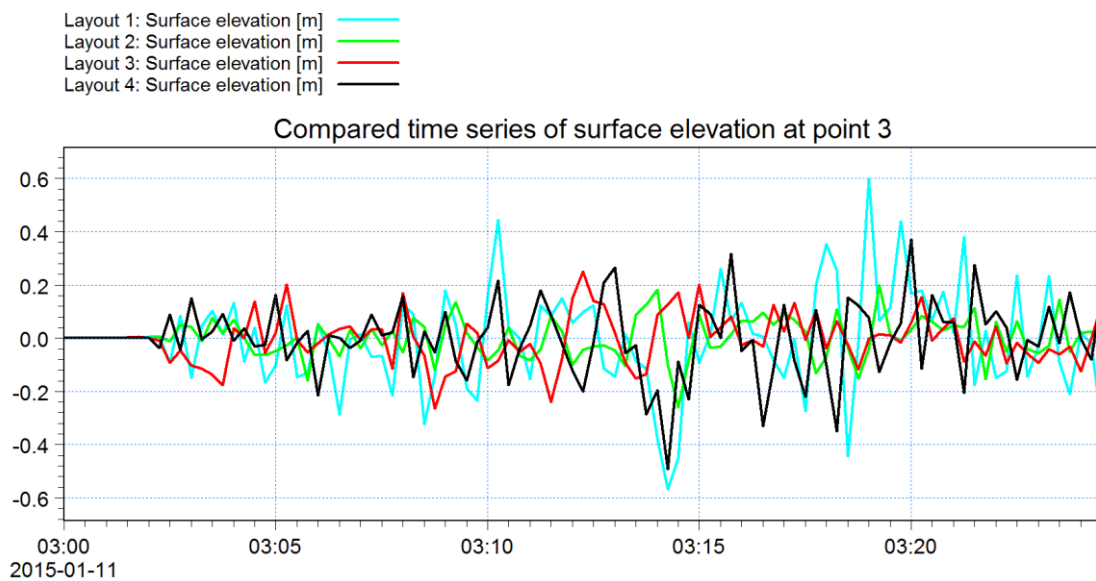
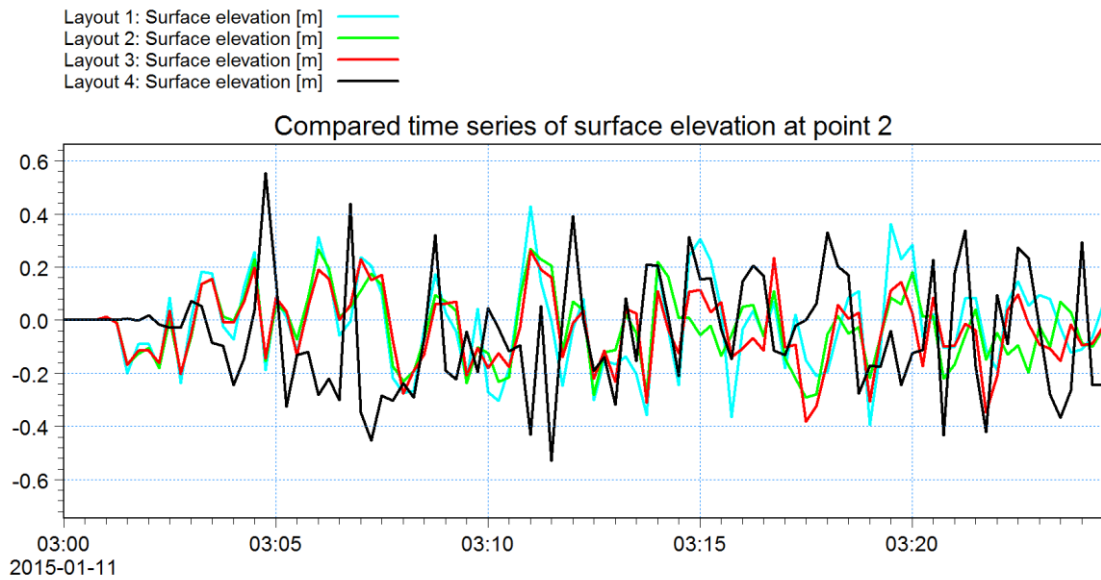
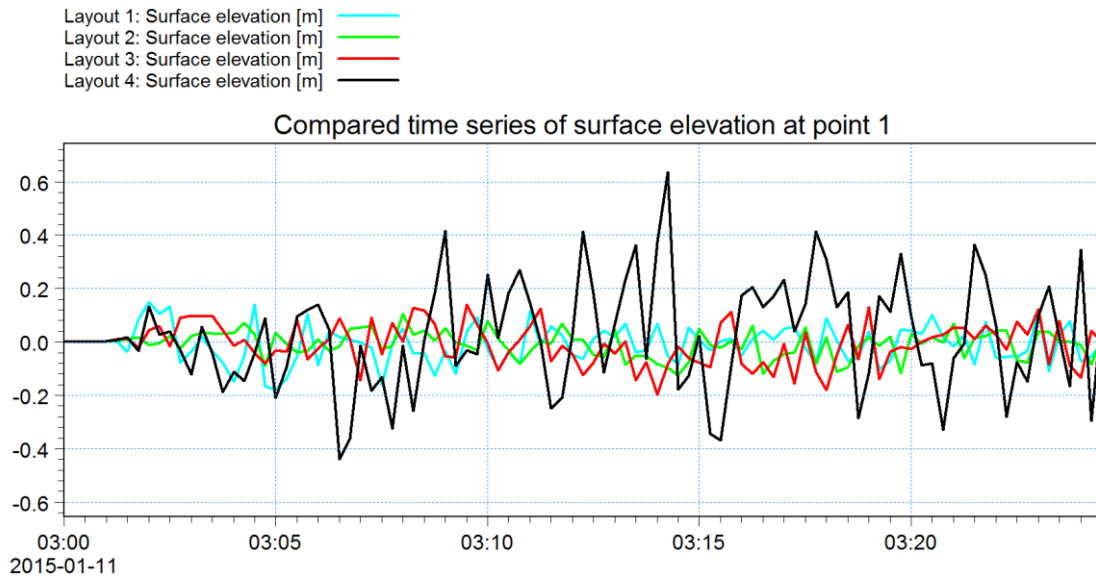
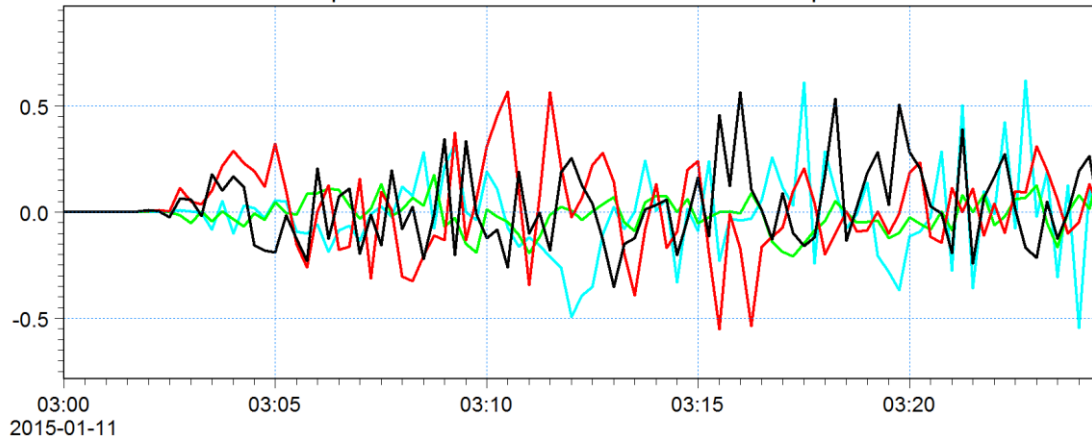


Figure 107 Compared wave height time series for waves coming from north-east (Points 1-3)

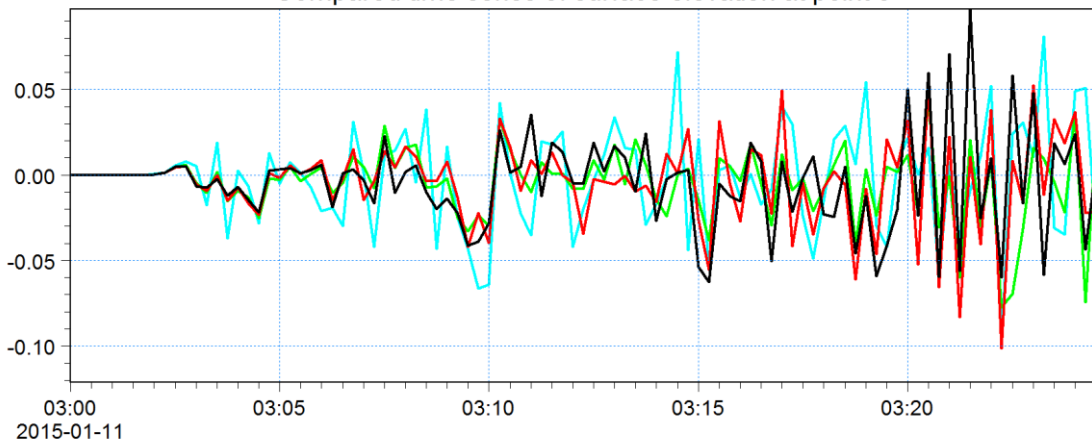
Layout 1: Surface elevation [m] —
 Layout 2: Surface elevation [m] —
 Layout 3: Surface elevation [m] —
 Layout 4: Surface elevation [m] —

Compared time series of surface elevation at point 4



Layout 1: Surface elevation [m] —
 Layout 2: Surface elevation [m] —
 Layout 3: Surface elevation [m] —
 Layout 4: Surface elevation [m] —

Compared time series of surface elevation at point 5



Layout 1: Surface elevation [m] —
 Layout 2: Surface elevation [m] —
 Layout 3: Surface elevation [m] —
 Layout 4: Surface elevation [m] —

Compared time series of surface elevation at point 6

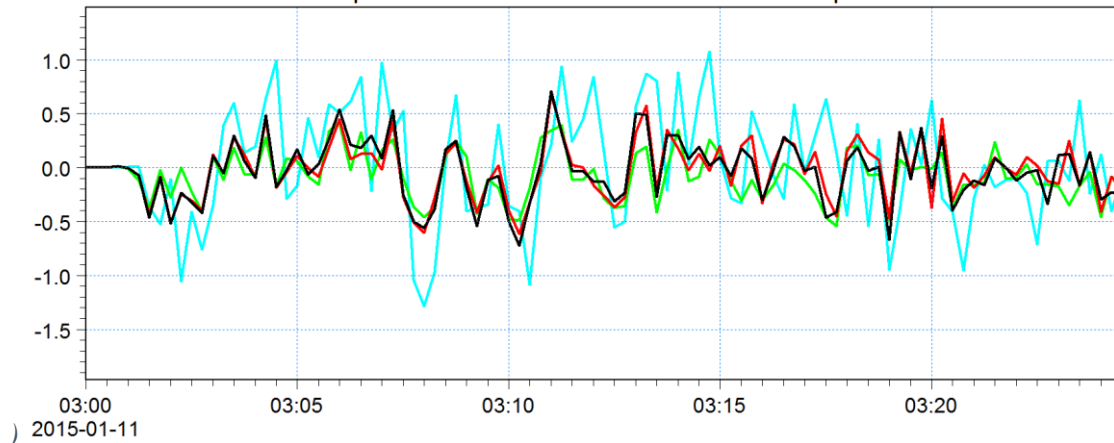


Figure 108 Compared wave height time series for waves coming from north-east (Points 4-6)

Table 12 Summary of max. wave height obtained from simulation with random waves from north-west. Colour green symbolize the lowest value while red the highest values.

Max. wave heights obtained from simulation with random waves from north-west				
Location	Layout 1	Layout 2	Layout 3	Layout 4
Point 1	0.78 m	1.04 m	1.36 m	0.78 m
Point 2	0.36 m	0.20 m	0.26 m	0.15 m
Point 3	0.28 m	0.09 m	0.10 m	0.22 m
Point 4	0.23 m	0.11 m	0.21 m	0.35 m
Point 5	0.13 m	0.14 m	0.16 m	0.14 m
Point 6	0.60 m	0.35 m	0.31 m	0.60 m

Table 13 Summary of max. wave height obtained from simulation with random waves from north-east. Colour green symbolize the lowest value while red the highest values.

Max. wave heights obtained from simulation with random waves from north-east				
Location	Layout 1	Layout 2	Layout 3	Layout 4
Point 1	0.18 m	0.12 m	0.20 m	0.63 m
Point 2	0.43 m	0.29 m	0.38 m	0.55 m
Point 3	0.60 m	0.26 m	0.26 m	0.49 m
Point 4	0.62 m	0.21 m	0.57 m	0.56 m
Point 5	0.10 m	0.08 m	0.10 m	0.10 m
Point 6	0.56 m	0.54 m	0.68 m	0.72 m

To obtain wave period from results obtained from BW simulation a Linear Spectra Analysis was performed with default setup values. Log files from those analyses are located at Appendices.

Table 14 Summary of mean wave period obtained from LSA of random waves from north-west.

Mean wave periods obtained from LSA with random waves from north-west				
Location	Layout 1	Layout 2	Layout 3	Layout 4
Point 3	4.86 s	4.94 s	4.51 s	4.66 s
Point 4	5.19 s	4.59 s	4.70 s	4.83 s
Point 5	4.40 s	5.90 s	5.97 s	5.63 s

Table 15 Summary of mean wave period obtained from LSA of random waves from north-east.

Mean wave periods obtained from LSA with random waves from north-east				
Location	Layout 1	Layout 2	Layout 3	Layout 4
Point 3	8.56 s	6.98 s	8.71 s	6.95 s
Point 4	9.50 s	9.54 s	8.68 s	5.89 s
Point 5	5.08 s	7.08 s	5.88 s	7.45 s

7. CONCLUSIONS AND RECOMMENDATIONS FOR FURTHER REASERCH

It is shown in this master thesis planning and designing the harbour layout is very complex task, dependent on wide range of factors, such us technical, environmental or economic aspects. As the main task for harbour structures is to ensure safe conditions for berthing and cargo handling operations, the wave climate provided by the geometry and construction solutions have to be thoroughly investigated. Numerical simulations are of great help with this task. With growing computational power of computers they are growing in popularity as are cheap and efficient way of checking proposed solutions, optimizing and making more reliable and durable constructions. To prepare a model that will give credible and reliable information is also a demanding and difficult process. One have to take into account a large variety of phenomena that take place in deep water and near the coastline. Numerous parameters have to be chosen wisely as they can significantly alter the results.

Obtaining representative input data is of highest importance, but is often quite troublesome, as measuring station are located far away from each other or do not take measurements at the same time. This was also the case in this study.

In spite of such difficulties effective analysis was conducted. Results from prepared numerical simulations of wave conditions provided by four different given concepts of new breakwater layouts indicate that the calmest wave climate is provided by the layout that was marked as Layout 2, that is the one without the detached breakwater and with large new oblong basin. For the two main directions checked it gave the smallest wave heights inside the harbour basins and at the entrance to the harbour.

Prepared model has some shortcomings that could be easily corrected, given more time and with additional data and resources available.

First of all, it lacks validation. This can be done in two ways. A scale model testing can be useful to check whether obtained wave patterns are realistic. This requires a facility with a wave basin and is quite expensive. Other method involves taking wave measurements inside the existing harbour and running additional numerical model with current geometry in order to calibrate all the parameters used in target models. This was impossible to prepare due to lack of input data for SW simulation from recent time.

The other drawback of the prepared model are simplifications used in order to make the model calculable on regular, not so powerful personal computers. With more powerful processors complex phenomena such as wave breaking could be taken into account.

Conducted analysis verified only the basic criterion, that is the wave climate inside the harbour. In order to make sure, that no additional unfavourable phenomena take place, prepared models should be extended by additional features. Due to the fact that old Ustka harbour is located at the river mouth and river flow connected with storm surge was causing quay stability problems, information about hydrodynamics (currents, river flow, storm surge) should be included into numerical model. This would give valuable information about the impact of new structures on the conditions inside the harbour during such adverse conditions.

Harbour oscillations and seiches can be also causing unfavourable effects, especially on mooring systems. This phenomenon should be investigated as well to make sure that water oscillations induced by pressure changes or long waves entering the harbour do not have similar frequencies to the natural frequencies water masses inside harbour basins.

Coastal structures affect natural processes that take place nearshore. This refers mainly to the sediment transport, that can be significantly disturbed by structures and induce disastrous effects and should be investigated additionally.

One last issue should also be noted. The research focused only on choosing the best layout out of four different concepts given by Maritime Office in Słupsk. Re-examination of the problem could possibly reveal another harbour layout, that will provide even better wave climate inside as well as meet other criteria not included in this study.

REFERENCES

- Agerschou et al. (2004) Planning and design of ports and marine terminals. 2nd Edition
- Bobin (2012), Appendix 6 to Regulation No. 1 of the Director of the Maritime Office in Słupsk of 17 May 2012. regarding Determining the port areas and public facilities, equipment and installations in the port infrastructure. Official Journal of the Pomeranian Voivodeship from 2012. Item. 2103 Official Journal of the West Pomeranian Voivodeship 2012 item. 1436. Słupsk, Poland*
- Bolt et al. (2015) Extract from the technical expertise concerning failure of Pilot Quay in Ustka.*
- Brzóska et al. (2011), Ustka Development Strategy by 2020. Department of Local Development and European Integration of the City of Ustka. Ustka, Poland*
- Christow (2007) The development strategy of the sea port in Ustka by 2021. In Proc. Business Mobility International Sp. Z o. o. *
- Czajewski (1988) Nautical Meteorology, Publishers of Communications and Connections, Warsaw.*
- Hasselmann, K., (1974), On the spectral dissipation of ocean waves due to whitecapping, Bound. Layer Meteor., 6, 107-127.
- Hasselmann, S., K. Hasselmann (1985), Computation and parametrizations of Non-linear Energy Transfer in a gravity-wave spectrum, Hamburger Geophys. Einzelschr., Serie A.
- Huler, S. (2004). Defining the Wind: The Beaufort Scale, and How a 19th-Century Admiral Turned Science into Poetry. Crown
- Jakusik (2006) Characteristics of waves in the southern part of the Baltic Sea. In Proc. Institute of Meteorology and Water Management, Warsaw, Poland.*
- Mike 21 BW, SW and HD (2016) User Guides and Scientific Manuals
- OCDI (2002) Technical Standards and Sommentaries for Port and Harbour Facilities in Japan
- Paplińska (2000) Modern methods of forecasting waves on the Baltic Sea. Inżynieria Morska i Geotechnika, 21, 5, 245-252.*
- Renewable Energy, <http://www.energetycznie.com.pl>, as of June 2016
- Sailing Poland, http://www.sailingpoland.pl/elocja/ustka_port, as of June 2016.
- Sawaragi (1995) Coastal Engineering – Waves, Beaches, Wave-Structure Interactions, Chapter 5. Osaka, Japan.
- Short Description, Mike 21 Spectral Waves FM. Denmark
- Takahashi et al. (2006) Technical Note of NILIM No.309 The National Institute for Land and Infrastructure Management in Japan
- Thoresen (2010), Port designer's handbook, 2nd edition. London, United Kingdom
- Trozzi, C. and Vaccaro, R. (2000) Environmental impact of port activities. Rome, Italy.
- Uscinowicz (2003) Exploration and Extraction of Sand and Gravel Resources in the Polish Exclusive Economic Zone of the Baltic Sea (2003). In Proc. European marine sand and

gravel—shaping the future, EMSAGG Conference 20–21 February 2003, Delft University, Netherlands.

**Reference in Polish*

APPENDICES

1. Mike Zero License Agreement



Application for MIKE by DHI Software Sponsorship Program

Application for free time-limited (max. 12 months at a time) licenses for MIKE by DHI software products.
Please submit to your local DHI office.

Applicant (Name): **Wiktor Wickland**
University: **Norwegian University of Science and Technology**
Professor: **Raed Lubbad**
Course of Studies: **Marine Civil Engineering**
Title of Thesis: **Expansion of the port in Ustka: simulation of wave conditions.**
Software Product(s): **MIKE 21 BW and MIKE 21 SW**

Short description of intended use of the MIKE by DHI software products in the project:

A new port is needed in Ustka. I will calculate wave conditions inside the port with different breakwater layouts. Master thesis is prepared together with a friend of mine Hubert Konkol.

I hereby apply for a free license of the MIKE by DHI software listed above for work related to my thesis. I agree to fulfil all the conditions listed on page 2 in case the sponsorship is granted.

Place: Trendelenburg, Date: 03.02.2016

Wiktor Wickland
Signature User

I confirm that the person having signed above is a student at my institution working on the above mentioned thesis. I support the use of the above listed MIKE by DHI software for the thesis work.

Raed Lubbad
Signature Professor

DHI internal: Assigned hardware key: _____



Application for MIKE by DHI Software Sponsorship Program

Application for free time-limited (max. 12 months at a time) licenses for MIKE by DHI software products.
Please submit to your local DHI office.

Applicant (Name): **Hubert Konkol**
University: **Norwegian University of Science and Technology**
Professor: **Raed Lubbad**
Course of Studies: **Marine Civil Engineering**
Title of Thesis: **Expansion of the port in Ustka: simulation of wave conditions.**
Software Product(s): **MIKE 21 BW and MIKE 21 SW**

Short description of intended use of the MIKE by DHI software products in the project:

A new port is needed in Ustka. I will calculate wave conditions inside the port with different breakwater layouts. Master thesis is prepared together with a friend of mine Wiktor Wickland.

I hereby apply for a free license of the MIKE by DHI software listed above for work related to my thesis. I agree to fulfil all the conditions listed on page 2 in case the sponsorship is granted.

Place: Trondheim, Date: 03.02.2016

Hubert Konkol
Signature User

I confirm that the person having signed above is a student at my institution working on the above mentioned thesis. I support the use of the above listed MIKE by DHI software for the thesis work.

Raed Lubbad
Signature Professor

DHI internal. Assigned hardware key: _____



Conditions of Use:

1. User may apply the MIKE by DHI license(s) provided by DHI exclusively for work directly related to the thesis.
2. The term of use ends with the day of hand-in of the thesis or the day of viva voce.
3. User shall return the provided hardware dongle to DHI immediately at the end of the term of use.
4. If renewing the MIKE by DHI license(s), the User must provide an update on the thesis to DHI, and a new agreement must be signed. It is the responsibility of the User to initiate this.
5. User may not copy the software or replicate/copy/bypass the dongle. The license(s) may not be used for any commercial purpose, no matter whether related to the thesis or not. The software license(s) may not be made available to third parties under any conditions.
6. User shall inform DHI immediately in case of changes regarding this agreement, including but not limited to changes in the title of thesis or premature ending of the work on the thesis.
7. After finishing the thesis, User agrees to provide DHI with a digital copy (PDF format) of the thesis. At the same time, User agrees to provide DHI with a one-page abstract (in English) of the thesis that DHI may publish with due reference to the original text and with author information.
8. For any written publications published or during verbal presentations, that include results derived from the MIKE by DHI Software, DHI must be acknowledged for the sponsored MIKE by DHI license file(s).
9. User understands and accepts that by breaching any of the conditions of this agreement, User is violating the intellectual property rights of DHI. In case of breach of the agreement, DHI reserves the right to claim a fee corresponding to 150% of the full commercial price of the licenses plus reasonable legal costs.
10. Any breach of this agreement will be prosecuted. User is personally responsible for any violations.
11. In addition to the above, User agrees to be bound by all standard conditions for use of MIKE by DHI software as described in the standard Software License Agreement, which is displayed during installation of the software.

2. Sample log files from Linear Spectra Analysis

2.1. Layout 1 point 3, waves from north-east

```
-----  
-----  
DHI Wave Synthesizer  
07-02-2016  
WS Spectral Analysis  
21:20:38  
-----  
-----
```

```
Parameter file: D:\...\WsLinearSpectralAnalysisPar1.wslsa  
-----  
-----
```

```
Input data file      : D:\...\Point3.dfs0  
Number of items     : 15  
Number of sets of items : 99  
Interval between sets : 15,0000 s
```

```
Item 1:  
  Name: P(850,630):Surface elevation  
  Type: Surface Elevation [100078]  
  Unit: meter [1000]  
  Base: meter [1000]  
  FRU: meter [1000]
```

```
Item 2:  
  Name: P(850,630):Water level  
  Type: Water Level [100000]  
  Unit: meter [1000]  
  Base: meter [1000]  
  FRU: meter [1000]  
-----  
-----
```

The following parameters are used for the linear spectral analysis

```
Start time          : 0,00 s  
Stop time           : 1470,00 s  
FFT parameters  
  Size of FFT block : 64  
  Overlap            : 0,667  
  Number of subseries : 2  
  FFT duration       : 1290,00 s  
  FFT utilization    : 86,9 %  
  Frequency step     : 0,001 Hz  
  Lower cut-off frequency : 0,000 Hz  
  Higher cut-off frequency : 0,033 Hz  
  Data window        : Hanning
```

```
Parameter set      : Period  
  Auto spectrum    : Yes  
    Parameters     : Spectral moments  
    Parameters     : Peak parameters  
    Parameters     : Spectral width  
    Parameters     : Peak to peak estimates
```

```

Parameters : Period parameters
Cross-spectrum : No
Frequency response spectrum : No
Coherence spectrum : No
Coherent power spectrum : No

```

Analyses to perform

```

Input/Parameter set : 1//Period
Input/Parameter set : 2//Period
Input/Parameter set : 3//Period
Input/Parameter set : 4//Period

```

Output data file

```

Spectra : D:\...\LSA_Point4.dfs0

```

```

*****
*****

```

Analysis : 1

```

Input : P(850,630):Surface elevation / 100078 / 1000 / True

```

Parameters derived from auto spectra

```

-----
Item      Spectral      Spectral      Spectral      Spectral
no        moment        moment        moment        moment
           m0          m1          m2          m4
-----
  1  3,4822E-02  4,0661E-04  6,8570E-06  3,0702E-09
  2  3,4823E-02  4,0661E-04  6,8570E-06  3,0702E-09
-----

```

```

-----
Item      Peak          Peak          Spectral
no        frequency      value         width
           fp          Gp          eps
-----
  1  1,5625E-02  3,4618E+00  7,4848E-01
  2  1,5625E-02  3,4618E+00  7,4848E-01
-----

```

```

-----
Item      Peak-Peak      Peak-Peak      Peak-Peak      Peak-Peak      Peak-Peak
no        Hm0          H10%          H1%          H0.1%          H0.01%
-----
  1  7,4643E-01  8,0091E-01  1,1327E+00  1,3872E+00  1,6018E+00
  2  7,4643E-01  8,0091E-01  1,1327E+00  1,3872E+00  1,6018E+00
-----

```

```

-----
Item      Period      Period      Period      Period
no        Tp          T01         T02         T24
-----
  1  6,4000E+01  8,5640E+01  7,1263E+01  4,7259E+01

```

2 6,4000E+01 8,5640E+01 7,1263E+01 4,7259E+01

Used output identification codes:

- AS Auto spectrum
- XA Cross-spectrum amplitude
- XP Cross-spectrum phase
- CS Co-spectrum (real)
- QS Quad-spectrum (imaginary)
- CO Coherence spectrum
- CP Coherent power spectrum
- RA Response amplitude spectrum
- RP Response phase spectrum

Output data file : D:\...\LSA_Point4.dfs0

Creation date : 07-02-2016
Creation time : 21:20:40
Number of items : 4
Number of sets of items : 32
Interval between sets : 0,0010 Hz

#	Min	Max	Mean	St. Dev
Del Description				
1 100260 7100	9,157E-02	3,462E+00	1,045E+00	9,294E-01
0 1 AS 1				
2 100260 7100	9,157E-02	3,462E+00	1,045E+00	9,294E-01
0 2 AS 2				
3 999 0	3,821E+00	1,757E+02	3,634E+01	3,622E+01
0 3 AS 3				
4 999 0	8,789E-02	3,369E+02	4,086E+01	6,494E+01
0 4 AS 4				

2.2. Layout 1 point 4, waves from north-east

DHI Wave Synthesizer
07-02-2016
WS Spectral Analysis
21:21:42

Parameter file: D:\...\WsLinearSpectralAnalysisPar1.wslsa

```

Input data file      : D:\...\Point4.dfs0
Number of items     : 3
Number of sets of items : 99
Interval between sets : 15,0000 s
Item 1:
  Name: P(734,405):Surface elevation
  Type: Surface Elevation [100078]
  Unit: meter [1000]
  Base: meter [1000]
  FRU: meter [1000]

```

The following parameters are used for the linear spectral analysis

```

Start time          : 0,00 s
Stop time           : 1470,00 s
FFT parameters
  Size of FFT block : 64
  Overlap            : 0,667
  Number of subseries : 2
  FFT duration       : 1290,00 s
  FFT utilization    : 86,9 %
  Frequency step     : 0,001 Hz
  Lower cut-off frequency : 0,000 Hz
  Higher cut-off frequency : 0,033 Hz
  Data window        : Hanning

```

```

Parameter set      : Period
Auto spectrum      : Yes
  Parameters        : Spectral moments
  Parameters        : Peak parameters
  Parameters        : Spectral width
  Parameters        : Peak to peak estimates
  Parameters        : Period parameters
Cross-spectrum     : No
Frequency response spectrum : No
Coherence spectrum : No
Coherent power spectrum : No

```

```

Analyses to perform
Input/Parameter set : 1//Period
Input/Parameter set : 2//Period
Input/Parameter set : 3//Period

```

```

Output data file
Spectra          : D:\...\LSA_Point4.dfs0

```

```

*****
*****

```

```

Analysis : 1
  Input  : P(734,405):Surface elevation / 100078 / 1000 / True

```

Parameters derived from auto spectra

```

-----
Item      Spectral      Spectral      Spectral      Spectral

```

no	moment m0	moment m1	moment m2	moment m4
1	3,2157E-02	3,3784E-04	6,9315E-06	4,8469E-09
2	0,0000E+00	0,0000E+00	0,0000E+00	0,0000E+00
3	0,0000E+00	0,0000E+00	0,0000E+00	0,0000E+00

Item no	Peak frequency fp	Peak value Gp	Spectral width eps
1	2,0833E-03	5,5232E+00	8,3171E-01
2	3,3333E-02	0,0000E+00	-1,0000E-35
3	3,3333E-02	0,0000E+00	-1,0000E-35

Item no	Peak-Peak Hm0	Peak-Peak H10%	Peak-Peak H1%	Peak-Peak H0.1%	Peak-Peak H0.01%
1	7,1730E-01	7,6965E-01	1,0884E+00	1,3331E+00	1,5393E+00
2	0,0000E+00	-1,0000E-35	-1,0000E-35	-1,0000E-35	-1,0000E-35
3	0,0000E+00	-1,0000E-35	-1,0000E-35	-1,0000E-35	-1,0000E-35

Item no	Period Tp	Period T01	Period T02	Period T24
1	4,8000E+02	9,5184E+01	6,8112E+01	3,7816E+01
2	3,0000E+01	-1,0000E-35	-1,0000E-35	-1,0000E-35
3	3,0000E+01	-1,0000E-35	-1,0000E-35	-1,0000E-35

Used output identification codes:

- AS Auto spectrum
- XA Cross-spectrum amplitude
- XP Cross-spectrum phase
- CS Co-spectrum (real)
- QS Quad-spectrum (imaginary)
- CO Coherence spectrum
- CP Coherent power spectrum
- RA Response amplitude spectrum
- RP Response phase spectrum

Output data file : D:\...\LSA_Point4.dfs0


```

-----
-----
Creation date           : 07-02-2016
Creation time          : 21:21:44
Number of items       : 3
Number of sets of items : 32
Interval between sets  : 0,0010 Hz
-----

```

```

-----
-----
#           Min           Max           Mean           St. Dev
Del Description
1 100260 7100 4,031E-02 5,523E+00 9,647E-01 1,250E+00
0 1 AS 1
2 100260 7100 0,000E+00 0,000E+00 0,000E+00 0,000E+00
0 2 AS 2
3 100260 7100 0,000E+00 0,000E+00 0,000E+00 0,000E+00
0 3 AS 3
-----
-----

```